Hypermetabolism in mice carrying a near complete human chromosome 21

Dylan C. Sarver[1,2], Cheng Xu[1,2], Susana Rodriguez[1,2], Susan Aja[2,3], Andrew E. Jaffe[4,5,6,7,8,9], Feng J. Gao[1], Michael Delannoy[10], Muthu Periasamy[11,12], Yasuhiro Kazuki[13,14], Mitsuo Oshimura[14], Roger H. Reeves[1,8], G. William Wong[1,2,*]

Affiliations:

[1]Department of Physiology, Johns Hopkins University School of Medicine, Baltimore, Maryland, USA

[2]Center for Metabolism and Obesity Research, Johns Hopkins University School of Medicine, Baltimore, Maryland, USA

[3]Department of Neuroscience, Johns Hopkins University School of Medicine, Baltimore, MD, USA

[4]Department of Psychiatry and Behavioral Sciences, Johns Hopkins University School of Medicine, Baltimore, MD, USA

[5]Department of Mental Health, Johns Hopkins Bloomberg School of Public Health, Baltimore, MD, USA.

[6]The Lieber Institute for Brain Development, Baltimore, MD, USA.

[7]Center for Computational Biology, Johns Hopkins University, Baltimore, MD, USA.

[8]Department of Genetic Medicine, Johns Hopkins University School of Medicine, Baltimore, MD, USA.

[9]Department of Biostatistics, Johns Hopkins Bloomberg School of Public Health, Baltimore, MD, USA.

[10]Department of Cell Biology, Johns Hopkins University School of Medicine, Baltimore, MD, USA.

[11]Department of Physiology and Cell Biology, The Ohio State University, Columbus, OH, USA.

[12]Burnett School of Biomedical Sciences, College of Medicine, University of Central Florida, Orlando, FL, USA

[13]Division of Genome and Cellular Functions, Department of Molecular and Cellular Biology, School of Life Science, Faculty of Medicine, Tottori University, Tottori, Japan

[14]Chromosome Engineering Research Center, Tottori University, Tottori, Japan.

*Correspondence: gwwong@jhmi.edu

ABSTRACT

The consequences of aneuploidy have traditionally been studied in cell and animal models in which the extrachromosomal DNA is from the same species. Here, we explore a fundamental question concerning the impact of aneuploidy on systemic metabolism using a non-mosaic transchromosomic mouse model (TcMAC21) carrying a near complete human chromosome 21. Independent of diets and housing temperatures, TcMAC21 mice consume more calories, are hyperactive and hypermetabolic, remain consistently lean and profoundly insulin sensitive, and have a higher body temperature. The hypermetabolism and elevated thermogenesis are due to sarcolipin overexpression in the skeletal muscle, resulting in futile sarco(endo)plasmic reticulum Ca^{2+} ATPase (SERCA) activity and energy dissipation. Mitochondrial respiration is also markedly increased in skeletal muscle to meet the high ATP demand created by the futile cycle. This serendipitous discovery provides proof-of-concept that sarcolipin-mediated thermogenesis via uncoupling of the SERCA pump can be harnessed to promote energy expenditure and metabolic health.

Key words: Aneuploidy, trisomy, hypermetabolism, sarcolipin, SERCA pump, futile cycle

INTRODUCTION

The presence of an extra chromosome in mammals is generally lethal during fetal development, due to widespread cellular havoc caused by misregulated gene expression arising from gene dosage imbalance (1). Down syndrome (DS), resulting from trisomy of chromosome 21, is one of the rare aneuploidies compatible with life although as many as 80% of trisomy 21 conceptuses miscarry (2). The increased expression of ~500 transcribed sequences of human chromosome 21 (Hsa21) affects many cell types and organ systems during development and in the postnatal period (3, 4). Humans with trisomy 21 have cognitive deficits, altered craniofacial development, and are at significantly higher risk for congenital heart defects, hearing and vision loss, leukemia, gastrointestinal disease, and early-onset dementia (2).

Given the significant impact of intellectual disability on the lives of individuals with DS, research emphasis has naturally focused on the neurological deficits underpinning trisomy 21 (5). In addition to developmental abnormalities associated with DS, there is an increasing awareness that adolescents and adults with DS also have an increased incidence of obesity, insulin resistance, and diabetes (6-8). Although this was first noted in the 1960s (9), the underlying cause for these metabolic dysregulations is mostly unknown and largely underexplored. Beyond clinical observations, limited studies have been conducted to determine the physiological underpinnings of metabolic impairments seen in DS [reviewed in (10)]. Our recent study on the Ts65Dn mouse model represents the most in-depth metabolic analysis, to date, of any Down syndrome mouse model (11). However, the segmental trisomic Ts65Dn mouse contains only ~55% of the orthologous protein-coding genes found on Hsa21 (12). In addition, it contains additional trisomic genes from the centromeric region of mouse chromosome 17 (Mmu17) not found in Hsa21, thus complicating the genotype-phenotype relationships (13, 14).

In the past two decades, more than 20 mouse models of DS have been generated (15). Despite their utility in advancing DS research, none of these models recapitulate the full spectrum of human DS. With the

exception of Tc1, all the DS mouse models are trisomic for some, but not all, of the orthologous mouse genes found in Hsa21 (15). Tc1 is the first mouse model with an independently segregating Hsa21 (16). However, Tc1 mice are missing >50 of the 220 protein coding genes on Hsa21 due to deletion and mutations (17). In addition, Tc1 mice show extensive mosaicism (i.e., the human chromosome is present in zygotes but is lost randomly from cells during development). As a consequence, every mouse has a unique developmental trajectory, complicating the interpretations of results obtained from Tc1 mice. To overcome the limitations of previously generated trisomic mouse models, a transchromosomic mouse model (TcMAC21) carrying an independently segregating and a near complete copy of Hsa21 was recently developed (18). TcMAC21 is not mosaic and contains 93% of HSA21q protein-coding genes (PCGs), and is considered the most representative mouse model of DS.

Both mouse and rat that carry a non-mosaic Hsa21 recapitulate many DS phenotypes related to the central nervous system (e.g., reduced cerebellum volume, learning and memory deficit), craniofacial skeleton, and heart (18, 19). The metabolic phenotype of TcMAC21, however, is unknown and has yet to be examined. The availability of the TcMAC21 mouse model has afforded a unique opportunity to address two fundamental questions: 1) what is the impact of aneuploidy on systemic metabolism; 2) what are the molecular, cellular, and physiological consequences of introducing a foreign (human) chromosome from an evolutionarily distant species into mice?

Unexpectedly, we discovered that TcMAC21 mice have all the hallmarks of hypermetabolism, driven by elevated mitochondrial respiration and futile sarco(endo)plasmic reticulum Ca^{2+} ATPase (SERCA) pump activity in the skeletal muscle as a consequence of endogenous sarcolipin (SLN) overexpression. Our study has provided further evidence and proof-of-concept that endogenous SLN-mediated uncoupling of the SERCA pump can be harnessed for energy dissipation, weight loss, and metabolic health.

RESULTS

Human chromosome 21 genes are differentially expressed and regulated in mouse adipose tissue, liver, and skeletal muscle

TcMAC21 mice carry a non-mosaic and independently segregating mouse artificial chromosome with a near complete copy of the long arm of human chromosome 21 (Hsa21q) (18). The Hsa21q in TcMAC21is comprised of ~37 Mb and 199 protein coding genes (Fig. 1A). RNA-sequencing showed that TcMAC21 mice are capable of expressing Hsa21-derived transcripts in each of the tissues examined, and that gene expression is regulated in a tissue-specific manner. The transcriptional activity map of Hsa21 shows regions of gene expression and repression (Fig. 1B). There are three large regions of Hsa21 with little or no transcription activity: 29.5-31.1 Mb, 44.5-44.8 Mb, and 45.3-46.2 Mb. The first gap of transcriptional inactivity contains the protein-coding genes *Cldn8* and *Cldn17*, *Girk1*, and 33 distinct *Krtap* (keratin-associated protein) genes. The second transcriptionally inactive area contains 16 *Krtap* genes, and the third transcriptionally inactive area contains 8 protein-coding genes (*Col6a1, Col6a2, Col18a1, Fctd, Lss, Pcbp3, Slc19a1*, and *Spatc1l*). By filtering the transcriptional map to display expressed-genes only, we highlighted all the genes with their differential expression profiles across five major metabolic tissues—brown adipose tissue (BAT), inguinal white adipose tissue (iWAT), gonadal white adipose tissue (gWAT), liver, and skeletal muscle (Fig. 1C).

One of the more striking differences in expression profile is between visceral (gonadal) and subcutaneous (inguinal) white adipose tissue (gWAT and iWAT respectively). gWAT expresses 115 human protein-coding genes (PCGs) while iWAT expresses only 27. A similar pattern can be seen in the non-protein-coding genes (NPCGs). We were unable to detect any Hsa21-derived non-protein-coding genes in the iWAT, while in gWAT we observed 37. Overlap analysis was carried out to assess how

similar expression profiles were between tissues (Fig. 1D). Of the 126 Hsa21-derived protein-coding genes expressed by at least one tissue, a majority (65 total) are shared between BAT, gWAT, liver, and skeletal muscle. Of the 109 Hsa21-derived non-protein-coding genes expressed by at least one tissue, the majority (53 total) are uniquely expressed by skeletal muscle. Of note, the liver uniquely expresses 6 PCGs and 2 NPCGs, gWAT 4 and 3, skeletal muscle 3 and 53, BAT 1 and 10, and iWAT 0 and 0. Together, these data indicate that Hsa21-derived transcripts are differentially expressed and regulated across major metabolic tissues in TcMAC21 mice.

Hypermetabolism in TcMAC21 mice

Having established that Hsa21-derived transcripts are differentially expressed and regulated in mouse organs and tissues, we next asked the impact of the extra human genetic material and genes on systemic metabolism. As previously documented, TcMAC21 pups are born at the same weight as their euploid littermates (18). However, by 3 months of age TcMAC21 mice fed a standard chow weighed significantly less (~8.5 g) than euploid littermates, and this weight difference remained stable over time (Fig. 2A). The size and body weight differences were not due to reduced plasma IGF-1 and growth hormone, as their circulating levels were in fact higher in TcMAC21 compared to euploid mice (Fig. S1). Body composition analysis showed that TcMAC21 have significantly reduced absolute and relative (normalized to body weight) fat mass (Fig. 2B). Although the absolute lean mass was reduced in TcMAC21 mice, the relative lean mass (normalized to body weight) was not different between genotypes. Tissue collection at termination of the study also showed smaller visceral and subcutaneous fat mass and liver weight in TcMAC21 mice (Table S1).

Differences in body weight were not due to reduced caloric intake, as TcMAC21 mice actually consumed a significantly higher amount of food relative to their body weight than euploid controls (Fig.

2C). Indirect calorimetry analysis indicated that TcMAC21 mice—regardless of the photocycle (light or dark phase) and metabolic states (*ad libitum* fed, fasted, refed)—were expending ~25% more energy and were significantly more active compared to euploid controls (Fig. 2D-E and Fig. S2 and Table S2). Despite much higher caloric intake per gram body mass, TcMAC21 mice were much leaner due to substantially elevated physical activity and energy expenditure. Hyperactivity and elevated energy expenditure were not due to altered circulating thyroid hormones, as serum triiodothyronine (T_3, the active form of TH) levels were not different between chow fed TcMAC21 and euploid mice (Fig. S1). Serum level of thyroxine (T_4), the precursor of T_3, were modestly elevated in TcMAC21 relative to euploid mice.

In accordance with the lean phenotype, TcMAC21 mice had significantly smaller adipocyte cell size in both subcutaneous (inguinal) and visceral (gonadal) fat depots (Fig. 2F-G), as well as significantly reduced fat accumulation in liver (Fig. 2H). Fasting triglyceride, non-esterified fatty acid (NEFA), and β-hydroxybutyrate levels were not different between genotypes; fasting cholesterol, however, was higher in TcMAC21 mice (Fig. 2I). Although fasting insulin levels were not different between groups, fasting blood glucose was significantly lower in TcMAC21 mice (Fig. 2J). The insulin resistance index (HOMA-IR), along with glucose and insulin tolerance tests suggested modest improvements in insulin sensitivity in TcMAC21 relative to euploid mice (Fig. 2K-M). Assessment of the pancreas showed that TcMAC21 mice have similar β-islet cross-sectional area (CSA), insulin and somatostatin content, and insulin granule and vesicle size compared to euploid controls (Fig. 2N-P). Taken together, these data indicate that chow-fed TcMAC21 mice at baseline are lean despite increased caloric intake, and this is largely due to elevated physical activity and energy expenditure.

MAC21 mice are resistant to diet-induced obesity and metabolic dysfunction

The hypermetabolic phenotypes seen in chow-fed TcMAC21 predicted that these mice would be resistant to diet-induced obesity and metabolic dysfunction. Indeed, after 8 weeks on high-fat diet (HFD), TcMAC21 mice gained only ~3 g of body weight, whereas the euploid controls gained >15 g of body weight over the same period. Consequently, TcMAC21 mice weighed ~50% less than euploid controls (Fig. 3A). Consistent with the lean phenotype, the absolute and relative (normalized to body weight) fat mass were markedly reduced compared to euploid controls (Fig. 3B). The weights of other organs (liver, kidney, BAT) at time of termination were also lower in TcMAC21 mice, but tibia length was not different between genotypes (Fig. S3 and Table S3). Complete blood count revealed no differences in erythroid, lymphoid, and myeloid cell numbers between genotypes (Table S4). Because relative lean mass was higher in TcMAC21 compared to euploid mice (Fig. 3B), the lean phenotype seen in HFD-fed TcMAC21 is largely due to reduced adiposity. Accordingly, TcMAC21 had significantly smaller adipocyte cell size in both subcutaneous (inguinal) and visceral (gonadal) fat depots, and a marked reduction in lipid accumulation in the liver (Fig. 3C-E).

Although fasting serum triglyceride, NEFA, and β-hydroxybutyrate levels were not different between genotypes, serum cholesterol was significantly lower in TcMAC21 mice (Fig. 3F). Fasting glucose and insulin levels, and the insulin resistance index (HOMA-IR), were markedly lower in TcMAC21 mice relative to euploid controls (Fig. 3G-H), indicative of enhanced insulin sensitivity. In glucose tolerance tests (GTT), even though the rate of glucose disposal was similar between TcMAC21 and euploid mice, the amount of serum insulin present during GTT (time 0, 15, and 30 min) was dramatically lower in TcMAC21 (Fig. 3I-J). This indicates that a substantially lower amount of insulin is sufficient to promote glucose clearance in TcMAC21 at a rate comparable to euploid mice, consistent with elevated insulin sensitivity in the peripheral tissues. Indeed, when we directly assessed insulin action via insulin tolerance tests (ITT), TcMAC21 mice clearly exhibited higher insulin sensitivity as indicated by the significant differences in insulin-stimulated glucose disposal (Fig. 3K).

To independently confirm TcMAC21 mice are more insulin sensitive, we fasted the mice overnight (16 hr) then reintroduced them to food. Under this fasting-refeeding condition, we could clearly see the resumption of food intake was successful at increasing blood glucose in TcMAC21 (Fig. 3L); however, the insulin response to food intake in TcMAC21 mice was strikingly smaller in magnitude compared to euploid controls (Fig. 3M). Again, these data indicate that TcMAC21 mice are significantly more insulin sensitive since a substantially lower insulin response during fasting-refeeding is sufficient for glucose clearance at a rate comparable to euploid mice.

These results prompted us to determine if there were developmental changes in the pancreas leading to reduced insulin secretion in response to glucose administration or food intake, independent of elevated insulin sensitivity in peripheral tissues. Quantification of β-islet size, pancreatic insulin and somatostatin content, as well as insulin granule and vesicle size did not reveal any intrinsic differences between TcMAC21 and euploid mice (Fig. 3N-Q), thus ruling out a developmental cause and arguing in favor of enhanced insulin action. Pancreatic acinar zymogen granule size was also not different between genotypes (Fig. S4), suggesting normal development of the exocrine pancreas. Taken together, these data indicate that TcMAC21 mice are remarkably resistant to HFD-induced obesity and insulin resistance.

Hypermetabolism of TcMAC21 mice is uncoupled from changes in adipose and liver transcriptomes

Next, we sought to uncover the physiological mechanisms responsible for TcMAC21 resistance to weight gain and developing insulin resistance when fed a high-fat diet. First, we wanted to rule out whether there is a change in caloric intake. TcMAC21 mice actually consumed a significantly higher amount of food

(relative to their body weight) compared to euploid controls (Fig. 4A and Table S5). To rule out any potential dysfunction of the gut that might adversely affect nutrient absorption, we collected, counted, weighed, and subjected fecal samples of each mouse to fecal bomb calorimetry. Neither fecal frequency, average fecal pellet weight, nor fecal energy content was different between TcMAC21 and euploid mice (Fig. 4B and Fig. S5). Fecal energy content trended lower in TcMAC21 (Fig. 4B), implying a modest increase in the efficiency of nutrient absorption. Since energy input (caloric intake per gram body weight) was significantly higher in TcMAC21 and outputs (left over fecal energy) were similar across genotypes, the data strongly support hypermetabolism being the cause of the lean phenotype seen in TcMAC21 mice. Indeed, when we measured energy expenditure (EE) and physical activity of both groups, we found that TcMAC21 mice have markedly higher EE and physical activity irrespective of circadian cycle and metabolic states (Fig. 4C-D and Fig. S6 and Table S5). The striking difference in EE was very similar to TcMAC21 fed a standard chow (Fig. 2D), but to an even greater extent when mice were fed a high-fat diet, presumably due to the greater availability of calorie-dense lipid substrates for oxidation.

Because TcMAC21 mice burned a large excess of energy, we measured the circulating levels of thyroid hormones as they are known to increase metabolic rate and energy expenditure (20). Both serum T_3 (the active form) and T_4 (precursor of T_3) levels were significantly higher in TcMAC21 relative to euploid mice (Fig. 4E). T_3 hormone, however, was not elevated in HFD-fed mice housed at thermoneutrality (30°C) (Fig. S1). If energy expenditure was elevated, body temperature of TcMAC21 mice would likely increase. Indeed, deep colon temperatures of TcMAC21 were elevated, most notably in the dark cycle when mice are active (Fig. 4F). Assessment with thermal imaging showed an elevated skin temperature around the interscapular region of TcMAC21 mice, whereas the tail skin temperature was not different between groups (Fig. 4F-G). Importantly, the differences in interscapular skin temperatures persisted in TcMAC21 even when compared to weight-matched wild-type mice (Fig. 4H-I), thus ruling out body weight (and hence surface area/volume ratio) as the cause of greater heat generation to

compensate for greater heat loss. Elevated body temperature, however, was not observed in chow-fed mice (Fig. S7), even though chow-fed TcMAC21 were also hyperactive and had higher energy expenditure.

Consistent with the thermal imaging data, histological analysis of the interscapular brown adipose tissue (BAT) revealed a marked reduction in fat accumulation and a "healthy" brown appearance in TcMAC21 mice when compared to euploid controls (Fig. 4J-K), presumably due to excess lipids being utilized. We therefore expected several key metabolic genes in BAT to be upregulated in TcMAC21. Surprisingly, we found minimal differences in key thermogenic and fat oxidation genes between the two groups of mice (Fig. 4L and Fig. S8). This led us to assume the differences in gene expression must be due to non-canonical and potentially novel pathways. To test this, we conducted an unbiased RNA-sequencing analysis of BAT, liver, gWAT, and iWAT. Again, to our surprise and contrary to expectation, we found the transcriptomes of BAT, liver, gWAT, and iWAT in TcMAC21 to be remarkably similar to euploid controls (Fig. 4M).

There was not a single tissue that had more than 0.3% of its transcriptome significantly altered (Fig. 4N and Table S6-S9). None of the significant changes in gene expression—small in number—could readily account for the striking differences in phenotypes between TcMAC21 and euploid mice. Corroborating the RNA-seq results, quantitative real-time PCR analyses of select metabolic genes in BAT, liver, gWAT, and iWAT also showed minimal changes in TcMAC21 regardless of diet (chow or HFD) and temperature (22°C or 30°) (Fig. S8-12). Together, these data indicate that TcMAC21 mice are hyperactive and hypermetabolic with elevated thermogenesis, but these phenotypes are largely uncoupled from transcriptomic changes in BAT, liver, gWAT, and iWAT.

Sarcolipin overexpression in skeletal muscle drives TcMAC21 hypermetabolism

Given the remarkable differences seen in body weight, adiposity, tissue histology and lipid contents, insulin sensitivity, body temperature, physical activity and metabolic rate between TcMAC21 and euploid mice, we were surprised by how few changes in transcriptomes—both in number and magnitude—were occurring in BAT, liver, and two major white adipose depots. This prompted us to examine the transcriptome of skeletal muscle, by far the largest metabolically active tissue that can substantially contribute to overall energy expenditure. RNA-sequencing of TcMAC21 skeletal muscle (gastrocnemius) revealed it to be the most transcriptionally dynamic tissue, with 4.2% of the transcriptome changed relative to euploid controls (Fig. 5A). Within the skeletal muscle of TcMAC21, there were 432 up-regulated genes and 501 down-regulated genes (Fig. S13 and Table S10). Gene ontology analysis of the differentially expressed genes highlighted up-regulated pathways related to thermogenesis, mitochondrial activity, and amino acid metabolism; and down-regulated pathways related to TGF-β, insulin, growth hormone, calcium, adrenergic, serine/threonine kinase, and cGMP-PKG signaling pathways (Fig. 5B).

To further confirm the RNA-sequencing results, we performed qPCR on a number of key genes related to skeletal muscle metabolism, fast- and slow-twitch fiber-types, futile-cycling, thyroid hormone action, and general calcium handling (Fig. 5C and Fig. S14). While a few of the genes were significantly different in expression, the most notable upregulated gene with the biggest magnitude of change was *Sln*, encoding the 31 amino acid single-pass membrane protein, sarcolipin (SLN). SLN is a regulator and an uncoupler of the sarco(endo)plasmic reticulum calcium ATPase (SERCA) (21, 22). Under normal circumstances, SERCA uses the energy derived from ATP hydrolysis to transport calcium from the cytosol back into the sarcoplasmic reticulum (SR) (23). When SLN binds to SERCA, it uncouples ATP hydrolysis from calcium transport into the SR (24); this results in futile SERCA pump activity, ATP hydrolysis, and heat generation (Fig. 5D) (22, 25, 26). In addition, increased cytosolic calcium transients

(due to less being transported into the SR) promotes calcium entry into mitochondria and activates mitochondrial respiration, as well as, calcium-dependent signaling that enhances oxidative metabolism in skeletal muscle (27, 28).

Interestingly, regardless of diet (chow or HFD) and temperature (22°C or 30°C), TcMAC21 mice consistently had ~20-30 fold upregulated *Sln* expression (Fig. 5E). The expression of other calcium handling genes—phospholamban (*Pln*), calmodulin (*Calm2*), SERCA1a (*Atp2a1*), SERCA2a (*Atp2a2*)—were not significantly different between TcMAC21 and euploid mice. Likewise, overexpressing SLN in skeletal muscle of transgenic mice also did not alter SERCA expression (29). The *Sln* gene is known to be upregulated in skeletal muscle by cold exposure (30-32). In contrast, the markedly upregulated *Sln* expression seen in TcMAC21 mice housed at ambient temperature (22°C) remained high even when the animals were housed at thermoneutrality (30°C). Consistent with the mRNA data, SLN protein levels were also strikingly upregulated in TcMAC21 skeletal muscle (gastrocnemius) (Fig. 5F-G). Immunofluorescence also indicated substantially more SLN positive muscle fibers in TcMAC21 mice (Fig. 5H-I). We included skeletal muscle lysate from SLN over-expression (OE) transgenic mouse (28) as our positive control. While the transgenic mouse had ~2.5 fold higher level of SLN compared to controls, the SLN protein levels in TcMAC21 were ~4.5 fold higher than the euploid mice (Fig. 5G). It is known that *Sln* can be induced in skeletal muscle as a compensatory response to muscle atrophy, dystrophy, and injury (33). However, none of the genes involved in muscle repair, wasting, and atrophy were significantly upregulated (Table S12), suggesting that *Sln* overexpression is not due to structural or functional deficit of the skeletal muscle in TcMAC21 mice. Collectively, our data suggest that a mechanism exists that can achieve upregulation of endogenous mouse SLN at a level substantially higher than that seen in artificially overexpressed transgenic mice under non-pathological condition.

Quantification of histological sections revealed that the average gastrocnemius muscle fiber cross-sectional area (CSA) in TcMAC21 was significantly smaller compared to euploid mice (Fig. 5J and Fig. S15). This suggests a shift from being a predominantly glycolytic muscle to a more oxidative muscle, as a smaller muscle fiber cross-sectional area is associated with a more oxidative muscle phenotype (34). In accordance, protein levels of mitochondrial complex I-V were significantly higher in TcMAC21 gastrocnemius muscle compared to euploid controls (Fig. 5K-L). Corroborating the Western blot data, immunofluorescence also showed substantially higher succinate dehydrogenase (SDHB) staining (marker of oxidative capacity) in gastrocnemius muscle of TcMAC21 mice (Fig. 5M-N).

To determine if TcMAC21 mice have higher mitochondrial activity compared to euploid controls, we conducted mitochondrial respiration analyses in liver, BAT, iWAT, gWAT, and different muscle types (quadriceps, extensor digitorum longus, gastrocnemius, plantaris, soleus, tongue, and heart). Except soleus and heart, most muscle types from TcMAC21 fed either chow or HFD—regardless of whether they were predominantly slow-twitch (oxidative), fast-twitch (glycolytic), or mixed—showed significantly elevated oxygen consumption due to elevated mitochondrial respiration (Fig. 4O-Q and Fig. S16-20). Enhanced mitochondrial complex I, II, and IV activities were more pronounced in glycolytic muscle tissues, suggesting that these normally glycolytic muscle fibers may assume a more oxidative phenotype in TcMAC21 mice. The greater oxidative phenotype in glycolytic muscle tissues was not due to changes in fiber type composition, as none of the fiber type-specific transcripts were different between genotypes (Fig. 5C). These data are consistent with similar results reported for skeletal muscle-specific SLN overexpression mice (27-29).

In contrast to muscle, mitochondrial activities of complex I and II in interscapular BAT was largely unchanged in TcMAC21 (Fig. 5Q and Fig. S18), despite the pronounced differences in BAT histology and lipid content between TcMAC21 and euploid mice (Fig. 4J-K). In chow-fed mice, however,

mitochondrial complex IV activity was higher in BAT of TcMAC21. In subcutaneous (inguinal) white adipose tissue, mitochondrial respiration was significantly reduced in chow-fed TcMAC21 mice but unchanged in HFD-fed mice (Fig. S21). In visceral (gonadal) white adipose tissue, mitochondrial respiration was also largely unchanged in either chow or HFD-fed TcMAC21 mice (Fig. S21). Unexpectedly and in striking contrast to muscle and BAT, mitochondrial complex I, II, IV activity was markedly reduced in the liver and heart of both chow- and HFD-fed TcMAC21 compared to euploid mice (Fig. 5Q and Fig. S19-20), despite the liver of TcMAC21 mice being significantly "healthier" with much reduced lipid accumulation (Fig. 2H and 3E).

All together, these data suggest that SLN-mediated futile SERCA activity in skeletal muscle is likely the dominant driver underlying the hypermetabolism phenotypes seen in TcMAC21 mice. Because the futile SERCA pump activity consumes ATP to generate heat without transporting calcium into SR (22, 24, 26, 35, 36), this creates a huge energy demand and markedly drives up the activity of mitochondrial respiration to supply the ATP needed for the futile cycling of Ca^{2+}. Presumably, this dominant effect results in systemic channeling of metabolic substrates (e.g., lipids) into skeletal muscle to fuel the elevated mitochondrial respiration rate. This in turn leads to secondary improvements and protection—reduced fat accumulation and smaller adipocyte—we observed in liver, BAT, gWAT, and iWAT despite minimal changes in the transcriptomes of these tissues.

Potential regulators of sarcolipin expression in skeletal muscle

Having established that SLN-mediated futile SERCA activity underlies hypermetabolism in TcMAC21 mice, we next asked what regulator(s) promote the upregulation of endogenous SLN, as little is known about what controls its expression in skeletal muscle. We took advantage of the observation that SLN overexpression appears to be locked in the "on" position in skeletal muscle and could not be

downregulated to control levels at thermoneutrality (Fig. 5E). Thyroid hormone (T_3) is likely not the driver of SLN overexpression since serum T_3 was not different between TcMAC21 and euploid housed at thermoneutrality (Fig. S1); in addition, SLN was shown to be upregulated in hypothyroid mice compared to euthyroid controls (37). When housed at thermoneutrality (30°C), TcMAC21 mice maintained their lean phenotypes with lower fasting insulin levels and elevated metabolic rate and energy expenditure despite higher caloric intake (Fig. 6A-E). Accordingly, TcMAC21 mice housed at thermoneutrality had smaller adipocyte cell size and lower lipid contents in BAT and liver (Fig. S22). Tissue collection at termination of the study also showed significantly smaller fat mass and reduced BAT and liver weight in TcMAC21 mice (Table S13).

From these data we surmised that the regulator(s) of SLN would likewise remain unchanged (i.e., continued to be up- or down-regulated) at thermoneutrality. We therefore performed RNA-sequencing on skeletal muscle isolated from HFD-fed TcMAC21 housed at thermoneutrality. RNA-seq data showed a total of 113 differentially expressed genes (DEGs) in the skeletal muscle of TcMAC21 mice, with 59 being up-regulated and 54 being down-regulated (Fig. 6F and Table S14). Of the 59 up-regulated genes, 56 were protein coding (PCGs) and 3 were non-protein coding (NPCGs); the down-regulated group had 51 PCGs and 3 NPCGs. Next, we compared the skeletal muscle transcriptomes of euploid vs TcMAC21 mice housed at 22°C with the transcriptomes of euploid vs TcMAC21 mice housed at 30°C. This tells us which genes are differentially expressed by TcMAC21 mice relative to euploid controls at both temperatures. There were 848 genes differentially expressed by only TcMAC21 mice housed at 22°C. This includes 392 up-regulated (299 PCGs and 93 NPCGs) and 456 down-regulated (386 PCGs and 70 NPCGs) genes (Fig. 6G). There were 31 genes differentially expressed by only TcMAC21 mice housed at 30°C, with 22 up-regulated (19 PCGs and 3 NPCGs) and 9 down-regulated (7 PCGs and 2 NPCGs) genes. Notably, there were 81 genes differentially expressed by TcMAC21 at both temperatures, with 37 up-regulated (all PCGs) and 44 down-regulated (43 PCGs and 1 NPCG) genes.

To further narrow our candidate *Sln* regulators, we directly compared the expression of mouse genes in the skeletal muscle of TcMAC21 mice housed at 22°C and 30°C. Because *Sln* expression was similarly upregulated in the skeletal muscle of TcMAC21 mice housed at 22°C and 30°C, we presumed the regulator(s) of *Sln* would also display minimal variation across both temperatures. We therefore focused on genes that remained unchanged at 22°C and 30°C in TcMAC21 skeletal muscle. We first filtered out all genes above or below Log2(FC) of 0.5 or -0.5, which left us with 3754 transcripts whose expression remained relatively unchanged at both temperatures. We next sorted the data by *P*-value, then compared the entire list of unchanged transcripts to the list of shared DEGs shown in Fig. 6G, and found that only 5 genes were present in both (Fig. 6H). This list contains one up-regulated gene (A930018M24Rik) and four down-regulated PCGs (*Csde1*, *Kmt5a*, *Vasp*, and *Calm1*). Again, these are the genes that are differentially expressed by TcMAC21 mice housed at 22°C and 30°C as compared to euploid, which remain unchanged in TcMAC21 mice across temperature. Thus, these are potential *Sln* regulators that are encoded in the mouse genome.

Alternatively, the regulator(s) of *Sln* expression could be one or more Hsa21-drived human genes. There was a total of 106 human transcripts expressed by TcMAC21 mice housed at 22°C and 30°C, with 94 PCGs and 12 are NPCGs (Fig. 6I). There were 4 human PCGs only expressed in TcMAC21 mice housed at 30°C and 83 human genes whose expression was turned off at 30°C. Interestingly, a majority (75 out of 83) of the human genes that were turned off at 30°C are NPCGs. The human genes that we postulated as most likely to regulate *Sln* expression would be those that change the least at 22°C and 30°C. We first calculated the difference in Log2(FC) values of all human genes expressed at 22°C and 30°C in TcMAC21 skeletal muscle [i.e., Log2(FC at 22°C) - Log2(FC at 30°C)]. Those values closest to zero represent genes with the most consistent expression across both housing temperatures. Genes with a negative Log2(FC) difference are expressed at higher levels at 30°C, and genes with a positive Log2(FC) difference are expressed at higher levels at 22°C. The ~20 genes with the closest-to-zero Log2(FC) difference are listed in yellow (Fig. 6J), and these would be considered potential regulators of *Sln* derived

from Hsa21. Altogether, our analysis has yielded a defined number of potential *Sln* regulators, from the mouse or human genome, that can be experimentally tested (either singly or in combination) in follow-up studies.

DISCUSSION

While assessing the systemic metabolic impact of cross-species aneuploidy (a human chromosome in mice), we made several striking and unexpected discoveries. Given that TcMAC21 mice recapitulate multiple features of human trisomy 21 — most notably structural and functional neurological deficits and craniofacial skeletal alterations (18) and also a small body size compared to their euploid littermates —we initially expected the animals to show metabolic changes such as obesity and glucose intolerance reminiscent of the DS population (7) or the metabolic dysregulation (e.g., insulin resistance and dyslipidemia) seen in the Ts65Dn Down syndrome mouse model (11). Instead, the TcMAC21 mice display hallmarks of hypermetabolism. They are lean despite greater caloric intake, and have markedly elevated oxidative metabolic rate as indicated by increased VO_2, energy expenditure, mitochondrial respiration in skeletal muscle, and by a shift to more a oxidative phenotype in skeletal muscle.

Although the higher prevalence of obesity and diabetes is well documented in the DS population (7), the mechanism of how gene dosage imbalance causes metabolic dysregulation *in vivo* is largely unknown and limited to only a few studies (10, 38). Until our recent study (11), the scope of the previous metabolic studies using DS mouse models was limited. Our present study represents one of the most comprehensive metabolic analyses carried out in DS mouse models to date. To our surprise, TcMAC21 phenotypes appear to be the opposite of what is seen in DS. We can speculate on possible reasons for this: 1) The strong and dominant physiological effects of *Sln* overexpression in the skeletal muscle of TcMAC21 override and mask potential deleterious effects of high-fat feeding seen in the euploid controls;

2) The unexpected phenotypes of TcMAC21 could be the result of complex interactions between human genes and the mouse genome that we do not fully understand. Further, the human proteins may alter the stoichiometric compositions of multi-protein complexes in an unpredictable way. For this reason, and for comparison, it is imperative to carry out similar comprehensive metabolic studies in other established DS mouse models (e.g., Dp(16)1Yey/+ and Ts66Yah) where all the trisomic genes are derived from the mouse instead of human, and also without extra trisomic genes not found in Hsa21 (39, 40). It is possible the trisomic mouse orthologs of Hsa21 genes are over-expressed and interact with the rest of the mouse genome in a manner that more closely reflects what might be seen in the adipose tissue, liver, and skeletal muscle of DS. This is an important issue to resolve in terms of selecting appropriate DS mouse models to best reflect the metabolic phenotypes seen in DS.

What could be the mechanism underlying the striking metabolic phenoytpes of TcMAC21? The key driver of hypermetabolism appears to be SLN overexpression in the skeletal muscle of TcMAC21 mice, leading to persistent uncoupling of the SERCA pumps, heat generation, and energy dissipation. This mechanism could explain multiple unexpected observations: despite a marked reduction in lipid accumulation in the liver, BAT, and WAT, surprisingly few changes were seen in the transcriptomes of these tissues, and none could account for the striking tissue histology. Importantly, none of the key genes (e.g., *Ucp1* in BAT and browning/beiging genes in iWAT) involved in thermogenesis and lipid metabolism were significantly different between TcMAC21 and euploid mice, and yet the mice had elevated deep colon temperature. While the metabolic activity (i.e., mitochondrial respiration) of BAT was largely unchanged, complex I, II, and IV activity in the liver were surprisingly downregulated. Mitochondrial respiration was either downregulated or unchanged in iWAT and gWAT. All these striking phenotypes could be explained by metabolic substrates (e.g., lipid) channeling away from liver, BAT, and WAT, and into skeletal muscle to fuel elevated mitochondrial respiration, as this was needed to meet the high ATP demand created by futile SERCA pump activity.

We largely ruled out the involvement of thyroid hormones in promoting hypermetabolism in TcMAC21 mice. Under the basal state when mice were fed a standard chow, or HFD-fed mice housed at thermoneutrality, circulating T_3 levels were not different between groups despite the hyperactivity and hypermetabolism of TcMAC21 mice. Although serum T_3 levels were elevated in HFD-fed TcMAC21 housed at room temperature (22°C), the predicted T_3 effects were largely absent. It is known that T_3 negatively regulates the expression of SLN, as hypothyroidic mice have significantly upregulated SLN mRNA and protein in skeletal muscle compared to euthyroid mice (37). Instead of the expected downregulation, SLN expression was dramatically elevated in the skeletal muscle of TcMAC21 mice. Through its nuclear hormone receptor, T_3 regulates many metabolic genes in adipose tissue, liver, and skeletal muscle (20), and yet none of the well-known T_3-regulated genes were upregulated in these tissues despite elevated T_3 levels. In addition, T_3 is a potent inducer of *Ucp1* expression in BAT (41) and white adipose tissue beiging (42), but *Ucp1* transcript levels were not upregulated in BAT or the white adipose tissue of TcMAC21 mice. This apparent T_3 resistance in HFD-fed TcMAC21 mice is likely a compensatory response to an already elevated body temperature and the hypermetabolism induced by SLN-mediated futile SERCA activity and heat generation in skeletal muscle. If T_3 further increased the metabolic rate of TcMAC21 mice, this would likely overtax the heat dissipation mechanism leading to hyperthermia and possible death.

By collapsing the proton motive force within the intermembrane space of mitochondria, UCP1-mediated mitochondrial uncoupling in BAT could raise body temperature and enhance energy expenditure (43). Although thermal imaging highlighted increased skin temperature around the interscapular BAT region of TcMAC21 mice, the thermal signal could be produced by local muscle around the interscapular area. Our gene expression, BAT transcriptomics, and functional data, however, do not support UCP1-mediated uncoupling in BAT as a probable mechanism for the hypermetabolism and elevated thermogenesis seen in TcMAC21 mice. Neither the expression of *Ucp1* nor mitochondrial activity was consistently elevated in the BAT of TcMAC21 mice fed chow or HFD. Housing mice at a

thermoneutral temperature would suppress BAT activity and beigeing in iWAT (44), yet TcMAC21 mice housed at thermoneutrality for an extended period (>2 months) retained elevated energy expenditure and lean body weight comparable to TcMAC21 mice housed at 22°C. Together, these data argue against BAT being a significant contributor to the thermogenesis seen in TcMAC21 mice.

Recent studies have also shown that creatine-driven futile substrate cycling and SERCA2b-mediated calcium cycling in beige fat can promote energy expenditure and thermogenesis (45, 46). Regardless of housing temperatures, none of the genes involved in creatine/phosphocreatine futile cycle (e.g, *Slc6a8*, *Gatm*, *Gamt*, *Ckmt1*, *Ckmt2*) or the SERCA2b-RyR2 pathway (*Atp2a2*, *Ryr2*) were upregulated in iWAT, suggesting that these pathways are likely not involved in the hypermetabolic phenotypes of TcMAC21. Promoting metabolic inefficiency in skeletal muscle by UCP1 or UCP3 overexpression can increase metabolic rate and prevent diet-induced obesity (47-49). In the skeletal muscle of TcMAC21 mice, *Ucp1* and *Ucp3* transcripts were not upregulated, suggesting that mitochondrial uncoupling by UCP1 or UCP3 is also unlikely to contribute to the observed lean and hypermetabolic phenotypes.

SLN plays a role in modulating body weight by promoting energy expenditure through its effects on the SERCA pump (25, 28, 50, 51). Binding of SLN to SERCA does not interfere with ATP hydrolysis of the pump, but reduces calcium transport into SR lumen through a calcium “slippage” mechanism (22, 26, 35, 36). Thus, SLN promotes futile cycling of the SERCA pumps, ATP hydrolysis, and heat generation. Consistent with this model, mice lacking SLN are cold intolerant and gain more weight on an HFD due to reduced energy expenditure (25, 50, 51); conversely, transgenic overexpression of SLN in skeletal muscle promotes a lean phenotype (28).

Under normal situations, SLN is mainly expressed in slow-twitch oxidative muscle tissues such as the soleus and diaphragm, with little expression in fast-twitch glycolytic muscle tissues such as the

gastrocnemius and quadriceps (52). In the case of hypothyroid mice, endogenous SLN is only markedly upregulated in oxidative muscle fibers (soleus and diaphragm) but not the large glycolytic muscle tissues (37). It has been argued that in rodents the futile SERCA activity and energy expenditure occurring in soleus and diaphragm (both are small in size) is quantitatively insufficient to effect significant changes in body weight (53). Notwithstanding the artificial overexpression of SLN in both fast-twitch glycolytic and slow-twitch oxidative muscle fibers (28), it is unclear whether endogenous SLN can be substantially induced in large glycolytic muscle tissues such as the gastrocnemius and quadriceps under non-pathological conditions. Our data helps to resolve this issue. In TcMAC21 mice, endogenous SLN is markedly upregulated in a largely glycolytic muscle (gastrocnemius), suggesting that a mechanism indeed exists that can substantially elevate SLN transcript and protein in muscle fiber types that normally have low expression. Corroborating this is the observation that mitochondrial respiration is significantly elevated in most muscle types—gastrocnemius (fast-twitch), quadriceps (fast-twitch), plantaris (mixed), and extensor digitorum longus (mixed).

The huge ATP demand created by the futile SERCA pump activity appears to be the cause of upregulated protein expression of complex I-IV, elevated mitochondrial respiration, and the assumption of an oxidative phenotype in muscle tissues that are normally glycolytic. This reprogramming of glycolytic muscle tissues into an oxidative phenotype is likely due to elevated cytosolic calcium transients (as less calcium is being transported into the SR due to uncoupling of the SERCA pumps), leading to calcium-dependent activation of mitochondrial respiration and calcium-dependent signaling that drives increased production of OXPHOS proteins (27, 28, 54-57). Since skeletal muscle makes up ~40% of the body's weight and is a major energy consuming tissue (58, 59), elevated energy expenditure via futile SERCA pump activity—especially the big muscles (gastrocnemius and quadriceps)—will have substantial impact on total energy balance and body weight. As an added benefit, increased fuel consumption for non-shivering thermogenesis driven by the futile SERCA pump would channel lipid substrates into skeletal muscle for oxidation and prevent excess lipid accumulation in liver, BAT, and

white adipose tissue, thus conferring an overall healthy metabolic profile with preserved systemic insulin sensitivity.

Although TcMAC21 mice also have increased voluntary physical activity, our data suggest that futile SERCA activity in skeletal muscle is the main driver of the hypermetabolic phenotype. Overexpression of SLN in skeletal muscle does not significantly alter voluntary physical activity at ambient room temperature or at thermoneutrality, yet the SLN transgenic mice consistently gained significantly less weight in response to high-fat feeding (28, 50). Further, SLN appears to be required for effective adiposity reduction in HFD-fed mice with access to a running wheel (60). Elevated locomotor activity in TcMAC21 mice, however, would likely amplify the effect of sarcolipin-mediated uncoupling of the SERCA pumps, as muscle movement results in greater SR Ca^{2+} cycling. In cultured myotubes, caffeine-induced release of Ca^{2+} from the SR via the ryanodine receptor/channel (RYR1) would only activate calcium-dependent signaling in the presence, but not absence, of SLN; conversely, inhibiting Ca^{2+} release through RYR1 using dantrolene blocks calcium-dependent signaling only in SLN-expressing, but not SLN-deficient, myotubes (27). Thus, increased SR Ca^{2+} cycling due to elevated physical activity would promote energy expenditure and also create a favorable cellular context to amplify the effects of sarcolipin overexpression on uncoupling of the SERCA pumps. Accordingly, energy expenditure and the degree of leanness seen in TcMAC21 mice are significantly greater in magnitude than the SLN transgenic mice.

To fully harness SLN-mediated futile SERCA activity for energy dissipation and weight loss requires an understanding of how endogenous SLN expression is regulated, but the mechanism of which remains largely unknown. TcMAC21 mice offer critical insights into the switches that control SLN expression in skeletal muscle. Regardless of temperatures (ambient or thermoneutral), elevated *Sln* expression in TcMAC21 appeared to be in the “on” position and could not be turned off. We exploited this information to zoom in on a defined set of mouse and Hsa21-derived transcripts—some of which are

transcription factors (e.g., *PKNOX1*, *ETS2*), RNA binding proteins (e.g., *Csde1*), and epigenetic regulators (e.g., *Kmt5a*)—that remain significantly up- or down-regulated in skeletal muscle at both 22°C and 30°C, and show <1% variability across the two temperatures. We presume that one or more of these genes could potentially be the sought after "switches" of *Sln* expression. Additional studies are needed to identify such critical on/off switches. A recent study has suggested that the C-terminal cleavage fragment of TUG can upregulate *Sln* expression in the skeletal muscle when it enters the nucleus and forms a complex with PPAR-γ and PGC-1α (61). However, this pathway is largely abrogated in mice fed an HFD; thus, we think this transcriptional mechanism is likely not involved in upregulating *Sln* expression in TcMAC21 mice fed an HFD.

Weight loss can be achieved by reducing caloric intake or promoting energy expenditure, and the latter can be physiologically accomplished by increasing physical activity (e.g., exercise) or through shivering and non-shivering thermogenesis (43, 62). SLN-mediated non-shivering thermogenesis offers an attractive approach for promoting energy expenditure and weight loss: Expression of SLN is restricted to the striated muscle of all mammals, including humans (63-66). Compared to BAT (~1.5% of body weight in young men) (67), the total mass of skeletal muscle (~40% of body weight) makes futile SERCA activity in this large tissue especially effective in energy dissipation (68). Importantly, overexpression of SLN in skeletal muscle does not appear to have adverse effects; rather, SLN transgenic mice have higher endurance capacity and improved muscle performance due to enhanced oxidative capacity (29). In summary, our work provides further proof-of-concept that endogenous SLN-mediated uncoupling of SERCA pumps to enhance energy expenditure can potentially be harnessed for systemic metabolic health.

MATERIALS AND METHODS

Mouse model

The transchromosomic TcMAC21 (simply referred to as MAC21) mice carrying a near complete human chromosome 21were generated and genotyped as previously described (18). Because MAC21 male mice are infertile, all the female mice were used for breeding. Hence, metabolic analyses were conducted on male mice only. MAC21 mice were initially maintained on an outbred background (ICR strain mice). After crossing for eight generations onto BDF1 (C57BL/6J (B6) x DBA/2J (D2)), MAC21 were transferred to the Riken Animal Resource (BRC No. RBRC05796 and STOCK Tc (HSA21q-MAC1)). Characterizations of MAC21 were performed on mice (75% B6/25% D2 on average) produced by crossing B6 males with trisomic B6D2 females (18). Euploid littermates were used as controls throughout the studies.

Mice were fed a standard chow (Envigo; 2018SX) or high-fat diet (HFD; 60% kcal derived from fat, #D12492, Research Diets, New Brunswick, NJ). Mice were housed in polycarbonate cages on a 12h:12h light-dark photocycle with ad libitum access to water and food. Standard chow was provided for 8 weeks, beginning at 12 weeks of age; HFD was provided for 16 weeks, beginning at 5 months of age. At termination of the study, all mice were fasted for 2 h and euthanized. Tissues were collected, snap-frozen in liquid nitrogen, and kept at 80°C until analysis.

For thermoneutral studies, mice were housed in a temperature regulated (ambient temp. maintained at 30 ± 1°C) animal facility at Johns Hopkins University School of Medicine. Mice were acclimatized for two full weeks prior to experimentation. All experimental procedures conducted on these mice (i.e., glucose and insulin tolerance tests, fasting-refeeding blood collections, tissue dissections, etc.) were completed within the 30°C housing unit to prevent temperature fluctuation.

All mouse protocols were approved by the Institutional Animal Care and Use Committee of the Johns Hopkins University School of Medicine (animal protocol # MO19M481). All animal experiments

were conducted in accordance with the National Institute of Health guidelines and followed the standards established by the Animal Welfare Acts.

Body composition analysis

Body composition analyses for total fat and lean mass, and water content were determined using a quantitative magnetic resonance instrument (Echo-MRI-100, Echo Medical Systems, Waco, TX) at the Mouse Phenotyping Core facility at Johns Hopkins University School of Medicine.

Complete blood count analysis

A complete blood count on blood samples was performed at the Pathology Phenotyping Core at Johns Hopkins University School of Medicine. Tail vein blood was collected using EDTA-coated blood collection tubes (Sarstedt, Nümbrecht, Germany) and analyzed using Procyte Dx analyzer (IDEXX Laboratories, Westbrook, ME).

Indirect calorimetry

Chow or HFD-fed MAC21 male mice and euploid littermates were used for simultaneous assessments of daily body weight change, food intake (corrected for spillage), physical activity, and whole-body metabolic profile in an open flow indirect calorimeter (Comprehensive Laboratory Animal Monitoring System, CLAMS; Columbus Instruments, Columbus, OH) as previously described (69). In brief, data were collected for three days to confirm mice were acclimatized to the calorimetry chambers (indicated by stable body weights, food intakes, and diurnal metabolic patterns), and data were analyzed from the subsequent three days. Mice were observed with ad libitum access to food, throughout the fasting process, and in response to refeeding. Rates of oxygen consumption ($\dot{V}_{O2}$; $mL \cdot kg^{-1} \cdot h^{-1}$) and carbon dioxide production ($\dot{V}_{CO2}$; $mL \cdot kg^{-1} \cdot h^{-1}$) in each chamber were measured every 24 min. Respiratory exchange ratio ($RER = \dot{V}_{CO2}/\dot{V}_{O2}$) was calculated by CLAMS software (version 4.93) to estimate relative oxidation of

carbohydrates (RER = 1.0) versus fats (RER = 0.7), not accounting for protein oxidation. Energy expenditure (EE) was calculated as EE= $\dot{V}_{O2}$× [3.815 + (1.232 × RER)] and normalized to lean mass. Physical activities (total and ambulatory) were measured by infrared beam breaks in the metabolic chamber. Average metabolic values were calculated per subject and averaged across subjects for statistical analysis by Student's t-test.

Fecal bomb calorimetry and assessment of fecal parameters

Fecal pellet frequency and average fecal pellet weight were monitored by housing each mouse singly in clean cages for 3 days and counting the number of fecal pellets and recording their weight at the end of each 24 h period. The average of the three days was used to generate a mouse average, which were then averaged within a group for comparison across genotype. Fecal pellets from 3 days were combined and shipped to the University of Michigan Animal Phenotyping Core for fecal bomb calorimetry. Briefly, fecal samples were dried overnight at 50°C prior to weighing and grinding them to powder. Each sample was mixed with wheat flour (90% wheat flour, 10% sample) and formed into 1.0 g pellet, which was then secured into the firing platform and surrounded by 100% oxygen. The bomb was lowered into water reservoir and ignited to release heat into the surrounding water. Together these data were used to calculate fecal pellet frequency (bowel movements/day), average fecal pellet weight (g/bowel movement), fecal energy (cal/g feces), and total fecal energy (kcal/day).

Thermography tests

Deep colonic temperature was measure by inserting a lubricated (Medline, water soluble lubricating jelly, MDS032280) probe (Physitemp, BAT-12 Microprobe Thermometer) into the anus at a depth of 2 cm. Stable numbers were recorded on three separate days in both the dark and light cycle for each mouse. Skin temperature measurements and images of the tail, abdomen, and suprascapular regions of mice were taken across three days, in both the dark and light cycle, using a thermal imaging camera (Teledyne FLIR, Sweden, FLIR-C2) set at a constant distance of ~16 inches away from the specimen.

Bone length measurements

Tibias were dissected and excess tissue was cleared away. A Mitutoyo Corp. digital caliper (500-196-30) was used to measure end-to-end bone length.

Glucose and insulin tolerance tests

For glucose tolerance tests (GTTs), mice were fasted for 6 h before glucose injection. Glucose (Sigma, St. Louis, MO) was reconstituted in saline (0.9 g NaCl/L), sterile-filtered, and injected intraperitoneally (i.p.) at 1 mg/g body weight. Blood glucose was measured at 0, 15, 30, 60, and 120 min after glucose injection using a glucometer (NovaMax Plus, Billerica, MA). Blood was collected at 0, 15, and 30 min time points for serum isolation followed by Insulin ELISA. For insulin tolerance tests (ITTs), food was removed 2 h before insulin injection. Insulin was diluted in saline, sterile-filtered, and injected i.p. at 1.0 U/kg body weight. Blood glucose was measured at 0, 15, 30, 60, and 90 min after insulin injection using a glucometer (NovaMax Plus).

Fasting-Refeeding insulin tests

Mice were fasted overnight (~16 h) then reintroduced to food. Blood glucose was monitored at the 16 h fast time point (time = 0 h refed) and at 1, 2, and 3 hours into the refeeding process. Blood was collected at the 16 h fast and 2 h refed time points for insulin ELISA. Homeostatic model assessment for insulin resistance (HOMA-IR) was calculated as follows (70): [fasting insulin (uIU/mL) X blood glucose (mmol/L)] / 22.5.

Blood and tissue chemistry analysis

Tail vein blood samples were allowed to clot on ice and then centrifuged for 10 min at 10,000 x *g*. Serum samples were stored at -80°C until analyzed. Serum triglycerides (TG) and cholesterol were measured according to manufacturer's instructions using an Infinity kit (Thermo Fisher Scientific, Middletown, VA). Non-esterified free fatty acids (NEFA) were measured using a Wako kit (Wako Chemicals, Richmond, VA). Serum β-hydroxybutyrate (ketone) concentrations were measured with a StanBio Liquicolor kit (StanBio Laboratory, Boerne, TX). Serum insulin (Crystal Chem, 90080), adiponectin (MilliporeSigma, EZMADP-60K), leptin (MilliporeSigma, EZML-82K), growth hormone (MilliporeSigma, EZRMGH-45K), IGF-1 (Crystal Chem, 80574), T3 (Calbiotech, T3043T-100), and T4 (Calbiotech, T4044T-100) levels were measured by ELISA according to manufacturer's instructions. Pancreatic insulin and somatostatin (SST) were isolated from pancreas samples using acid-ethanol extraction. Briefly, pancreatic samples were in a solution of acid-ethanol (1.5% HCl in 70% EtOH) and incubated overnight at -20°C. They were then homogenized and incubated for an additional night at -20°C. The following day, samples were centrifuged at 4°C to pellet debris. The aqueous protein-rich solution was transferred to a new tube and neutralized with 1M Tris pH7.5. Prior to Insulin quantification by ELISA, samples were diluted 1:1000 with ELISA sample diluent. Following ELISA quantification of pancreatic insulin (Mercodia, 10-1247-01) and SST (Phoenix Pharmaceuticals Inc., EK-060-03) protein concentrations of pancreatic samples were quantified using a Bradford assay (Sigma-Aldrich, B6916). Insulin and SST values were then normalized to protein concentration, averaged, and compared across groups.

Histology and quantification

Inguinal (subcutaneous) white adipose tissue (iWAT), gonadal (visceral) white adipose tissue (gWAT), liver, pancreas, suprascapular brown adipose tissue (BAT), and gastrocnemius muscle were dissected and fixed in formalin. Paraffin embedding, tissue sectioning, and staining with hematoxylin and eosin were performed at the Pathology Core facility at Johns Hopkins University School of Medicine. Images were captured with a Keyence BZ-X700 All-in-One fluorescence microscope (Keyence Corp., Itasca, IL).

Adipocyte (gWAT and iWAT) and gastrocnemius cross-sectional area (CSA), as well as the total area covered by lipid droplets in hepatocytes and brown adipose tissue adipocytes, were measured on hematoxylin and eosin-stained slides using ImageJ software (71). For CSA measurements, all cells in one field of view at 100X magnification per tissue section per mouse were analyzed. For iWAT and gWAT adipocyte CSA, at least 150 cells were quantified per mouse. For pancreatic β-islet CSA, 40X magnification images were stitched together from sections at two depths of the pancreas for a single mouse. All β-islets across the two stitched images were quantified per mouse. Image capturing and quantifications were carried out blinded to genotype.

Immunohistochemistry and quantification

All paraffin sections used for immunofluorescence staining were deparaffinized with SafeClear (Fisher HealthCare, 23-044192), rehydrated using graded concentrations of ethanol in water (100% EtOH, 95%, 75%, 50%, then dH_2O), then subjected to antigen retrieval with a pressure cooker for 5 min in sodium citrate buffer (10 mM sodium citrate, 0.05% Tween 20, pH 6.0). Specimens were washed with a TBS + 0.025% Trion X-100 buffer, blocked with 10% normal goat serum at RT for 1 h, and incubated at 4°C overnight with the appropriate primary antibody. Muscle cells expressing sarcolipin or oxidative fibers were labeled with a rabbit polyclonal anti-sarcolipin Ab (Millipore Sigma, ABT13) or mouse monoclonal Ab to SDHB (Abcam, ab14714), respectively. Primary antibodies were used at a concentration of 1:200 in TBS buffer (with 1% BSA), followed by the appropriate secondary antibody at 1:1000 (diluted in TBS + 1% BSA) and incubated for 1 h at RT. Secondary antibodies used were goat anti-mouse (Invitrogen, Alexa Fluor 594, A21135) and goat anti-rabbit (Invitrogen, Alexa Fluor 488, A11008). All specimens were additionally stained with WGA (Wheat Germ Agglutinin, Alexa Fluor 647, W32466) at a concentration of 1:250 in TBS and mounted with a coverslip using ProLong Gold antifade reagent with DAPI (Invitrogen, P36935). Images were captured with a Keyence BZ-X700 All-in-One fluorescence microscope (Keyence Corp., Itasca, IL). Muscle cell cross-sectional area analysis was completed on

specimens stained with WGA. At least 1000 cells of the gastrocnemius muscle were quantified per mouse using ImageJ (71).

Western blots analysis

Protein was isolated from skeletal muscle samples using RIPA buffer as previously described (72). Protein lysates used for sarcolipin immunoblots were boiled for 5 min in a loading buffer (50 mM Tris, 2% SDS, 1% β-ME, 6% glycerol, 0.01% bromophenol blue), while those used for mitochondrial oxidative phosphorylation complex immunoblots were heated for 3 min at 50°C in the same buffer. Total protein was quantified by BCA assay (Thermo Scientific, 23225), loaded in equal amounts and volume, and run on a 4-20% gradient gel (Biorad, 4561096). Protein was transferred to nitrocellulose or PVDF membrane (sarcolipin and OXPHOS blots, respectively) and blocked in PBS containing 0.2% Tween 20 and 5% non-fat milk for 1 h, then incubated overnight at 4°C on a shaker with the antibody. Sarcolipin was detected using the Millipore Sigma antibody (ABT13, rabbit polyclonal) at a concentration of 1:500. Mitochondrial oxidative phosphorylation complexes were detected with the Abcam OXPHOS cocktail antibody (ab110413, mouse monoclonal) at a concentration of 1:5000. GAPDH was detected using the Proteintech antibody (60004-1-Ig, mouse monoclonal) at a concentration of 1:20,000. Anti-rabbit or anti-mouse secondary antibodies conjugated to HRP were used to recognize the primary antibody. Immunoblots were developed using HRP substrate ECL (GE Healthcare), visualized with a MultiImage III FluorChem Q (Alpha Innotech), and quantified with ImageJ. For the OXPHOS membrane, the blot was re-probed with the GAPDH antibody after stripping with ReBlot Plus Strong Antibody Stripping Solution (MilliporeSigma, 2504).

Electron microscopy and quantification

Mouse pancreas was dissected and sectioned into six pieces (~1 mm^3) for fixation with freshly prepared electron microscopy-grade 2% paraformaldehyde, 2% glutaraldehyde in 100 mM Sorenson's phosphate buffer containing 3 mM $MgCl_2$, pH 7.4, and 1,144 mOsm overnight at 4 °C on slow rocker. Samples were

rinsed with the same buffer containing 3% sucrose, 316 mOsm, and osmicated in 2% osmium tetroxide reduced in 1.5% potassium ferrocyanide for 2 h at 4°C. Tissue was then rinsed in 100 mM maleate buffer containing 3% sucrose pH 6.2 and en bloc stained in 2% uranyl acetate in maleate buffer for 1 h at 4°C in the dark. Samples were dehydrated in a graded ethanol series, brought to room temperature in 70% ethanol, and completely dehydrated in 100% ethanol. Samples were resin-embedded (Epon 812, T. Pella) after a propylene oxide transition step and further infiltrated and cured the next day. 80-nm-thin compression free sections were obtained with a Diatome diamond knife (35 degree). Sections were picked up on 1 x 2-mm formvar-coated copper slot grids (Polysciences) and further stained with uranyl acetate followed by lead citrate. Grids were examined on a Hitachi H-7600 transmission electron microscope operating at 80 kV. Images of β-cells and acinar cells were digitally captured at magnifications of 5,000 and 10,000X from six unique locations in the pancreas of each mouse with an AMT XR 50-5 megapixel CCD camera. Within each of the six locations, at least 600 zymogen granules and 200 insulin granules (dense insulin core and vesicle) were measured for CSA quantification using ImageJ software. Analyses were performed on a total of 6 randomly selected male chow-fed mice (WT, n = 3; KO, n = 3) and 6 randomly selected HFD-fed mice (WT, n = 3; KO, n = 3). Of the six unique locations from a single mouse, values were averaged to generate a mouse average. Therefore, each data point represents a mouse average comprised of at least 3,600 zymogen granules, 1,200 dense insulin cores, or 1,200 insulin vesicles.

Quantitative real-time PCR analysis

Total RNA was isolated from tissues using Trizol reagent (Thermo Fisher Scientific) according to the manufacturer's instructions. Purified total RNA was reverse transcribed using an iScript cDNA Synthesis Kit (Bio-rad). Real-time quantitative PCR analysis was performed on a CFX Connect Real-Time System (Bio-rad) using iTaq™ Universal SYBR Green Supermix (Bio-rad) per manufacturer's instructions. Data were normalized to *36B4* gene (encoding the acidic ribosomal phosphoprotein P0) and expressed as relative mRNA levels using the ΔΔCt method (73). Fold change data were log transformed to ensure

normal distribution and statistics were performed. Real-time qPCR primers used are listed in supplemental Table S14.

RNA-sequencing analysis

A total of 50 samples were sequenced with paired-end 50-bp reads (2x50bp) across two batches that were balanced for genotype (n = 40 across liver, brown fat, subcutaneous fat and visceral fat and n = 10 of skeletal muscle). Raw sequencing reads from all samples were aligned to a custom concatenated Gencode hg38 + mm10 reference genome using HISAT2 2.0.4 (74). Genes were quantified with featureCounts v1.5.0-p3 (75) to a custom concatenated hg38+mm10 gtf file within each sample. We retained 24,016 genes with mean RPKM > 0.1 across the mouse genome (N=23,801 genes) and chr21 in the human genome (N=215 genes) above this cutoff, and subsequently dropped two samples with outlier RNA-seq quality metrics (one SubQ_MAC21 sample with low gene assignment and high mitochondrial rates and one Skeletal_MAC21 sample with low read alignment rate), leaving a total of 48 samples. High-throughput sequencing data from this study have been submitted to the NCBI Sequence Read Archive (SRA) under accession number PRJNA877694.

We interrogated the effects of MAC21 genotype, tissue, and the statistical interaction between genotype and tissue on the transcriptome, further adjusting for confounders of gene assignment rate and mitochondrial mapping rate, using the limma voom approach (76). Given that four of the tissues were derived from the same animals, we used linear mixed effect using the animal ID as a random intercept. We accounted for multiple testing by controlling for the Benjamini-Hochberg false discovery rate across all mouse genes (since human genes were highly enriched for being DEGs given these defined the genotype effect). As a secondary analysis, we modeled the effect of MAC21 genotype within each tissue (also adjusting for the same two sequencing-derived confounders as the full model) using linear regression (since there were no repeated measures within a tissue). Gene set enrichment analyses were performed using clusterProfiler (77) and accounted for the false discovery rate.

Respirometry of frozen tissue samples

Respirometry was conducted on frozen tissue samples to assay for mitochondrial activity as described previously (78). Briefly, all tissues were dissected, snap frozen in liquid nitrogen, and stored at -80°C freezer for later analysis. Samples were thawed in MAS buffer (70mM sucrose, 220 mM mannitol, 5 mM KH_2PO_4, 5 mM $MgCl_2$, 1 mM EGTA, 2 mM HEPES pH 7.4), finely minced with scissors, then homogenized with a glass Dounce homogenizer. The resulting homogenate was spun at 1000 *g* for 10 min at 4°C. The supernatant was collected and immediately used for protein quantification by BCA assay (Thermo Scientific, 23225). Each well of the Seahorse microplate was loaded with 8 µg of homogenate protein for all tissue types, except for brown adipose tissue (BAT) and heart of which 4 µg was loaded. Each biological replicate is comprised of three technical replicates. Samples from all tissues were treated separately with NADH (1 mM) as a complex I substrate or Succinate (a complex II substrate, 5 mM) in the presence of rotenone (a complex I inhibitor, 2 µM), then with the inhibitors rotenone (2 µM) and Antimycin A (4 µM), followed by TMPD (0.45 mM) and Ascorbate (1 mM) to activate complex IV, and finally treated with Azide (40 mM) to assess non-mitochondrial respiration.

Statistical analyses

All results are expressed as mean ± standard error of the mean (SEM). Statistical analysis was performed with Prism 9 software (GraphPad Software, San Diego, CA). Data were analyzed with two-tailed Student's *t*-tests or by repeated measures ANOVA. For two-way ANOVA, we performed Bonferroni post hoc tests. $P < 0.05$ was considered statistically significant.

ACKNOWLEDGEMENTS

The work was funded, in part, by grants from the National Institutes of Health (DK084171 to GWW, HD098540 and HD038384 to RHR), Japan Society for the Promotion of Science (25221308 to MO), and the Core Research for Evolutional Science and Technology (JPMJCR18S4 to YK). The presented information and its interpretation do not necessarily reflect those of the funding agencies. We thank Nanami Senoo from the Claypool lab for technical advice on conducting the mitochondrial respiration experiments using Seahorse machine.

AUTHOR CONTRIBUTIONS

DCS, RHR, GWW conceived the project. DCS, CX, SR, SA, MD, GWW performed the experiments. DCS, SA, AJ, GWW analyzed and interpreted the data. FG bred and maintained the mouse lines. YK, MO, and RHR provided the TcMAC21 mouse model. MP provided reagents and inputs to the project. GWW and DCS wrote the manuscript with inputs from all authors.

COMPETING INTERESTS

M.O. is CEO, employee, and shareholder of Trans Chromosomics, Inc. which manages commercial use of the TcMAC21 mouse. We declare that none of the authors has a conflict of interest.

REFERENCES

1. Zhu J, Tsai HJ, Gordon MR, and Li R. Cellular stress associated with aneuploidy. *Dev Cell.* 2018;44(4):420-31.
2. Antonarakis SE, Skotko BG, Rafii MS, Strydom A, Pape SE, Bianchi DW, Sherman SL, and Reeves RH. Down syndrome. *Nat Rev Dis Primers.* 2020;6(1):9.
3. Korenberg JR, Chen XN, Schipper R, Sun Z, Gonsky R, Gerwehr S, Carpenter N, Daumer C, Dignan P, Disteche C, et al. Down syndrome phenotypes: the consequences of chromosomal imbalance. *Proc Natl Acad Sci U S A.* 1994;91(11):4997-5001.
4. Antonarakis SE. Down syndrome and the complexity of genome dosage imbalance. *Nat Rev Genet.* 2017;18(3):147-63.
5. Potier MC, and Reeves RH. Editorial: Intellectual disabilities in Down syndrome from birth and throughout life: assessment and treatment. *Front Behav Neurosci.* 2016;10(120.
6. Van Goor JC, Massa GG, and Hirasing R. Increased incidence and prevalence of diabetes mellitus in Down's syndrome. *Arch Dis Child.* 1997;77(2):186.
7. Bertapelli F, Pitetti K, Agiovlasitis S, and Guerra-Junior G. Overweight and obesity in children and adolescents with Down syndrome-prevalence, determinants, consequences, and interventions: A literature review. *Res Dev Disabil.* 2016;57(181-92.
8. Fonseca CT, Amaral DM, Ribeiro MG, Beserra IC, and Guimaraes MM. Insulin resistance in adolescents with Down syndrome: a cross-sectional study. *BMC Endocr Disord.* 2005;5(6.
9. Milunsky A, and Neurath PW. Diabetes mellitus in Down's Syndrome. *Arch Environ Health.* 1968;17(3):372-6.
10. Dierssen M, Fructuoso M, Martinez de Lagran M, Perluigi M, and Barone E. Down Syndrome Is a Metabolic Disease: Altered Insulin Signaling Mediates Peripheral and Brain Dysfunctions. *Front Neurosci.* 2020;14(670.
11. Sarver DC, Xu C, Velez LM, Aja S, Jaffe AE, Seldin MM, Reeves RH, and Wong GW. Dysregulated systemic metabolism in a Down syndrome mouse model. *Mol Metab.* 2022:101666.
12. Gupta M, Dhanasekaran AR, and Gardiner KJ. Mouse models of Down syndrome: gene content and consequences. *Mamm Genome.* 2016;27(11-12):538-55.
13. Duchon A, Raveau M, Chevalier C, Nalesso V, Sharp AJ, and Herault Y. Identification of the translocation breakpoints in the Ts65Dn and Ts1Cje mouse lines: relevance for modeling Down syndrome. *Mamm Genome.* 2011;22(11-12):674-84.
14. Reinholdt LG, Ding Y, Gilbert GJ, Czechanski A, Solzak JP, Roper RJ, Johnson MT, Donahue LR, Lutz C, and Davisson MT. Molecular characterization of the translocation breakpoints in the Down syndrome mouse model Ts65Dn. *Mamm Genome.* 2011;22(11-12):685-91.
15. Herault Y, Delabar JM, Fisher EMC, Tybulewicz VLJ, Yu E, and Brault V. Rodent models in Down syndrome research: impact and future opportunities. *Dis Model Mech.* 2017;10(10):1165-86.
16. O'Doherty A, Ruf S, Mulligan C, Hildreth V, Errington ML, Cooke S, Sesay A, Modino S, Vanes L, Hernandez D, et al. An aneuploid mouse strain carrying human chromosome 21 with Down syndrome phenotypes. *Science.* 2005;309(5743):2033-7.
17. Gribble SM, Wiseman FK, Clayton S, Prigmore E, Langley E, Yang F, Maguire S, Fu B, Rajan D, Sheppard O, et al. Massively parallel sequencing reveals the complex structure of an irradiated human chromosome on a mouse background in the Tc1 model of Down syndrome. *PLoS One.* 2013;8(4):e60482.
18. Kazuki Y, Gao FJ, Li Y, Moyer AJ, Devenney B, Hiramatsu K, Miyagawa-Tomita S, Abe S, Kazuki K, Kajitani N, et al. A non-mosaic transchromosomic mouse model of down syndrome carrying the long arm of human chromosome 21. *Elife.* 2020;9(
19. Kazuki Y, Gao FJ, Yamakawa M, Hirabayashi M, Kazuki K, Kajitani N, Miyagawa-Tomita S, Abe S, Sanbo M, Hara H, et al. A transchromosomic rat model with human chromosome 21 shows robust Down syndrome features. *Am J Hum Genet.* 2022;109(2):328-44.

20. Mullur R, Liu YY, and Brent GA. Thyroid hormone regulation of metabolism. *Physiol Rev.* 2014;94(2):355-82.
21. Bal NC, and Periasamy M. Uncoupling of sarcoendoplasmic reticulum calcium ATPase pump activity by sarcolipin as the basis for muscle non-shivering thermogenesis. *Philos Trans R Soc Lond B Biol Sci.* 2020;375(1793):20190135.
22. Wang S, Gopinath T, Larsen EK, Weber DK, Walker C, Uddigiri VR, Mote KR, Sahoo SK, Periasamy M, and Veglia G. Structural basis for sarcolipin's regulation of muscle thermogenesis by the sarcoplasmic reticulum Ca(2+)-ATPase. *Sci Adv.* 2021;7(48):eabi7154.
23. Toyoshima C, and Inesi G. Structural basis of ion pumping by Ca2+-ATPase of the sarcoplasmic reticulum. *Annu Rev Biochem.* 2004;73(269-92.
24. Smith WS, Broadbridge R, East JM, and Lee AG. Sarcolipin uncouples hydrolysis of ATP from accumulation of Ca2+ by the Ca2+-ATPase of skeletal-muscle sarcoplasmic reticulum. *Biochem J.* 2002;361(Pt 2):277-86.
25. Bal NC, Maurya SK, Sopariwala DH, Sahoo SK, Gupta SC, Shaikh SA, Pant M, Rowland LA, Bombardier E, Goonasekera SA, et al. Sarcolipin is a newly identified regulator of muscle-based thermogenesis in mammals. *Nat Med.* 2012;18(10):1575-9.
26. Mall S, Broadbridge R, Harrison SL, Gore MG, Lee AG, and East JM. The presence of sarcolipin results in increased heat production by Ca(2+)-ATPase. *J Biol Chem.* 2006;281(48):36597-602.
27. Maurya SK, Herrera JL, Sahoo SK, Reis FCG, Vega RB, Kelly DP, and Periasamy M. Sarcolipin Signaling Promotes Mitochondrial Biogenesis and Oxidative Metabolism in Skeletal Muscle. *Cell reports.* 2018;24(11):2919-31.
28. Maurya SK, Bal NC, Sopariwala DH, Pant M, Rowland LA, Shaikh SA, and Periasamy M. Sarcolipin Is a Key Determinant of the Basal Metabolic Rate, and Its Overexpression Enhances Energy Expenditure and Resistance against Diet-induced Obesity. *J Biol Chem.* 2015;290(17):10840-9.
29. Sopariwala DH, Pant M, Shaikh SA, Goonasekera SA, Molkentin JD, Weisleder N, Ma J, Pan Z, and Periasamy M. Sarcolipin overexpression improves muscle energetics and reduces fatigue. *J Appl Physiol (1985).* 2015;118(8):1050-8.
30. Pant M, Bal NC, and Periasamy M. Cold adaptation overrides developmental regulation of sarcolipin expression in mice skeletal muscle: SOS for muscle-based thermogenesis? *J Exp Biol.* 2015;218(Pt 15):2321-5.
31. Rowland LA, Bal NC, Kozak LP, and Periasamy M. Uncoupling Protein 1 and Sarcolipin Are Required to Maintain Optimal Thermogenesis, and Loss of Both Systems Compromises Survival of Mice under Cold Stress. *J Biol Chem.* 2015;290(19):12282-9.
32. Bal NC, Maurya SK, Singh S, Wehrens XH, and Periasamy M. Increased Reliance on Muscle-based Thermogenesis upon Acute Minimization of Brown Adipose Tissue Function. *J Biol Chem.* 2016;291(33):17247-57.
33. Chambers PJ, Juracic ES, Fajardo VA, and Tupling AR. Role of SERCA and sarcolipin in adaptive muscle remodeling. *Am J Physiol Cell Physiol.* 2022;322(3):C382-C94.
34. van Wessel T, de Haan A, van der Laarse WJ, and Jaspers RT. The muscle fiber type-fiber size paradox: hypertrophy or oxidative metabolism? *Eur J Appl Physiol.* 2010;110(4):665-94.
35. Sahoo SK, Shaikh SA, Sopariwala DH, Bal NC, Bruhn DS, Kopec W, Khandelia H, and Periasamy M. The N Terminus of Sarcolipin Plays an Important Role in Uncoupling Sarco-endoplasmic Reticulum Ca2+-ATPase (SERCA) ATP Hydrolysis from Ca2+ Transport. *J Biol Chem.* 2015;290(22):14057-67.
36. Sahoo SK, Shaikh SA, Sopariwala DH, Bal NC, and Periasamy M. Sarcolipin protein interaction with sarco(endo)plasmic reticulum Ca2+ ATPase (SERCA) is distinct from phospholamban protein, and only sarcolipin can promote uncoupling of the SERCA pump. *J Biol Chem.* 2013;288(10):6881-9.

37. Kaspari RR, Reyna-Neyra A, Jung L, Torres-Manzo AP, Hirabara SM, and Carrasco N. The paradoxical lean phenotype of hypothyroid mice is marked by increased adaptive thermogenesis in the skeletal muscle. *Proc Natl Acad Sci U S A.* 2020;117(36):22544-51.
38. Fructuoso M, Rachdi L, Philippe E, Denis RG, Magnan C, Le Stunff H, Janel N, and Dierssen M. Increased levels of inflammatory plasma markers and obesity risk in a mouse model of Down syndrome. *Free Radic Biol Med.* 2018;114(122-30.
39. Li Z, Yu T, Morishima M, Pao A, LaDuca J, Conroy J, Nowak N, Matsui S, Shiraishi I, and Yu YE. Duplication of the entire 22.9 Mb human chromosome 21 syntenic region on mouse chromosome 16 causes cardiovascular and gastrointestinal abnormalities. *Hum Mol Genet.* 2007;16(11):1359-66.
40. Duchon A, Del Mar Muniz Moreno M, Chevalier C, Nalesso V, Andre P, Fructuoso-Castellar M, Mondino M, Po C, Noblet V, Birling MC, et al. Ts66Yah, a mouse model of Down syndrome with improved construct and face validity. *Dis Model Mech.* 2022;15(12).
41. Yau WW, Singh BK, Lesmana R, Zhou J, Sinha RA, Wong KA, Wu Y, Bay BH, Sugii S, Sun L, et al. Thyroid hormone (T3) stimulates brown adipose tissue activation via mitochondrial biogenesis and MTOR-mediated mitophagy. *Autophagy.* 2019;15(1):131-50.
42. Johann K, Cremer AL, Fischer AW, Heine M, Pensado ER, Resch J, Nock S, Virtue S, Harder L, Oelkrug R, et al. Thyroid-Hormone-Induced Browning of White Adipose Tissue Does Not Contribute to Thermogenesis and Glucose Consumption. *Cell reports.* 2019;27(11):3385-400 e3.
43. Chouchani ET, Kazak L, and Spiegelman BM. New Advances in Adaptive Thermogenesis: UCP1 and Beyond. *Cell Metab.* 2019;29(1):27-37.
44. Gonzalez-Hurtado E, Lee J, Choi J, and Wolfgang MJ. Fatty acid oxidation is required for active and quiescent brown adipose tissue maintenance and thermogenic programing. *Mol Metab.* 2018;7(45-56.
45. Kazak L, Chouchani ET, Jedrychowski MP, Erickson BK, Shinoda K, Cohen P, Vetrivelan R, Lu GZ, Laznik-Bogoslavski D, Hasenfuss SC, et al. A creatine-driven substrate cycle enhances energy expenditure and thermogenesis in beige fat. *Cell.* 2015;163(3):643-55.
46. Ikeda K, Kang Q, Yoneshiro T, Camporez JP, Maki H, Homma M, Shinoda K, Chen Y, Lu X, Maretich P, et al. UCP1-independent signaling involving SERCA2b-mediated calcium cycling regulates beige fat thermogenesis and systemic glucose homeostasis. *Nat Med.* 2017;23(12):1454-65.
47. Clapham JC, Arch JR, Chapman H, Haynes A, Lister C, Moore GB, Piercy V, Carter SA, Lehner I, Smith SA, et al. Mice overexpressing human uncoupling protein-3 in skeletal muscle are hyperphagic and lean. *Nature.* 2000;406(6794):415-8.
48. Son C, Hosoda K, Ishihara K, Bevilacqua L, Masuzaki H, Fushiki T, Harper ME, and Nakao K. Reduction of diet-induced obesity in transgenic mice overexpressing uncoupling protein 3 in skeletal muscle. *Diabetologia.* 2004;47(1):47-54.
49. Li B, Nolte LA, Ju JS, Han DH, Coleman T, Holloszy JO, and Semenkovich CF. Skeletal muscle respiratory uncoupling prevents diet-induced obesity and insulin resistance in mice. *Nat Med.* 2000;6(10):1115-20.
50. Bombardier E, Smith IC, Gamu D, Fajardo VA, Vigna C, Sayer RA, Gupta SC, Bal NC, Periasamy M, and Tupling AR. Sarcolipin trumps beta-adrenergic receptor signaling as the favored mechanism for muscle-based diet-induced thermogenesis. *FASEB J.* 2013;27(9):3871-8.
51. MacPherson RE, Gamu D, Frendo-Cumbo S, Castellani L, Kwon F, Tupling AR, and Wright DC. Sarcolipin knockout mice fed a high-fat diet exhibit altered indices of adipose tissue inflammation and remodeling. *Obesity (Silver Spring).* 2016;24(7):1499-505.
52. Babu GJ, Bhupathy P, Carnes CA, Billman GE, and Periasamy M. Differential expression of sarcolipin protein during muscle development and cardiac pathophysiology. *J Mol Cell Cardiol.* 2007;43(2):215-22.
53. Campbell KL, and Dicke AA. Sarcolipin Makes Heat, but Is It Adaptive Thermogenesis? *Front Physiol.* 2018;9(714.

54. Robb-Gaspers LD, Burnett P, Rutter GA, Denton RM, Rizzuto R, and Thomas AP. Integrating cytosolic calcium signals into mitochondrial metabolic responses. *EMBO J.* 1998;17(17):4987-5000.
55. Jouaville LS, Pinton P, Bastianutto C, Rutter GA, and Rizzuto R. Regulation of mitochondrial ATP synthesis by calcium: evidence for a long-term metabolic priming. *Proc Natl Acad Sci U S A.* 1999;96(24):13807-12.
56. Tarasov AI, Griffiths EJ, and Rutter GA. Regulation of ATP production by mitochondrial Ca(2+). *Cell Calcium.* 2012;52(1):28-35.
57. Glancy B, Willis WT, Chess DJ, and Balaban RS. Effect of calcium on the oxidative phosphorylation cascade in skeletal muscle mitochondria. *Biochemistry.* 2013;52(16):2793-809.
58. Rolfe DF, and Brown GC. Cellular energy utilization and molecular origin of standard metabolic rate in mammals. *Physiol Rev.* 1997;77(3):731-58.
59. Zurlo F, Larson K, Bogardus C, and Ravussin E. Skeletal muscle metabolism is a major determinant of resting energy expenditure. *J Clin Invest.* 1990;86(5):1423-7.
60. Gamu D, Trinh A, Bombardier E, and Tupling AR. Persistence of diet-induced obesity despite access to voluntary activity in mice lacking sarcolipin. *Physiol Rep.* 2015;3(9).
61. Habtemichael EN, Li DT, Camporez JP, Westergaard XO, Sales CI, Liu X, Lopez-Giraldez F, DeVries SG, Li H, Ruiz DM, et al. Insulin-stimulated endoproteolytic TUG cleavage links energy expenditure with glucose uptake. *Nat Metab.* 2021;3(3):378-93.
62. Roesler A, and Kazak L. UCP1-independent thermogenesis. *Biochem J.* 2020;477(3):709-25.
63. Paran CW, Verkerke AR, Heden TD, Park S, Zou K, Lawson HA, Song H, Turk J, Houmard JA, and Funai K. Reduced efficiency of sarcolipin-dependent respiration in myocytes from humans with severe obesity. *Obesity (Silver Spring).* 2015;23(7):1440-9.
64. Rowland LA, Bal NC, and Periasamy M. The role of skeletal-muscle-based thermogenic mechanisms in vertebrate endothermy. *Biol Rev Camb Philos Soc.* 2015;90(4):1279-97.
65. Vangheluwe P, Schuermans M, Zador E, Waelkens E, Raeymaekers L, and Wuytack F. Sarcolipin and phospholamban mRNA and protein expression in cardiac and skeletal muscle of different species. *Biochem J.* 2005;389(Pt 1):151-9.
66. Fajardo VA, Bombardier E, Vigna C, Devji T, Bloemberg D, Gamu D, Gramolini AO, Quadrilatero J, and Tupling AR. Co-expression of SERCA isoforms, phospholamban and sarcolipin in human skeletal muscle fibers. *PLoS One.* 2013;8(12):e84304.
67. Leitner BP, Huang S, Brychta RJ, Duckworth CJ, Baskin AS, McGehee S, Tal I, Dieckmann W, Gupta G, Kolodny GM, et al. Mapping of human brown adipose tissue in lean and obese young men. *Proc Natl Acad Sci U S A.* 2017;114(32):8649-54.
68. Smith IC, Bombardier E, Vigna C, and Tupling AR. ATP consumption by sarcoplasmic reticulum Ca(2)(+) pumps accounts for 40-50% of resting metabolic rate in mouse fast and slow twitch skeletal muscle. *PLoS One.* 2013;8(7):e68924.
69. Sarver DC, Stewart AN, Rodriguez S, Little HC, Aja S, and Wong GW. Loss of CTRP4 alters adiposity and food intake behaviors in obese mice. *Am J Physiol Endocrinol Metab.* 2020;319(6):E1084-E100.
70. Matthews DR, Hosker JP, Rudenski AS, Naylor BA, Treacher DF, and Turner RC. Homeostasis model assessment: insulin resistance and beta-cell function from fasting plasma glucose and insulin concentrations in man. *Diabetologia.* 1985;28(7):412-9.
71. Schneider CA, Rasband WS, and Eliceiri KW. NIH Image to ImageJ: 25 years of image analysis. *Nat Methods.* 2012;9(7):671-5.
72. Rodriguez S, Lei X, Petersen PS, Tan SY, Little HC, and Wong GW. Loss of CTRP1 disrupts glucose and lipid homeostasis. *Am J Physiol Endocrinol Metab.* 2016;311(E678-E97.
73. Schmittgen TD, and Livak KJ. Analyzing real-time PCR data by the comparative C(T) method. *Nat Protoc.* 2008;3(6):1101-8.
74. Kim D, Paggi JM, Park C, Bennett C, and Salzberg SL. Graph-based genome alignment and genotyping with HISAT2 and HISAT-genotype. *Nat Biotechnol.* 2019;37(8):907-15.

75. Liao Y, Smyth GK, and Shi W. featureCounts: an efficient general purpose program for assigning sequence reads to genomic features. *Bioinformatics.* 2014;30(7):923-30.
76. Law CW, Chen Y, Shi W, and Smyth GK. voom: Precision weights unlock linear model analysis tools for RNA-seq read counts. *Genome Biol.* 2014;15(2):R29.
77. Yu G, Wang LG, Han Y, and He QY. clusterProfiler: an R package for comparing biological themes among gene clusters. *OMICS.* 2012;16(5):284-7.
78. Acin-Perez R, Benador IY, Petcherski A, Veliova M, Benavides GA, Lagarrigue S, Caudal A, Vergnes L, Murphy AN, Karamanlidis G, et al. A novel approach to measure mitochondrial respiration in frozen biological samples. *EMBO J.* 2020;39(13):e104073.

FIGURE LEGENDS

Figure 1. Human chromosome 21 genes are differentially expressed and regulated in mouse adipose tissue, liver, and skeletal muscle. A) Graphical representation of human chromosome 21 (Hsa21) and the entire long arm (Hsa21q) region carried by a mouse artificial chromosome in the transchromosomic mouse model (TcMAC21). Four deletions that occurred during generation of the transchromosomic mice eliminate 14/213 protein coding genes (PCGs; 7%) and 105/487 predicted or known non-protein coding genes (NPCGs; 22%) (18). **B)** Global view of transcriptionally expressed and repressed protein and non-protein coding gene regions over the entire Hsa21q across five tissues. Gray box denotes transcript that is not detected. **C)** Transcriptional activity map showing only Hsa21 genes expressed by at least one tissue. Gray box denotes transcript that is not detected. **D)** Overlap analysis showing shared expression of human protein coding and non-protein coding genes across five tissues. Of the 235 unique human genes expressed by the MAC21, 54% are protein coding and 46% are non-protein coding genes. PCGs, protein coding genes; NPCGs, non-protein coding genes; B, brown adipose tissue; iW, inguinal white adipose tissue; gW, gonadal white adipose tissue; L, liver; M, skeletal muscle (gastrocnemius); n.d., not detected. n = 5 RNA samples per group per tissue-type. Mice were on high-fat diet for 16 weeks at the time of tissue collection.

Figure 2. Hypermetabolism in TcMAC21 mice. A) Body weights of mice fed standard chow. **B)** Body composition analysis of fat and lean mass (relative to body weight). **C)** Food intake over a 24 h period. **D-E)** Energy expenditure (EE) and physical activity level over 24 hr period in chow-fed mice. **F)** Hematoxylin and eosin (H&E) stained sections of inguinal white adipose tissue (iWAT), and adipocyte cross-sectional area (CSA) quantification. **G)** Histology of gonadal white adipose tissue (gWAT), and adipocyte CSA quantification. **H)** Histology of liver tissues with quantification of area covered by lipid droplets per focal plane. **I)** Fasting serum triglyceride, cholesterol, non-esterified fatty acids (NEFA), β-

hydroxybutyrate (ketone) levels. **J)** fasting blood glucose and insulin levels. **K)** Insulin resistance index (homeostatic model assessment for insulin resistance (HOMA-IR). **L)** Glucose tolerance tests. **M)** Insulin tolerance tests. **N)** Histology of pancreas and quantification of β-islet CSA. **O)** Pancreatic insulin and somatostatin (SST) contents (normalized to pancreatic protein input). **P)** Electron micrographs (EM) of pancreatic β-cells showing dense insulin granules and their surrounding vesicles, and the quantification of insulin granule CSA, insulin vesicle CSA, and the ratio of insulin granule to insulin vesicle. *n* = 8 euploid and 9 TcMAC21 mice for all graphs from A to Y. *n* = 8-10 euploid and 5-8 TcMAC21 samples used for pancreatic analysis by H&E and protein quantification, graphs N and P. *n* = 3 euploid and 3 TcMAC21 used for EM quantification; each data point represents 1,200 insulin granules and 1,200 insulin vesicles quantified across 6 unique locations per mouse, graphs P.

Figure 3. TcMAC21 mice are resistant to diet-induced obesity and metabolic dysfunction. A) Body weights over time on a high-fat diet and representative mouse images. **B)** Body composition analysis of fat and lean mass. **C)** Histology of inguinal white adipose tissue (iWAT), and quantification of adipocyte cross-sectional area (CSA). **D)** Histology of gonadal white adipose tissue (gWAT), and quantification of adipocyte CSA. **E)** Histology of liver tissues, and quantification of area covered by lipid droplets per focal plane. **F)** Fasting serum triglyceride, cholesterol, non-esterified fatty acids (NEFA), β-hydroxybutyrate (ketone) levels. **G)** Fasting blood glucose and insulin levels. **H)** Insulin resistance index (homeostatic model assessment for insulin resistance (HOMA-IR). **I)** Glucose tolerance tests (GTT). **J)** Serum insulin levels during GTT**. K)** Insulin tolerance tests. **L)** Blood glucose levels after an overnight (16 h) fast and 1, 2, and 3 h of food reintroduction. **M)** Serum insulin levels after a 16 h fast and 2 h of refeeding. **N)** Pancreas histology and quantification of β-islet CSA. **O-P)** Pancreatic insulin and somatostatin (SST) contents (normalized to pancreatic protein input). **Q)** Electron micrographs (EM) of pancreatic β-cells showing dense insulin granules and their surrounding vesicles, and quantification of insulin granule CSA, insulin vesicle CSA, and the ratio of insulin granule to insulin vesicle. *n* = 8 euploid

and 8-9 TcMAC21 mice for all graphs from A to P. *n* = 3 euploid and 3 TcMAC21 used for EM quantification; each data point represents 1,200 insulin granules and 1,200 insulin vesicles quantified across 6 unique locations per mouse, graphs Q.

Figure 4. Hypermetabolism of TcMAC21 mice on HFD is uncoupled from changes in adipose and liver transcriptomes. A) Food intake in mice fed a high-fat diet (HFD). **B)** Fecal energy content. **C-D)** Energy expenditure (EE) and activity level over 24 h period in HFD-fed mice. **E)** Serum Triiodothyronine (T_3) and Thyroxine (T_4) levels. **F)** Deep colonic and tail temperature measured over three days in both the light and dark cycle. **G)** Representative infrared images of mice. **H)** Body weights of euploid, TcMAC21, and weight-matched (WM) control C57BL/6 mice. **I)** Interscapular skin temperature of euploid, TcMAC21, and WM control mice. **J)** Representative histology of brown adipose tissue (BAT). **K)** Quantification of percent total lipid area coverage per focal plane in BAT of euploid and TcMAC21. **L)** Expression of mouse genes (by qPCR) known to play major metabolic roles in BAT. **M)** Differentially expressed mouse genes (DEGs), both protein coding (PCG) and non-protein coding genes (NPCG) in BAT, liver, gonadal white adipose tissue (gWAT), and inguinal white adipose tissue (iWAT). All data is relative to euploid, and presented as Log2(FC). The list of genes shown is all the up and down regulated mouse genes (significant by adjusted p-value cut-off) for all 4 tissues. The red bars indicate up regulated genes and the blue bars indicate down regulated genes. **N)** General view and summary of transcriptional changes in BAT, Liver, gWAT, and iWAT to highlight the strikingly minimal changes in the mouse transcriptome across the four tissues. Only a combined total of 114 differentially expressed genes (DEGs) across four tissues, with the relative percentage (out of the 114 DEGs) shown for each tissue. Of the 114 DEGs, 105 are protein-coding genes (PCGs; dark yellow bar) and 9 are non-protein coding genes (NPCGs; light yellow bar). Of the 114 DEGs, 46 are upregulated (red bar) and 68 are down regulated (blue bar). In total, only a combined 0.53% change is noted in the transcriptome of all four tissues (out of the 21,752 RNAs detected).

Figure 5. Sarcolipin overexpression in skeletal muscle drives TcMAC21 hypermetabolism. A) RNA-sequencing analysis reveals changes in TcMAC21 relative to euploid skeletal muscle (gastrocnemius). Volcano plot of skeletal muscle transcriptome (transcripts from the mouse genome only). The lower dotted line denotes significance at the adjusted *P* value cut-off (adj. $P = 0.05$). The vertical dotted lines denote a Log2(FC) of -0.5 or 0.5. **B)** Gene Ontology analysis of RNA-sequencing results using ClusterProfiler (77). **C)** Expression of genes (by qPCR) known to be involved in metabolism, fast- or slow-twitch fiber types, futile cycling, thyroid hormone action, and calcium handling in skeletal muscle (gastrocnemius). **D)** Graphical representation of the sarco(endo)plasmic reticulum Ca^{2+} ATPase (SERCA) and its regulator, sarcolipin (SLN). SERCA pump uses the energy derived from ATP hydrolysis to translocate Ca^{2+} from the cytosol back into the sarcoplasmic reticulum (SR), promoting muscle relaxation and restoring intracellular Ca^{2+} level following muscle contraction. SLN binds to SERCA and uncouples its Ca^{2+} transport activity from ATP hydrolysis and heat generation, thus promoting futile SERCA activity. **E)** qPCR analysis of sarcolipin (*Sln*) expression in euploid and TcMAC21 mice fed a standard chow, high-fat diet (HFD), and HFD while housed at thermoneutrality (30°C). **F)** Immunoblot of SLN and GAPDH (loading control) in muscle lysates of Euploid, TcMAC21, and SLN overexpression (OE) transgenic mice. **G)** Immunoblot quantification of SLN using GAPDH as a loading control. The dotted line marks the OE (SLN overexpression mouse model) level of SLN expression. **H-I)** Gastrocnemius immunofluorescent labeling of SLN-expressing muscle fibers. **J)** Muscle fiber cross-sectional area (CSA) quantification from WGA-stained gastrocnemius. **K)** Immunoblot of OXPHOS complex levels, with GAPDH as a loading control. **L)** Quantification of OXPHOS complex levels relative to GAPDH. **M-N)** Gastrocnemius immunofluorescent labeling of Succinate dehydrogenase subunit B (SDHB)-expressing muscle fibers. **O-P)** Seahorse respirometry analyses of frozen tissue samples. Shown here are the quadricep group average tracings for oxygen consumption rate (OCR) across the experimental time course. **Q)** OCR of TcMAC21 mitochondrial complex I, II, and IV relative to Euploid, for eleven separate

tissues (quadricep, Qd; extensor digitorum longus, EDL; gastrocnemius, Gast; Plantaris, Plnt; Soleus, Sol; Tongue, Tng; Brown adipose tissue, BAT; Liver, Liv; Heart, Hrt; Inguinal white adipose tissue, iWAT; Gonadal white adipose tissue, gWAT) and two dietary conditions (Chow and HFD). DEGs, differentially expressed genes; PCGs, protein coding genes; NPCGs, non-protein coding genes. *n* = 5 euploid and 4 TcMAC21 for RNA-sequencing experiments. *n* = 8-9 euploid and 7-8 TcMAC21 for HFD qPCR. *n* = 7-10 euploid and TcMAC21 for Chow qPCR. *n* = 4-5 euploid and TcMAC21 for HFD + thermoneutrality qPCR. *n* = 6 euploid and 6 TcMAC21 for all immunoblots. *n* = 7 Euploid and 8 TcMAC21 for gastrocnemius CSA quantification. *n* = 6 euploid and 4 TcMAC21 for all mitochondrial respiration assays; each biological replicate represents the average of three technical replicates.

Figure 6. Potential regulators of sarcolipin expression in skeletal muscle. A.) Body weights at thermoneutrality (30°C) for 8 weeks. B) Body composition analysis of fat and lean mass. C) Fasting insulin levels. D) Energy expenditure in the dark and light cycles. E) Food intake. F) Volcano plot of skeletal muscle transcriptome (transcripts from the mouse genome only). The lower dotted line denotes significance at the *P* value cut-off (*P* = 0.05), and the upper dotted line denotes significance at the adjusted *P* value cut-off (adj. *P* = 0.05). The vertical dotted lines denote a Log 2 (Fold Change) of -0.5 or 0.5. Flanking the Volcano plot are the top down- and up-regulated mouse genes. G) Comparison of differentially expressed genes (DEGs) shared and not shared by TcMAC21 mice housed at 22°C vs. 30°C. Heat map showing all significantly up- or down-regulated shared genes. H) Direct comparison of TcMAC21 mice housed at 22°C and 30°C for most stably expressed mouse genes. Data filtered first by genes with Log2(FC) within ±0.5 (least change), then by lowest significance, and finally compared to the shared DEGs found in G. Table shows DEGs with least variation in expression at 22°C and 30°C. I) Overlap analysis of Hsa21-derived human transcripts expressed in TcMAC21 mice (skeletal muscle) housed at 22°C and 30°C. J) Graph showing the most stably expressed Hsa21-derived human genes in the TcMAC21 gastrocnemius. Top axis refers to the difference in Log2(FC) between human genes in

TcMAC21 mice housed at 22°C and 30°C. Bottom axis shows the Log2(FC) value of a particular gene at 22°C and 30°C. The gene list shows all the human genes expressed by both groups with the least amount of change between the two temperatures.

Fig. 1

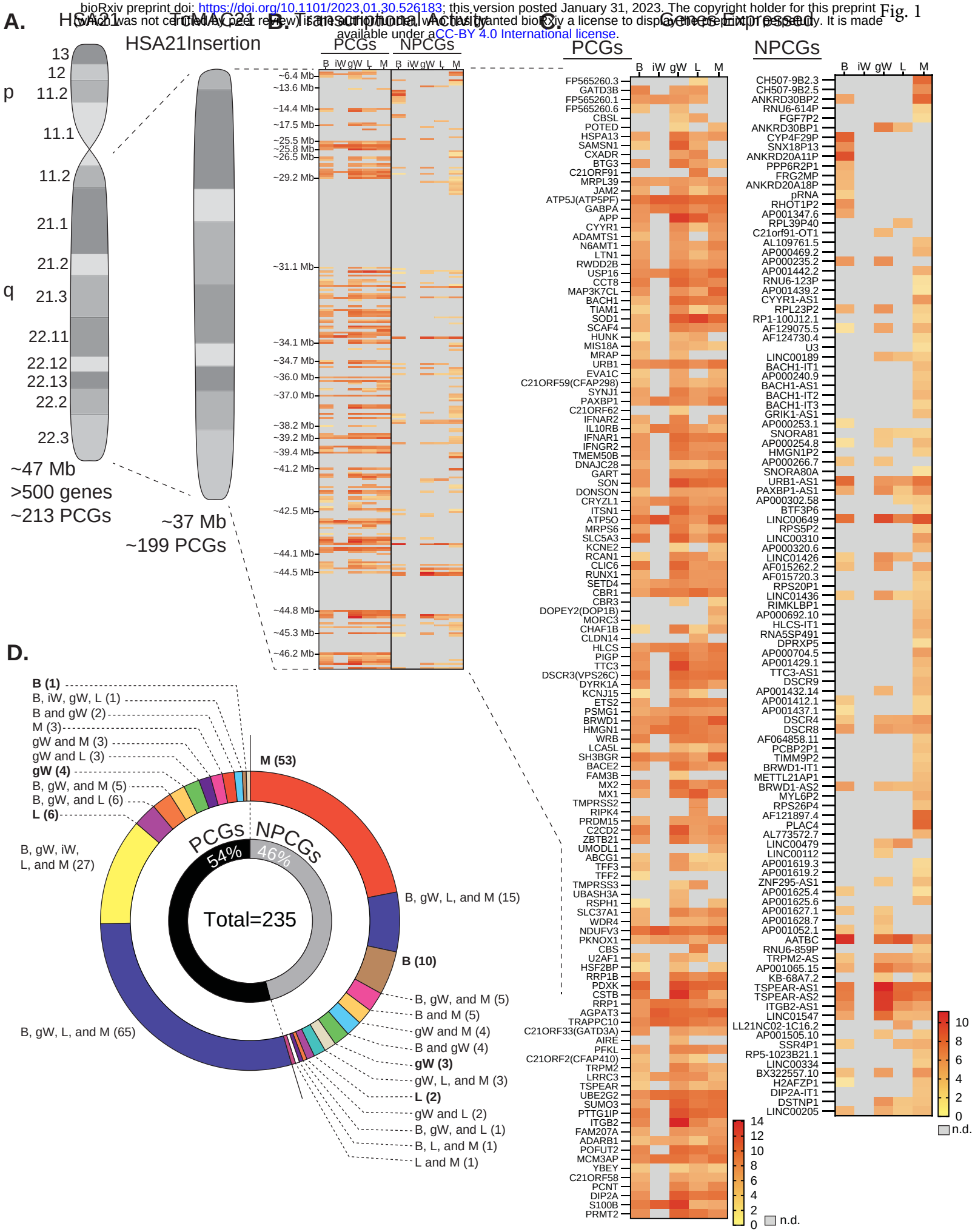

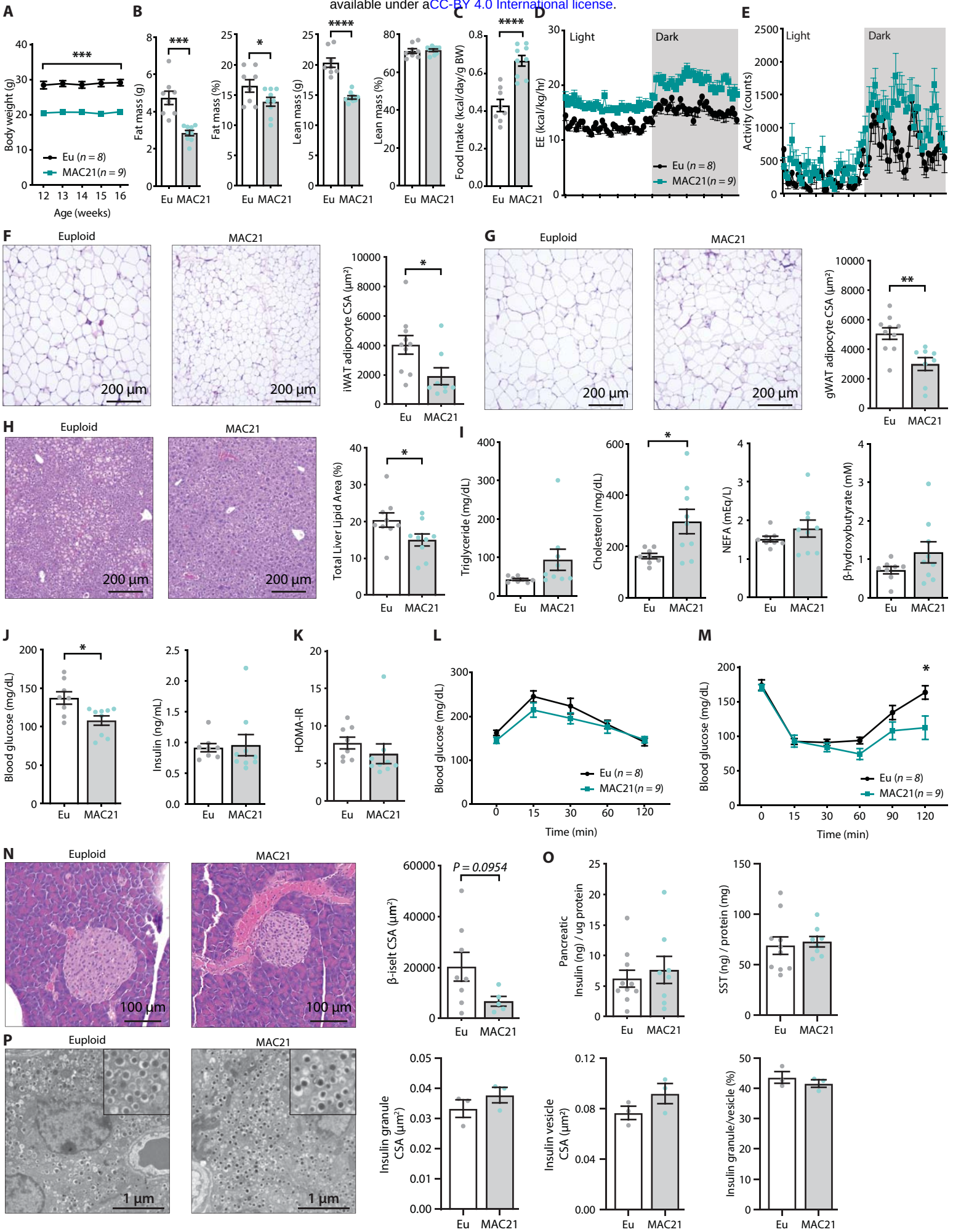

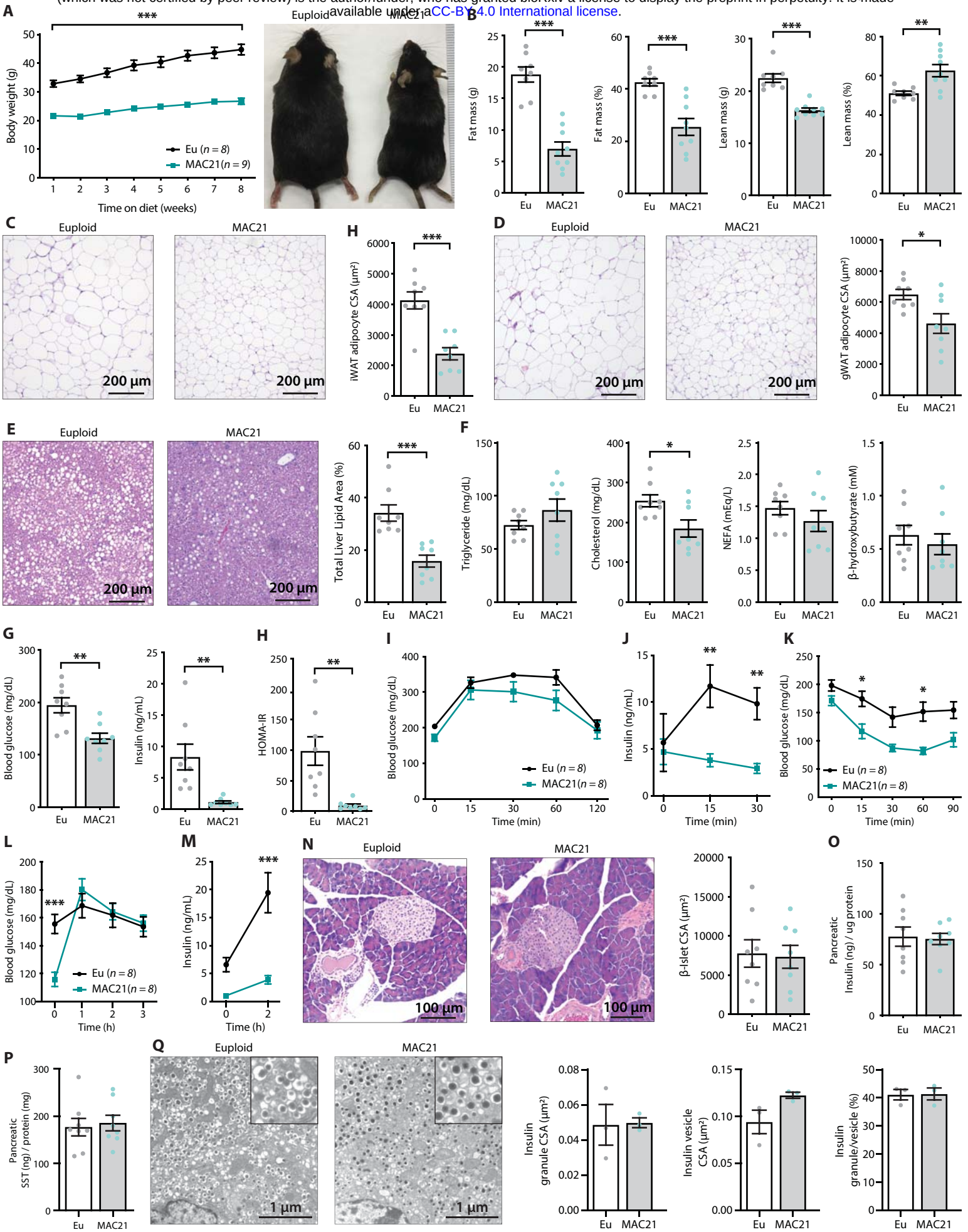

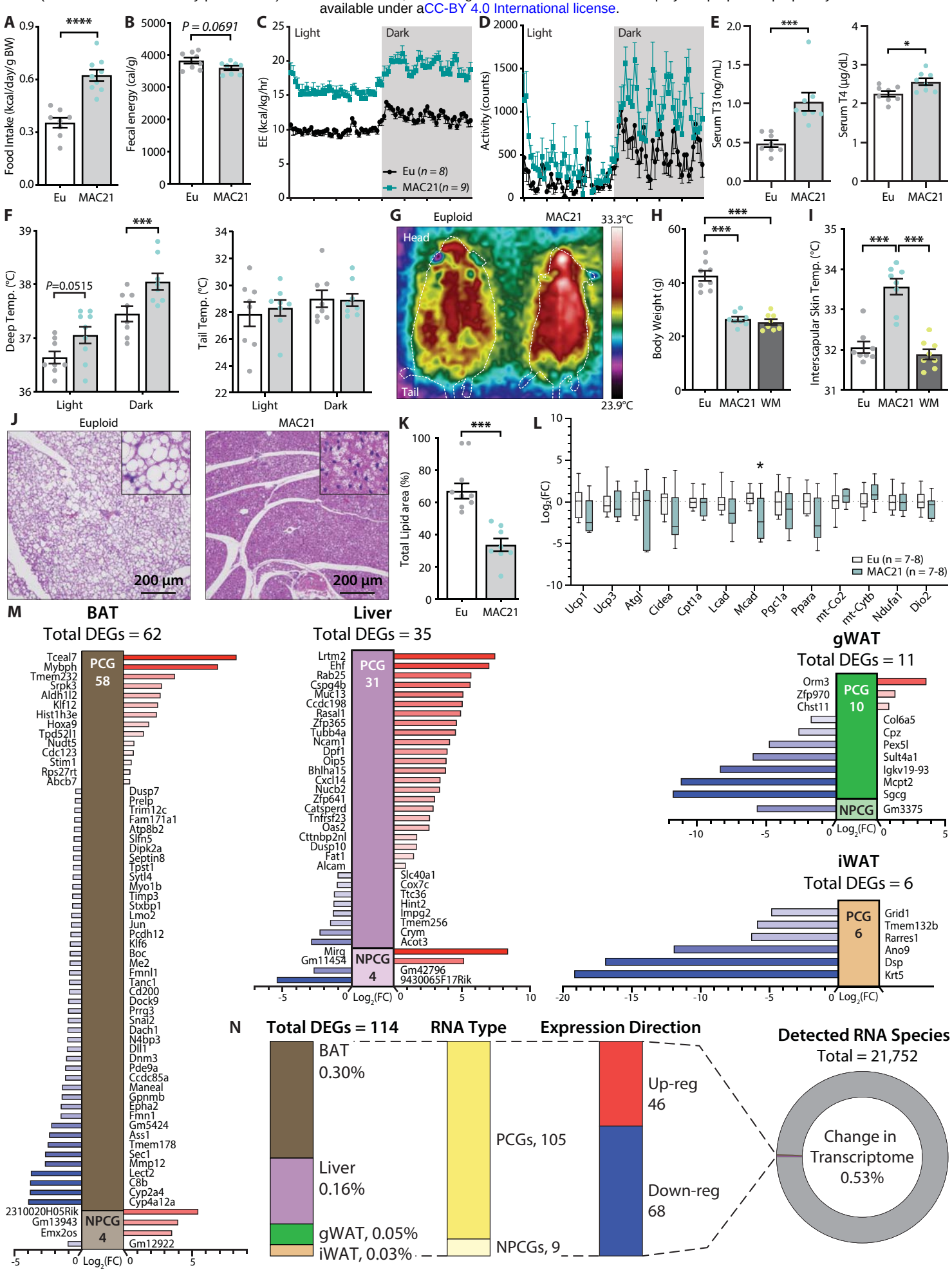

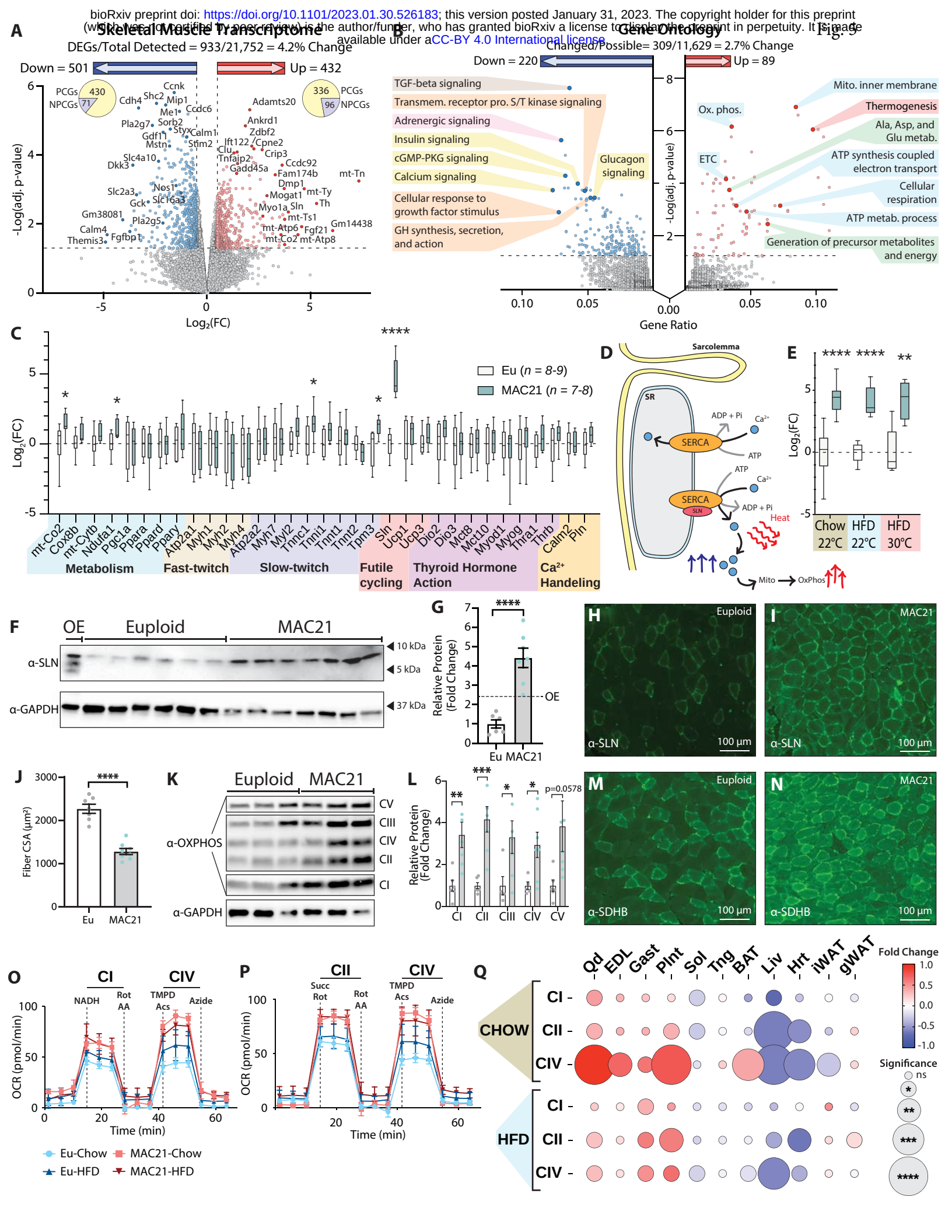

Thermoneutrality (30°C HFD)

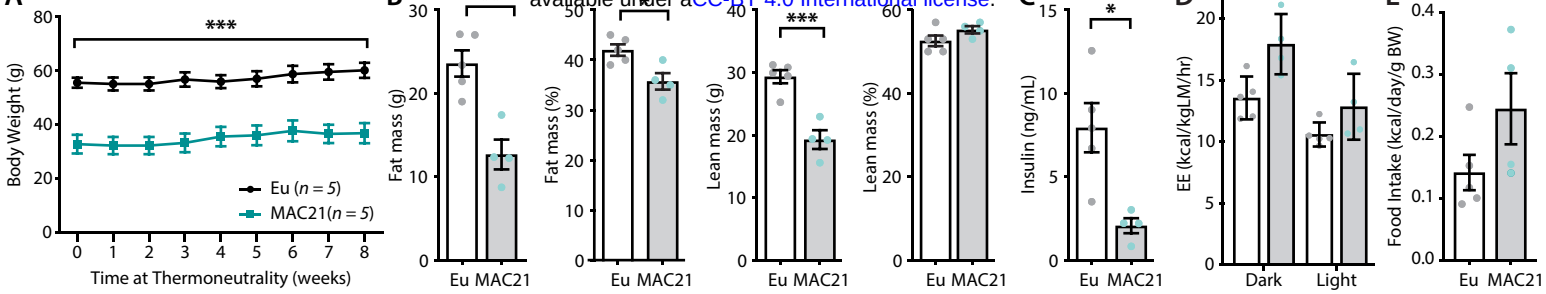

F

Mouse DEGS: Top Down-Regulated

Gene Symbol	Log_2(FC)	adj. P. Val
Cdh4	-3.28	0.0078
Shc2	-2.79	0.0337
Nhs	-2.73	0.0211
Cntnap2	-2.42	0.0195
Gdf11	-2.34	0.0004
Pla2g7	-2.20	0.0027
Aurka	-2.11	0.0288
Ctxn3	-1.90	0.0006
Mss51	-1.80	0.0007
Col24a1	-1.77	0.0229
Mib1	-1.69	0.0016
Ces1d	-1.67	0.0467
Aebp1	-1.60	0.0001
Nos1	-1.48	0.0456
Wbscr17	-1.48	0.0177
Col22a1	-1.46	0.0031
Sorbs2	-1.43	0.0020
Enox2	-1.35	0.0134
Tpbgl	-1.35	0.0220
Mettl11b	-1.26	0.0275
Mstn	-1.25	0.0013
Rasd2	-1.24	0.0006

Skeletal Muscle Transcriptome (Mouse Genome)
HFD fed mice housed at 30°C

DEGs/Total Detected = 113/17,329 = 0.65% Change

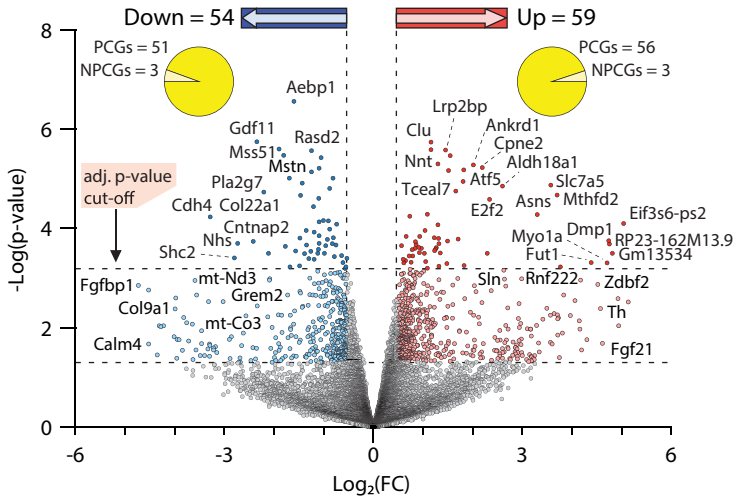

Mouse DEGS: Top Up-Regulated

Gene Symbol	Log_2(FC)	adj. P. Val
Eif3s6-ps2	5.04	0.0101
Gm13534	4.81	0.0288
RP23-162M13.9	4.76	0.0214
Dmp1	4.74	0.0192
Myo1a	4.71	0.0403
Fut1	4.39	0.0403
Ccdc92	3.77	0.0467
Mthfd2	3.70	0.0031
Slc7a5	3.57	0.0021
Asns	3.30	0.0071
Aldh18a1	2.60	0.0022
E2f2	2.34	0.0037
A930003A15Rik	2.29	0.0288
Cpne2	2.19	0.0012
Ankrd1	2.01	0.0010
Aldh1l2	1.83	0.0451
Atf5	1.82	0.0012
Tceal7	1.81	0.0019
Spag5	1.71	0.0182
Itga9	1.66	0.0026
Tnfaip2	1.55	0.0007
Cdkn1a	1.52	0.0013

G

Mouse DEG Overlap analysis

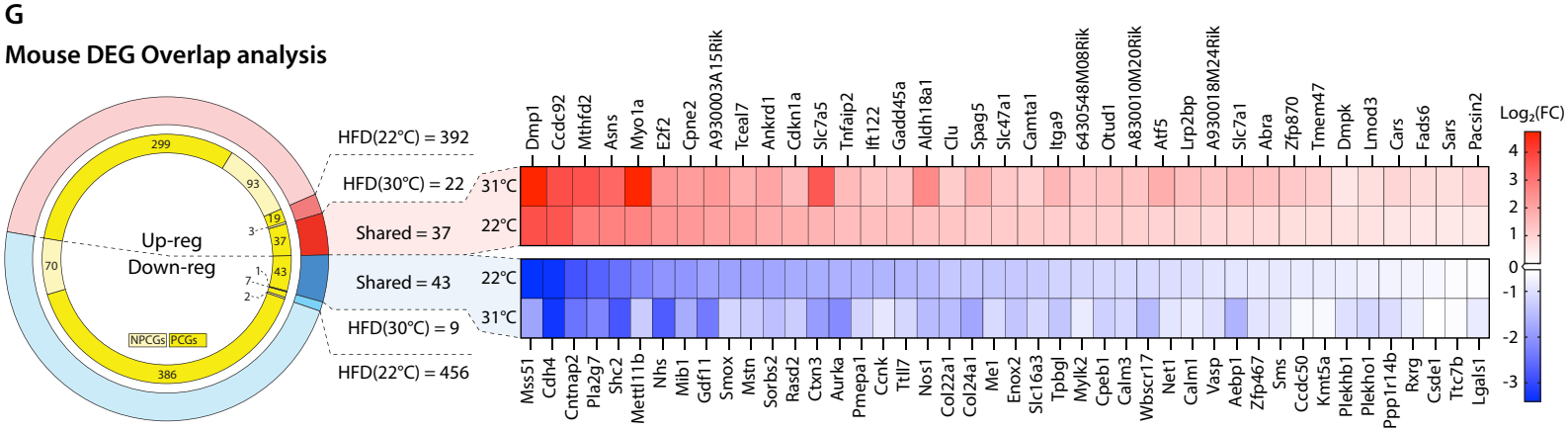

H

MAC21 (22°C) vs (30°C)

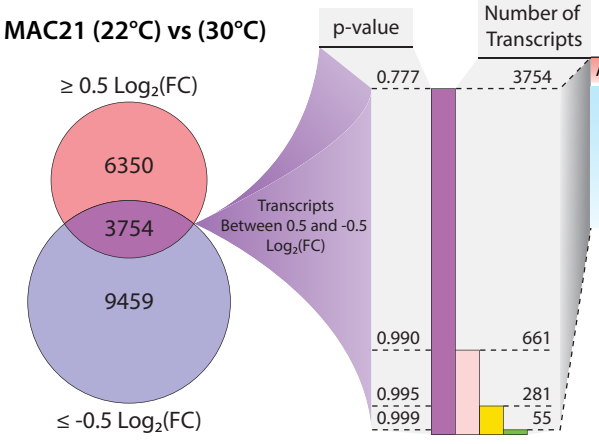

Total non-significanct transcripts expressed = 19563

Most temperature stable genes that are also shared DEGs (Mouse Genome)

Gene Symbol	Description
A930018M24Rik	RIKEN cDNA A930018M24 gene
Csde1	Cold shock domain containing E, RNA binding
Kmt5a	Lysine methyltransferase 5A
Vasp	Vasodilator-stimulated phosphoprotein
Calm1	Calmodulin 1

I

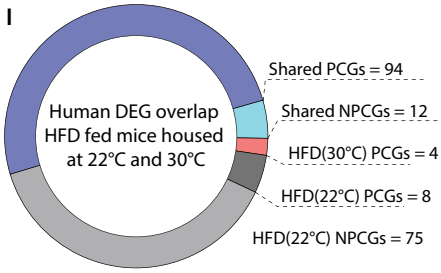

J

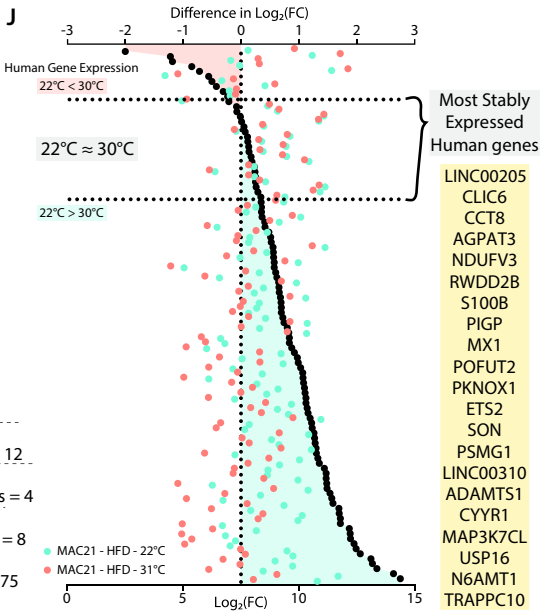

Fig. SI

Mice fed a standard chow, housed at room temperature (22°C)

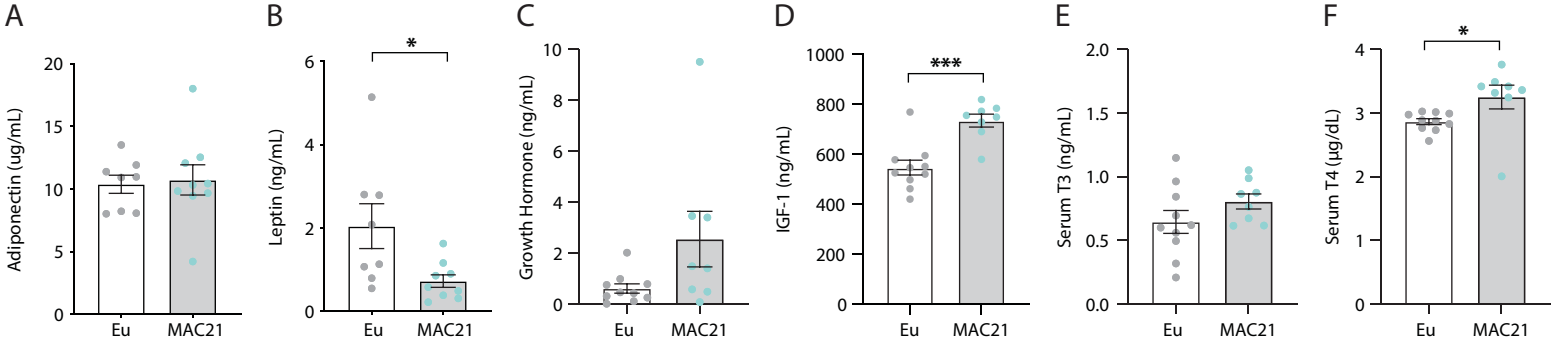

Mice fed an HFD, housed at room temperature (22°C)

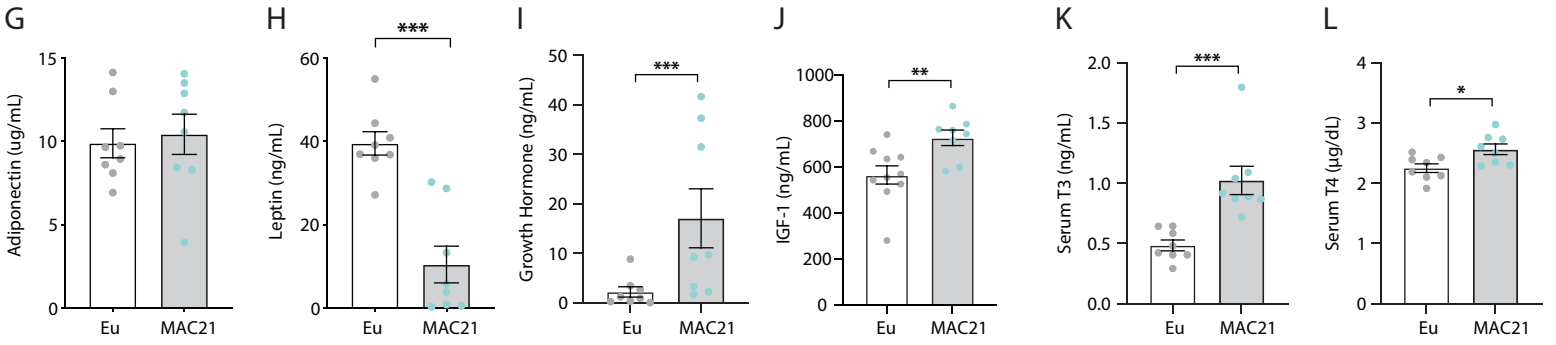

Mice fed an HFD, housed at thermoneutrality (31°C)

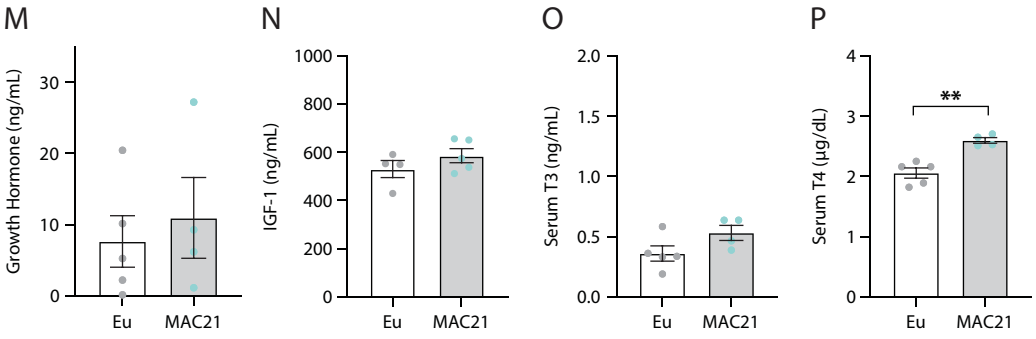

Figure S1. ELISA data from Euploid and MAC21 mice. Circulating levels of adiponectin (A), leptin (B), growth hormone (C), IGF-1 (D), thyroid hormone (T3, E), and thyroxine (T4, F) in chow-fed mice housed at room temperature (22°C). Circulating levels of adiponectin (G), leptin (H), growth hormone (I), IGF-1 (J), T3 (K), and T4 (L) in HFD-fed mice housed at 22°C. Circulating levels of growth hormone (M), IGF-1 (N), T3 (O), and T4 (P) in HFD-fed mice housed at thermoneutrality (30°C).

Fig. S2

Chow diet.

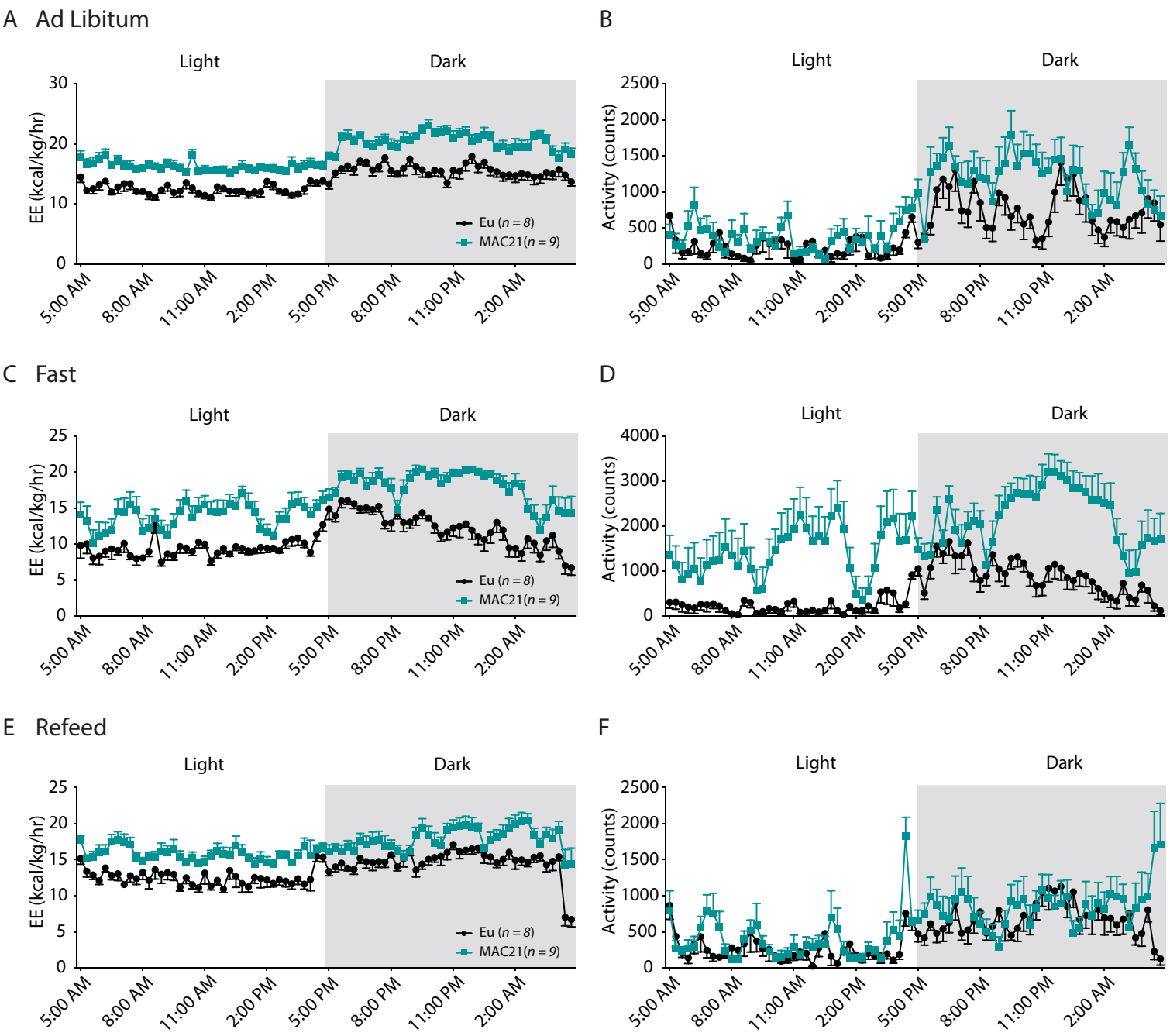

Figure S2. Indirect calorimetry of energy expenditure and physical activity in Euploid and MAC21 mice fed a standard chow. A-B) Energy expenditure (EE) and physical activity over a 24 h period in ad libitum chow-fed mice. **C-D)** Energy expenditure (EE) and physical activity over a 24 h period in fasted mice. **E-F)** Energy expenditure (EE) and physical activity over a 24 h period of refeeding after a fast.

Fig. S3

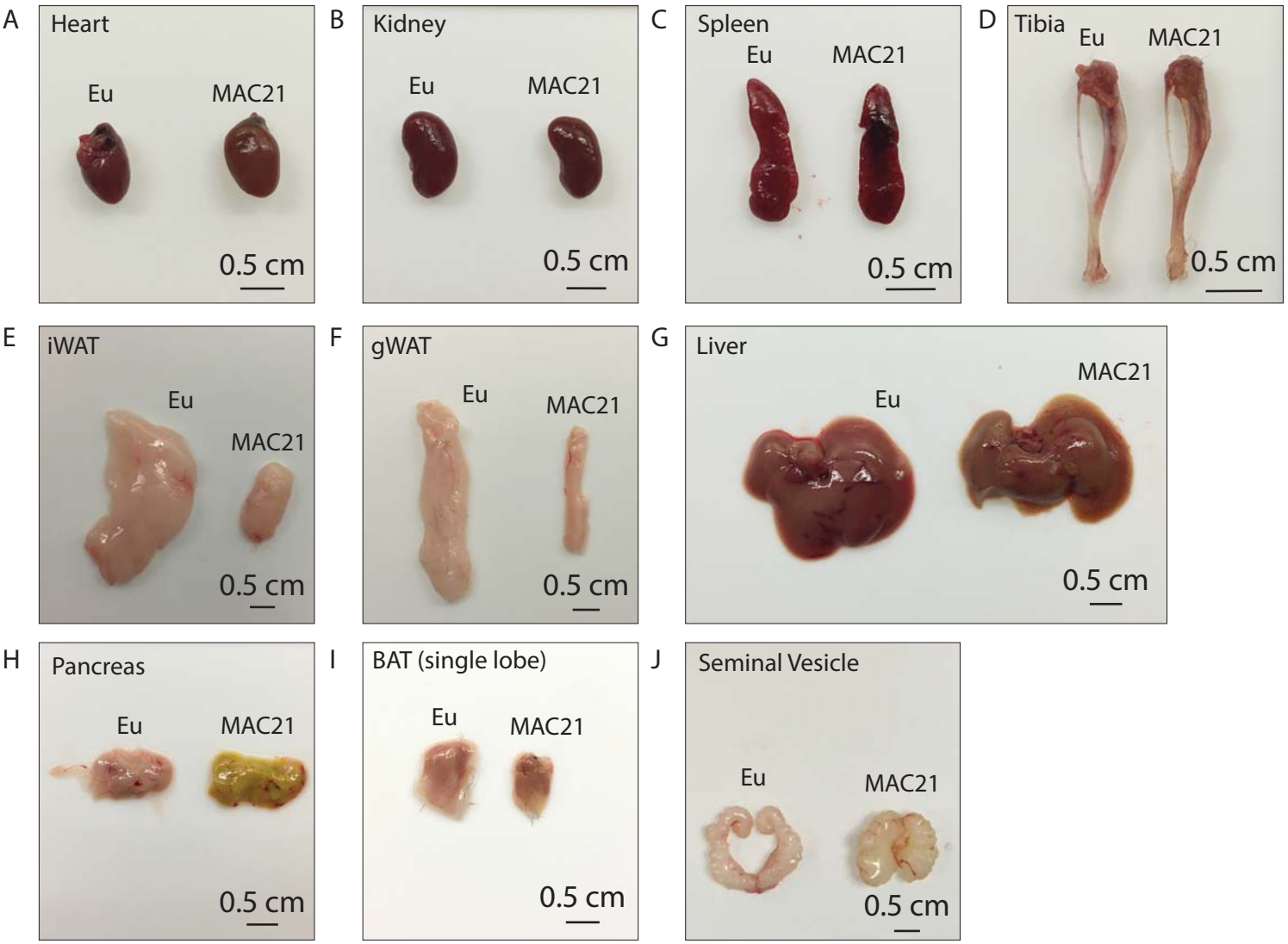

Figure S3. Representative tissue dissection images of Euploid and MAC21 mice fed a high-fat diet.

Representative side-by-side dissection images of **A)** heart, **B)** kidney, **C)** spleen, **D)** tibia, **E)** inguinal white adipose tissue (iWAT), **F)** gonadal white adipose tissue (gWAT), **G)** liver, **H)** pancreas, **I)** brown adipose tissue (BAT), and **J)** seminal vesicle. Mice were housed at ambient room temperature (22°C).

Fig. S4

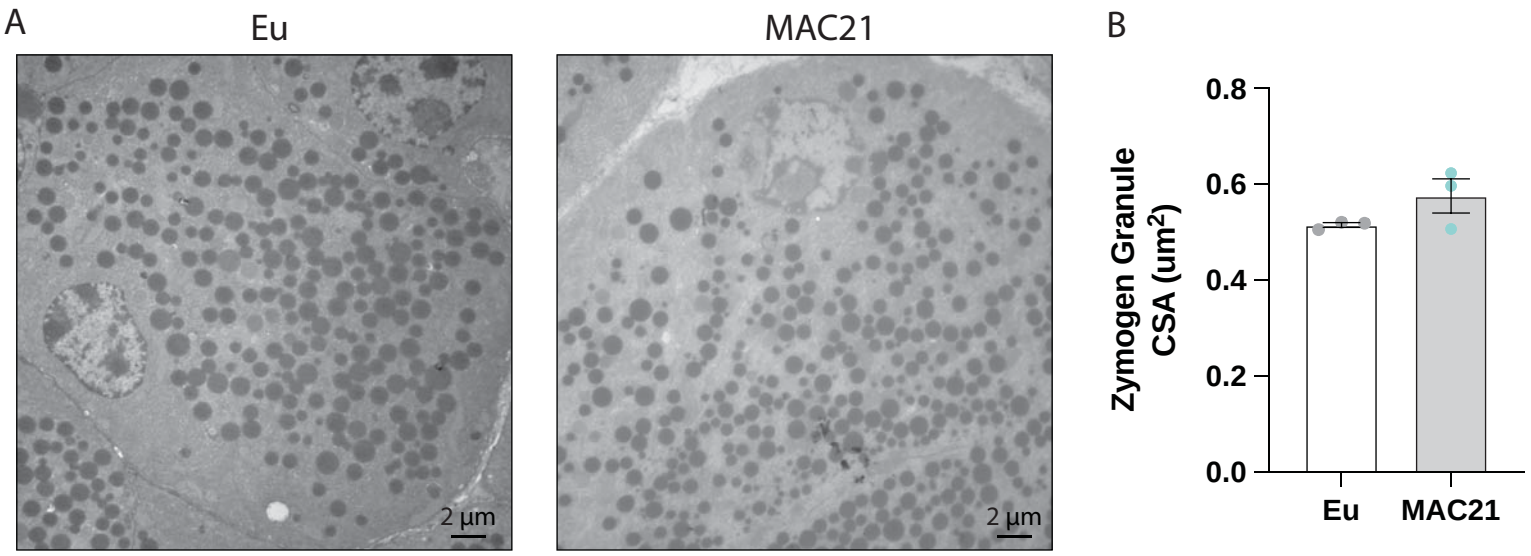

Figure S4. Electron micrograph quantification of pancreatic acinar cell zymogen granules. A and B) Representative Euploid and MAC21 acinar cells. **C)** Average zymogen granule cross-sectional area (CSA) quantification. Each data point represents a mouse average comprised of at least 3,600 zymogen granules from six unique locations within the pancreas. Analyses were performed on a total of 6 randomly selected HFD-fed mice (WT, $n = 3$; KO, $n = 3$).

Fig. S5

Fecal energy data from HFD-fed mice housed at 22°C

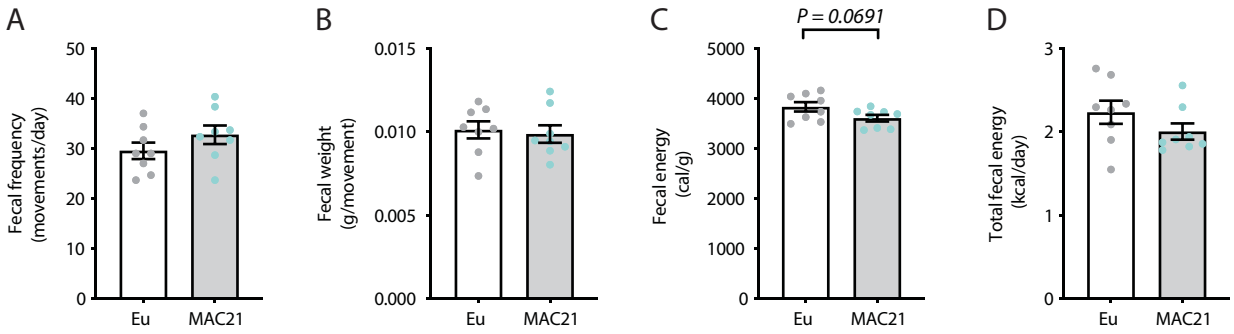

Fecal data from HFD-fed mice housed at thermoneutrality (30°C)

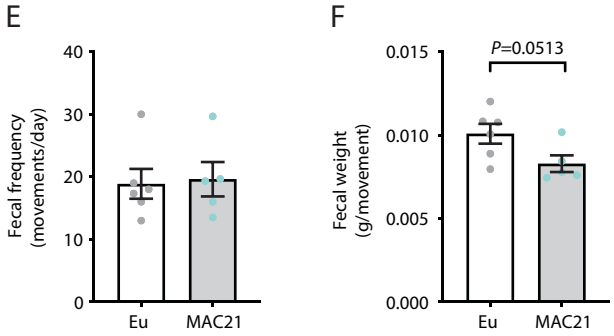

Figure S5. Fecal data from Euploid and MAC21 mice fed a high-fat diet at room temperature (22°C) or thermoneutrality (30°C). Fecal energy data from HFD-fed mice housed at room temperature (22°C) showing **A)** rate of fecal pellet production (bowel movement), **B)** Average fecal pellet weight, and **C-D)** Fecal energy composition as measure by fecal bomb calorimetry. Fecal data from mice fed a high-fat diet housed at thermoneutrality showing **E)** rate of fecal pellet production and **F)** average fecal weight per pellet.

Fig. S6

High-fat diet

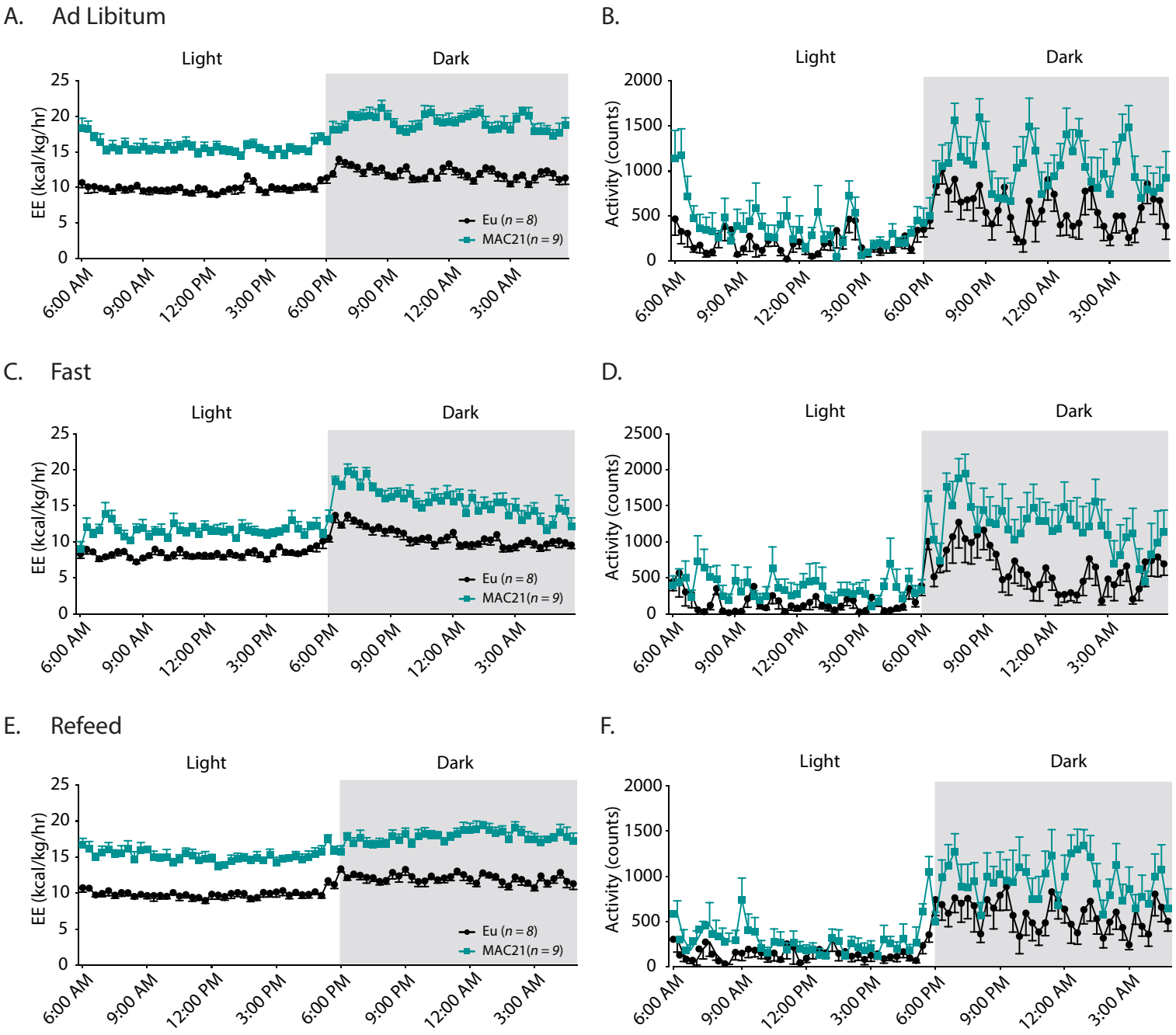

Figure S6. Indirect calorimetry of energy expenditure and physical activity in Euploid and MAC21 mice fed a high-fat diet. A-B) Energy expenditure (EE) and physical activity over a 24 h period in ad libitum HFD-fed mice. **C-D)** Energy expenditure (EE) and physical activity over a 24 h period in fasted mice. **E-F)** Energy expenditure (EE) and physical activity over a 24 h period of refeeding after a fast.

Fig. S7

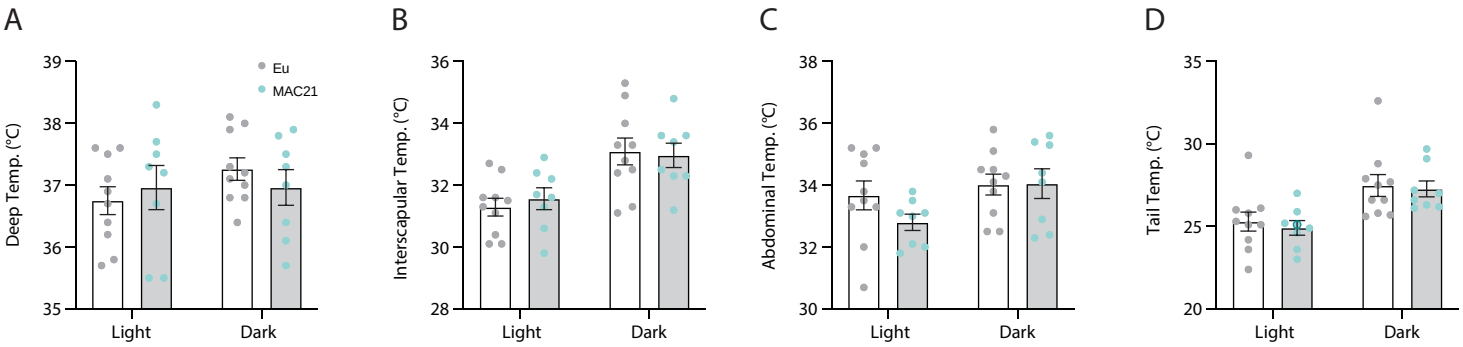

Figure S7. Light and dark cycle body temperature of Euploid and MAC21 mice fed a standard chow. A) Deep colonic temperature. **B)** Interscapular skin temperature. **C)** Abdominal Skin temperature. **D)** Tail skin temperature. Each data point represents the average of three days of independent data collection.

Fig. S8

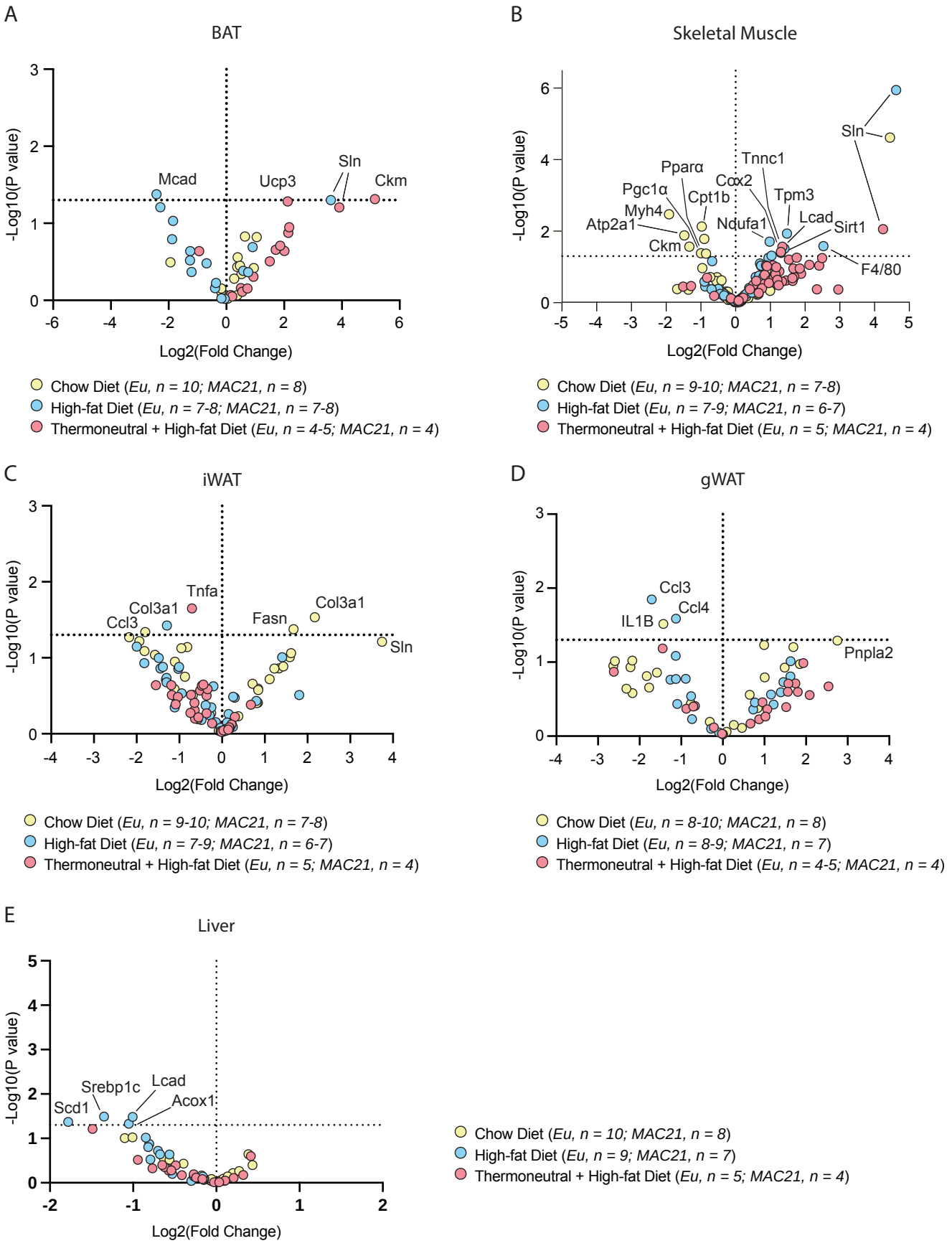

Figure S8. Volcano plot of all qPCR results from BAT, skeletal muscle, and white adipose tissue. Overlaid results of Euploid and MAC21 mice across all conditions assayed (chow diet at 22°C, high-fat diet at 22°C, and high-fat diet at 30°C) for **A)** Brown adipose tissue (BAT), **B)** Gastrocnemius (skeletal muscle), **C)** inguinal white adipose tissue (iWAT), **D)** gonadal white adipose tissue (gWAT), and **E)** Liver. Significant and/or relevant genes are labeled. Thermoneutral = 30°C housing condition.

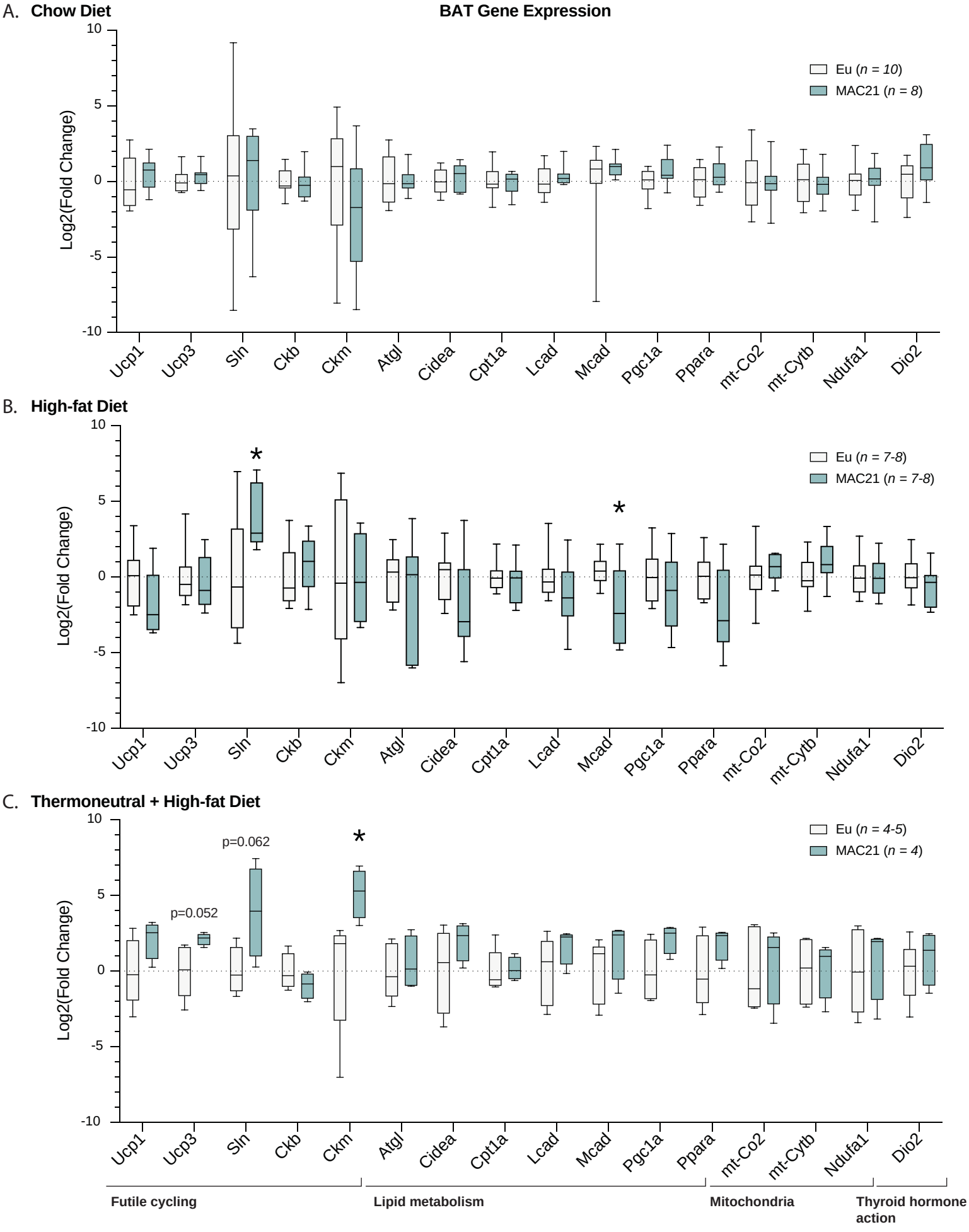

Figure S9. Gene expression analysis in brown adipose tissue. qPCR analysis of brown adipose tissue genes important for futile cycling, lipid metabolism, mitochondrial function, and thyroid hormone action in Euploid and MAC21 male mice fed a standard chow and housed at 22°C (A), fed a high-fat diet and housed at 22°C (B), and fed a high-fat diet and housed at thermoneutral 30°C (C)**.**

Fig. S10

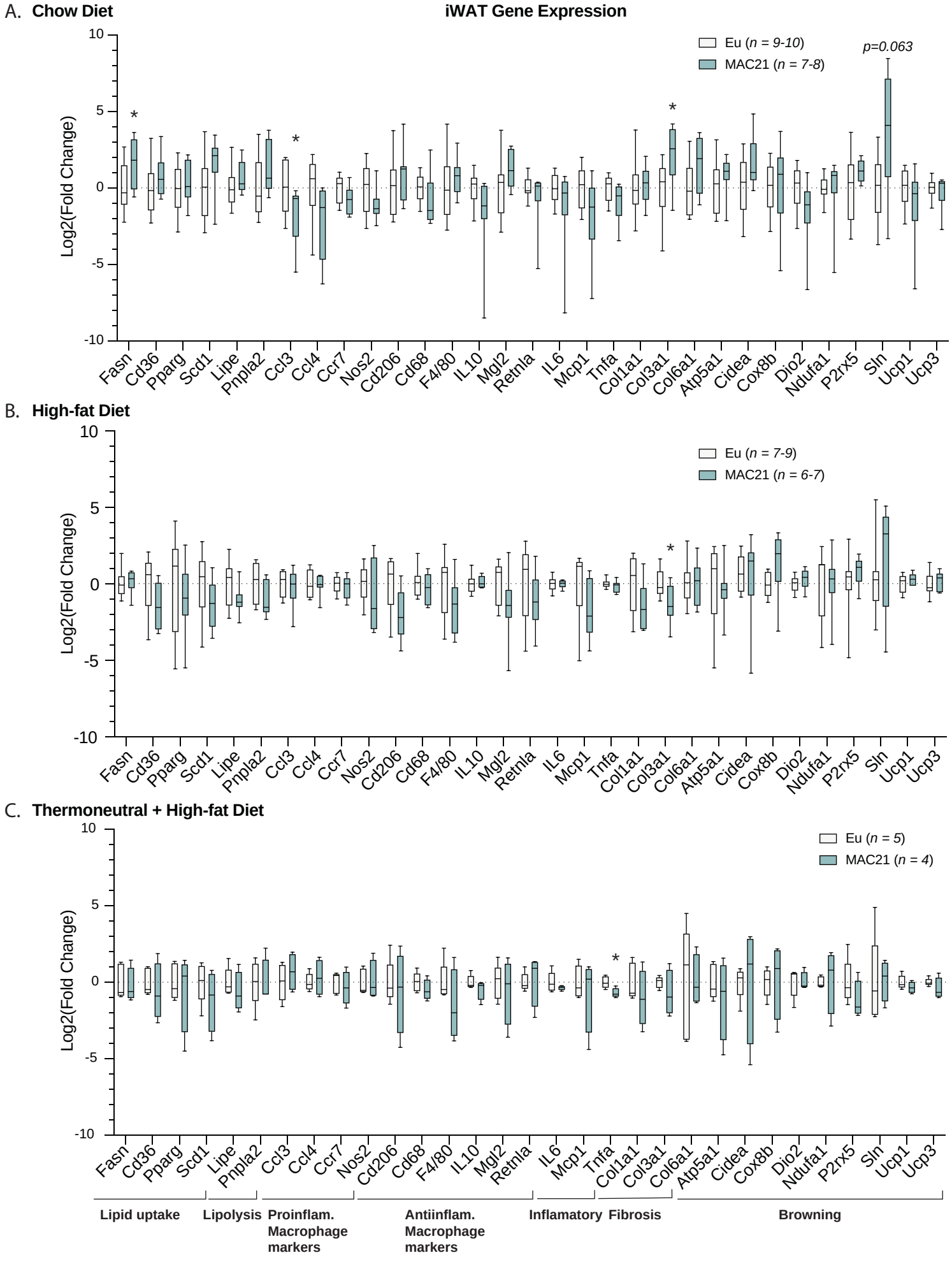

Figure S10. Gene expression analysis in inguinal white adipose tissue. qPCR analysis of inguinal white adipose tissue (iWAT) genes important for lipid uptake, lipolysis, inflammation, fibrosis, and browning in Euploid and MAC21 male mice fed a standard chow diet and housed at 22°C (A), fed a high-fat diet and housed at 22°C (B), and fed a high-fat diet and housed at thermoneutral 30°C (C)**.**

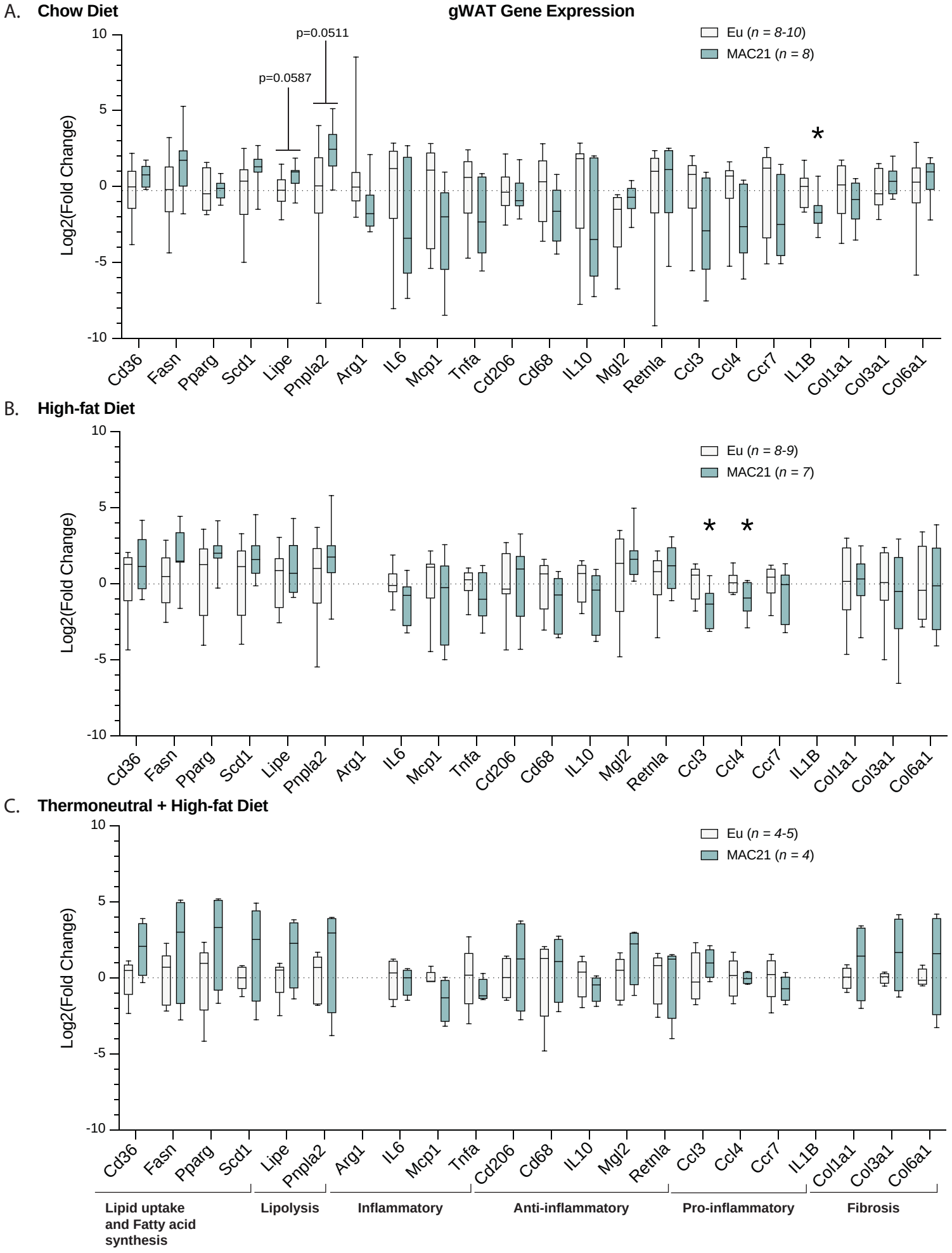

Figure S11. Gene expression analysis in gonadal white adipose tissue. qPCR analysis of gonadal white adipose tissue (gWAT) genes important for lipid uptake, fatty acid synthesis, lipolysis, inflammation, and fibrosis in Euploid and MAC21 male mice fed a standard chow diet and housed at 22°C (A), fed a high-fat diet and housed at 22°C (B), and fed a high-fat diet and housed at thermoneutral 30°C (C)**.**

Fig S2

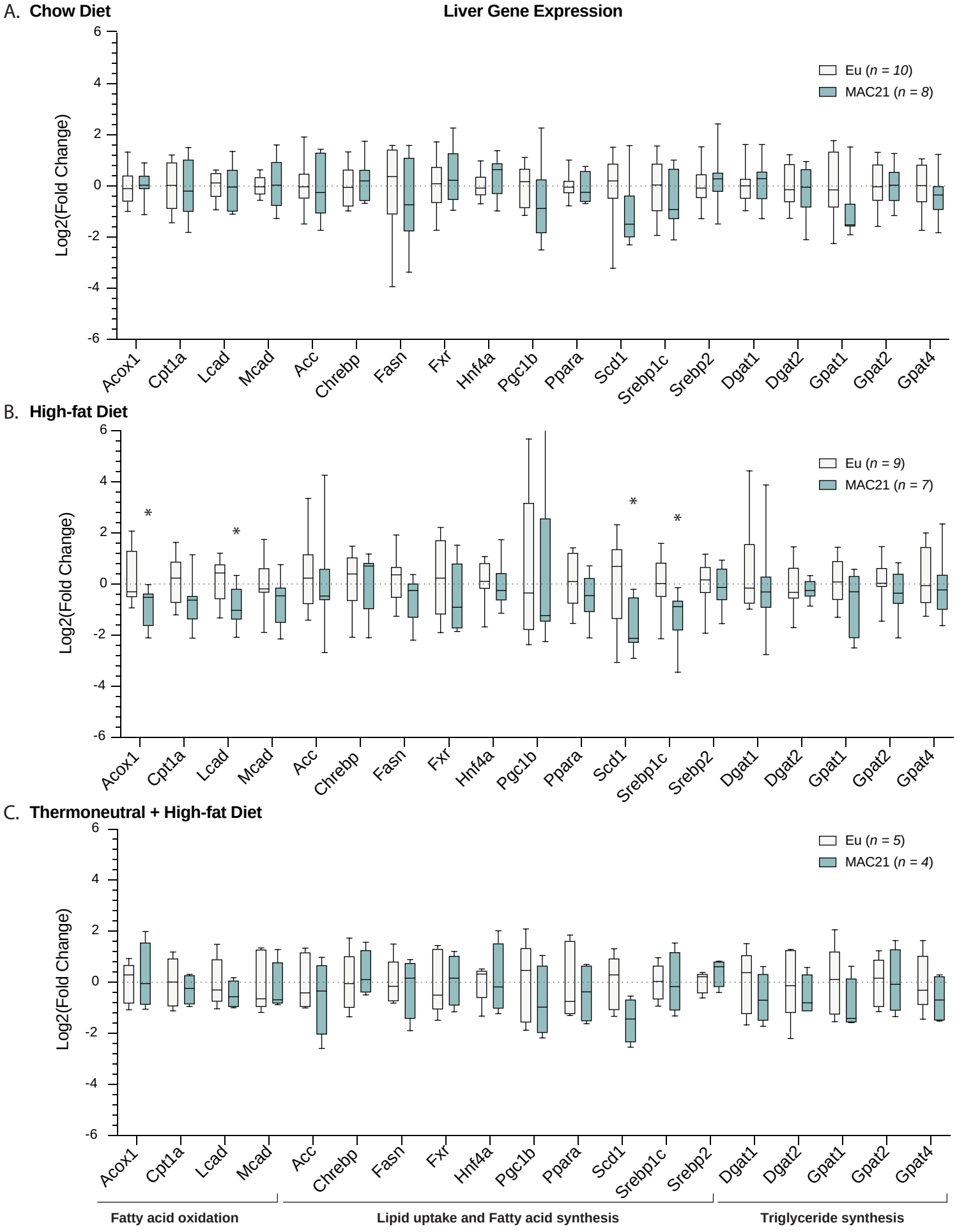

Figure S12. Gene expression analysis in liver. qPCR analysis of liver genes important for lipid uptake, fatty acid synthesis and oxidation, and triglyceride synthesis in Euploid and MAC21 male mice fed a standard chow and housed at 22°C (A), fed a high-fat diet and housed at 22°C (B), and fed a high-fat diet and housed at thermoneutral 30°C (C)**.**

Fig. 9F3

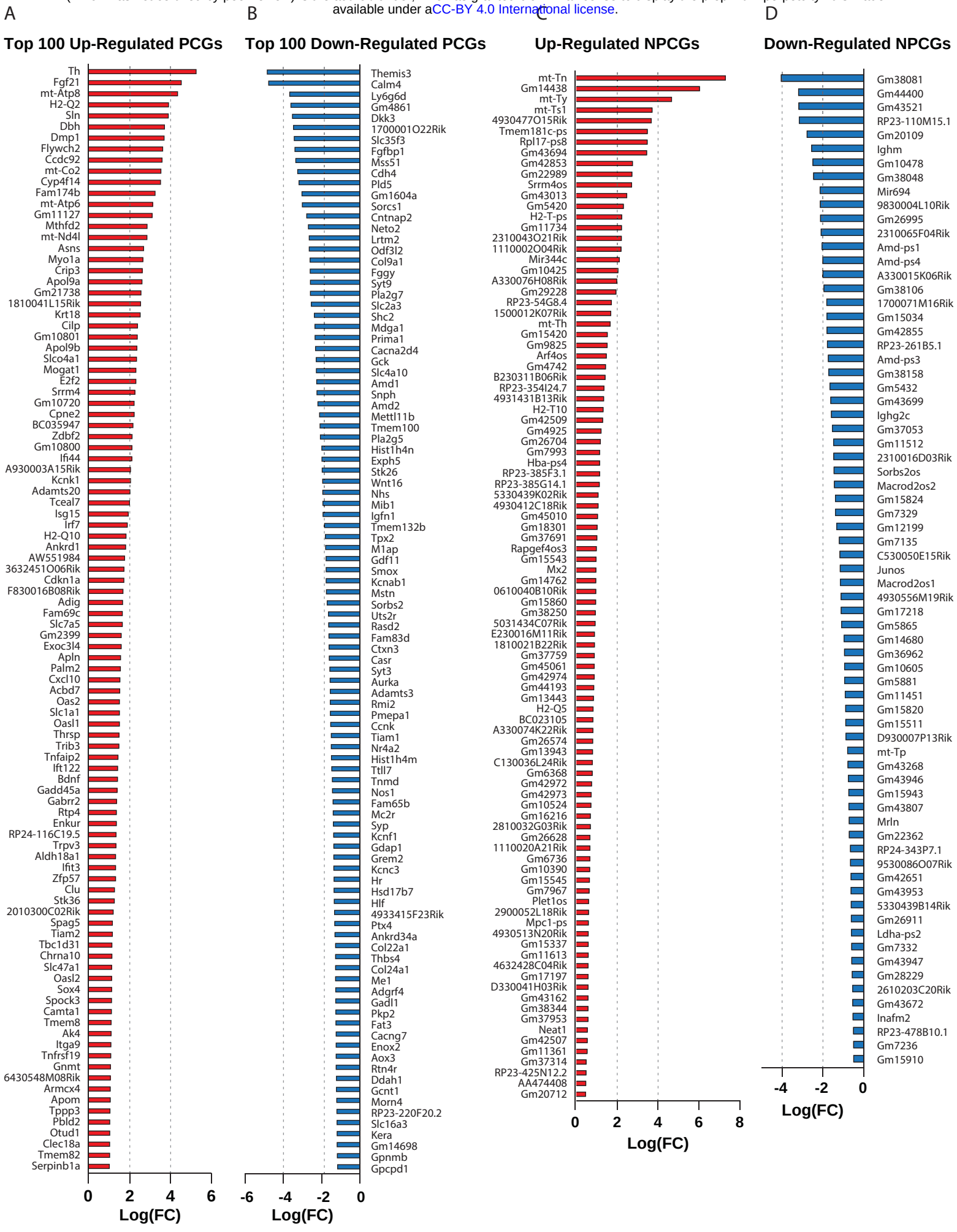

Figure S13. The top up- and down-regulated genes in skeletal muscle based on RNA-seq data. A) Top 100 up-regulated protein-coding genes. **B)** Top 100 down-regulated protein-coding genes. **C)** All up-regulated non-protein-coding genes. **D)** All down-regulated non-protein-coding genes. *n* = 5 Euploid and 4 MAC21 for RNA-sequencing experiments. All mice were fed a high-fat diet and housed at ambient room temperature (22°C).

Fig 3/4

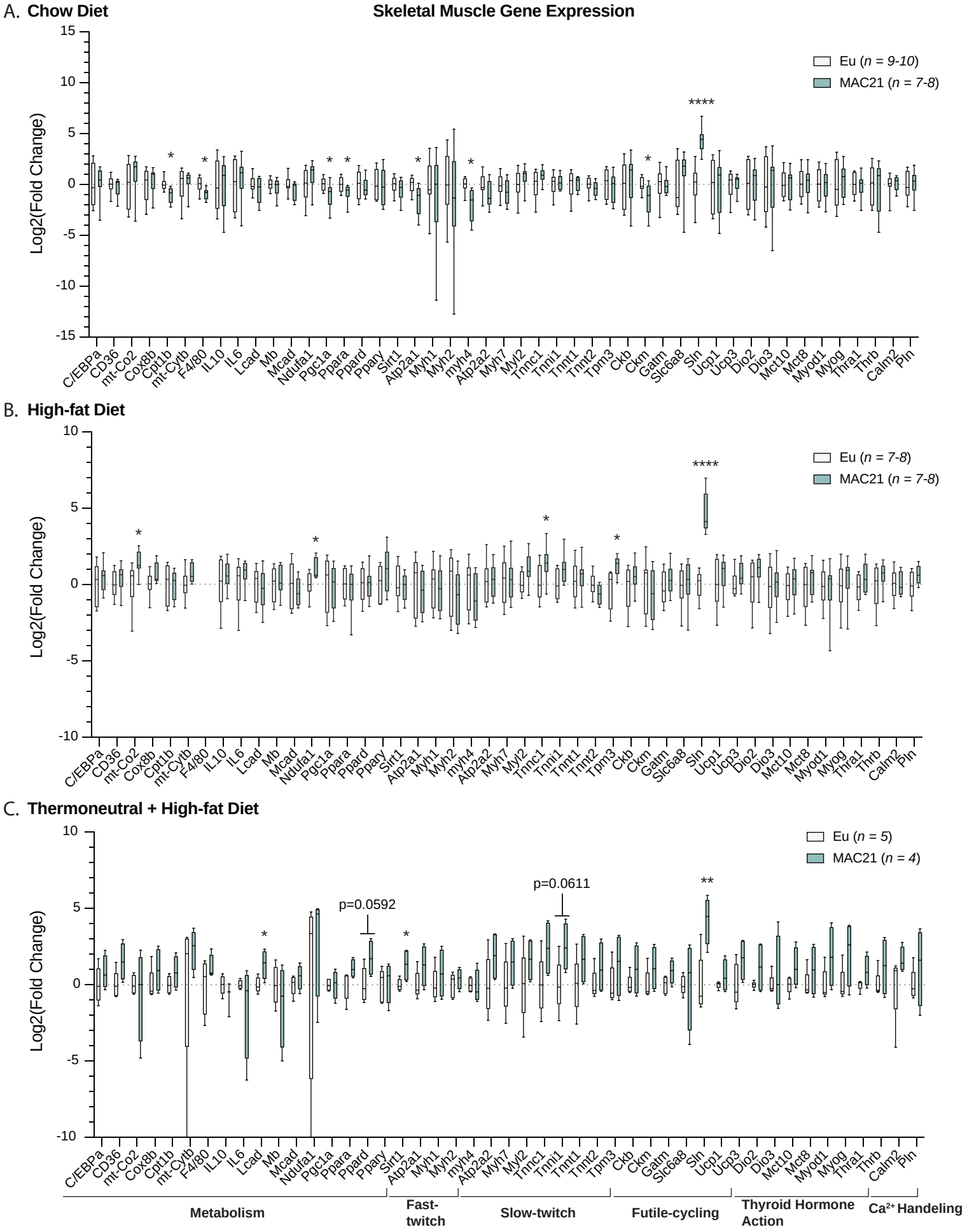

Figure S14. Gene expression analysis in skeletal muscle. qPCR analysis of gastrocnemius skeletal muscle genes important for general metabolism, fast- and slow-twitch fiber types, futile cycling, thyroid hormone action, and calcium handling in Euploid and MAC21 male mice fed a standard chow diet and housed at 22°C (A), fed a high-fat diet and housed at 22°C (B), and fed a high-fat diet and housed at thermoneutral 30°C (C)**.**

Fig. S15

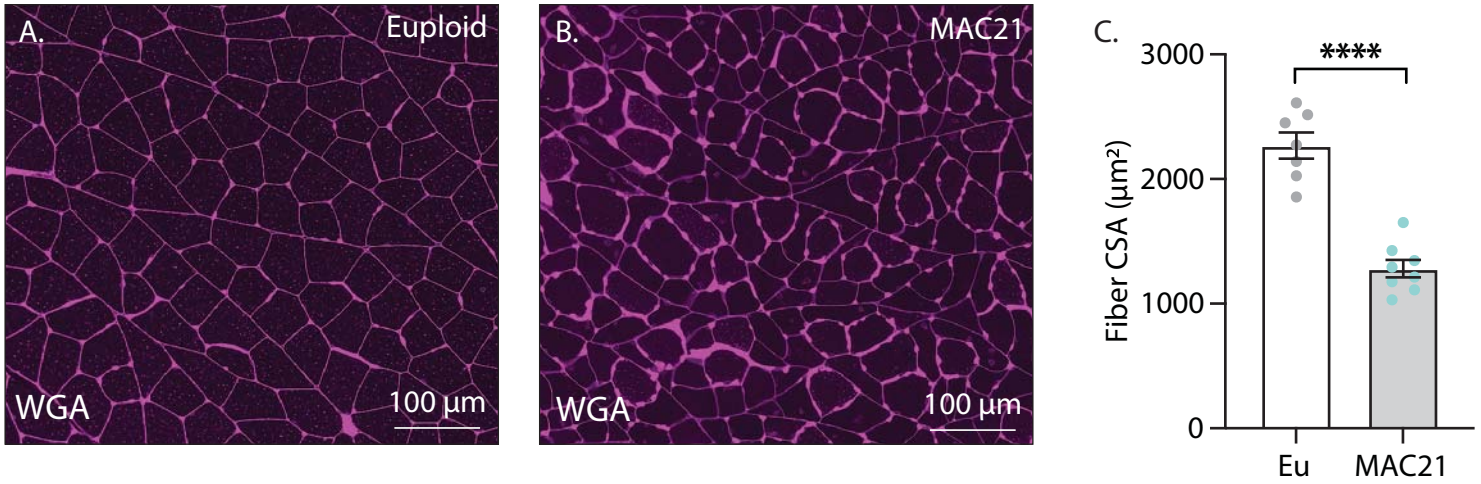

Figure S15. Skeletal muscle cross-sectional area analysis of MAC21 and Euploid mice fed a high-fat diet. A-B) Representative wheat-germ agglutinin (WGA) stained gastrocnemius skeletal muscle samples**. C)** Muscle fiber cross-sectional area (CSA) analysis. Mice were housed at ambient room temperature (22°C).

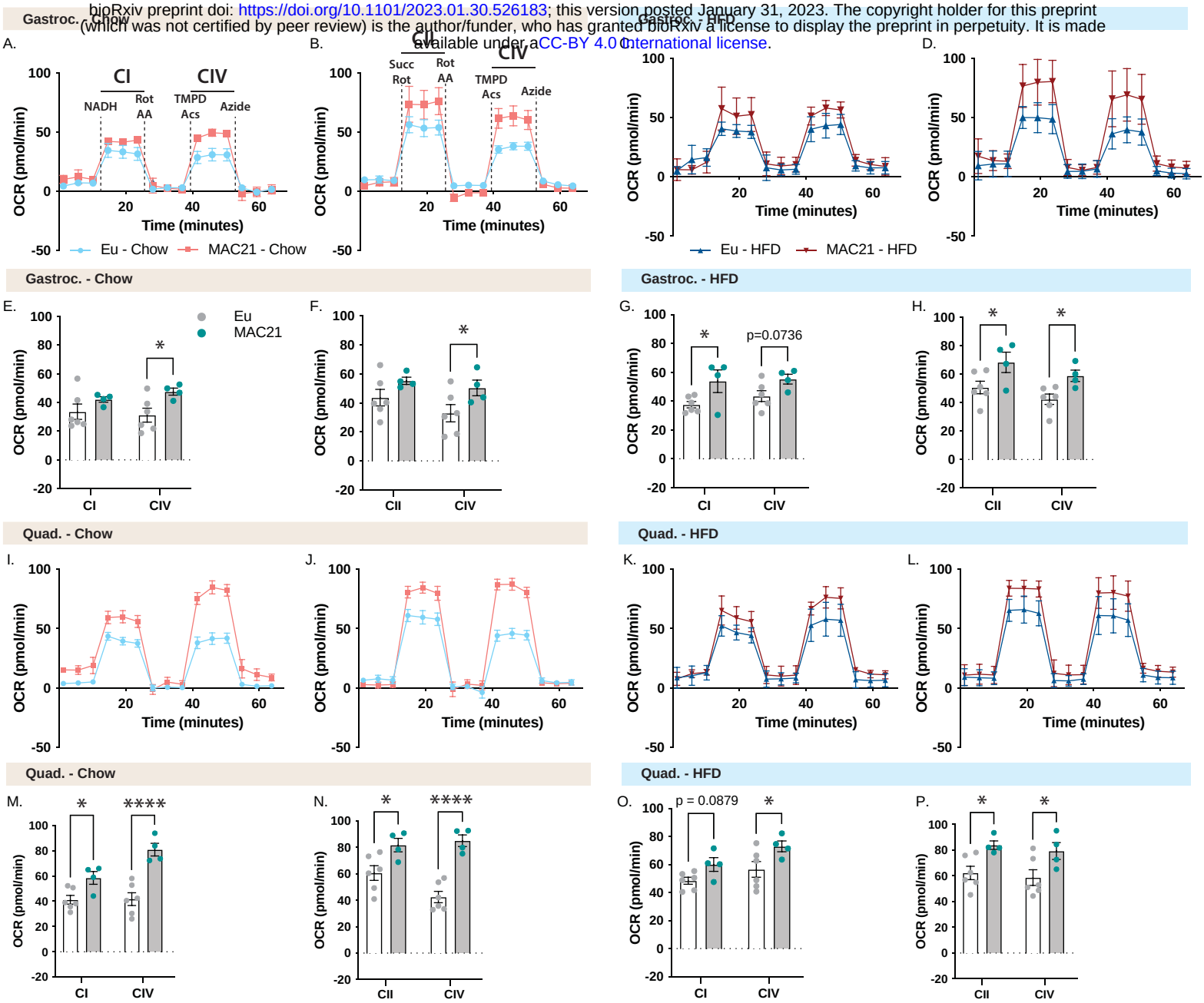

Fig. S16

Figure S16. Mitochondrial respirometry analysis of gastrocnemius and quadricep muscle. A and C) Average group gastrocnemius (Gastroc) oxygen consumption rate (OCR) traces using NADH as a substrate for Euploid (Eu) and MAC21 male mice fed a standard chow or high-fat diet (HFD), respectively. **B and D)** Average group Gastroc OCR traces using succinate as a substrate in the presence of rotenone (Rot) for Euploid and MAC21 mice fed a standard chow or HFD, respectively. **E and G)** Mitochondrial complex I, and IV OCR quantification for A and C, respectively. **F and H)** Mitochondrial complex II and IV OCR quantification for B and D, respectively. **I and K)** Average group quadricep (Quad) OCR traces using NADH as a substrate for Euploid and MAC21 mice fed a standard chow or HFD, respectively. **J and L)** Average group Quad OCR traces using succinate as a substrate in the presence of rotenone (Rot) for Euploid and MAC21 mice fed a standard chow or HFD, respectively. **M and O)** Mitochondrial complex I and IV OCR quantification for I and K, respectively. **N and P)** Mitochondrial complex II and IV OCR quantification for J and L, respectively. All mice used for respirometry were house at ambient room temperature (22°C). AA, antimycin A; TMPD, N,N,N',N'-tetramethyl-p-phenylenediamine; Acs, ascorbate; CI, mitochondrial complex I; CII, mitochondrial complex II; CIV, mitochondrial complex IV.

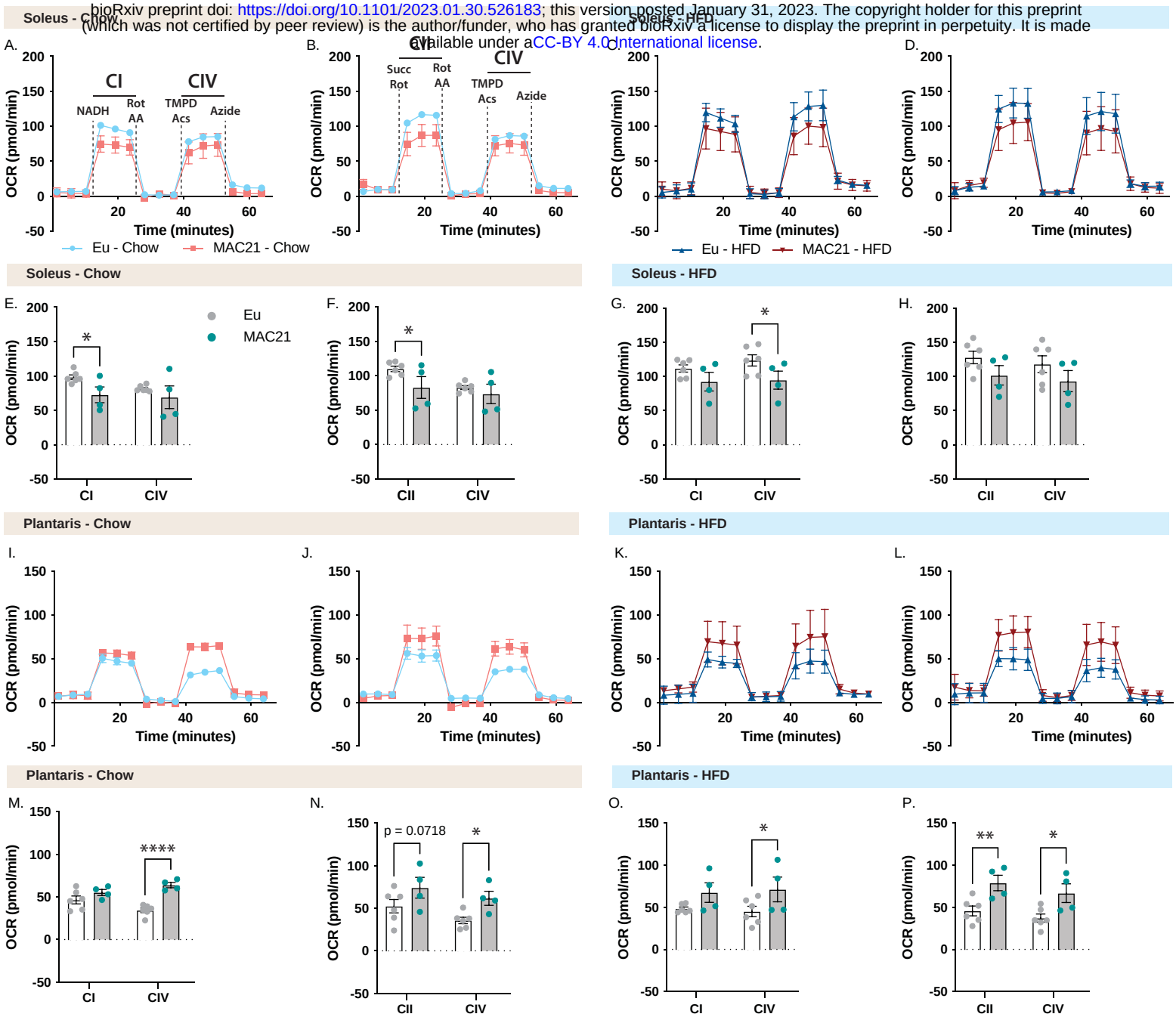

Fig. S17

Figure S17. Mitochondrial respirometry analysis of soleus and plantaris muscle. A and C) Average group soleus oxygen consumption rate (OCR) traces using NADH as a substrate for Euploid (Eu) and MAC21 male mice fed a standard chow or high-fat diet (HFD), respectively. **B and D)** Average group soleus OCR traces using succinate as a substrate in the presence of Rotenone (Rot) for Euploid and MAC21 mice fed a standard chow or HFD, respectively. **E and G)** Mitochondrial complex I and IV OCR quantification for A and C, respectively. **F and H)** Mitochondrial complex II and IV OCR quantification for B and D, respectively. **I and K)** Average group plantaris OCR traces using NADH as a substrate for Euploid and MAC21 mice fed a standard chow or HFD, respectively. **J and L)** Average group plantaris OCR traces using succinate as a substrate in the presence of rotenone (Rot) for Euploid and MAC21 mice fed a standard chow or HFD, respectively. **M and O)** Mitochondrial complex I and IV OCR quantification for I and K, respectively. **N and P)** Mitochondrial complex II and IV OCR quantification for J and L, respectively. All mice used for respirometry were house at ambient room temperature (22°C). AA, antimycin A; TMPD, N,N,N',N'-tetramethyl-p-phenylenediamine; Acs, ascorbate; CI, mitochondrial complex I; CII, mitochondrial complex II; CIV, mitochondrial complex IV.

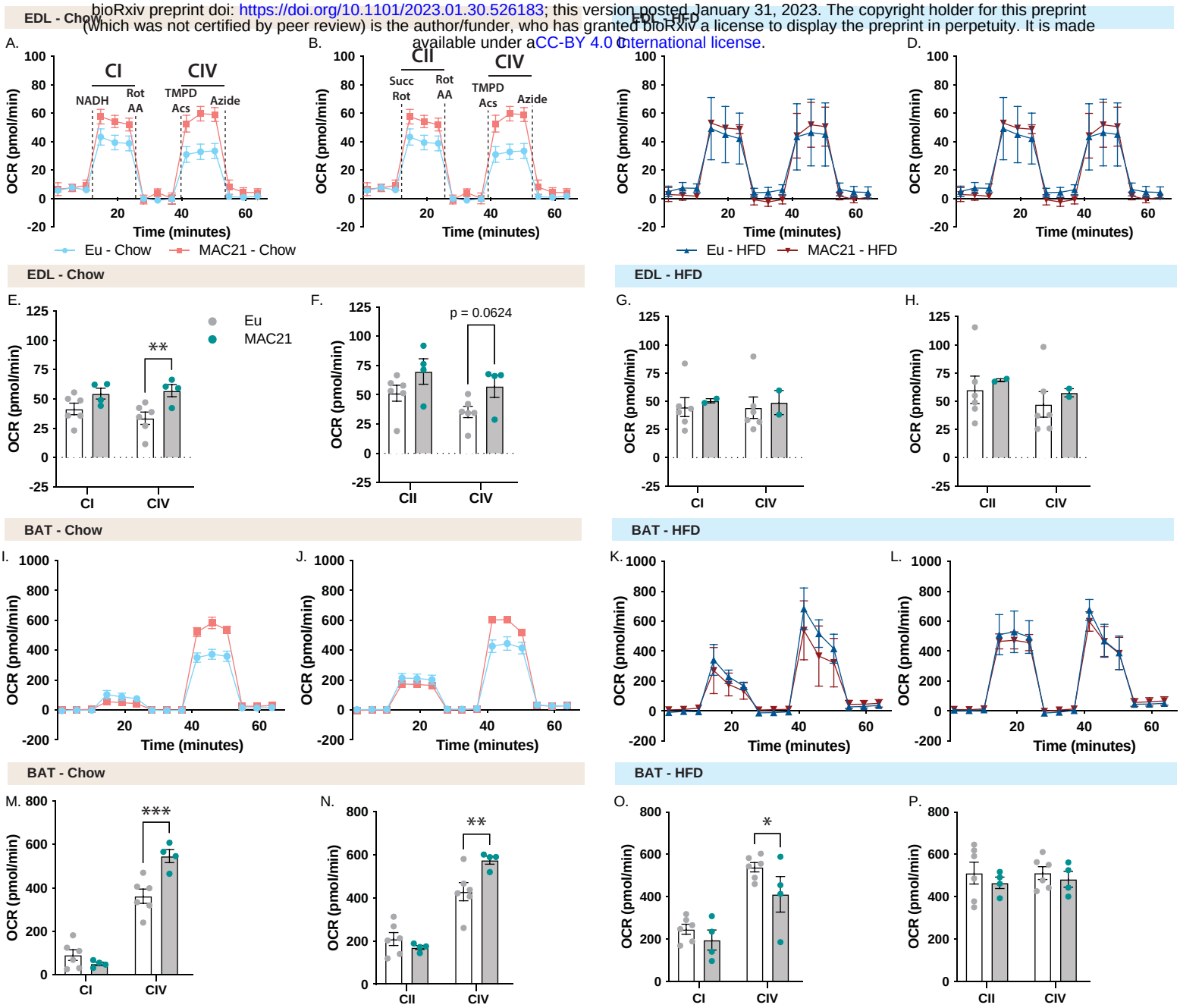

Fig. S18

Figure S18. Mitochondrial respirometry analysis of EDL and BAT. A and C) Average group extensor digitorum longus (EDL) oxygen consumption rate (OCR) traces using NADH as a substrate for Euploid (Eu) and MAC21 male mice fed a standard chow or high-fat diet (HFD), respectively. **B and D)** Average group EDL OCR traces using succinate as a substrate in the presence of rotenone (Rot) for Euploid and MAC21 mice fed a standard chow or HFD, respectively. **E and G)** Mitochondrial complex I and IV OCR quantification for A and C, respectively. **F and H)** Mitochondrial complex II and IV OCR quantification for B and D, respectively. **I and K)** Average group brown adipose tissue (BAT) OCR traces using NADH as a substrate for Euploid and MAC21 mice fed a standard chow or HFD, respectively. **J and L)** Average group brown adipose tissue (BAT) OCR traces using succinate as a substrate in the presence of rotenone (Rot) for Euploid and MAC21 mice fed a standard chow or HFD, respectively. **M and O)** Mitochondrial complex I and IV OCR quantification for I and K, respectively. **N and P)** Mitochondrial complex II and IV OCR quantification for J and L, respectively. All mice used for respirometry were house at ambient room temperature (22°C). AA, antimycin A; TMPD, N,N,N',N'-tetramethyl-p-phenylenediamine; Acs, ascorbate; CI, mitochondrial complex I; CII, mitochondrial complex II; CIV, mitochondrial complex IV.

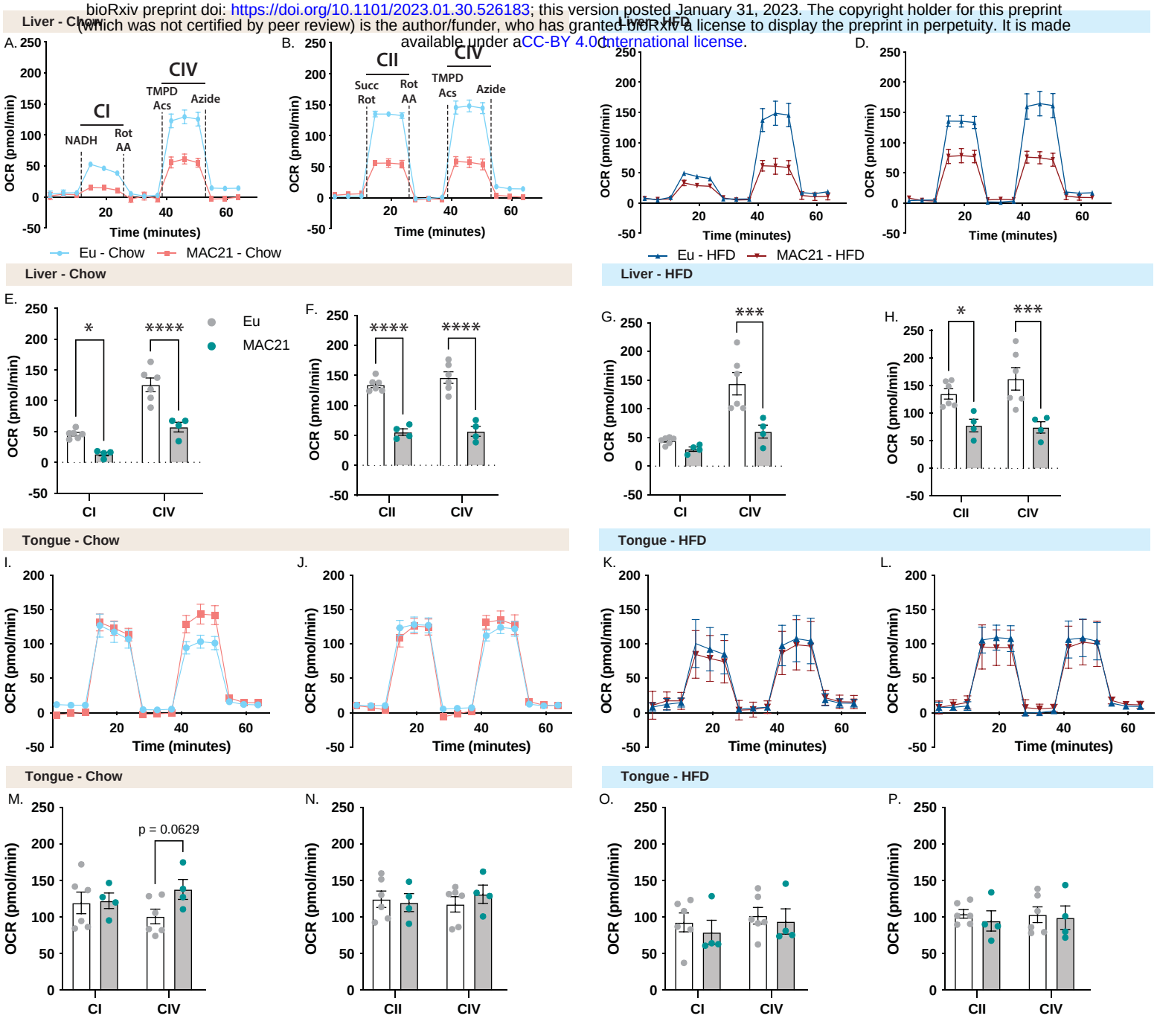

Fig. S19

Figure S19. Mitochondrial respirometry analysis of liver and tongue. A and C) Average group liver oxygen consumption rate (OCR) traces using NADH as a substrate for Euploid (Eu) and MAC21 male mice fed a standard chow or high-fat diet (HFD), respectively. **B and D)** Average group liver OCR traces using succinate as a substrate in the presence of rotenone (Rot) for Euploid and MAC21 mice fed a standard chow or HFD, respectively. **E and G)** Mitochondrial complex I and IV OCR quantification for A and C, respectively. **F and H)** Mitochondrial complex II and IV OCR quantification for B and D, respectively. **I and K)** Average group tongue OCR traces using NADH as a substrate for Euploid and MAC21 mice fed a standard chow or HFD, respectively. **J and L)** Average group tongue OCR traces using succinate as a substrate in the presence of rotenone (Rot) for Euploid and MAC21 mice fed a standard chow or HFD, respectively. **M and O)** Mitochondrial complex I and IV OCR quantification for I and K, respectively. **N and P)** Mitochondrial complex II and IV OCR quantification for J and L, respectively. All mice used for respirometry were house at ambient room temperature (22°C). AA, antimycin A; TMPD, N,N,N',N'-tetramethyl-p-phenylenediamine; Acs, ascorbate; CI, mitochondrial complex I; CII, mitochondrial complex II; CIV, mitochondrial complex IV.

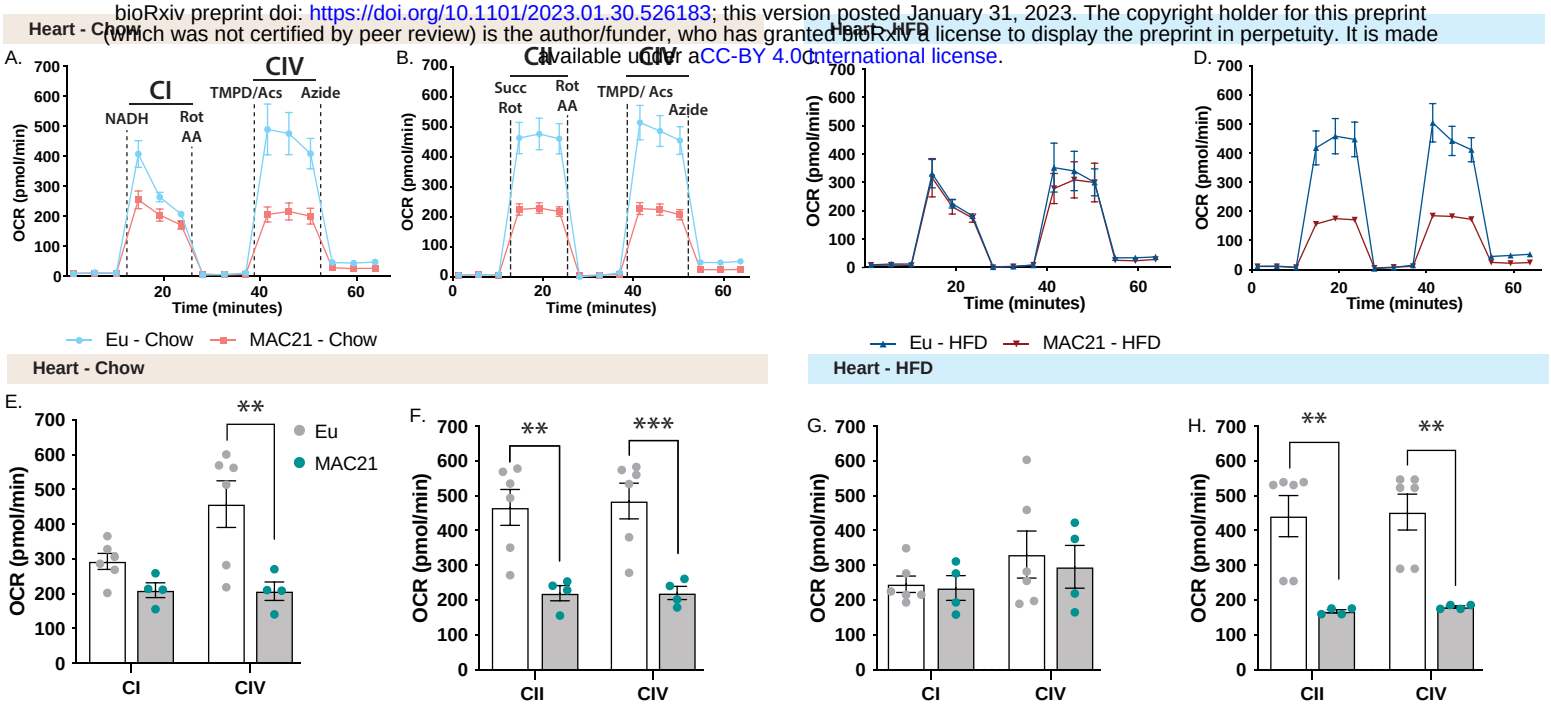

Fig. S20

Figure S20. Mitochondrial respirometry analysis of heart. A and C) Average group heart oxygen consumption rate (OCR) traces using NADH as a substrate for Euploid (Eu) and MAC21 male mice fed a standard chow or high-fat diet (HFD), respectively. **B and D)** Average group heart OCR traces using succinate as a substrate in the presence of rotenone (Rot) for Euploid and MAC21 mice fed a standard chow or HFD, respectively. **E and G)** Mitochondrial complex I and IV OCR quantification for A and C, respectively. **F and H)** Mitochondrial complex II and IV OCR quantification for B and D, respectively. All mice used for respirometry were house at ambient room temperature (22°C). AA, antimycin A; TMPD, N,N,N',N'-tetramethyl-p-phenylenediamine; Acs, ascorbate; CI, mitochondrial complex I; CII, mitochondrial complex II; CIV, mitochondrial complex IV.

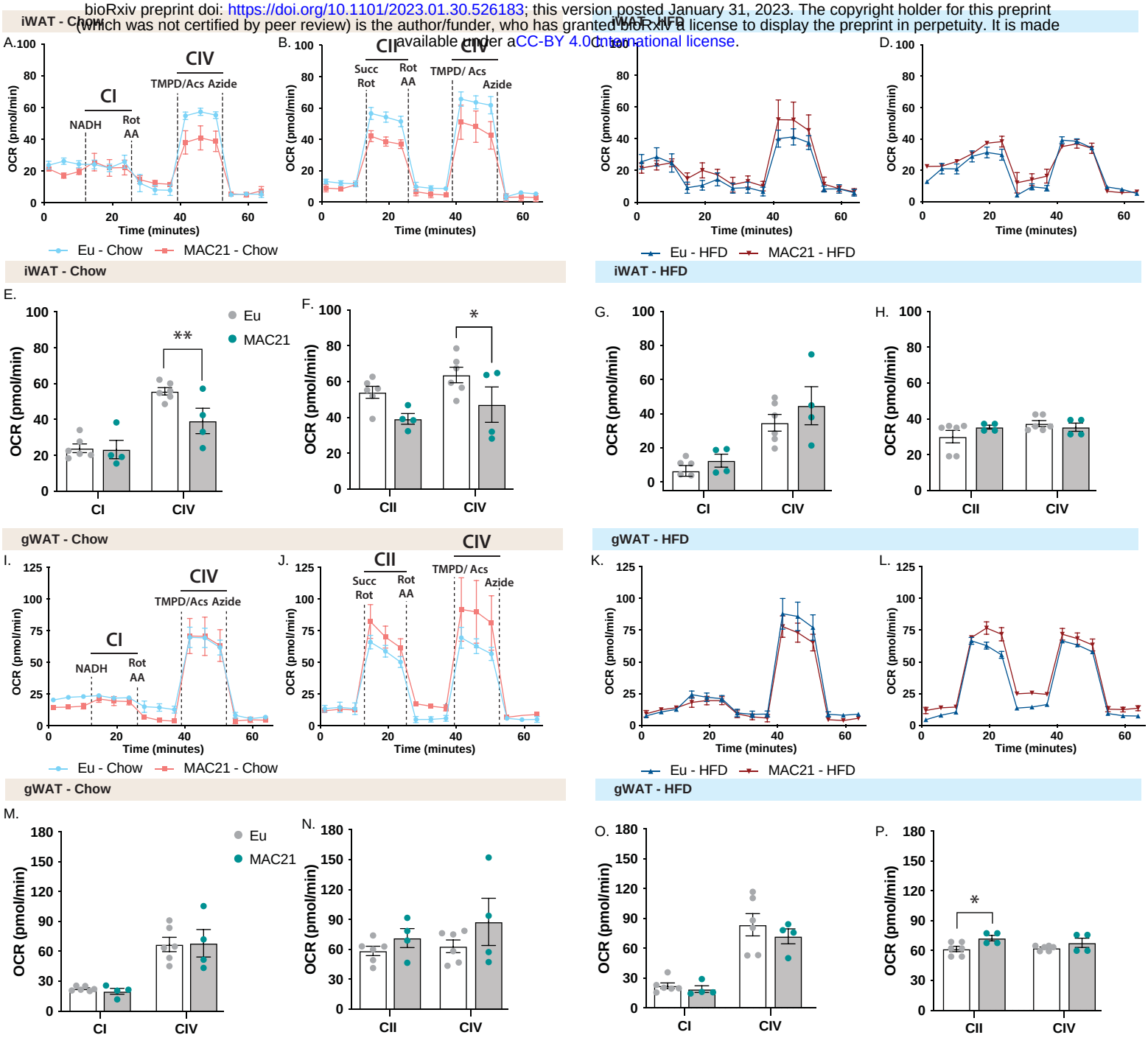

Fig. S21

Figure S21. Mitochondrial respirometry analysis of inguinal (iWAT) and gonadal (gWAT) white adipose tissue. A and C) Average group iWAT oxygen consumption rate (OCR) traces using NADH as a substrate for Euploid (Eu) and MAC21 male mice fed a standard chow or high-fat diet (HFD), respectively. **B and D)** Average group liver OCR traces using succinate as a substrate in the presence of rotenone (Rot) for Euploid and MAC21 mice fed a standard chow or HFD, respectively. **E and G)** Mitochondrial complex I and IV OCR quantification for A and C, respectively. **F and H)** Mitochondrial complex II and IV OCR quantification for B and D, respectively. **I and K)** Average group gWAT OCR traces using NADH as a substrate for Euploid and MAC21 mice fed a standard chow or HFD, respectively. **J and L)** Average group gWAT OCR traces using succinate as a substrate in the presence of rotenone (Rot) for Euploid and MAC21 mice fed a standard chow or HFD, respectively. **M and O)** Mitochondrial complex I and IV OCR quantification for I and K, respectively. **N and P)** Mitochondrial complex II and IV OCR quantification for J and L, respectively. All mice used for respirometry were house at ambient room temperature (22°C). AA, antimycin A; TMPD, N,N,N',N'-tetramethyl-p-phenylenediamine; Acs, ascorbate; CI, mitochondrial complex I; CII, mitochondrial complex II; CIV, mitochondrial complex IV.

Fig. S22

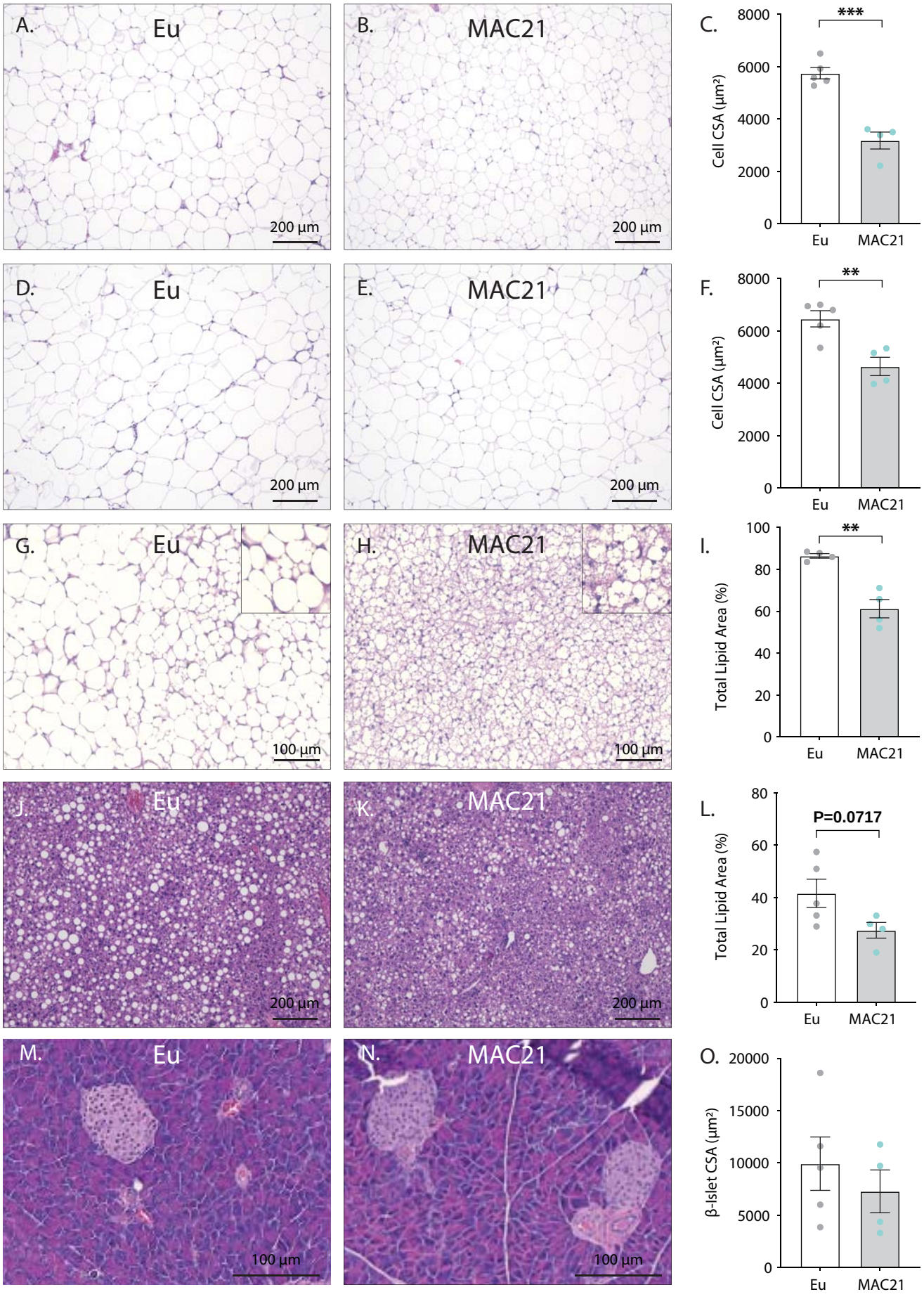

Figure S22. Histology of HFD-fed Euploid and MAC21 mice housed at thermoneutrality (30°C). Representative hematoxylin and eosin (H&E) stained sections of inguinal white adipose tissue (iWAT, A-B), gonadal white adipose tissue (gWAT, D and E), brown adipose tissue (BAT, H and I), liver (J and K), and pancreas (M and N). **C)** Average iWAT adipocyte cross-sectional area (CSA) quantification. **F)** Average gWAT adipocyte CSA quantification. **I)** Average BAT area covered by lipid droplets per focal plane. **L)** Average liver area covered by lipid droplets per focal plane. **O)** Average pancreas β-islet CSA quantification.

Table S1. Tissue weights of chow-fed Euploid and MAC21 male mice at termination of the study.

	Eu	MAC21	*P*
N	7	6	
BW (g)	**47.17 ± 3.73**	**26.77 ± 3.14**	**0.002**
gWAT (g)	**1.47 ± 0.29**	**0.60 ± 0.19**	**0.040**
iWAT (g)	1.15 ± 0.30	0.43 ± 0.20	0.080
Liver (g)	**2.42 ± 0.31**	**1.54 ± 0.18**	**0.034**
Pancreas (g)	0.30 ± 0.02	0.27 ± 0.01	0.109
Kidney (g)	0.19 ± 0.01	0.15 ± 0.02	0.051
Heart (g)	**0.16 ± 0.01**	**0.14 ± 0.01**	**0.025**

Eu: Euploid; BW: body weight; gWAT: gondal white adipose tissue; iWAT: inguinal white adipose tissue; BAT: brown adipose tissue

Table S2. Indirect calorimetry analysis of male (16.5 weeks of age) Euploid and MAC21 littermate mice fed a standard chow

	Eu	MAC21	*P*	Eu	MAC21	*P*	Eu	MAC21	*P*
Low-fat chow diet (Male)	***Ad-libitum* (dark cycle)**			***Ad-libitum* (light cycle)**			***Ad-libitum* (24 hr)**		
N	8	9		8	9		8	9	
Body weight (g)							**28.9 ± 1.09**	**20.6 ± 0.29**	**<0.001**
Food intake (kcal)	9.76 ± 0.65	10.66 ± 0.58	0.320	2.44 ± 0.45	2.67 ± 0.20	0.639	12.2 ± 0.92	13.3 ± 0.56	0.302
VO2 (mL/kg lean mass/h)	**4381 ± 180**	**5674 ± 69**	**<0.001**	**3589 ± 123**	**4616 ± 83**	**<0.001**	**3984 ± 151**	**5145 ± 79**	**<0.001**
VCO2 (mL/kg lean mass/h)	**4231 ± 182**	**5600 ± 97**	**<0.001**	**3158 ± 122**	**4170 ± 109**	**<0.001**	**3695 ± 150**	**4889 ± 81**	**<0.001**
RER (VCO2/VO2)	**0.96 ± 0.006**	**0.99 ± 0.007**	**0.030**	0.88 ± 0.008	0.90 ± 0.010	0.099	**0.92 ± 0.006**	**0.94 ± 0.005**	**0.011**
EE (kcal/kg lean mass/h)	**21.9 ± 0.91**	**28.5 ± 0.49**	**<0.001**	**17.6 ± 0.62**	**22.7 ± 0.45**	**<0.001**	**19.8 ± 0.76**	**25.6 ± 0.40**	**<0.001**
Total activity (beam breaks)	**30160 ± 2377**	**47055 ± 5532**	**0.017**	**9639 ± 1589**	**14530 ± 1107**	**0.021**	**39798 ± 3869**	**61586 ± 6366**	**0.013**
Ambulatory activity (counts)	**16577 ± 3138**	**28148 ± 4020**	**0.042**	4605 ± 1662	7135 ± 778	0.172	21181 ± 4736	35283 ± 4680	0.052
	Fasting (dark cycle)			**Fasting (light cycle)**			**Fasting (24 hr)**		
Body weight (g)							**25.5 ± 1.15**	**16.6 ± 0.41**	**<0.001**
Food intake (kcal)	0	0		0	0		0	0	
VO2 (mL/kg lean mass/h)	**3604 ± 118**	**5151 ± 149**	**<0.001**	**2794 ± 60**	**4099 ± 199**	**<0.001**	**3199 ± 83**	**4675 ± 169**	**<0.001**
VCO2 (mL/kg lean mass/h)	**2800 ± 98**	**4115 ± 106**	**<0.001**	**2107 ± 57**	**3098 ± 161**	**<0.001**	**2454 ± 71**	**3606 ± 129**	**<0.001**
RER (VCO2/VO2)	0.77 ± 0.002	0.78 ± 0.006	0.105	0.75 ± 0.006	0.75 ± 0.008	0.982	0.76 ± 0.003	0.77 ± 0.006	0.492
EE (kcal/kg lean mass/h)	**17.2 ± 0.57**	**25.1 ± 0.69**	**<0.001**	**13.3 ± 0.30**	**19.5 ± 0.95**	**<0.001**	**15.2 ± 0.41**	**22.3 ± 0.80**	**<0.001**
Total activity (beam breaks)	**36169 ± 1838**	**87131 ± 11695**	**0.001**	**9221 ± 1546**	**56436 ± 14366**	**0.008**	**45389 ± 3068**	**143567 ± 25225**	**0.002**
Ambulatory activity (counts)	**21867 ± 1863**	**62399 ± 9337**	**0.001**	**4886 ± 1252**	**42324 ± 11664**	**0.009**	**26753 ± 2956**	**104723 ± 20414**	**0.003**
	Re-feed (dark cycle)			**Re-feed (light cycle)**			**Re-feed (24 hr)**		
Body weight (g)							**27.9 ± 1.03**	**19.4 ± 0.55**	**<0.001**
Food intake (kcal)	12.9 ± 0.62	13.4 ± 0.36	0.524	3.41 ± 0.37	4.01 ± 0.47	0.337	17.6 ± 1.05	17.3 ± 0.49	0.836
VO2 (mL/kg lean mass/h)	**4216 ± 145**	**4980 ± 184**	**0.006**	**3459 ± 154**	**4356 ± 126**	**<0.001**	**3850 ± 147**	**4678 ± 132**	**<0.001**
VCO2 (mL/kg lean mass/h)	**4200 ± 159**	**4966 ± 179**	**0.008**	**3502 ± 186**	**4431 ± 177**	**0.003**	**3873 ± 167**	**4706 ± 132**	**0.001**
RER (VCO2/VO2)	1.00 ± 0.005	1.00 ± 0.006	0.517	1.01 ± 0.014	1.01 ± 0.020	0.920	1.01 ± 0.009	1.00 ± 0.011	0.921
EE (kcal/kg lean mass/h)	**21.3 ± 0.75**	**25.1 ± 0.92**	**0.006**	**17.5 ± 0.81**	**22.1 ± 0.69**	**<0.001**	**19.5 ± 0.76**	**23.6 ± 0.66**	**<0.001**
Total activity (beam breaks)	**49750 ± 4033**	**65119 ± 5703**	**0.048**	9175 ± 1219	12966 ± 1506	0.073	37102 ± 4356	45853 ± 7582	0.349
Ambulatory activity (counts)	27781 ± 4810	38270 ± 3686	0.099	4326 ± 1186	6693 ± 1045	0.153	19302 ± 4436	26753 ± 5461	0.314

Eu: Euploid; VO2: rate of oxygen consumption; VCO2: rate of carbon dioxide production; RER: respiratory exchange ratio; EE: energy expenditure

Table S3. Tissue weight of high fat diet-fed male mice (33 weeks of age; fed diet for 16.5 weeks) at termination of the study

	Eu	MAC21	*P*
N	8	8	
Body weight (g)	**46.62 ± 2.16**	**28.16 ±1.76**	**<0.001**
Gondal fat (gWAT, g)	**1.09 ±0.11**	**0.64 ±0.12**	**0.016**
Inguinal fat (iWAT, g)	**1.02 ±0.06**	**0.32 ±0.08**	**<0.001**
Liver (g)	**2.02 ±0.22**	**1.39 ±0.08**	**0.018**
Pancreas (g)	0.25 ±0.03	0.25 ±0.01	0.933
Kidney (g)	**0.18 ±0.01**	**0.15 ±0.01**	**0.026**
Spleen (g)	0.09 ±0.01	0.09 ±0.01	0.851
Diaphragm (g)	**0.11 ±0.01**	**0.09 ±0.01**	**0.010**
Heart (g)	0.18 ±0.02	0.16 ±0.01	0.266
BAT (g)	**0.32 ±0.04**	**0.12 ±0.02**	**0.001**
Brain (g)	**0.45 ±0.01**	**0.48 ±0.005**	**0.004**
Tibia (mm)	18.25 ±0.21	18.04 ±0.15	0.421

Eu: Euploidy; gWAT: gondal white adipose tissue; iWAT: inguinal white adipose tissue; BAT: brown adipose tissue

Table S4. Complete blood count of Euploid and MAC21 mice fed a high-fat diet (50 weeks of age; on diet for 13 weeks)

	Eu	MAC21	*P*
N	5	6	
RBC (10^6/μL)	8.66±0.61	9.22±0.26	0.452
HGB (g/dL)	12.85±1.24	14.02±0.31	0.424
HCT (%)	41.88±3.59	42.88±1.09	0.813
MCV (fL)	48.12±1.46	46.56±0.54	0.381
MCH (pg)	14.72±0.59	15.26±0.16	0.436
MCHC (g/dL)	30.53±0.58	32.80±0.28	0.009
RET (10^3/μL)	747.12±141.32	412.34±25.07	0.063
PLT (10^3/μL)	722.33±176.68	1230.40±86.03	0.039
WBC (10^3/μL)	9.62±2.41	9.93±0.47	0.902
NEUT (10^3/μL)	2.29±0.87	1.55±0.04	0.421
LYMPH (10^3/μL)	7.86±2.06	7.95±0.43	0.969
MONO (10^3/μL)	0.31±0.13	0.19±0.05	0.370
EO (10^3/μL)	0.23±0.10	0.22±0.03	0.985
BASO (10^3/μL)	0.01±0.01	0.03±0.01	0.267

RBC, red blood cell count; HGB hemoglobin; HCT, hematocrit; MCV, mean corpuscular (erythrocyte) volume; MCH, mean corpuscular hemoglobin; MCHC, mean corpuscular hemoglobin concentration; RET, reticulocyte count; PLT, platelet count; WBC, white blood cells count; NEUT, neutrophil count; LYMPH, lymphocyte count; MONO, monocyte count; EO, eosinophil count; BASO, basophil count; Eu, euploid

Table S5. Indirect calorimetry analysis of male (25 weeks of age) Euploid and MAC21 littermate mice fed a high-fat diet (8.5 weeks on diet)

	Eu	MAC21	*P*	Eu	MAC21	*P*	Eu	MAC21	*P*
High-fat diet (Male)	***Ad-libitum* (dark cycle)**			***Ad-libitum* (light cycle)**			***Ad-libitum* (24 hr)**		
N	8	9		8	9		8	9	
Body weight (g)							**43.0 ± 1.99**	**25.8 ± 1.06**	**<0.001**
Food intake (kcal)	11.7 ± 1.02	12.6 ± 0.78	0.502	3.6 ± 0.61	3.6 ± 0.34	0.987	15.3 ± 1.20	16.2 ± 0.83	0.556
VO2 (mL/kg lean mass/h)	**4871 ± 107**	**6378 ± 316**	**<0.001**	**4046 ± 74**	**5222 ± 250**	**<0.001**	**4459 ± 84**	**5800 ± 281**	**<0.001**
VCO2 (mL/kg lean mass/h)	**3956 ± 88**	**5316 ± 255**	**<0.001**	**3270 ± 65**	**4274 ± 216**	**<0.001**	**3613 ± 68**	**4795 ± 232**	**<0.001**
RER (VCO2/VO2)	**0.81 ± 0.004**	**0.83 ± 0.003**	**0.001**	0.81 ± 0.004	0.82 ± 0.006	0.244	**0.81 ± 0.003**	**0.83 ± 0.004**	**0.011**
EE (kcal/kg lean mass/h)	**23.5 ± 0.51**	**30.9 ± 1.52**	**<0.001**	**19.5 ± 0.36**	**25.2 ± 1.22**	**<0.001**	**21.5 ± 0.40**	**28.0 ± 1.36**	**<0.001**
Total activity (beam breaks)	**22378 ± 1644**	**41249 ± 4280**	**0.001**	**8153 ± 1249**	**14099 ± 1570**	**0.011**	**30531 ± 2553**	**16508 ± 5503**	**0.001**
Ambulatory activity (counts)	**11114 ± 1669**	**20126 ± 2350**	**0.008**	3571 ± 1295	5798 ± 730	0.144	**14685 ± 2859**	**25924 ± 2898**	**0.015**
	Fasting (dark cycle)			**Fasting (light cycle)**			**Fasting (24 hr)**		
Body weight (g)							**40.3 ± 1.89**	**23.1 ± 1.06**	**<0.001**
Food intake (kcal)	0	0		0	0		0	0	
VO2 (mL/kg lean mass/h)	**4389 ± 138**	**5063 ± 238**	**0.028**	3475 ± 84	3832 ± 176	0.089	**3932 ± 108**	**4447 ± 201**	**0.040**
VCO2 (mL/kg lean mass/h)	**3317 ± 101**	**3887 ± 172**	**0.013**	2650 ± 64	2953 ± 131	0.057	**2984 ± 80**	**3419 ± 146**	**0.020**
RER (VCO2/VO2)	0.76 ± 0.002	0.77 ± 0.007	0.096	0.76 ± 0.003	0.77 ± 0.004	0.149	0.76 ± 0.002	0.77 ± 0.005	0.109
EE (kcal/kg lean mass/h)	**20.8 ± 0.65**	**24.1 ± 1.12**	**0.024**	16.5 ± 0.40	18.3 ± 0.83	0.081	**18.7 ± 0.51**	**21.2 ± 0.94**	**0.035**
Total activity (beam breaks)	**25504 ± 3251**	**47893 ± 5189**	**0.003**	**6259 ± 815**	**14298 ± 1499**	**<0.001**	**31763 ± 3793**	**62191 ± 6644**	**0.001**
Ambulatory activity (counts)	**13987 ± 1797**	**28435 ± 3571**	**0.003**	**2381 ± 392**	**7565 ± 1177**	**<0.001**	**16368 ± 1981**	**36000 ± 4676**	**0.002**
	Re-feed (dark cycle)			**Re-feed (light cycle)**			**Re-feed (24 hr)**		
Body weight (g)							**41.4 ± 1.93**	**25.5 ± 0.90**	**<0.001**
Food intake (kcal)	12.9 0.62	13.4 ± 0.38	0.524	2.90 ± 0.62	3.6 ± 0.34	0.353	**13.0 ± 0.87**	**17.7 ± 0.82**	**0.002**
VO2 (mL/kg lean mass/h)	**4907 ± 133**	**5707 ± 225**	**0.008**	**3981 ± 77**	**4829 ± 187**	**<0.001**	**4459 ± 100**	**5282 ± 203**	**0.003**
VCO2 (mL/kg lean mass/h)	**3916 ± 104**	**4812 ± 164**	**<0.001**	**3233 ± 65**	**4130 ± 162**	**<0.001**	**3586 ± 79**	**4482 ± 159**	**<0.001**
RER (VCO2/VO2)	**0.80 ± 0.005**	**0.84 ± 0.008**	**<0.001**	**0.81 ± 0.004**	**0.86 ± 0.011**	**0.002**	**0.80 ± 0.004**	**0.85 ± 0.009**	**<0.001**
EE (kcal/kg lean mass/h)	**23.5 ± 0.63**	**27.7 ± 1.06**	**0.005**	**19.2 ± 0.37**	**23.5 ± 0.90**	**<0.001**	**21.4 ± 0.48**	**25.7 ± 0.97**	**0.001**
Total activity (beam breaks)	**49750 ± 4033**	**65119 ± 6049**	**0.048**	**5118 ± 712**	**9820 ± 1222**	**0.005**	**27579 ± 2805**	**46524 ± 5236**	**0.007**
Ambulatory activity (counts)	27781 ± 4810	38270 ± 3910	0.100	**1618 ± 186**	**3424 ± 434**	**0.002**	**11970 ± 847**	**22377 ± 2708**	**0.003**

Eu: Euploid; VO2: rate of oxygen consumption; VCO2: rate of carbon dioxide production; RER: respiratory exchange ratio; EE: energy expenditure

Table S6

Human genes expressed Gonadal White Adipose Tissue (HFD, 22 C)

Gene Symbol	Log(Fold Change)	Adj.p-Value	Gene Type	GenecodeID	EntrezID
DSCR3	10.74	6.24E-07	protein_coding	ENSG00000157538.13	10311
MCM3AP	10.31	6.24E-07	protein_coding	ENSG00000160294.10	8888
TRAPPC10	10.92	6.24E-07	protein_coding	ENSG00000160218.12	7109
USP16	10.61	6.24E-07	protein_coding	ENSG00000156256.14	10600
PTTG1IP	12.07	6.24E-07	protein_coding	ENSG00000183255.11	754
PRMT2	11.14	6.24E-07	protein_coding	ENSG00000160310.16	3275
BRWD1	10.52	6.24E-07	protein_coding	ENSG00000185658.13	54014
IFNGR2	10.30	6.24E-07	protein_coding	ENSG00000159128.14	3460
PIGP	10.71	6.24E-07	protein_coding	ENSG00000185808.13	51227
HMGN1	10.55	6.24E-07	protein_coding	ENSG00000205581.10	3150
SUMO3	11.29	6.24E-07	protein_coding	ENSG00000184900.15	6612
C2CD2	11.70	6.24E-07	protein_coding	ENSG00000157617.16	25966
TTC3	12.50	6.24E-07	protein_coding	ENSG00000182670.13	7267
APP	13.12	6.24E-07	protein_coding	ENSG00000142192.20	351
MX2	10.87	6.24E-07	protein_coding	ENSG00000183486.12	4600
S100B	13.02	6.24E-07	protein_coding	ENSG00000160307.9	6285
HLCS	9.83	7.70E-07	protein_coding	ENSG00000159267.14	3141
CRYZL1	9.72	7.70E-07	protein_coding	ENSG00000205758.11	9946
BTG3	10.05	7.70E-07	protein_coding	ENSG00000154640.14	10950
ATP5J	11.35	7.70E-07	protein_coding	ENSG00000154723.12	522
IFNAR1	10.75	7.70E-07	protein_coding	ENSG00000142166.12	3454
TSPEAR-AS1	11.19	7.70E-07	antisense	ENSG00000235890.2	NA
GABPA	10.39	7.93E-07	protein_coding	ENSG00000154727.10	2551
PAXBP1	9.31	7.93E-07	protein_coding	ENSG00000159086.14	94104
ATP5O	9.47	7.93E-07	protein_coding	ENSG00000241837.6	539
RRP1B	10.07	8.08E-07	protein_coding	ENSG00000160208.12	23076
TMEM50B	9.68	8.08E-07	protein_coding	ENSG00000142188.16	757
CCT8	11.07	8.08E-07	protein_coding	ENSG00000156261.12	10694
PDXK	12.34	8.08E-07	protein_coding	ENSG00000160209.18	8566
DYRK1A	10.18	8.08E-07	protein_coding	ENSG00000157540.19	1859
BACE2	10.18	8.08E-07	protein_coding	ENSG00000182240.15	25825
SLC37A1	9.40	8.08E-07	protein_coding	ENSG00000160190.13	54020
TSPEAR-AS2	10.46	8.08E-07	antisense	ENSG00000182912.6	NA
SCAF4	9.65	8.34E-07	protein_coding	ENSG00000156304.14	57466
RUNX1	9.80	8.34E-07	protein_coding	ENSG00000159216.18	861
DIP2A	11.62	1.06E-06	protein_coding	ENSG00000160305.17	23181
UBE2G2	10.76	1.19E-06	protein_coding	ENSG00000184787.18	7327
CBR1	9.67	1.23E-06	protein_coding	ENSG00000159228.12	873
LINC00649	9.71	1.24E-06	antisense	ENSG00000237945.7	100506334
SYNJ1	9.77	1.25E-06	protein_coding	ENSG00000159082.17	8867
SETD4	8.93	1.25E-06	protein_coding	ENSG00000185917.13	54093
NDUFV3	10.48	1.25E-06	protein_coding	ENSG00000160194.17	4731
ETS2	9.78	1.25E-06	protein_coding	ENSG00000157557.11	2114
SON	12.02	1.25E-06	protein_coding	ENSG00000159140.18	6651
RWDD2B	8.94	1.43E-06	protein_coding	ENSG00000156253.6	10069
RRP1	10.20	1.61E-06	protein_coding	ENSG00000160214.12	8568
WRB	9.77	1.75E-06	protein_coding	ENSG00000182093.14	7485
URB1	9.90	1.76E-06	protein_coding	ENSG00000142207.6	9875
PSMG1	8.59	2.01E-06	protein_coding	ENSG00000183527.11	8624
PKNOX1	8.48	2.04E-06	protein_coding	ENSG00000160199.14	5316
PRDM15	8.20	2.06E-06	protein_coding	ENSG00000141956.13	63977
ZBTB21	10.33	2.15E-06	protein_coding	ENSG00000173276.13	49854
PFKL	9.27	2.31E-06	protein_coding	ENSG00000141959.16	5211
HSPA13	10.09	2.31E-06	protein_coding	ENSG00000155304.5	6782
IFNAR2	9.48	2.33E-06	protein_coding	ENSG00000159110.19	3455
N6AMT1	8.08	2.49E-06	protein_coding	ENSG00000156239.11	29104
CYYR1	8.86	2.49E-06	protein_coding	ENSG00000166265.11	116159
ADAMTS1	8.42	2.66E-06	protein_coding	ENSG00000154734.14	9510
IL10RB	9.62	2.74E-06	protein_coding	ENSG00000243646.9	3588
ITSN1	11.09	2.83E-06	protein_coding	ENSG00000205726.14	6453
AGPAT3	10.66	3.98E-06	protein_coding	ENSG00000160216.18	56894
SH3BGR	9.20	4.62E-06	protein_coding	ENSG00000185437.13	6450
SOD1	11.57	4.79E-06	protein_coding	ENSG00000142168.14	6647
CLIC6	11.05	4.81E-06	protein_coding	ENSG00000159212.12	54102
DONSON	7.83	5.33E-06	protein_coding	ENSG00000159147.17	29980
CH507-9B2.5	8.41	5.52E-06	protein_coding	ENSG00000275464.4	102724159
ITGB2-AS1	10.41	5.92E-06	antisense	ENSG00000227039.6	100505746
ABCG1	8.34	6.16E-06	protein_coding	ENSG00000160179.18	9619
MX1	9.88	9.40E-06	protein_coding	ENSG00000157601.13	4599
C21orf59	7.62	9.53E-06	protein_coding	ENSG00000159079.18	56683
LTN1	8.26	9.53E-06	protein_coding	ENSG00000198862.13	26046
AP001065.15	8.02	9.97E-06	lincRNA	ENSG00000228709.1	NA
MAP3K7CL	8.76	1.01E-05	protein_coding	ENSG00000156265.15	56911
TFF3	8.29	1.11E-05	protein_coding	ENSG00000160180.15	7033
MRPL39	8.29	1.12E-05	protein_coding	ENSG00000154719.13	54148
U2AF1	7.36	1.15E-05	protein_coding	ENSG00000160201.11	7307
CSTB	13.49	1.15E-05	protein_coding	ENSG00000160213.5	1476
JAM2	8.61	1.20E-05	protein_coding	ENSG00000154721.14	58494
TSPEAR	7.99	1.73E-05	protein_coding	ENSG00000175894.14	54084
ADARB1	7.52	1.84E-05	protein_coding	ENSG00000197381.15	104
MRPS6	9.88	1.84E-05	protein_coding	ENSG00000243927.5	64968
LRRC3	8.99	1.85E-05	protein_coding	ENSG00000160233.7	81543
AP000235.2	6.96	2.25E-05	lincRNA	ENSG00000226983.2	339622
EVA1C	7.49	2.28E-05	protein_coding	ENSG00000166979.12	59271
PAXBP1-AS1	7.03	2.49E-05	antisense	ENSG00000238197.5	100506215
LINC01547	8.45	2.49E-05	lincRNA	ENSG00000183250.11	84536
TRPM2	9.51	2.52E-05	protein_coding	ENSG00000142185.16	7226
MIS18A	7.08	2.59E-05	protein_coding	ENSG00000159055.3	54069
CXADR	7.87	2.88E-05	protein_coding	ENSG00000154639.18	1525
BACH1	10.86	3.05E-05	protein_coding	ENSG00000156273.15	571
POFUT2	10.87	3.22E-05	protein_coding	ENSG00000186866.16	23275
CH507-9B2.3	7.95	3.31E-05	protein_coding	ENSG00000280071.3	102724023
RCAN1	9.20	3.31E-05	protein_coding	ENSG00000159200.17	1827
AATBC	8.52	3.54E-05	antisense	ENSG00000215458.8	284837
AIRE	6.54	3.60E-05	protein_coding	ENSG00000160224.16	326
SLC5A3	11.26	3.73E-05	protein_coding	ENSG00000198743.6	6526
DNAJC28	6.64	3.79E-05	protein_coding	ENSG00000177692.11	54943
C21orf33	8.07	5.04E-05	protein_coding	ENSG00000160221.16	8209
CHAF1B	9.77	5.58E-05	protein_coding	ENSG00000159259.7	8208
C21orf2	6.81	5.77E-05	protein_coding	ENSG00000160226.15	755
ANKRD30BP2	7.08	5.77E-05	transcribed_unprocessed_pseudogene	ENSG00000224309.7	NA
KCNJ15	7.41	5.77E-05	protein_coding	ENSG00000157551.17	3772
GART	9.42	5.82E-05	protein_coding	ENSG00000159131.16	2618
MRAP	6.45	6.31E-05	protein_coding	ENSG00000170262.12	56246
PCNT	9.44	6.57E-05	protein_coding	ENSG00000160299.16	5116
DSCR8	6.34	6.63E-05	protein_coding	ENSG00000198054.11	84677
HUNK	6.50	7.11E-05	protein_coding	ENSG00000142149.8	30811
CH507-9B2.9	6.27	7.83E-05	protein_coding	ENSG00000280433.1	102724200
LCA5L	6.61	7.98E-05	protein_coding	ENSG00000157578.13	150082
LINC01436	6.51	7.98E-05	lincRNA	ENSG00000231106.2	NA
WDR4	6.88	8.44E-05	protein_coding	ENSG00000160193.11	10785
TRPM2-AS	6.00	9.22E-05	antisense	ENSG00000230061.2	NA
URB1-AS1	6.63	1.47E-04	lincRNA	ENSG00000256073.3	84996
AF015262.2	6.60	1.47E-04	lincRNA	ENSG00000234703.1	NA
TIAM1	8.88	1.85E-04	protein_coding	ENSG00000156299.13	7074
HSF2BP	6.05	2.00E-04	protein_coding	ENSG00000160207.8	11077
BX322557.10	6.29	2.21E-04	processed_transcript	ENSG00000215447.7	NA
ITGB2	14.12	2.52E-04	protein_coding	ENSG00000160255.17	3689
FAM207A	8.51	2.66E-04	protein_coding	ENSG00000160256.12	85395
RPL23P2	6.74	2.85E-04	processed_pseudogene	ENSG00000176054.6	NA
UBASH3A	6.51	3.56E-04	protein_coding	ENSG00000160185.14	53347
LINC00205	5.54	6.66E-04	lincRNA	ENSG00000223768.1	NA
LINC01426	6.95	7.00E-04	antisense	ENSG00000234380.1	100506385
DSCR4	5.72	7.48E-04	protein_coding	ENSG00000184029.9	10281
BRWD1-AS2	5.16	7.67E-04	antisense	ENSG00000255568.3	103091865
SAMSN1	11.44	7.67E-04	protein_coding	ENSG00000155307.17	64092
DSTNP1	6.75	1.10E-03	processed_pseudogene	ENSG00000230982.1	NA
CBSL	5.37	1.10E-03	protein_coding	ENSG00000274276.4	102724560
C21orf58	7.65	1.18E-03	protein_coding	ENSG00000160298.17	54058
ANKRD30BP1	7.72	1.43E-03	unprocessed_pseudogene	ENSG00000175302.5	NA
21NC02-1C1£	6.06	1.80E-03	antisense	ENSG00000272825.1	NA
LINC00479	5.07	3.25E-03	lincRNA	ENSG00000236384.7	150135
AF129075.5	5.93	3.40E-03	sense_intronic	ENSG00000231125.2	NA
FAM3B	5.17	3.85E-03	protein_coding	ENSG00000183844.16	54097
C21orf62	4.91	4.17E-03	protein_coding	ENSG00000205929.10	56245
AP001505.10	4.58	4.85E-03	lincRNA	ENSG00000276529.1	NA
TMPRSS3	5.24	5.16E-03	protein_coding	ENSG00000160183.13	64699
CBR3	5.57	5.16E-03	protein_coding	ENSG00000159231.5	874
RSPH1	6.75	5.16E-03	protein_coding	ENSG00000160188.9	89765
AP001628.7	4.74	6.12E-03	lincRNA	ENSG00000231754.2	NA
AP001432.14	5.26	7.95E-03	lincRNA	ENSG00000242553.1	NA
KCNE2	4.58	8.49E-03	protein_coding	ENSG00000159197.3	9992
YBEY	4.81	8.74E-03	protein_coding	ENSG00000182362.13	54059
LINC00112	4.10	9.20E-03	antisense	ENSG00000232401.1	54089
SNORA81	4.16	1.23E-02	snoRNA	ENSG00000238390.1	NA
AP000266.7	4.43	1.28E-02	antisense	ENSG00000232623.1	NA
AP001052.1	4.10	1.31E-02	pseudogene	ENSG00000281420.1	NA
AP001627.1	4.14	1.51E-02	antisense	ENSG00000225731.1	NA
ZNF295-AS1	4.23	2.39E-02	lincRNA	ENSG00000237232.7	150142
POTED	4.39	2.39E-02	protein_coding	ENSG00000166351.10	317754
AP000254.8	4.08	3.03E-02	antisense	ENSG00000273271.1	NA
KB-68A7.2	4.13	3.63E-02	lincRNA	ENSG00000277352.1	NA
LINC00189	5.51	3.87E-02	sense_overlapping	ENSG00000215533.8	193629
AP001625.4	4.15	4.06E-02	sense_intronic	ENSG00000239930.2	101930094

Mouse genes expressed

Gene Symbol	Log(Fold Change)	Adj.p-Value	Gene Type	GenecodeID	EntrezID
Orm3	3.68	3.12E-02	protein_coding	ENSMUSG00000028359.4	18407
Zfp970	1.44	4.62E-02	protein_coding	ENSMUSG00000078866.10	628308
Chst11	0.99	4.89E-02	protein_coding	ENSMUSG00000034612.7	58250

Mouse genes repressed

Gene Symbol	Log(Fold Change)	Adj.p-Value	Gene Type	GenecodeID	EntrezID
Sgcg	-11.75	2.27E-02	protein_coding	ENSMUSG00000035296.13	24053
Mcpt2	-11.17	2.33E-02	protein_coding	ENSMUSG00000022226.5	17225
Igkv19-93	-8.37	1.67E-02	IG_V_gene	ENSMUSG00000098814.2	NA
Sult4a1	-6.01	7.08E-03	protein_coding	ENSMUSG00000018865.8	29859
Gm3375	-5.67	4.69E-03	processed_pseudogene	ENSMUSG00000107470.1	NA
Pex5l	-4.85	1.35E-02	protein_coding	ENSMUSG00000027674.16	58869
Cpz	-2.73	2.70E-02	protein_coding	ENSMUSG00000036596.6	242939
Col6a5	-1.84	4.47E-02	protein_coding	ENSMUSG00000091345.8	665033

Table S7 Inguinal White Adipose Tissue (HFD, 22°C)

Human genes expressed

Gene Symbol	Log(Fold Change)	Adj.p-Value	Gene Type	GencodeID	EntrezID
ATP5O	12.02	0.014	protein_coding	ENSG00000241837.6	539
NDUFV3	11.81	0.021	protein_coding	ENSG00000160194.17	4731
AGPAT3	11.50	0.003	protein_coding	ENSG00000160216.18	56894
ATP5J	11.47	0.021	protein_coding	ENSG00000154723.12	522
S100B	11.44	0.022	protein_coding	ENSG00000160307.9	6285
TRAPPC10	11.08	0.003	protein_coding	ENSG00000160218.12	7109
UBE2G2	10.53	0.015	protein_coding	ENSG00000184787.18	7327
RRP1	10.35	0.014	protein_coding	ENSG00000160214.12	8568
MCM3AP	10.33	0.014	protein_coding	ENSG00000160294.10	8888
HMGN1	10.28	0.024	protein_coding	ENSG00000205581.10	3150
IL10RB	10.06	0.017	protein_coding	ENSG00000243646.9	3588
GABPA	9.82	0.017	protein_coding	ENSG00000154727.10	2551
PAXBP1	9.80	0.014	protein_coding	ENSG00000159086.14	94104
CBR1	9.77	0.014	protein_coding	ENSG00000159228.12	873
HLCS	9.40	0.007	protein_coding	ENSG00000159267.14	3141
CRYZL1	9.10	0.014	protein_coding	ENSG00000205758.11	9946
USP16	9.09	0.037	protein_coding	ENSG00000156256.14	10600
URB1	9.07	0.018	protein_coding	ENSG00000142207.6	9875
BRWD1	8.78	0.017	protein_coding	ENSG00000185658.13	54014
CH507-9B2.5	8.60	0.014	protein_coding	ENSG00000275464.4	102724159
SH3BGR	8.48	0.018	protein_coding	ENSG00000185437.13	6450
LRRC3	8.25	0.030	protein_coding	ENSG00000160233.7	81543
SETD4	8.17	0.017	protein_coding	ENSG00000185917.13	54093
PSMG1	8.06	0.014	protein_coding	ENSG00000183527.11	8624
PKNOX1	8.01	0.038	protein_coding	ENSG00000160199.14	5316
MRPL39	7.72	0.017	protein_coding	ENSG00000154719.13	54148
ADARB1	7.27	0.034	protein_coding	ENSG00000197381.15	104

Mouse up-regulated genes

Gene Symbol	Log(Fold Change)	Adj.p-Value	Gene Type	GencodeID	EntrezID
NONE					

Mouse down-regulated genes

Gene Symbol	Log(Fold Change)	Adj.p-Value	Gene Type	GencodeID	EntrezID
Krt5	-19.19	0.046	protein_coding	ENSMUSG00000061527.6	110308
Dsp	-16.95	0.014	protein_coding	ENSMUSG00000054889.9	109620
Ano9	-11.97	0.027	protein_coding	ENSMUSG00000054662.8	71345
Rarres1	-6.35	0.030	protein_coding	ENSMUSG00000049404.7	109222
Tmem132b	-5.93	0.014	protein_coding	ENSMUSG00000070498.3	208151
Grid1	-4.89	0.018	protein_coding	ENSMUSG00000041078.6	14803

Table S8 Liver (HFD, 22°C)

Human genes expressed

Gene Symbol	Log(Fold Change)	Adj.p-Value	Gene Type	GencodeID	EntrezID
SOD1	12.78	7.85E-07	protein_coding	ENSG00000142168.14	6647
MX1	11.52	2.61E-05	protein_coding	ENSG00000157601.13	4599
APP	11.48	7.85E-07	protein_coding	ENSG00000142192.20	351
PDXK	11.13	5.31E-06	protein_coding	ENSG00000160209.18	8566
PTTG1IP	10.80	9.91E-07	protein_coding	ENSG00000183255.11	754
SON	10.76	7.23E-06	protein_coding	ENSG00000159140.18	6651
CBR1	10.65	1.44E-05	protein_coding	ENSG00000159228.12	873
ATP5J	10.59	1.61E-06	protein_coding	ENSG00000154723.12	522
AGPAT3	10.51	4.02E-05	protein_coding	ENSG00000160216.18	56894
CSTB	10.14	2.54E-06	protein_coding	ENSG00000160213.5	1476
POFUT2	10.14	1.47E-05	protein_coding	ENSG00000186866.16	23275
DSCR3	10.11	1.07E-06	protein_coding	ENSG00000157538.13	10311
PRMT2	10.08	4.17E-06	protein_coding	ENSG00000160310.16	3275
UBE2G2	10.06	2.16E-06	protein_coding	ENSG00000184787.18	7327
DIP2A	10.00	5.84E-05	protein_coding	ENSG00000160305.17	23181
NDUFV3	9.92	6.07E-06	protein_coding	ENSG00000160194.17	4731
SUMO3	9.88	1.95E-06	protein_coding	ENSG00000184900.15	6612
BACH1	9.83	2.53E-05	protein_coding	ENSG00000156273.15	571
TRAPPC10	9.83	2.54E-06	protein_coding	ENSG00000160218.12	7109
WRB	9.82	1.25E-06	protein_coding	ENSG00000182093.14	7485
HMGN1	9.79	7.00E-06	protein_coding	ENSG00000205581.10	3150
CCT8	9.77	2.16E-06	protein_coding	ENSG00000156261.12	10694
ETS2	9.74	2.69E-04	protein_coding	ENSG00000157557.11	2114
C21orf91	9.73	2.36E-05	protein_coding	ENSG00000154642.10	54149
CBS	9.73	2.87E-06	protein_coding	ENSG00000160200.17	875
BRWD1	9.66	1.44E-05	protein_coding	ENSG00000185658.13	54014
IFNAR1	9.65	6.01E-06	protein_coding	ENSG00000142166.12	3454
TTC3	9.53	1.15E-05	protein_coding	ENSG00000182670.13	7267
GART	9.46	2.54E-06	protein_coding	ENSG00000159131.16	2618
AATBC	9.46	6.93E-04	antisense	ENSG00000215458.8	284837
DYRK1A	9.40	2.16E-06	protein_coding	ENSG00000157540.19	1859
ITGB2	9.38	1.74E-04	protein_coding	ENSG00000160255.17	3689
USP16	9.26	9.29E-06	protein_coding	ENSG00000156256.14	10600
PFKL	9.20	2.54E-05	protein_coding	ENSG00000141959.16	5211
CXADR	9.07	2.16E-06	protein_coding	ENSG00000154639.18	1525
MCM3AP	9.01	2.16E-06	protein_coding	ENSG00000160294.10	8888
ITSN1	8.98	2.16E-06	protein_coding	ENSG00000205726.14	6453
GABPA	8.89	7.99E-06	protein_coding	ENSG00000154727.10	2551
PIGP	8.86	2.16E-06	protein_coding	ENSG00000185808.13	51227
SCAF4	8.85	2.41E-04	protein_coding	ENSG00000156304.14	57466
TMEM50B	8.85	3.94E-06	protein_coding	ENSG00000142188.16	757
RRP1	8.84	1.34E-05	protein_coding	ENSG00000160214.12	8568
RRP1B	8.80	2.27E-05	protein_coding	ENSG00000160208.12	23076
HLCS	8.75	3.53E-04	protein_coding	ENSG00000159267.14	3141
LRRC3	8.72	2.63E-03	protein_coding	ENSG00000160233.7	81543
TSPEAR-AS2	8.71	9.97E-06	antisense	ENSG00000182912.6	NA
URB1	8.70	2.54E-06	protein_coding	ENSG00000142207.6	9875
BACE2	8.64	1.47E-05	protein_coding	ENSG00000182240.15	25825
RCAN1	8.60	4.02E-05	protein_coding	ENSG00000159200.17	1827
TSPEAR-AS1	8.59	6.07E-06	antisense	ENSG00000235890.2	NA
IFNGR2	8.57	2.36E-05	protein_coding	ENSG00000159128.14	3460
MX2	8.54	1.77E-04	protein_coding	ENSG00000183486.12	4600
ATP5O	8.46	9.29E-06	protein_coding	ENSG00000241837.6	539
TMPRSS2	8.40	1.47E-05	protein_coding	ENSG00000184012.11	7113
RUNX1	8.36	2.64E-05	protein_coding	ENSG00000159216.18	861
TMPRSS3	8.31	1.71E-03	protein_coding	ENSG00000160183.13	64699
SETD4	8.31	3.80E-06	protein_coding	ENSG00000185917.13	54093
PSMG1	8.31	3.69E-06	protein_coding	ENSG00000183527.11	8624
RIPK4	8.30	7.72E-05	protein_coding	ENSG00000183421.11	54101
CH507-9B2.3	8.19	1.47E-05	protein_coding	ENSG00000280071.3	102724023
CLIC6	8.18	3.20E-03	protein_coding	ENSG00000159212.12	54102
RWDD2B	8.13	9.29E-06	protein_coding	ENSG00000156253.6	10069
PRDM15	8.12	3.94E-06	protein_coding	ENSG00000141956.13	63977
IFNAR2	8.07	4.98E-05	protein_coding	ENSG00000159110.19	3455
SLC37A1	8.07	1.47E-05	protein_coding	ENSG00000160190.13	54020
SLC5A3	8.05	2.41E-04	protein_coding	ENSG00000198743.6	6526
PAXBP1	8.01	8.78E-06	protein_coding	ENSG00000159086.14	94104
SYNJ1	7.99	1.44E-05	protein_coding	ENSG00000159082.17	8867
FAM207A	7.99	6.53E-05	protein_coding	ENSG00000160256.12	85395
CRYZL1	7.94	7.23E-06	protein_coding	ENSG00000205758.11	9946
C2CD2	7.92	1.27E-05	protein_coding	ENSG00000157617.16	25966
IL10RB	7.87	8.65E-06	protein_coding	ENSG00000243646.9	3588
BTG3	7.82	7.72E-05	protein_coding	ENSG00000154640.14	10950
SH3BGR	7.75	6.07E-06	protein_coding	ENSG00000185437.13	6450
DONSON	7.71	7.80E-05	protein_coding	ENSG00000159147.17	29980
TRPM2	7.70	1.44E-05	protein_coding	ENSG00000142185.16	7226
ZBTB21	7.65	2.23E-05	protein_coding	ENSG00000173276.13	49854
CBSL	7.52	2.71E-03	protein_coding	ENSG00000274276.4	102724560
MRPL39	7.52	7.30E-05	protein_coding	ENSG00000154719.13	54148
LINC00649	7.46	7.30E-05	antisense	ENSG00000237945.7	100506334
HSPA13	7.42	1.53E-04	protein_coding	ENSG00000155304.5	6782
PCNT	7.36	3.30E-05	protein_coding	ENSG00000160299.16	5116
HUNK	7.36	3.27E-05	protein_coding	ENSG00000142149.8	30811
N6AMT1	7.35	7.30E-05	protein_coding	ENSG00000156239.11	29104
CH507-9B2.5	7.31	6.86E-05	protein_coding	ENSG00000275464.4	102724159
MAP3K7CL	7.28	1.74E-04	protein_coding	ENSG00000156265.15	56911
CLDN14	7.15	2.95E-03	protein_coding	ENSG00000159261.10	23562
PKNOX1	7.14	1.76E-05	protein_coding	ENSG00000160199.14	5316
C21orf33	7.12	7.30E-05	protein_coding	ENSG00000160221.16	8209
SAMSN1	7.01	1.37E-02	protein_coding	ENSG00000155307.17	64092
AP001065.1S	6.93	1.59E-04	lincRNA	ENSG00000228709.1	NA
WDR4	6.89	2.69E-04	protein_coding	ENSG00000160193.11	10785
MRPS6	6.87	3.13E-04	protein_coding	ENSG00000243927.5	64968
C21orf58	6.86	6.53E-05	protein_coding	ENSG00000160298.17	54058
S100B	6.80	9.01E-03	protein_coding	ENSG00000160307.9	6285
LINC00479	6.78	4.60E-02	lincRNA	ENSG00000236384.7	150135
ITGB2-AS1	6.73	1.09E-03	antisense	ENSG00000227039.6	100505746
YBEY	6.54	1.10E-04	protein_coding	ENSG00000182362.13	54059
MIS18A	6.44	4.11E-04	protein_coding	ENSG00000159055.3	54069
URB1-AS1	6.41	2.63E-03	lincRNA	ENSG00000256073.3	84996
DNAJC28	6.36	1.74E-04	protein_coding	ENSG00000177692.11	54943
LTN1	6.22	2.70E-04	protein_coding	ENSG00000198862.13	26046
C21orf59	6.21	1.33E-04	protein_coding	ENSG00000159079.18	56683
TSPEAR	6.06	1.91E-02	protein_coding	ENSG00000175894.14	54084
TRPM2-AS	5.96	1.27E-03	antisense	ENSG00000230061.2	NA
DSCR8	5.95	2.41E-04	protein_coding	ENSG00000198054.11	84677
U2AF1	5.93	2.27E-03	protein_coding	ENSG00000160201.11	7307
TFF3	5.91	4.05E-03	protein_coding	ENSG00000160180.15	7033
DSCR4	5.80	1.13E-03	protein_coding	ENSG00000184029.9	10281
CYYR1	5.80	4.62E-04	protein_coding	ENSG00000166265.11	116159
JAM2	5.49	9.67E-03	protein_coding	ENSG00000154721.14	58494
ADARB1	5.47	4.66E-04	protein_coding	ENSG00000197381.15	104
LINC01426	5.44	2.99E-02	antisense	ENSG00000234380.1	100506385
LCA5L	5.44	6.96E-03	protein_coding	ENSG00000157578.13	150082
RPL23P2	5.34	1.75E-03	processed_pseudogene	ENSG00000176054.6	NA
KCNJ15	5.26	4.96E-02	protein_coding	ENSG00000157551.17	3772
SSR4P1	5.24	1.12E-03	transcribed_processed_pseudogene	ENSG00000235374.2	728039
LINC01547	5.08	1.13E-03	lincRNA	ENSG00000183250.11	84536
C21orf91-OT1	5.07	1.70E-03	lincRNA	ENSG00000240770.5	246312
RPL39P40	5.07	2.71E-03	processed_pseudogene	ENSG00000226580.1	NA
ANKRD30BP2	4.97	1.56E-02	transcribed_unprocessed_pseudogene	ENSG00000224309.7	NA
BRWD1-AS2	4.90	1.05E-02	antisense	ENSG00000255568.3	103091865
CHAF1B	4.75	4.98E-02	protein_coding	ENSG00000159259.7	8208
TIAM1	4.72	3.17E-03	protein_coding	ENSG00000156299.13	7074
LINC00189	4.70	3.34E-02	sense_overlapping	ENSG00000215533.8	193629
C21orf2	4.70	5.70E-03	protein_coding	ENSG00000160226.15	755
ABCG1	4.60	1.20E-02	protein_coding	ENSG00000160179.18	9619
DSTNP1	4.29	1.81E-02	processed_pseudogene	ENSG00000230982.1	NA
PAXBP1-AS1	4.21	1.75E-02	antisense	ENSG00000238197.5	100506215
LINC00205	4.16	8.46E-03	lincRNA	ENSG00000223768.1	NA
CH507-9B2.1	4.01	1.62E-02	protein_coding	ENSG00000277117.4	102723996
AP000302.58	3.73	4.09E-02	antisense	ENSG00000231355.1	NA
LINC01436	3.69	4.35E-02	lincRNA	ENSG00000231106.2	NA
SNORA81	3.64	4.39E-02	snoRNA	ENSG00000238390.1	NA

Mouse up-regulated genes

Gene Symbol	Log(Fold Change)	Adj.p-Value	Gene Type	GencodeID	EntrezID
Mirg	8.40	0.016	lincRNA	ENSMUSG00000097391.8	NA
Lrtm2	7.46	0.022	protein_coding	ENSMUSG00000055003.14	211187
Ehf	7.03	0.017	protein_coding	ENSMUSG00000012350.15	13661
Rab25	5.71	0.001	protein_coding	ENSMUSG00000008601.12	53868
BC067074	5.66	0.015	protein_coding	ENSMUSG00000021763.16	408066
Gm11454	5.18	0.050	lincRNA	ENSMUSG00000086152.1	NA
Muc13	5.13	0.015	protein_coding	ENSMUSG00000022824.12	17063
Ccdc198	5.08	0.050	protein_coding	ENSMUSG00000021850.13	67082
Rasal1	4.96	0.037	protein_coding	ENSMUSG00000029602.11	19415
Zfp365	4.65	0.017	protein_coding	ENSMUSG00000037855.15	216049
Tubb4a	4.58	0.009	protein_coding	ENSMUSG00000062591.5	22153
Ncam1	4.15	0.037	protein_coding	ENSMUSG00000039542.15	17967
Dpf1	3.97	0.009	protein_coding	ENSMUSG00000030584.14	29861
Oip5	3.89	0.049	protein_coding	ENSMUSG00000072980.3	70645
Bhlha15	3.86	0.041	protein_coding	ENSMUSG00000052271.7	17341
Cxcl14	3.45	0.027	protein_coding	ENSMUSG00000021508.10	57266
Nucb2	3.41	0.016	protein_coding	ENSMUSG00000030659.14	53322
Zfp641	3.06	0.050	protein_coding	ENSMUSG00000022987.11	239652
Catsperd	2.95	0.042	protein_coding	ENSMUSG00000040828.9	106757
Tnfrsf23	2.69	0.033	protein_coding	ENSMUSG00000037613.16	79201
Oas2	2.65	0.047	protein_coding	ENSMUSG00000032690.16	246728
Cttnbp2nl	1.75	0.038	protein_coding	ENSMUSG00000062127.11	80281
Dusp10	1.74	0.022	protein_coding	ENSMUSG00000039384.8	63953
Fat1	1.52	0.047	protein_coding	ENSMUSG00000070047.13	14107
Alcam	0.92	0.037	protein_coding	ENSMUSG00000022636.13	11658

Mouse down-regulated genes

Gene Symbol	Log(Fold Change)	Adj.p-Value	Gene Type	GencodeID	EntrezID
Acot3	-2.94	0.037	protein_coding	ENSMUSG00000021228.14	171281
Gm42796	-2.77	0.037	TEC	ENSMUSG00000105192.1	NA
Crym	-2.34	0.030	protein_coding	ENSMUSG00000030905.5	12971
Tmem256	-1.58	0.020	protein_coding	ENSMUSG00000070394.10	69186
Impg2	-1.39	0.037	protein_coding	ENSMUSG00000035270.15	224224
Hint2	-1.34	0.012	protein_coding	ENSMUSG00000028470.10	68917
Ttc36	-1.31	0.047	protein_coding	ENSMUSG00000039438.6	192653
Cox7c	-1.10	0.047	protein_coding	ENSMUSG00000017778.14	12867
Slc40b1	-1.04	0.047	protein_coding	ENSMUSG00000025993.10	53945

Table S9

Human genes expressed Brown Adipose Tissue (HFD, 22 C)

Gene Symbol	Log(Fold Change)	Adj.p-Value	Gene Type	GencodeID	EntrezID
PDXK	11.14	4.20E-05	protein_coding	ENSG00000160209.18	8566
AATBC	10.77	4.20E-05	antisense	ENSG00000215458.8	284837
SLC5A3	10.17	2.12E-06	protein_coding	ENSG00000198743.6	6526
NDUFV3	10.16	4.06E-05	protein_coding	ENSG00000160194.17	4731
ATP5O	10.01	6.31E-05	protein_coding	ENSG00000241837.6	539
CLIC6	9.89	3.42E-06	protein_coding	ENSG00000159212.12	54102
ATP5J	9.85	1.42E-04	protein_coding	ENSG00000154723.12	522
CSTB	9.82	1.94E-05	protein_coding	ENSG00000160213.5	1476
S100B	9.76	6.31E-05	protein_coding	ENSG00000160307.9	6285
SH3BGR	9.71	1.08E-04	protein_coding	ENSG00000185437.13	6450
ANKRD20A11P	9.61	2.49E-05	transcribed_unprocessed_pseudogene	ENSG00000215559.8	391267
PTTG1IP	9.60	7.18E-06	protein_coding	ENSG00000183255.11	754
CCT8	9.55	4.09E-05	protein_coding	ENSG00000156261.12	10694
DSCR3	9.54	1.98E-06	protein_coding	ENSG00000157538.13	10311
C2CD2	9.53	1.86E-06	protein_coding	ENSG00000157617.16	25966
WRB	9.44	8.11E-05	protein_coding	ENSG00000182093.14	7485
CH507-9B2.3	9.36	7.56E-05	protein_coding	ENSG00000280071.3	102724023
POFUT2	9.21	5.99E-04	protein_coding	ENSG00000186866.16	23275
ITGB2	9.07	1.20E-05	protein_coding	ENSG00000160255.17	3689
TRAPPC10	9.04	3.05E-05	protein_coding	ENSG00000160218.12	7109
CYP4F29P	8.92	1.95E-05	transcribed_unprocessed_pseudogene	ENSG00000228314.1	54055
USP16	8.87	4.20E-05	protein_coding	ENSG00000156256.14	10600
MCM3AP	8.79	1.32E-05	protein_coding	ENSG00000160294.10	8888
PRMT2	8.77	5.89E-05	protein_coding	ENSG00000160310.16	3275
UBE2G2	8.76	6.19E-04	protein_coding	ENSG00000184787.18	7327
MX2	8.74	2.73E-05	protein_coding	ENSG00000183486.12	4600
DIP2A	8.69	7.88E-05	protein_coding	ENSG00000160305.17	23181
PIGP	8.67	2.49E-05	protein_coding	ENSG00000185808.13	51227
SON	8.66	3.69E-04	protein_coding	ENSG00000159140.18	6651
GART	8.64	4.09E-05	protein_coding	ENSG00000159131.16	2618
C21orf33	8.63	7.24E-04	protein_coding	ENSG00000160221.16	8209
URB1	8.60	6.83E-05	protein_coding	ENSG00000142207.6	9875
BRWD1	8.56	3.58E-04	protein_coding	ENSG00000185658.13	54014
URB1-AS1	8.54	4.00E-05	lincRNA	ENSG00000256073.3	84996
RWDD2B	8.54	2.12E-06	protein_coding	ENSG00000156253.6	10069
MAP3K7CL	8.53	1.85E-04	protein_coding	ENSG00000156265.15	56911
GABPA	8.49	2.12E-06	protein_coding	ENSG00000154727.10	2551
RRP1B	8.47	2.73E-05	protein_coding	ENSG00000160208.12	23076
DYRK1A	8.44	8.94E-05	protein_coding	ENSG00000157540.19	1859
APP	8.43	8.35E-04	protein_coding	ENSG00000142192.20	351
AGPAT3	8.39	8.91E-04	protein_coding	ENSG00000160216.18	56894
HMGN1	8.36	1.53E-04	protein_coding	ENSG00000205581.10	3150
RRP1	8.35	1.02E-05	protein_coding	ENSG00000160214.12	8568
IFNAR1	8.35	5.89E-05	protein_coding	ENSG00000142166.12	3454
IFNGR2	8.34	2.12E-06	protein_coding	ENSG00000159128.14	3460
TTC3	8.34	1.24E-04	protein_coding	ENSG00000182670.13	7267
LINC00649	8.29	3.42E-06	antisense	ENSG00000237945.7	100506334
BTG3	8.27	2.61E-05	protein_coding	ENSG00000154640.14	10950
ITSN1	8.26	6.09E-05	protein_coding	ENSG00000205726.14	6453
ZBTB21	8.21	2.58E-06	protein_coding	ENSG00000173276.13	49854
CH507-9B2.5	8.20	2.12E-06	protein_coding	ENSG00000275464.4	102724159
TMEM50B	8.17	3.05E-05	protein_coding	ENSG00000142188.16	757
BACE2	8.08	2.12E-06	protein_coding	ENSG00000182240.15	25825
MRPL39	8.03	7.56E-05	protein_coding	ENSG00000154719.13	54148
HLCS	7.98	1.98E-04	protein_coding	ENSG00000159267.14	3141
CRYZL1	7.90	1.94E-04	protein_coding	ENSG00000205758.11	9946
LTN1	7.89	2.12E-06	protein_coding	ENSG00000198862.13	26046
SUMO3	7.89	2.41E-04	protein_coding	ENSG00000184900.15	6612
TSPEAR-AS1	7.87	5.08E-05	antisense	ENSG00000235890.2	NA
N6AMT1	7.85	5.08E-05	protein_coding	ENSG00000156239.11	29104
MRPS6	7.76	7.88E-05	protein_coding	ENSG00000243927.5	64968
CYYR1	7.75	7.76E-05	protein_coding	ENSG00000166265.11	116159
TSPEAR-AS2	7.74	7.51E-06	antisense	ENSG00000182912.6	NA
CBR1	7.73	8.00E-04	protein_coding	ENSG00000159228.12	873
SYNJ1	7.73	2.12E-06	protein_coding	ENSG00000159082.17	8867
PFKL	7.50	8.00E-04	protein_coding	ENSG00000141959.16	5211
PCNT	7.49	3.81E-05	protein_coding	ENSG00000160299.16	5116
PAXBP1	7.49	5.95E-05	protein_coding	ENSG00000159086.14	94104
ETS2	7.47	1.98E-04	protein_coding	ENSG00000157557.11	2114
HSPA13	7.47	3.42E-06	protein_coding	ENSG00000155304.5	6782
MX1	7.37	8.72E-03	protein_coding	ENSG00000157601.13	4599
SETD4	7.34	3.58E-04	protein_coding	ENSG00000185917.13	54093
FAM207A	7.22	4.09E-05	protein_coding	ENSG00000160256.12	85395
PSMG1	7.22	3.40E-05	protein_coding	ENSG00000183527.11	8624
IFNAR2	7.21	2.12E-06	protein_coding	ENSG00000159110.19	3455
DNAJC28	7.17	2.61E-05	protein_coding	ENSG00000177692.11	54943
JAM2	7.07	1.00E-03	protein_coding	ENSG00000154721.14	58494
SNX18P13	7.01	3.40E-05	processed_pseudogene	ENSG00000230965.1	NA
WDR4	6.98	3.42E-06	protein_coding	ENSG00000160193.11	10785
ITGB2-AS1	6.98	3.21E-05	antisense	ENSG00000227039.6	100505746
PRDM15	6.97	9.83E-04	protein_coding	ENSG00000141956.13	63977
SLC37A1	6.93	3.35E-05	protein_coding	ENSG00000160190.13	54020
C21orf58	6.89	7.23E-04	protein_coding	ENSG00000160298.17	54058
PKNOX1	6.87	2.73E-05	protein_coding	ENSG00000160199.14	5316
RUNX1	6.87	3.01E-04	protein_coding	ENSG00000159216.18	861
SCAF4	6.87	1.38E-03	protein_coding	ENSG00000156304.14	57466
SOD1	6.83	4.65E-03	protein_coding	ENSG00000142168.14	6647
RHOT1P2	6.80	2.95E-05	processed_pseudogene	ENSG00000203616.2	NA
MIS18A	6.76	1.36E-04	protein_coding	ENSG00000159055.3	54069
AP000235.2	6.58	1.33E-04	lincRNA	ENSG00000226983.2	339622
TRPM2	6.58	7.53E-05	protein_coding	ENSG00000142185.16	7226
BACH1	6.47	2.59E-04	protein_coding	ENSG00000156273.15	571
BRWD1-AS2	6.39	3.56E-05	antisense	ENSG00000255568.3	103091865
DSCR8	6.32	1.71E-05	protein_coding	ENSG00000198054.11	84677
TFF3	6.27	5.89E-05	protein_coding	ENSG00000160180.15	7033
MRAP	6.25	3.77E-04	protein_coding	ENSG00000170262.12	56246
ADAMTS1	6.25	3.22E-05	protein_coding	ENSG00000154734.14	9510
U2AF1	6.24	8.73E-05	protein_coding	ENSG00000160201.11	7307
DONSON	6.14	1.36E-04	protein_coding	ENSG00000159147.17	29980
C21orf59	6.08	1.95E-05	protein_coding	ENSG00000159079.18	56683
IL10RB	6.04	1.24E-04	protein_coding	ENSG00000243646.9	3588
C21orf2	6.03	8.94E-05	protein_coding	ENSG00000160226.15	755
CH507-9B2.9	5.95	5.89E-05	protein_coding	ENSG00000280433.1	102724200
ADARB1	5.94	2.73E-05	protein_coding	ENSG00000197381.15	104
ANKRD30BP2	5.93	2.59E-05	transcribed_unprocessed_pseudogene	ENSG00000224309.7	NA
AP001347.6	5.90	8.11E-05	antisense	ENSG00000224905.6	NA
LINC01547	5.87	9.20E-05	lincRNA	ENSG00000183250.11	84536
ABCG1	5.77	3.26E-05	protein_coding	ENSG00000160179.18	9619
LRRC3	5.76	1.24E-03	protein_coding	ENSG00000160233.7	81543
PAXBP1-AS1	5.73	5.60E-04	antisense	ENSG00000238197.5	100506215
LCA5L	5.65	4.09E-05	protein_coding	ENSG00000157578.13	150082
AP001065.15	5.46	2.61E-05	lincRNA	ENSG00000228709.1	NA
PPP6R2P1	5.44	1.80E-02	unprocessed_pseudogene	ENSG00000233442.2	NA
RPL23P2	5.43	1.04E-04	processed_pseudogene	ENSG00000176054.6	NA
YBEY	5.37	2.61E-05	protein_coding	ENSG00000182362.13	54059
SAMSN1	5.28	1.00E-03	protein_coding	ENSG00000155307.17	64092
EVA1C	5.25	7.18E-04	protein_coding	ENSG00000166979.12	59271
LINC00205	5.14	6.31E-05	lincRNA	ENSG00000223768.1	NA
FRG2MP	5.13	6.33E-05	processed_pseudogene	ENSG00000275170.1	NA
TSPEAR	5.05	8.00E-04	protein_coding	ENSG00000175894.14	54084
ANKRD20A18P	5.04	7.35E-03	unprocessed_pseudogene	ENSG00000249493.1	NA
RCAN1	4.79	1.37E-03	protein_coding	ENSG00000159200.17	1827
AF015262.2	4.77	1.05E-04	lincRNA	ENSG00000234703.1	NA
BX322557.10	4.74	9.83E-05	processed_transcript	ENSG00000215447.7	NA
TIAM1	4.70	9.70E-04	protein_coding	ENSG00000156299.13	7074
AP001052.1	4.54	1.24E-03	pseudogene	ENSG00000281420.1	NA
AP001627.1	4.50	1.35E-03	antisense	ENSG00000225731.1	NA
TRPM2-AS	4.46	2.67E-03	antisense	ENSG00000230061.2	NA
AP000266.7	4.36	4.84E-03	antisense	ENSG00000232623.1	NA
DSCR4	4.30	2.21E-03	protein_coding	ENSG00000184029.9	10281
LINC01436	4.18	3.58E-04	lincRNA	ENSG00000231106.2	NA
CHAF1B	4.14	9.03E-04	protein_coding	ENSG00000159259.7	8208
AP001412.1	4.12	1.99E-03	antisense	ENSG00000272948.2	NA
SSR4P1	4.03	2.99E-03	transcribed_processed_pseudogene	ENSG00000235374.2	728039
LINC01426	3.92	4.32E-04	antisense	ENSG00000234380.1	100506385
HUNK	3.83	1.63E-02	protein_coding	ENSG00000142149.8	30811
TFF2	3.80	1.22E-02	protein_coding	ENSG00000160181.8	7032
pRNA	3.78	3.54E-03	misc_RNA	ENSG00000277572.1	NA
HSF2BP	3.69	1.98E-03	protein_coding	ENSG00000160207.8	11077
KCNJ15	3.42	5.83E-03	protein_coding	ENSG00000157551.17	3772
RSPH1	3.23	2.14E-02	protein_coding	ENSG00000160188.9	89765
AP000253.1	2.82	8.22E-03	lincRNA	ENSG00000234509.1	NA
AP001437.1	2.74	3.31E-02	antisense	ENSG00000273210.1	NA
AP000254.8	2.56	4.61E-02	antisense	ENSG00000273271.1	NA
AF129075.5	2.44	1.41E-02	sense_intronic	ENSG00000231125.2	NA
H2AFZP1	2.17	3.36E-02	processed_pseudogene	ENSG00000213440.2	NA

Human up-regulated genes

Gene Symbol	Log(Fold Change)	Adj.p-Value	Gene Type	GencodeID	EntrezID
Tceal7	8.25	0.007	protein_coding	ENSMUSG00000079428.8	100040972
Mybph	6.91	0.028	protein_coding	ENSMUSG00000042451.12	53311
2310020H05Rik	5.39	0.030	lincRNA	ENSMUSG00000100410.1	NA
Gm13943	3.95	0.048	lincRNA	ENSMUSG00000085277.1	NA
Tmem232	3.77	0.013	protein_coding	ENSMUSG00000045036.14	381107
Emx2os	3.51	0.015	antisense	ENSMUSG00000087095.2	NA
Srpk3	2.83	0.022	protein_coding	ENSMUSG00000002007.5	56504
Aldh1l2	2.73	0.044	protein_coding	ENSMUSG00000020256.14	216188
Kif12	2.54	0.006	protein_coding	ENSMUSG00000072294.4	16597
Hist1h3e	2.45	0.021	protein_coding	ENSMUSG00000069273.2	319151
Hoxa9	1.89	0.032	protein_coding	ENSMUSG00000038227.15	15405
Tpd52l1	1.51	0.027	protein_coding	ENSMUSG00000000296.7	21987
Nudt5	0.82	0.009	protein_coding	ENSMUSG00000025817.12	53893
Cdc123	0.78	0.009	protein_coding	ENSMUSG00000039128.13	98828
Stim1	0.62	0.033	protein_coding	ENSMUSG00000030987.5	20866
Rps27rt	0.53	0.032	protein_coding	ENSMUSG00000050621.6	100043813
Abcb7	0.51	0.026	protein_coding	ENSMUSG00000031333.7	11306
Rnf34	0.50	0.050	protein_coding	ENSMUSG00000029474.7	80751
Sgcb	0.48	0.037	protein_coding	ENSMUSG00000029156.11	24051

Mouse down-regulated genes

Gene Symbol	Log(Fold Change)	Adj.p-Value	Gene Type	GencodeID	EntrezID
Cyp4a12a	-4.00	0.037	protein_coding	ENSMUSG00000066071.6	277753
Cyp2a4	-3.87	0.018	protein_coding	ENSMUSG00000074254.4	13086
C8b	-3.86	0.045	protein_coding	ENSMUSG00000029656.13	110382
Lect2	-3.80	0.047	protein_coding	ENSMUSG00000021539.8	16841
Mmp12	-2.76	0.015	protein_coding	ENSMUSG00000049723.14	17381
Sec1	-2.75	0.032	protein_coding	ENSMUSG00000040364.8	56546
Tmem178	-2.57	0.017	protein_coding	ENSMUSG00000024245.4	68027
Ass1	-2.45	0.027	protein_coding	ENSMUSG00000076441.9	11898
Gm5424	-2.29	0.009	protein_coding	ENSMUSG00000046687.5	NA
Fmn1	-1.60	0.013	protein_coding	ENSMUSG00000044042.18	14260
Epha2	-1.58	0.005	protein_coding	ENSMUSG00000006445.3	13836
Gpnmb	-1.52	0.010	protein_coding	ENSMUSG00000029816.10	93695
Maneal	-1.50	0.032	protein_coding	ENSMUSG00000042763.9	215090
Ccdc85a	-1.27	0.009	protein_coding	ENSMUSG00000032878.16	216613
Pde9a	-1.26	0.009	protein_coding	ENSMUSG00000041119.11	18585
Dnm3	-1.19	0.023	protein_coding	ENSMUSG00000040265.16	103967
Dll1	-1.13	0.031	protein_coding	ENSMUSG00000014773.13	13388
N4bp3	-1.10	0.017	protein_coding	ENSMUSG00000001053.15	212706
Dach1	-1.09	0.024	protein_coding	ENSMUSG00000055639.16	13134
Snai2	-1.07	0.011	protein_coding	ENSMUSG00000022676.6	20583
Prrg3	-1.05	0.025	protein_coding	ENSMUSG00000033361.13	208748
Dock9	-1.04	0.046	protein_coding	ENSMUSG00000025558.16	105445
Gm12922	-1.03	0.026	processed_pseudogene	ENSMUSG00000081170.1	NA
Cd200	-0.98	0.032	protein_coding	ENSMUSG00000022661.14	17470
Tanc1	-0.97	0.022	protein_coding	ENSMUSG00000035168.16	66860
Fmnl1	-0.97	0.031	protein_coding	ENSMUSG00000055805.14	57778
Me2	-0.94	0.004	protein_coding	ENSMUSG00000024556.3	107029
Boc	-0.93	0.041	protein_coding	ENSMUSG00000022687.11	117606
Klf6	-0.91	0.033	protein_coding	ENSMUSG00000000078.6	23849
Pcdh12	-0.87	0.027	protein_coding	ENSMUSG00000024440.12	53601
Jun	-0.84	0.020	protein_coding	ENSMUSG00000052684.4	16476
Lmo2	-0.81	0.043	protein_coding	ENSMUSG00000032698.15	16909
Stxbp1	-0.75	0.034	protein_coding	ENSMUSG00000026797.16	20910
Timp3	-0.74	0.041	protein_coding	ENSMUSG00000020044.13	21859
Myo1b	-0.72	0.039	protein_coding	ENSMUSG00000018417.14	17912
Sytl4	-0.71	0.049	protein_coding	ENSMUSG00000031255.14	27359
Tpst1	-0.69	0.023	protein_coding	ENSMUSG00000034118.15	22021
Sept8	-0.69	0.035	protein_coding	ENSMUSG00000018398.18	20362
1190002N15Rik	-0.67	0.017	protein_coding	ENSMUSG00000045414.7	68861
Slfn5	-0.63	0.024	protein_coding	ENSMUSG00000054404.12	327978
Atp8b2	-0.62	0.046	protein_coding	ENSMUSG00000060671.12	54667
Fam171a1	-0.59	0.046	protein_coding	ENSMUSG00000050530.14	269233
Trim12c	-0.57	0.024	protein_coding	ENSMUSG00000057143.15	319236
Prelp	-0.56	0.036	protein_coding	ENSMUSG00000041577.5	116847
Dusp7	-0.52	0.013	protein_coding	ENSMUSG00000053716.9	235584
Smarcd2	-0.43	0.036	protein_coding	ENSMUSG00000078619.10	83796

Table S10 Skeletal muscle (HFD, 22°C)

Human genes expressed

Gene Symbol	Log(Fold Change)	Adj.p-Value	Gene Type	GencodeID	EntrezID
BRWD1	11.67	1.19E-06	protein_coding	ENSG00000185658.13	54014
SH3BGR	11.39	3.52E-06	protein_coding	ENSG00000185437.13	6450
MAP3K7CL	11.11	3.34E-05	protein_coding	ENSG00000156265.15	56911
ATP5O	11.11	1.19E-06	protein_coding	ENSG00000241837.6	539
AGPAT3	11.05	1.19E-06	protein_coding	ENSG00000160216.18	56894
SOD1	10.92	1.19E-06	protein_coding	ENSG00000142168.14	6647
USP16	10.89	1.19E-06	protein_coding	ENSG00000156256.14	10600
NDUFV3	10.84	1.19E-06	protein_coding	ENSG00000160194.17	4731
PDXK	10.77	1.19E-06	protein_coding	ENSG00000160209.18	8566
ATP5J	10.55	1.19E-06	protein_coding	ENSG00000154723.12	522
UBE2G2	10.51	1.19E-06	protein_coding	ENSG00000184787.18	7327
SON	10.41	1.19E-06	protein_coding	ENSG00000159140.18	6651
PTTG1IP	10.40	3.07E-06	protein_coding	ENSG00000183255.11	754
MCM3AP	10.38	1.19E-06	protein_coding	ENSG00000160294.10	8888
DIP2A	10.34	1.81E-06	protein_coding	ENSG00000160305.17	23181
DSCR3	10.31	1.19E-06	protein_coding	ENSG00000157538.13	10311
SUMO3	10.27	1.81E-06	protein_coding	ENSG00000184900.15	6612
URB1	10.13	1.19E-06	protein_coding	ENSG00000142207.6	9875
HLCS	10.06	1.89E-06	protein_coding	ENSG00000159267.14	3141
RRP1B	10.01	1.45E-06	protein_coding	ENSG00000160208.12	23076
GABPA	9.95	1.19E-06	protein_coding	ENSG00000154727.10	2551
SLC5A3	9.95	3.14E-06	protein_coding	ENSG00000198743.6	6526
GART	9.94	1.19E-06	protein_coding	ENSG00000159131.16	2618
IFNAR1	9.88	1.81E-06	protein_coding	ENSG00000142166.12	3454
TTC3	9.73	3.62E-06	protein_coding	ENSG00000182670.13	7267
PAXBP1	9.72	1.19E-06	protein_coding	ENSG00000159086.14	94104
BACH1	9.66	2.39E-06	protein_coding	ENSG00000156273.15	571
PIGP	9.59	1.19E-06	protein_coding	ENSG00000185808.13	51227
MX2	9.53	1.81E-06	protein_coding	ENSG00000183486.12	4600
LINC00649	9.47	6.36E-06	antisense	ENSG00000237945.7	100506334
ETS2	9.46	8.66E-05	protein_coding	ENSG00000157557.11	2114
POFUT2	9.44	1.19E-06	protein_coding	ENSG00000186866.16	23275
N6AMT1	9.38	1.19E-06	protein_coding	ENSG00000156239.11	29104
TMEM50B	9.35	1.84E-06	protein_coding	ENSG00000142188.16	757
TRAPPC10	9.33	3.29E-06	protein_coding	ENSG00000160218.12	7109
WRB	9.30	1.67E-06	protein_coding	ENSG00000182093.14	7485
ITSN1	9.22	1.81E-06	protein_coding	ENSG00000205726.14	6453
CBR1	9.14	1.41E-06	protein_coding	ENSG00000159228.12	873
SLC37A1	9.14	1.67E-06	protein_coding	ENSG00000160190.13	54020
PCNT	9.12	2.64E-06	protein_coding	ENSG00000160299.16	5116
APP	9.08	5.05E-06	protein_coding	ENSG00000142192.20	351
CCT8	9.06	3.57E-06	protein_coding	ENSG00000156261.12	10694
HMGN1	9.06	2.31E-06	protein_coding	ENSG00000205581.10	3150
C2CD2	8.96	1.88E-06	protein_coding	ENSG00000157617.16	25966
PRMT2	8.80	1.84E-06	protein_coding	ENSG00000160310.16	3275
PLAC4	8.74	2.15E-06	TEC	ENSG00000280109.1	NA
ANKRD30BP2	8.71	3.52E-06	transcribed_unprocessed_pseudogene	ENSG00000224309.7	NA
ADARB1	8.64	1.88E-06	protein_coding	ENSG00000197381.15	104
CLIC6	8.63	5.36E-06	protein_coding	ENSG00000159212.12	54102
CH507-9B2.3	8.62	3.15E-05	protein_coding	ENSG00000280071.3	102724023
SCAF4	8.62	2.75E-06	protein_coding	ENSG00000156304.14	57466
TSPEAR-AS1	8.60	1.84E-06	antisense	ENSG00000235890.2	NA
SYNJ1	8.59	2.67E-06	protein_coding	ENSG00000159082.17	8867
AF121897.4	8.56	7.01E-06	processed_pseudogene	ENSG00000235012.1	NA
MRPL39	8.54	3.29E-06	protein_coding	ENSG00000154719.13	54148
CYYR1	8.54	3.29E-06	protein_coding	ENSG00000166265.11	116159
IFNGR2	8.52	3.11E-06	protein_coding	ENSG00000159128.14	3460
RWDD2B	8.47	3.29E-06	protein_coding	ENSG00000156253.6	10069
SETD4	8.46	3.14E-06	protein_coding	ENSG00000185917.13	54093
PFKL	8.45	4.36E-06	protein_coding	ENSG00000141959.16	5211
PKNOX1	8.44	3.52E-06	protein_coding	ENSG00000160199.14	5316
PRDM15	8.41	4.04E-06	protein_coding	ENSG00000141956.13	63977
MX1	8.37	4.76E-06	protein_coding	ENSG00000157601.13	4599
HSPA13	8.32	3.52E-06	protein_coding	ENSG00000155304.5	6782
RUNX1	8.29	3.29E-06	protein_coding	ENSG00000159216.18	861
CRYZL1	8.28	5.36E-06	protein_coding	ENSG00000205758.11	9946
RRP1	8.28	3.29E-06	protein_coding	ENSG00000160214.12	8568
LTN1	8.17	2.11E-05	protein_coding	ENSG00000198862.13	26046
FAM207A	8.15	3.14E-06	protein_coding	ENSG00000160256.12	85395
ZBTB21	8.14	2.31E-06	protein_coding	ENSG00000173276.13	49854
URB1-AS1	8.12	2.63E-06	lincRNA	ENSG00000256073.3	84996
ADAMTS1	8.07	3.62E-06	protein_coding	ENSG00000154734.14	9510
MRPS6	8.05	5.05E-06	protein_coding	ENSG00000243927.5	64968
PSMG1	8.05	4.70E-06	protein_coding	ENSG00000183527.11	8624
WDR4	7.91	6.19E-06	protein_coding	ENSG00000160193.11	10785
IFNAR2	7.87	1.74E-05	protein_coding	ENSG00000159110.19	3455
CHAF1B	7.84	6.65E-06	protein_coding	ENSG00000159259.7	8208
TSPEAR-AS2	7.82	3.14E-06	antisense	ENSG00000182912.6	NA
JAM2	7.81	3.29E-06	protein_coding	ENSG00000154721.14	58494
DYRK1A	7.79	1.19E-06	protein_coding	ENSG00000157540.19	1859
BACE2	7.72	4.36E-06	protein_coding	ENSG00000182240.15	25825
ITGB2	7.65	4.24E-04	protein_coding	ENSG00000160255.17	3689
DONSON	7.54	4.04E-06	protein_coding	ENSG00000159147.17	29980
DNAJC28	7.44	3.55E-06	protein_coding	ENSG00000177692.11	54943
C21orf33	7.43	4.24E-06	protein_coding	ENSG00000160221.16	8209
S100B	7.27	2.46E-04	protein_coding	ENSG00000160307.9	6285
LCA5L	7.25	4.70E-06	protein_coding	ENSG00000157578.13	150082
DOPEY2	7.22	2.16E-04	protein_coding	ENSG00000142197.12	9980
TIAM1	7.21	1.25E-05	protein_coding	ENSG00000156299.13	7074
UMODL1	7.14	1.61E-05	protein_coding	ENSG00000177398.18	89766
CSTB	7.05	7.03E-05	protein_coding	ENSG00000160213.5	1476
TRPM2	7.04	2.25E-04	protein_coding	ENSG00000142185.16	7226
TSPEAR	7.02	7.01E-06	protein_coding	ENSG00000175894.14	54084
C21orf59	7.02	7.01E-06	protein_coding	ENSG00000159079.18	56683
CH507-9B2.5	6.98	3.24E-04	protein_coding	ENSG00000275464.4	102724159
PAXBP1-AS1	6.82	6.47E-06	antisense	ENSG00000238197.5	100506215
C21orf58	6.79	7.83E-06	protein_coding	ENSG00000160298.17	54058
BX322557.10	6.71	2.91E-05	processed_transcript	ENSG00000215447.7	NA
DSCR4	6.68	4.05E-05	protein_coding	ENSG00000184029.9	10281
BTG3	6.66	1.84E-05	protein_coding	ENSG00000154640.14	10950
EVA1C	6.61	2.11E-05	protein_coding	ENSG00000166979.12	59271
RCAN1	6.56	1.75E-04	protein_coding	ENSG00000159200.17	1827
CYYR1-AS1	6.52	1.67E-05	antisense	ENSG00000197934.8	100996571
POTED	6.47	2.51E-05	protein_coding	ENSG00000166351.10	317754
IL10RB	6.46	3.61E-04	protein_coding	ENSG00000243646.9	3588
LINC00310	6.37	1.26E-04	lincRNA	ENSG00000227456.7	114036
AATBC	6.36	2.07E-05	antisense	ENSG00000215458.8	284837
AP000704.5	6.31	6.58E-05	lincRNA	ENSG00000224790.2	NA
LRRC3	6.30	1.10E-04	protein_coding	ENSG00000160233.7	81543
RSPH1	6.25	6.95E-05	protein_coding	ENSG00000160188.9	89765
AP001065.15	6.20	1.74E-05	lincRNA	ENSG00000228709.1	NA
DSCR8	6.16	1.67E-05	protein_coding	ENSG00000198054.11	84677
MORC3	6.09	1.29E-04	protein_coding	ENSG00000159256.12	23515
KCNE2	6.00	2.26E-05	protein_coding	ENSG00000159197.3	9992
AF015262.2	5.95	4.12E-05	lincRNA	ENSG00000234703.1	NA
ITGB2-AS1	5.93	6.65E-05	antisense	ENSG00000227039.6	100505746
MYL6P2	5.59	5.20E-05	processed_pseudogene	ENSG00000235808.1	NA
SSR4P1	5.50	5.48E-05	transcribed_processed_pseudogene	ENSG00000235374.2	728039
HLCS-IT1	5.47	1.14E-04	sense_intronic	ENSG00000237646.1	NA
HSF2BP	5.46	9.59E-05	protein_coding	ENSG00000160207.8	11077
AP001442.2	5.42	6.76E-05	processed_transcript	ENSG00000233783.7	NA
TFF3	5.34	6.40E-04	protein_coding	ENSG00000160180.15	7033
MIS18A	5.34	1.75E-04	protein_coding	ENSG00000159055.3	54069
AF129075.5	5.27	7.03E-05	sense_intronic	ENSG00000231125.2	NA
AP000469.2	5.26	1.14E-04	lincRNA	ENSG00000224832.1	101927869
AL773572.7	5.21	2.19E-04	antisense	ENSG00000225745.8	NA
AP001625.6	5.19	5.26E-04	antisense	ENSG00000235772.1	NA
LINC01547	5.17	1.32E-04	lincRNA	ENSG00000183250.11	84536
DSCR9	5.15	2.25E-04	lincRNA	ENSG00000230366.9	257203
AP000320.6	5.08	3.61E-04	antisense	ENSG00000225555.1	NA
AP001432.14	5.08	9.59E-05	lincRNA	ENSG00000242553.1	NA
BACH1-IT2	5.06	1.99E-04	lincRNA	ENSG00000228817.4	NA
YBEY	5.04	1.54E-03	protein_coding	ENSG00000182362.13	54059
AP001429.1	5.03	2.68E-04	sense_intronic	ENSG00000270116.1	NA
TRPM2-AS	5.02	3.06E-04	antisense	ENSG00000230061.2	NA
ABCG1	5.01	3.38E-04	protein_coding	ENSG00000160179.18	9619
BRWD1-AS2	4.97	1.52E-04	antisense	ENSG00000255568.3	103091865
RNA5SP491	4.97	1.67E-03	rRNA	ENSG00000199806.1	NA
AP000254.8	4.94	4.15E-04	antisense	ENSG00000273271.1	NA
LINC00205	4.94	1.94E-04	lincRNA	ENSG00000223768.1	NA
AP000692.10	4.84	1.75E-04	antisense	ENSG00000273199.1	NA
BACH1-IT1	4.83	2.66E-04	sense_intronic	ENSG00000248476.1	NA

Mouse up-regulated genes

Gene Symbol	Log(Fold Change)	Adj.p-Value	Gene Type	GencodeID	EntrezID
mt-Tn	7.35	0.001	Mt_tRNA	ENSMUSG00000064348.1	NA
Gm14438	6.08	0.015	processed_pseudogene	ENSMUSG00000084323.4	NA
Th	5.31	0.003	protein_coding	ENSMUSG00000000214.11	21823
mt-Ty	4.71	0.001	Mt_tRNA	ENSMUSG00000064350.1	NA
Fgf21	4.58	0.012	protein_coding	ENSMUSG00000030827.5	56636
mt-Atp8	4.40	0.020	protein_coding	ENSMUSG00000064356.3	17706
H2-Q2	3.96	0.048	protein_coding	ENSMUSG00000091705.8	15013
Sln	3.94	0.004	protein_coding	ENSMUSG00000042045.5	66402
Dbh	3.76	0.040	protein_coding	ENSMUSG00000000889.8	13166
mt-Ts1	3.76	0.007	Mt_tRNA	ENSMUSG00000064352.1	NA
Dmp1	3.74	0.001	protein_coding	ENSMUSG00000029307.7	13406
4930477O15Rik	3.72	0.012	TEC, lincRNA	ENSMUSG00000104999.1	NA
Flywch2	3.67	0.005	protein_coding	ENSMUSG00000023911.12	76917
Ccdc92	3.64	0.000	protein_coding	ENSMUSG00000037979.13	215707
mt-Co2	3.58	0.020	protein_coding	ENSMUSG00000064354.1	17709
Cyp4f14	3.57	0.014	protein_coding	ENSMUSG00000024292.14	64385
Tmem181c-ps	3.52	0.006	unprocessed_pseudogene	ENSMUSG00000093880.2	NA
Rpl17-ps8	3.52	0.033	processed_pseudogene	ENSMUSG00000082035.1	NA
Gm43694	3.49	0.042	TEC	ENSMUSG00000107018.1	NA
Fam174b	3.30	0.000	protein_coding	ENSMUSG00000078670.3	100038347
mt-Atp6	3.18	0.019	protein_coding	ENSMUSG00000064357.1	17705
Gm11127	3.16	0.007	protein_coding	ENSMUSG00000079492.2	100529082
Mthfd2	2.90	0.001	protein_coding	ENSMUSG00000005667.8	17768
mt-Nd4l	2.90	0.050	protein_coding	ENSMUSG00000065947.3	17720
Gm42853	2.80	0.025	TEC	ENSMUSG00000107021.1	NA
Gm22989	2.77	0.021	snRNA	ENSMUSG00000088938.1	NA
Srrm4os	2.76	0.002	antisense	ENSMUSG00000086219.7	76798
Asns	2.74	0.011	protein_coding	ENSMUSG00000029752.12	27053
Myo1a	2.70	0.006	protein_coding	ENSMUSG00000025401.8	432516
Crip3	2.67	0.000	protein_coding	ENSMUSG00000023968.15	114570
Apol9a	2.66	0.011	protein_coding	ENSMUSG00000057346.11	223672
Gm21738	2.61	0.018	protein_coding	ENSMUSG00000095280.1	NA
1810041L15Rik	2.59	0.001	protein_coding	ENSMUSG00000062760.10	72301
Krt18	2.57	0.007	protein_coding	ENSMUSG00000023043.6	16668
Gm43013	2.52	0.031	processed_pseudogene	ENSMUSG00000106058.1	NA
Cilp	2.44	0.010	protein_coding	ENSMUSG00000042254.14	214425
Gm10801	2.43	0.005	protein_coding	ENSMUSG00000075015.3	NA
Apol9b	2.41	0.045	protein_coding	ENSMUSG00000068246.5	71898
Slco4a1	2.39	0.004	protein_coding	ENSMUSG00000038963.15	108115
Mogat1	2.36	0.003	protein_coding	ENSMUSG00000012187.13	68393
E2f2	2.36	0.000	protein_coding	ENSMUSG00000018983.9	242705
Gm5420	2.35	0.003	lincRNA	ENSMUSG00000056716.9	432436
Srrm4	2.31	0.005	protein_coding	ENSMUSG00000063919.10	68955
Gm10720	2.27	0.048	protein_coding	ENSMUSG00000074564.3	NA
Cpne2	2.27	0.000	protein_coding	ENSMUSG00000034361.10	234577
H2-T-ps	2.27	0.024	unprocessed_pseudogene	ENSMUSG00000073405.6	667803
Gm11734	2.26	0.000	lincRNA	ENSMUSG00000085419.1	NA
2310043O21Rik	2.26	0.012	lincRNA	ENSMUSG00000102106.1	69679
1110002O04Rik	2.23	0.033	lincRNA	ENSMUSG00000102531.1	NA
BC035947	2.22	0.007	protein_coding	ENSMUSG00000090486.2	NA
Zdbf2	2.17	0.000	protein_coding	ENSMUSG00000027520.15	73884
Gm10800	2.16	0.000	protein_coding	ENSMUSG00000075014.1	NA
Ifi44	2.16	0.005	protein_coding	ENSMUSG00000028037.13	99899
Mir344c	2.15	0.042	miRNA	ENSMUSG00000077107.1	100526506
A930003A15Rik	2.10	0.002	protein_coding	ENSMUSG00000075330.3	NA
Kcnk1	2.10	0.004	protein_coding	ENSMUSG00000033998.9	16525
Gm10425	2.09	0.001	lincRNA	ENSMUSG00000097081.1	NA
Adamts20	2.07	0.000	protein_coding	ENSMUSG00000022449.14	223838
Tceal7	2.05	0.000	protein_coding	ENSMUSG00000079428.8	100040972
A330076H08Rik	2.02	0.004	processed_transcript	ENSMUSG00000109321.1	320026
Gm29228	1.99	0.041	processed_pseudogene	ENSMUSG00000101682.1	NA
Isg15	1.99	0.030	protein_coding	ENSMUSG00000035692.6	100038882
Irf7	1.94	0.004	protein_coding	ENSMUSG00000025498.15	54123
H2-Q10	1.87	0.030	protein_coding	ENSMUSG00000067235.14	15007
Ankrd1	1.86	0.000	protein_coding	ENSMUSG00000024803.8	107765
AW551984	1.81	0.050	protein_coding	ENSMUSG00000038112.15	244810
3632451O06Rik	1.77	0.004	protein_coding	ENSMUSG00000036242.14	67419
Cdkn1a	1.77	0.005	protein_coding	ENSMUSG00000023067.13	12575
RP23-54G8.4	1.76	0.006	lincRNA	ENSMUSG00000109394.1	319893
1500012K07Rik	1.74	0.047	processed_transcript	ENSMUSG00000097247.2	68954
F830016B08Rik	1.73	0.001	protein_coding	ENSMUSG00000090942.1	240328
Adig	1.71	0.012	protein_coding	ENSMUSG00000044405.4	246747
mt-Th	1.70	0.010	Mt_tRNA	ENSMUSG00000064364.1	NA
Fam69c	1.69	0.036	protein_coding	ENSMUSG00000047992.10	240479
Slc7a5	1.69	0.003	protein_coding	ENSMUSG00000040010.10	20539
Gm2399	1.64	0.024	protein_coding	ENSMUSG00000078141.2	NA
Exoc3l4	1.64	0.004	protein_coding	ENSMUSG00000021280.8	74190
Apln	1.61	0.016	protein_coding	ENSMUSG00000037010.7	30878
Palm2	1.60	0.025	protein_coding	ENSMUSG00000090053.9	677884
Cxcl10	1.57	0.028	protein_coding	ENSMUSG00000034855.13	15945
Acbd7	1.57	0.041	protein_coding	ENSMUSG00000026644.6	78245
Gm15420	1.56	0.047	antisense	ENSMUSG00000087387.1	NA
Gm9825	1.56	0.009	processed_pseudogene	ENSMUSG00000096403.2	NA
Oas2	1.55	0.003	protein_coding	ENSMUSG00000032690.16	246728
Slc1a1	1.55	0.016	protein_coding	ENSMUSG00000024935.10	20510
Oasl1	1.55	0.021	protein_coding	ENSMUSG00000041827.15	231655
Thrsp	1.53	0.027	protein_coding	ENSMUSG00000035686.8	21835
Trib3	1.53	0.006	protein_coding	ENSMUSG00000032715.9	228775
Arf4os	1.52	0.034	antisense	ENSMUSG00000090861.1	NA
Tnfaip2	1.49	0.000	protein_coding	ENSMUSG00000021281.15	21928
Gm4742	1.48	0.032	processed_pseudogene	ENSMUSG00000105461.1	NA
Ift122	1.46	0.000	protein_coding	ENSMUSG00000030323.13	81896
Bdnf	1.46	0.031	protein_coding	ENSMUSG00000048482.14	12064
B230311B06Rik	1.46	0.038	lincRNA	ENSMUSG00000109284.1	381914
Gadd45a	1.44	0.000	protein_coding	ENSMUSG00000036390.8	13197
Gabrr2	1.42	0.013	protein_coding	ENSMUSG00000023267.10	14409
Rtp4	1.40	0.001	protein_coding	ENSMUSG00000033355.6	67775
RP23-354I24.7	1.40	0.005	lincRNA	ENSMUSG00000110656.1	NA
Enkur	1.40	0.046	protein_coding	ENSMUSG00000026679.3	71233
RP24-116C19.5	1.39	0.040	protein_coding	ENSMUSG00000109739.1	NA
Trpv3	1.39	0.005	protein_coding	ENSMUSG00000043029.2	246788
4931431B13Rik	1.38	0.014	processed_transcript	ENSMUSG00000108354.1	70973
Aldh18a1	1.37	0.017	protein_coding	ENSMUSG00000025007.13	56454
Ifit3	1.37	0.013	protein_coding	ENSMUSG00000074896.3	15959
Zfp57	1.36	0.019	protein_coding	ENSMUSG00000036036.15	22715
H2-T10	1.36	0.035	polymorphic_pseudogene	ENSMUSG00000079491.9	NA
Gm42509	1.34	0.017	TEC	ENSMUSG00000105042.1	NA
Clu	1.31	0.000	protein_coding	ENSMUSG00000022037.14	12759
Stk36	1.30	0.018	protein_coding	ENSMUSG00000033276.18	269209
Gm4925	1.26	0.048	transcribed_processed_pseudogene	ENSMUSG00000069540.4	237433
2010300C02Rik	1.25	0.011	protein_coding	ENSMUSG00000026090.16	72097
Gm26704	1.23	0.037	lincRNA	ENSMUSG00000097875.1	NA
Spag5	1.21	0.002	protein_coding	ENSMUSG00000002055.9	54141
Tiam2	1.21	0.004	protein_coding	ENSMUSG00000023800.14	24001
Gm7993	1.19	0.033	processed_pseudogene	ENSMUSG00000107092.1	NA
Hba-ps4	1.19	0.035	unprocessed_pseudogene	ENSMUSG00000084893.3	NA
RP23-385F3.1	1.19	0.003	processed_pseudogene	ENSMUSG00000110131.1	NA
Tbc1d31	1.19	0.002	protein_coding	ENSMUSG00000022364.14	210544
Chrna10	1.18	0.002	protein_coding	ENSMUSG00000066279.3	504186
RP23-385G14.1	1.18	0.007	transcribed_unprocessed_pseudogene	ENSMUSG00000110298.1	NA
Slc47a1	1.17	0.002	protein_coding	ENSMUSG00000010122.14	67473
Oasl2	1.17	0.011	protein_coding	ENSMUSG00000029561.17	23962
Sox4	1.17	0.038	protein_coding	ENSMUSG00000076431.4	20677
Spock3	1.17	0.033	protein_coding	ENSMUSG00000054162.15	72902
Camta1	1.16	0.005	protein_coding	ENSMUSG00000014592.19	100072
Tmem8	1.15	0.012	protein_coding	ENSMUSG00000024180.13	60455
Ak4	1.14	0.047	protein_coding	ENSMUSG00000028527.18	11639
Itga9	1.13	0.002	protein_coding	ENSMUSG00000039115.13	104099
Tnfrsf19	1.13	0.001	protein_coding	ENSMUSG00000060548.12	29820
Gnmt	1.11	0.035	protein_coding	ENSMUSG00000002769.8	14711
5330439K02Rik	1.11	0.046	lincRNA	ENSMUSG00000097827.1	NA
4930412C18Rik	1.11	0.016	processed_transcript	ENSMUSG00000085558.7	NA
6430548M08Rik	1.11	0.003	protein_coding	ENSMUSG00000031824.15	234797
Armcx4	1.11	0.001	protein_coding	ENSMUSG00000049804.9	100503043
Apom	1.10	0.040	protein_coding	ENSMUSG00000024391.7	55938
Tppp3	1.09	0.001	protein_coding	ENSMUSG00000014846.12	67971
Gm45010	1.09	0.037	TEC	ENSMUSG00000109015.1	NA
Pbld2	1.08	0.030	protein_coding	ENSMUSG00000020072.14	67307
Otud1	1.08	0.002	protein_coding	ENSMUSG00000043415.5	71198
Clec18a	1.07	0.006	protein_coding	ENSMUSG00000033633.13	353287
Tmem82	1.07	0.031	protein_coding	ENSMUSG00000043085.14	213989
Gm18301	1.07	0.044	unprocessed_pseudogene	ENSMUSG00000099569.1	NA

Mouse down-regulated genes

Gene Symbol	Log(Fold Change)	Adj.p-Value	Gene Type	GencodeID	EntrezID
Themis3	-4.90	0.033	protein_coding	ENSMUSG00000024105.2	74556
Calm4	-4.83	0.020	protein_coding	ENSMUSG00000033765.4	80796
Gm38081	-4.07	0.008	TEC	ENSMUSG00000104363.1	NA
Ly6g6d	-3.73	0.016	protein_coding	ENSMUSG00000073413.9	114654
Gm4861	-3.67	0.011	protein_coding	ENSMUSG00000055138.9	229862
Dkk3	-3.58	0.000	protein_coding	ENSMUSG00000030772.6	50781
1700001O22Rik	-3.53	0.004	protein_coding	ENSMUSG00000044320.14	73598
Slc35f3	-3.49	0.027	protein_coding	ENSMUSG00000057060.7	210027
Fgfbp1	-3.45	0.014	protein_coding	ENSMUSG00000048373.8	14181
Mss51	-3.41	0.001	protein_coding	ENSMUSG00000021815.3	74843
Cdh4	-3.31	0.000	protein_coding	ENSMUSG00000000305.12	12561
Pld5	-3.24	0.001	protein_coding	ENSMUSG00000055214.15	319455
Gm44400	-3.22	0.021	TEC	ENSMUSG00000107488.1	NA
Gm43521	-3.21	0.029	TEC	ENSMUSG00000106511.1	NA
RP23-110M15.1	-3.19	0.030	lincRNA	ENSMUSG00000109853.1	102635797
Gm1604a	-3.09	0.025	protein_coding	ENSMUSG00000094083.1	381059
Sorcs1	-3.07	0.006	protein_coding	ENSMUSG00000043531.16	58178
Cntnap2	-2.84	0.002	protein_coding	ENSMUSG00000039419.17	66797
Gm20109	-2.80	0.032	lincRNA	ENSMUSG00000097714.1	NA
Neto2	-2.75	0.004	protein_coding	ENSMUSG00000036902.10	74513
Lrtm2	-2.71	0.046	protein_coding	ENSMUSG00000055003.14	211187
Odf3l2	-2.71	0.001	protein_coding	ENSMUSG00000035963.8	382384
Col9a1	-2.66	0.025	protein_coding	ENSMUSG00000026147.16	12839
Fggy	-2.66	0.001	protein_coding	ENSMUSG00000028573.18	75578
Syt9	-2.65	0.017	protein_coding	ENSMUSG00000062542.11	60510
Pla2g7	-2.64	0.000	protein_coding	ENSMUSG00000023913.17	27226
Slc2a3	-2.59	0.001	protein_coding	ENSMUSG00000003153.10	20527
Ighm	-2.58	0.001	IG_C_gene	ENSMUSG00000076617.9	NA
Gm10478	-2.52	0.042	pseudogene	ENSMUSG00000073179.3	NA
Gm38048	-2.49	0.005	sense_overlapping	ENSMUSG00000102437.1	NA
Shc2	-2.44	0.000	protein_coding	ENSMUSG00000020312.11	216148
Mdga1	-2.41	0.000	protein_coding	ENSMUSG00000043557.15	74762
Prima1	-2.41	0.013	protein_coding	ENSMUSG00000041669.15	170952
Cacna2d4	-2.38	0.029	protein_coding	ENSMUSG00000041460.14	319734
Gck	-2.34	0.002	protein_coding	ENSMUSG00000041798.15	103988
Slc4a10	-2.34	0.000	protein_coding	ENSMUSG00000026904.17	94229
Amd1	-2.32	0.000	protein_coding	ENSMUSG00000075232.4	11702
Snph	-2.31	0.003	protein_coding	ENSMUSG00000027457.15	241727
Amd2	-2.25	0.001	protein_coding	ENSMUSG00000063953.2	100041585
Mir694	-2.17	0.034	miRNA	ENSMUSG00000076147.1	751558
Mettl11b	-2.17	0.000	protein_coding	ENSMUSG00000040113.14	240879
9830004L10Rik	-2.16	0.001	lincRNA	ENSMUSG00000099552.1	NA
Gm26995	-2.15	0.050	antisense	ENSMUSG00000098072.1	NA
Tmem100	-2.15	0.002	protein_coding	ENSMUSG00000069763.3	67888
Pla2g5	-2.13	0.009	protein_coding	ENSMUSG00000041193.15	18784
2310065F04Rik	-2.12	0.000	lincRNA	ENSMUSG00000087410.7	74184
Amd-ps1	-2.07	0.005	processed_pseudogene	ENSMUSG00000083823.3	NA
Hist1h4n	-2.05	0.045	protein_coding	ENSMUSG00000069305.3	319161
Exph5	-2.04	0.001	protein_coding	ENSMUSG00000034584.3	320051
Amd-ps4	-2.03	0.020	processed_pseudogene	ENSMUSG00000019836.5	NA
A330015K06Rik	-2.03	0.004	antisense	ENSMUSG00000104093.1	102637797
Stk26	-2.03	0.000	protein_coding	ENSMUSG00000031112.10	70415
Wnt16	-2.01	0.005	protein_coding	ENSMUSG00000029671.15	93735
Nhs	-2.00	0.000	protein_coding	ENSMUSG00000059493.13	195727
Mib1	-1.99	0.000	protein_coding	ENSMUSG00000024294.13	225164
Igfn1	-1.99	0.006	protein_coding	ENSMUSG00000051985.12	226438
Gm38106	-1.98	0.025	TEC	ENSMUSG00000102266.1	NA
Tmem132b	-1.90	0.013	protein_coding	ENSMUSG00000070498.3	208151
Tpx2	-1.86	0.000	protein_coding	ENSMUSG00000027469.16	72119
M1ap	-1.85	0.006	protein_coding	ENSMUSG00000030041.9	110958
1700071M16Rik	-1.84	0.001	antisense	ENSMUSG00000090307.7	73504
Gm15034	-1.83	0.012	processed_pseudogene	ENSMUSG00000081320.1	NA
Gm42855	-1.83	0.047	processed_pseudogene	ENSMUSG00000105706.1	NA
Gdf11	-1.83	0.000	protein_coding	ENSMUSG00000025352.6	14561
Smox	-1.82	0.002	protein_coding	ENSMUSG00000027333.18	228608
Kcnab1	-1.82	0.001	protein_coding	ENSMUSG00000027827.16	16497
RP23-261B5.1	-1.81	0.000	TEC	ENSMUSG00000110411.1	NA
Mstn	-1.81	0.000	protein_coding	ENSMUSG00000026100.6	17700
Sorbs2	-1.77	0.000	protein_coding	ENSMUSG00000031626.17	234214
Amd-ps3	-1.76	0.005	processed_pseudogene	ENSMUSG00000060096.4	NA
Gm38158	-1.74	0.004	processed_pseudogene	ENSMUSG00000103367.1	NA
Uts2r	-1.70	0.037	protein_coding	ENSMUSG00000039321.1	217369
Gm5432	-1.69	0.017	lincRNA	ENSMUSG00000097580.1	NA
Rasd2	-1.69	0.001	protein_coding	ENSMUSG00000034472.13	75141
Fam83d	-1.67	0.007	protein_coding	ENSMUSG00000027654.2	71878
Ctxn3	-1.67	0.000	protein_coding	ENSMUSG00000069372.3	629147
Casr	-1.66	0.035	protein_coding	ENSMUSG00000051980.13	12374
Gm43699	-1.64	0.028	lincRNA	ENSMUSG00000107244.1	NA
Syt3	-1.62	0.002	protein_coding	ENSMUSG00000030731.13	20981
Ighg2c	-1.62	0.050	IG_C_gene	ENSMUSG00000076612.7	NA
Aurka	-1.62	0.000	protein_coding	ENSMUSG00000027496.15	20878
Adamts3	-1.61	0.012	protein_coding	ENSMUSG00000043635.12	330119
Rmi2	-1.61	0.030	protein_coding	ENSMUSG00000037991.9	223970
Pmepa1	-1.60	0.003	protein_coding	ENSMUSG00000038400.15	65112
Ccnk	-1.58	0.000	protein_coding	ENSMUSG00000021258.9	12454
Gm37053	-1.56	0.010	TEC	ENSMUSG00000103348.1	NA
Tiam1	-1.55	0.000	protein_coding	ENSMUSG00000002489.15	21844
Nr4a2	-1.55	0.019	protein_coding	ENSMUSG00000026826.13	18227
Hist1h4m	-1.55	0.003	protein_coding	ENSMUSG00000069306.5	100041230
Ttll7	-1.53	0.001	protein_coding	ENSMUSG00000036745.15	70892
Gm11512	-1.51	0.026	processed_pseudogene	ENSMUSG00000081043.1	NA
2310016D03Rik	-1.50	0.037	lincRNA	ENSMUSG00000102098.1	69566
Tnmd	-1.50	0.011	protein_coding	ENSMUSG00000031250.8	64103
Nos1	-1.49	0.001	protein_coding	ENSMUSG00000029361.18	18125
Sorbs2os	-1.48	0.001	antisense	ENSMUSG00000085440.1	319940
Macrod2os2	-1.47	0.021	antisense	ENSMUSG00000074763.5	NA
Fam65b	-1.46	0.008	protein_coding	ENSMUSG00000036006.19	193385
Mc2r	-1.45	0.004	protein_coding	ENSMUSG00000045569.6	17200
Syp	-1.44	0.008	protein_coding	ENSMUSG00000031144.15	20977
Kcnf1	-1.43	0.049	protein_coding	ENSMUSG00000051726.6	382571
Gdap1	-1.42	0.006	protein_coding	ENSMUSG00000025777.8	14545
Grem2	-1.42	0.009	protein_coding	ENSMUSG00000050069.3	23893
Kcnc3	-1.42	0.006	protein_coding	ENSMUSG00000062785.14	16504
Gm15824	-1.42	0.017	processed_pseudogene	ENSMUSG00000083435.2	NA
Gm7329	-1.42	0.033	processed_pseudogene	ENSMUSG00000100774.1	NA
Hr	-1.41	0.000	protein_coding	ENSMUSG00000022096.14	15460
Hsd17b7	-1.41	0.001	protein_coding	ENSMUSG00000026675.12	15490
Hlf	-1.40	0.001	protein_coding	ENSMUSG00000003949.16	217082
4933415F23Rik	-1.38	0.033	protein_coding	ENSMUSG00000073730.2	66755
Ptx4	-1.37	0.038	protein_coding	ENSMUSG00000044172.6	68509
Ankrd34a	-1.36	0.030	protein_coding	ENSMUSG00000049097.9	545554
Gm12199	-1.36	0.034	antisense	ENSMUSG00000087080.1	NA
Col22a1	-1.33	0.002	protein_coding	ENSMUSG00000079022.9	69700
Thbs4	-1.33	0.001	protein_coding	ENSMUSG00000021702.7	21828
Col24a1	-1.33	0.013	protein_coding	ENSMUSG00000028197.4	71355
Me1	-1.33	0.000	protein_coding	ENSMUSG00000032418.15	17436
Adgrf4	-1.32	0.007	protein_coding	ENSMUSG00000023918.12	78249
Gadl1	-1.32	0.012	protein_coding	ENSMUSG00000056880.12	73748
Pkp2	-1.31	0.002	protein_coding	ENSMUSG00000041957.15	67451
Fat3	-1.31	0.001	protein_coding	ENSMUSG00000074505.4	270120
Cacng7	-1.30	0.002	protein_coding	ENSMUSG00000069806.5	81904
Enox2	-1.30	0.000	protein_coding	ENSMUSG00000031109.16	209224
Aox3	-1.30	0.019	protein_coding	ENSMUSG00000064294.12	71724
Rtn4r	-1.30	0.002	protein_coding	ENSMUSG00000043811.5	65079
Ddah1	-1.29	0.043	protein_coding	ENSMUSG00000028194.15	69219
Gcnt1	-1.28	0.025	protein_coding	ENSMUSG00000038843.17	14537
Morn4	-1.27	0.002	protein_coding	ENSMUSG00000049670.8	226123
RP23-220F20.2	-1.26	0.016	protein_coding	ENSMUSG00000110344.1	NA
Slc16a3	-1.26	0.001	protein_coding	ENSMUSG00000025161.16	80879
Kera	-1.25	0.003	protein_coding	ENSMUSG00000019932.7	16545
Gm14698	-1.25	0.000	protein_coding	ENSMUSG00000071748.2	NA
Gpnmb	-1.23	0.029	protein_coding	ENSMUSG00000029816.10	93695
Gm7135	-1.23	0.045	transcribed_unprocessed_pseudogene	ENSMUSG00000101348.6	634346
Gpcpd1	-1.22	0.000	protein_coding	ENSMUSG00000027346.15	74182
Tubb2b	-1.21	0.048	protein_coding	ENSMUSG00000045136.5	73710
Myl4	-1.21	0.033	protein_coding	ENSMUSG00000061086.12	17896
C530050E15Rik	-1.20	0.010	lincRNA	ENSMUSG00000097838.1	NA
Adra1a	-1.20	0.010	protein_coding	ENSMUSG00000045875.12	11549
Nov	-1.19	0.026	protein_coding	ENSMUSG00000037362.8	18133
Eif3j1	-1.19	0.021	protein_coding	ENSMUSG00000027236.8	78655
Junos	-1.19	0.000	antisense	ENSMUSG00000087366.7	NA
Tbc1d1	-1.18	0.005	protein_coding	ENSMUSG00000029174.18	57915

METTL21AP1	4.82	3.76E-03	processed_pseudogene	ENSG00000229623.1	NA
CBR3	4.81	1.77E-04	protein_coding	ENSG00000159231.5	874
ZNF295-AS1	4.73	4.51E-04	lincRNA	ENSG00000237232.7	150142
AL109761.5	4.69	2.40E-04	antisense	ENSG00000244676.5	NA
GRIK1-AS1	4.68	3.51E-04	antisense	ENSG00000174680.9	NA
H2AFZP1	4.55	3.21E-04	processed_pseudogene	ENSG00000213440.2	NA
BACH1-AS1	4.53	4.86E-04	lincRNA	ENSG00000232118.2	NA
DSTNP1	4.52	3.63E-04	processed_pseudogene	ENSG00000230982.1	NA
RPS26P4	4.49	4.77E-04	processed_pseudogene	ENSG00000228349.1	NA
PCBP2P1	4.49	5.03E-04	processed_pseudogene	ENSG00000235701.1	NA
TTC3-AS1	4.49	7.20E-04	antisense	ENSG00000228677.1	NA
RIMKLBP1	4.46	1.05E-03	processed_pseudogene	ENSG00000189089.5	NA
BRWD1-IT1	4.42	4.90E-04	sense_overlapping	ENSG00000237373.1	NA
DIP2A-IT1	4.40	8.06E-04	sense_intronic	ENSG00000223692.1	100862692
RP5-1023B21.1	4.33	1.74E-03	lincRNA	ENSG00000267857.2	NA
AF015720.3	4.23	7.95E-04	lincRNA	ENSG00000230794.1	NA
AP000240.9	4.21	5.58E-04	sense_intronic	ENSG00000273017.1	NA
LINC01436	4.21	4.29E-03	lincRNA	ENSG00000231106.2	NA
AF064858.11	4.12	6.34E-04	lincRNA	ENSG00000237721.1	NA
RNU6-859P	4.10	7.22E-04	snRNA	ENSG00000199598.1	NA
AP001505.10	4.09	2.75E-03	lincRNA	ENSG00000276529.1	NA
AP000302.58	4.07	1.51E-03	antisense	ENSG00000231355.1	NA
KB-68A7.2	3.99	2.67E-03	lincRNA	ENSG00000277352.1	NA
TIMM9P2	3.96	3.39E-03	processed_pseudogene	ENSG00000232608.1	NA
LINC00189	3.91	4.13E-03	sense_overlapping	ENSG00000215533.8	193629
LINC00334	3.82	1.42E-03	lincRNA	ENSG00000182586.7	114042
HMGN1P2	3.78	2.16E-03	processed_pseudogene	ENSG00000229046.1	NA
RPS20P1	3.75	2.09E-03	processed_pseudogene	ENSG00000229761.1	NA
RPS5P2	3.70	2.45E-03	processed_pseudogene	ENSG00000224598.1	NA
RPL23P2	3.70	1.91E-03	processed_pseudogene	ENSG00000176054.6	NA
SNORA81	3.49	4.34E-03	snoRNA	ENSG00000238390.1	NA
RNU6-614P	3.43	4.75E-03	snRNA	ENSG00000207097.1	NA
BTF3P6	3.43	2.55E-03	processed_pseudogene	ENSG00000233956.1	NA
BACH1-IT3	3.40	3.97E-03	sense_intronic	ENSG00000234293.1	NA
AP001412.1	3.36	3.40E-03	antisense	ENSG00000272948.2	NA
AP001437.1	3.35	9.28E-03	antisense	ENSG00000273210.1	NA
AF124730.4	3.27	9.00E-03	antisense	ENSG00000224649.1	NA
RP1-100J12.1	3.18	5.00E-03	antisense	ENSG00000273254.1	NA
AP001619.2	3.18	4.13E-03	sense_intronic	ENSG00000227698.1	NA
AP001619.3	3.05	8.81E-03	antisense	ENSG00000236545.1	NA
FGF7P2	2.88	2.98E-02	unprocessed_pseudogene	ENSG00000185390.2	NA
DPRXP5	2.79	4.53E-02	processed_pseudogene	ENSG00000270652.1	NA
U3	2.74	1.81E-02	snoRNA	ENSG00000212479.2	NA
AP001625.4	2.59	3.25E-02	sense_intronic	ENSG00000239930.2	101930094
RNU6-123P	2.48	3.98E-02	snRNA	ENSG00000251972.1	NA
SNORA80A	2.40	4.11E-02	snoRNA	ENSG00000200792.1	677846
AP001439.2	2.33	4.77E-02	antisense	ENSG00000224541.1	NA

Serpinb1a	1.06	0.026	protein_coding	ENSMUSG00000044734.15	66222
Gm37691	1.06	0.005	TEC	ENSMUSG00000104348.1	NA
Rapgefl1	1.05	0.033	protein_coding	ENSMUSG00000038020.5	268480
Fam83g	1.04	0.004	protein_coding	ENSMUSG00000042377.8	69640
Sh2d4a	1.04	0.006	protein_coding	ENSMUSG00000053886.4	72281
A830010M20Rik	1.04	0.004	protein_coding	ENSMUSG00000044060.18	NA
Sbsn	1.03	0.031	protein_coding	ENSMUSG00000046056.15	282619
Rapgef4os3	1.03	0.038	antisense	ENSMUSG00000086231.1	NA
Katnal2	1.03	0.015	protein_coding	ENSMUSG00000025420.13	71206
Gm15543	1.02	0.029	antisense	ENSMUSG00000086863.1	105242817
Snai3	1.01	0.001	protein_coding	ENSMUSG00000006587.6	30927
Adam1b	1.01	0.046	protein_coding	ENSMUSG00000062438.4	280667
Atf5	1.01	0.008	protein_coding	ENSMUSG00000038539.15	107503
Mx2	1.00	0.038	polymorphic_pseudogene	ENSMUSG00000023341.14	17858
Tmem116	1.00	0.014	protein_coding	ENSMUSG00000029452.18	77462
Fam166a	1.00	0.047	protein_coding	ENSMUSG00000026969.3	68222
Gm14762	1.00	0.042	lincRNA	ENSMUSG00000078314.2	NA
Zfp69	1.00	0.043	protein_coding	ENSMUSG00000064141.14	381549
0610040B10Rik	1.00	0.004	antisense	ENSMUSG00000089889.2	NA
Gm15860	1.00	0.026	antisense	ENSMUSG00000087336.2	NA
Mterf1a	0.99	0.033	protein_coding	ENSMUSG00000040429.6	545725
Mogat2	0.99	0.032	protein_coding	ENSMUSG00000052396.7	233549
Iigp1	0.99	0.032	protein_coding	ENSMUSG00000054072.11	60440
Arid5a	0.98	0.001	protein_coding	ENSMUSG00000037447.16	214855
Gm38250	0.98	0.049	antisense	ENSMUSG00000104168.1	NA
Vash2	0.97	0.036	protein_coding	ENSMUSG00000037568.12	226841
Lrp2bp	0.97	0.001	protein_coding	ENSMUSG00000031637.13	67620
5031434C07Rik	0.97	0.006	antisense	ENSMUSG00000044574.5	NA
Gm5617	0.97	0.005	protein_coding	ENSMUSG00000042293.7	434402
Rad51	0.97	0.033	protein_coding	ENSMUSG00000027323.10	19361
Osbp2	0.97	0.017	protein_coding	ENSMUSG00000020435.17	74309
Pdp2	0.97	0.006	protein_coding	ENSMUSG00000048371.8	382051
Lsmem1	0.96	0.000	protein_coding	ENSMUSG00000071342.4	380755
Dqx1	0.95	0.030	protein_coding	ENSMUSG00000009145.6	93838
Actn2	0.95	0.006	protein_coding	ENSMUSG00000052374.14	11472
Cmpk2	0.95	0.025	protein_coding	ENSMUSG00000020638.7	22169
Tlcd2	0.94	0.022	protein_coding	ENSMUSG00000038217.13	380712
Prkcz	0.94	0.042	protein_coding	ENSMUSG00000029053.16	18762
Aqp4	0.94	0.021	protein_coding	ENSMUSG00000024411.9	11829
E230016M11Rik	0.94	0.016	processed_transcript	ENSMUSG00000087231.7	320172
1810021B22Rik	0.94	0.011	processed_transcript	ENSMUSG00000087331.8	69120
Dnaja4	0.93	0.005	protein_coding	ENSMUSG00000032285.15	58233
Xirp1	0.93	0.007	protein_coding	ENSMUSG00000079243.2	22437
Gm37759	0.93	0.036	antisense	ENSMUSG00000102717.1	NA
Plin3	0.93	0.002	protein_coding	ENSMUSG00000024197.9	66905
Gm45061	0.93	0.030	TEC	ENSMUSG00000108075.1	NA
Gm42974	0.92	0.033	TEC	ENSMUSG00000104963.1	NA
Bbc3	0.92	0.024	protein_coding	ENSMUSG00000002083.13	170770
4930451G09Rik	0.91	0.019	protein_coding	ENSMUSG00000022543.8	74684
Gm44193	0.91	0.016	TEC	ENSMUSG00000107559.1	NA
Ccdc189	0.90	0.043	protein_coding	ENSMUSG00000057176.4	233899
Tmem71	0.90	0.003	protein_coding	ENSMUSG00000036944.5	213068
Actc1	0.90	0.025	protein_coding	ENSMUSG00000068614.7	11464
Sytl2	0.89	0.009	protein_coding	ENSMUSG00000030616.15	83671
Gm13443	0.88	0.007	processed_pseudogene	ENSMUSG00000075391.6	NA
Trim43a	0.88	0.020	protein_coding	ENSMUSG00000090693.3	547109
Lmcd1	0.88	0.003	protein_coding	ENSMUSG00000057604.9	30937
Nab2	0.87	0.014	protein_coding	ENSMUSG00000025402.12	17937
H2-Q5	0.87	0.037	polymorphic_pseudogene	ENSMUSG00000055413.12	15016
A930018M24Rik	0.87	0.006	protein_coding	ENSMUSG00000091089.1	NA
BC023105	0.86	0.006	pseudogene	ENSMUSG00000063388.4	NA
A330074K22Rik	0.86	0.015	lincRNA	ENSMUSG00000097960.1	434353
Slc7a1	0.86	0.009	protein_coding	ENSMUSG00000041313.14	11987
Slc25a13	0.85	0.033	protein_coding	ENSMUSG00000015112.15	50799
Gm26574	0.85	0.035	antisense	ENSMUSG00000097925.1	NA
Sacs	0.85	0.003	protein_coding	ENSMUSG00000048279.17	50720
Spsb2	0.85	0.006	protein_coding	ENSMUSG00000038451.13	14794
Ephb1	0.85	0.049	protein_coding	ENSMUSG00000032537.14	270190
Ptprq	0.84	0.036	protein_coding	ENSMUSG00000035916.7	237523
Dynlt1c	0.84	0.017	protein_coding	ENSMUSG00000000579.14	100040563
Gm13943	0.84	0.006	lincRNA	ENSMUSG00000085277.1	NA
Nudt5	0.84	0.005	protein_coding	ENSMUSG00000025817.12	53893
Cxx1b	0.83	0.001	protein_coding	ENSMUSG00000067924.4	553127
C130036L24Rik	0.83	0.012	processed_transcript	ENSMUSG00000073627.7	NA
Tspan13	0.83	0.001	protein_coding	ENSMUSG00000020577.15	66109
Egf	0.83	0.001	protein_coding	ENSMUSG00000028017.7	13645
Gm6368	0.83	0.043	processed_pseudogene	ENSMUSG00000080775.1	NA
Parp14	0.82	0.002	protein_coding	ENSMUSG00000034422.14	547253
Abra	0.82	0.011	protein_coding	ENSMUSG00000042895.5	223513
Nxpe3	0.82	0.048	protein_coding	ENSMUSG00000075033.3	385658
Tbx6	0.82	0.037	protein_coding	ENSMUSG00000030699.16	21389
Slc25a34	0.82	0.047	protein_coding	ENSMUSG00000040740.7	384071
Gm9920	0.80	0.048	protein_coding	ENSMUSG00000053749.12	100503794
Sept1	0.80	0.010	protein_coding	ENSMUSG00000000486.13	54204
Ifih1	0.80	0.003	protein_coding	ENSMUSG00000026896.14	71586
Gpt	0.80	0.002	protein_coding	ENSMUSG00000022546.4	76282
Prrxl1	0.80	0.041	protein_coding	ENSMUSG00000041730.13	107751
Gm42972	0.80	0.040	TEC	ENSMUSG00000105445.1	NA
Rhou	0.80	0.025	protein_coding	ENSMUSG00000039960.5	69581
Arhgef2	0.79	0.000	protein_coding	ENSMUSG00000028059.15	16800
Pank1	0.79	0.025	protein_coding	ENSMUSG00000033610.15	75735
Aspa	0.79	0.008	protein_coding	ENSMUSG00000020774.9	11484
Rsad2	0.79	0.049	protein_coding	ENSMUSG00000020641.15	58185
Gm42973	0.78	0.046	TEC	ENSMUSG00000105733.1	NA
Got1	0.78	0.001	protein_coding	ENSMUSG00000025190.13	14718
Galnt7	0.77	0.006	protein_coding	ENSMUSG00000031608.13	108150
Obsl1	0.77	0.012	protein_coding	ENSMUSG00000026211.17	98733
Prkg1	0.77	0.023	protein_coding	ENSMUSG00000052920.14	19091
Gm10524	0.76	0.045	TEC	ENSMUSG00000097141.2	NA
Tal2	0.76	0.038	protein_coding	ENSMUSG00000028417.3	21350
Hmga1-rs1	0.76	0.018	protein_coding	ENSMUSG00000078249.5	111241
Ift27	0.76	0.033	protein_coding	ENSMUSG00000016637.6	67042
Ckmt2	0.75	0.009	protein_coding	ENSMUSG00000021622.3	76722
P2ry1	0.75	0.017	protein_coding	ENSMUSG00000027765.6	18441
Perm1	0.75	0.001	protein_coding	ENSMUSG00000078486.3	74183
2210011C24Rik	0.75	0.013	protein_coding	ENSMUSG00000074217.8	70134
Myog	0.75	0.050	protein_coding	ENSMUSG00000026459.5	17928
Ifit1	0.75	0.035	protein_coding	ENSMUSG00000034459.8	15957
Trp63	0.74	0.001	protein_coding	ENSMUSG00000022510.14	22061
Slc16a1	0.74	0.003	protein_coding	ENSMUSG00000032902.1	20501
Esrrg	0.74	0.033	protein_coding	ENSMUSG00000026610.13	26381
Apobec2	0.74	0.002	protein_coding	ENSMUSG00000040694.3	11811
Gm16216	0.74	0.036	processed_pseudogene	ENSMUSG00000082107.1	NA
Fam83h	0.73	0.012	protein_coding	ENSMUSG00000046761.12	105732
2810032G03Rik	0.73	0.048	lincRNA	ENSMUSG00000037735.7	72669
Zfp870	0.73	0.028	protein_coding	ENSMUSG00000095325.1	240066
Kdr	0.73	0.019	protein_coding	ENSMUSG00000062960.10	16542
Btnl9	0.73	0.032	protein_coding	ENSMUSG00000040283.14	237754
Rad9b	0.72	0.028	protein_coding	ENSMUSG00000038569.13	231724
Gmnn	0.72	0.016	protein_coding	ENSMUSG00000006715.11	57441
Mvd	0.72	0.027	protein_coding	ENSMUSG00000006517.5	192156
Coq8a	0.72	0.001	protein_coding	ENSMUSG00000026489.13	67426
Gm26628	0.72	0.048	antisense	ENSMUSG00000097133.1	102632638
Tbc1d4	0.72	0.015	protein_coding	ENSMUSG00000033083.16	210789
1110020A21Rik	0.72	0.043	lincRNA	ENSMUSG00000097047.1	68531
Habp2	0.72	0.026	protein_coding	ENSMUSG00000025075.14	226243
Evc	0.72	0.005	protein_coding	ENSMUSG00000029122.11	59056
Tmem47	0.71	0.010	protein_coding	ENSMUSG00000025666.16	192216
Gm6736	0.71	0.033	processed_pseudogene	ENSMUSG00000071414.4	NA
Fam69b	0.71	0.033	protein_coding	ENSMUSG00000036186.5	56279
Snn	0.70	0.027	protein_coding	ENSMUSG00000037972.6	20621
Plet1	0.70	0.038	protein_coding	ENSMUSG00000032068.14	76509
Amot	0.70	0.001	protein_coding	ENSMUSG00000041688.16	27494
Gm10390	0.70	0.022	antisense	ENSMUSG00000097368.2	100503427
Deptor	0.70	0.017	protein_coding	ENSMUSG00000022419.15	97998
Stc2	0.70	0.042	protein_coding	ENSMUSG00000020303.2	20856
Cdkl3	0.70	0.005	protein_coding	ENSMUSG00000020389.19	213084
Ptpn14	0.70	0.002	protein_coding	ENSMUSG00000026604.17	19250
Gm35339	0.70	0.026	protein_coding	ENSMUSG00000109179.1	102638882
Ache	0.70	0.013	protein_coding	ENSMUSG00000023328.14	11423
Bche	0.69	0.043	protein_coding	ENSMUSG00000027792.11	12038
Ppm1k	0.69	0.001	protein_coding	ENSMUSG00000037826.5	243382
Lrrc74b	0.69	0.025	protein_coding	ENSMUSG00000022759.13	74685
Gm15545	0.69	0.033	antisense	ENSMUSG00000087138.1	100502630
Stbd1	0.69	0.039	protein_coding	ENSMUSG00000047963.7	52331
Kctd1	0.69	0.047	protein_coding	ENSMUSG00000036225.14	106931

Fxyd2	-1.18	0.030	protein_coding	ENSMUSG00000059412.6	11936
Macrod2os1	-1.18	0.014	antisense	ENSMUSG00000086450.1	NA
Xpr1	-1.16	0.001	protein_coding	ENSMUSG00000026469.14	19775
Styx	-1.16	0.000	protein_coding	ENSMUSG00000053205.8	56291
Nos1ap	-1.16	0.035	protein_coding	ENSMUSG00000038473.14	70729
Tpbgl	-1.15	0.002	protein_coding	ENSMUSG00000096606.2	100503386
Lrtm1	-1.14	0.016	protein_coding	ENSMUSG00000045776.2	319476
Whrn	-1.14	0.014	protein_coding	ENSMUSG00000039137.18	73750
Cdk19	-1.14	0.002	protein_coding	ENSMUSG00000038481.12	78334
4930556M19Rik	-1.14	0.005	lincRNA	ENSMUSG00000096971.1	75259
Gm17218	-1.14	0.011	antisense	ENSMUSG00000091078.1	NA
Wnt4	-1.13	0.002	protein_coding	ENSMUSG00000036856.4	22417
Gm5865	-1.12	0.006	processed_pseudogene	ENSMUSG00000104923.1	NA
Spred3	-1.11	0.002	protein_coding	ENSMUSG00000037239.8	101809
Mylk2	-1.10	0.001	protein_coding	ENSMUSG00000027470.9	228785
Tnc	-1.10	0.001	protein_coding	ENSMUSG00000028364.15	21923
Sema3a	-1.09	0.006	protein_coding	ENSMUSG00000028883.17	20346
Mfap3l	-1.09	0.003	protein_coding	ENSMUSG00000031647.10	71306
Ngf	-1.08	0.034	protein_coding	ENSMUSG00000027859.10	18049
Comp	-1.08	0.038	protein_coding	ENSMUSG00000031849.9	12845
Stab2	-1.08	0.005	protein_coding	ENSMUSG00000035459.15	192188
Fmod	-1.08	0.002	protein_coding	ENSMUSG00000041559.7	14264
Cpeb1	-1.07	0.004	protein_coding	ENSMUSG00000025586.17	12877
Spns2	-1.07	0.000	protein_coding	ENSMUSG00000040447.15	216892
Bcl2	-1.06	0.001	protein_coding	ENSMUSG00000057329.7	12043
Calm3	-1.06	0.000	protein_coding	ENSMUSG00000019370.10	12315
Wbscr17	-1.05	0.004	protein_coding	ENSMUSG00000034040.16	212996
Ccdc146	-1.04	0.041	protein_coding	ENSMUSG00000064280.13	75172
Smarca1	-1.04	0.038	protein_coding	ENSMUSG00000031099.16	93761
AI854703	-1.03	0.004	protein_coding	ENSMUSG00000053297.14	NA
Stim2	-1.03	0.000	protein_coding	ENSMUSG00000039156.19	116873
Mc5r	-1.02	0.049	protein_coding	ENSMUSG00000007480.3	17203
Xylt1	-1.02	0.002	protein_coding	ENSMUSG00000030657.11	233781
Shisa3	-1.02	0.023	protein_coding	ENSMUSG00000050010.8	330096
Pde4b	-1.02	0.003	protein_coding	ENSMUSG00000028525.16	18578
Tspyl5	-1.01	0.013	protein_coding	ENSMUSG00000038984.3	239364
Actr3b	-1.01	0.000	protein_coding	ENSMUSG00000056367.14	242894
Npnt	-1.01	0.031	protein_coding	ENSMUSG00000040998.18	114249
Net1	-1.01	0.000	protein_coding	ENSMUSG00000021215.14	56349
Fam78a	-1.01	0.005	protein_coding	ENSMUSG00000050592.8	241303
Gm7694	-1.01	0.046	protein_coding	ENSMUSG00000102752.1	665574
Fras1	-1.00	0.036	protein_coding	ENSMUSG00000034687.8	231470
Lrrc55	-1.00	0.049	protein_coding	ENSMUSG00000075224.8	241528
Nkain1	-1.00	0.000	protein_coding	ENSMUSG00000078532.9	67149
Phex	-1.00	0.022	protein_coding	ENSMUSG00000057457.11	18675
Zfp52	-1.00	0.008	protein_coding	ENSMUSG00000051341.5	22710
Gm14680	-0.99	0.005	processed_pseudogene	ENSMUSG00000081752.3	NA
Calm1	-0.99	0.000	protein_coding	ENSMUSG00000001175.13	12313
Slc30a2	-0.98	0.031	protein_coding	ENSMUSG00000028836.14	230810
Phka1	-0.98	0.000	protein_coding	ENSMUSG00000034055.16	18679
Slc16a10	-0.98	0.001	protein_coding	ENSMUSG00000019838.10	72472
Gm36962	-0.97	0.007	TEC	ENSMUSG00000103931.1	NA
Gm10605	-0.97	0.023	lincRNA	ENSMUSG00000097974.1	NA
Gm5881	-0.97	0.008	processed_pseudogene	ENSMUSG00000107747.1	NA
Rnase13	-0.97	0.042	protein_coding	ENSMUSG00000068392.2	497071
Tmem233	-0.97	0.000	protein_coding	ENSMUSG00000079278.1	545798
Tifa	-0.96	0.042	protein_coding	ENSMUSG00000046688.14	211550
Tcte2	-0.96	0.017	protein_coding	ENSMUSG00000038347.14	21646
Smarcd3	-0.96	0.000	protein_coding	ENSMUSG00000028949.13	66993
Gm10118	-0.96	0.032	protein_coding	ENSMUSG00000062561.3	NA
Fam69a	-0.96	0.004	protein_coding	ENSMUSG00000029270.10	67266
Fbp2	-0.95	0.001	protein_coding	ENSMUSG00000021456.7	14120
D1Ertd622e	-0.95	0.004	protein_coding	ENSMUSG00000044768.16	52392
D430041D05Rik	-0.94	0.004	protein_coding	ENSMUSG00000068373.14	241589
Gm11451	-0.94	0.035	processed_pseudogene	ENSMUSG00000083567.3	NA
Wnk3	-0.94	0.004	protein_coding	ENSMUSG00000041245.13	279561
Tppp	-0.93	0.003	protein_coding	ENSMUSG00000021573.14	72948
Nek5	-0.93	0.045	protein_coding	ENSMUSG00000037738.10	330721
Adgre1	-0.93	0.041	protein_coding	ENSMUSG00000004730.14	13733
Nmbr	-0.93	0.039	protein_coding	ENSMUSG00000019865.9	18101
Gpr155	-0.93	0.000	protein_coding	ENSMUSG00000041762.16	68526
Map9	-0.92	0.030	protein_coding	ENSMUSG00000033900.13	213582
Ccdc6	-0.92	0.000	protein_coding	ENSMUSG00000048701.13	76551
Vasp	-0.92	0.003	protein_coding	ENSMUSG00000030403.9	22323
Gm15820	-0.92	0.033	processed_pseudogene	ENSMUSG00000107105.1	NA
Hoxa11	-0.92	0.040	protein_coding	ENSMUSG00000038210.10	15396
Gm15511	-0.91	0.037	antisense	ENSMUSG00000086648.1	102642202
Slc38a4	-0.91	0.005	protein_coding	ENSMUSG00000022464.13	69354
Map2k6	-0.91	0.002	protein_coding	ENSMUSG00000020623.11	26399
D930007P13Rik	-0.90	0.050	lincRNA	ENSMUSG00000097003.1	432989
Fgf7	-0.90	0.017	protein_coding	ENSMUSG00000027208.14	14178
Aebp1	-0.90	0.029	protein_coding	ENSMUSG00000020473.13	11568
Ptgfr	-0.90	0.048	protein_coding	ENSMUSG00000028036.6	19220
Scamp5	-0.89	0.033	protein_coding	ENSMUSG00000040722.6	56807
Pdgfc	-0.89	0.043	protein_coding	ENSMUSG00000028019.9	54635
Itga4	-0.89	0.000	protein_coding	ENSMUSG00000027009.18	16401
Slc37a4	-0.89	0.010	protein_coding	ENSMUSG00000032114.8	14385
Col11a1	-0.89	0.012	protein_coding	ENSMUSG00000027966.20	12814
Il1rl1	-0.88	0.036	protein_coding	ENSMUSG00000026069.15	17082
Fam189b	-0.88	0.007	protein_coding	ENSMUSG00000032657.15	68521
Gcnt2	-0.88	0.006	protein_coding	ENSMUSG00000021360.15	14538
Vit	-0.88	0.030	protein_coding	ENSMUSG00000024076.9	74199
Col8a2	-0.88	0.046	protein_coding	ENSMUSG00000056174.8	329941
Polk	-0.87	0.000	protein_coding	ENSMUSG00000021668.14	27015
Tbx18	-0.87	0.037	protein_coding	ENSMUSG00000032419.8	76365
Odc1	-0.87	0.024	protein_coding	ENSMUSG00000011179.7	18263
Gm38393	-0.87	0.003	protein_coding	ENSMUSG00000000948.16	NA
Fibin	-0.87	0.012	protein_coding	ENSMUSG00000074971.4	67606
Mylk4	-0.86	0.004	protein_coding	ENSMUSG00000044951.13	238564
Tigd4	-0.86	0.009	protein_coding	ENSMUSG00000047819.3	403175
Chodl	-0.86	0.049	protein_coding	ENSMUSG00000022860.14	246048
Tfcp2l1	-0.86	0.016	protein_coding	ENSMUSG00000026380.10	81879
Auts2	-0.85	0.008	protein_coding	ENSMUSG00000029673.17	319974
Srcin1	-0.85	0.004	protein_coding	ENSMUSG00000038453.16	56013
Tdrkh	-0.85	0.005	protein_coding	ENSMUSG00000041912.12	72634
Zfp467	-0.85	0.003	protein_coding	ENSMUSG00000068551.12	68910
Mpp3	-0.85	0.031	protein_coding	ENSMUSG00000052373.14	13384
Aph1c	-0.84	0.047	protein_coding	ENSMUSG00000053040.13	68318
Smtnl2	-0.84	0.005	protein_coding	ENSMUSG00000045667.14	276829
Sms	-0.84	0.003	protein_coding	ENSMUSG00000071708.11	20603
Adgrl1	-0.83	0.007	protein_coding	ENSMUSG00000013033.16	330814
Hoxa13	-0.83	0.013	protein_coding	ENSMUSG00000038203.18	15398
Pdlim7	-0.83	0.000	protein_coding	ENSMUSG00000021493.15	67399
Klf2	-0.83	0.045	protein_coding	ENSMUSG00000055148.7	16598
Ccdc50	-0.82	0.000	protein_coding	ENSMUSG00000038127.14	67501
mt-Tp	-0.82	0.001	Mt_tRNA	ENSMUSG00000064372.1	NA
Ppp1r14c	-0.82	0.001	protein_coding	ENSMUSG00000040653.5	76142
Ccnyl1	-0.82	0.003	protein_coding	ENSMUSG00000070871.10	227210
Rnf126	-0.82	0.003	protein_coding	ENSMUSG00000035890.8	70294
Gnao1	-0.82	0.002	protein_coding	ENSMUSG00000031748.16	14681
Arnt2	-0.82	0.048	protein_coding	ENSMUSG00000015709.9	11864
Ybx3	-0.81	0.000	protein_coding	ENSMUSG00000030189.15	56449
Kmt5a	-0.80	0.001	protein_coding	ENSMUSG00000049327.17	67956
Gm43268	-0.80	0.027	TEC	ENSMUSG00000107182.1	NA
Mtss1l	-0.80	0.004	protein_coding	ENSMUSG00000033763.14	244654
Zfp277	-0.80	0.017	protein_coding	ENSMUSG00000055917.14	246196
Myh4	-0.80	0.003	protein_coding	ENSMUSG00000057003.12	17884
Hacd1	-0.80	0.001	protein_coding	ENSMUSG00000063275.15	30963
Cd109	-0.80	0.013	protein_coding	ENSMUSG00000046186.8	235505
Gnpnat1	-0.80	0.001	protein_coding	ENSMUSG00000037722.7	54342
Cys1	-0.79	0.048	protein_coding	ENSMUSG00000062563.14	12879
Acvr1b	-0.79	0.005	protein_coding	ENSMUSG00000000532.10	11479
Pde7a	-0.79	0.002	protein_coding	ENSMUSG00000069094.12	18583
Gid4	-0.78	0.000	protein_coding	ENSMUSG00000018415.14	66771
Gm43946	-0.78	0.009	TEC	ENSMUSG00000107720.1	NA
Plekhb1	-0.78	0.004	protein_coding	ENSMUSG00000030701.17	27276
Gm14326	-0.78	0.005	protein_coding	ENSMUSG00000078862.10	665211
Cpeb2	-0.77	0.002	protein_coding	ENSMUSG00000039782.14	231207
Sap30	-0.77	0.026	protein_coding	ENSMUSG00000031609.3	60406
Igfbp5	-0.77	0.013	protein_coding	ENSMUSG00000026185.8	16011
Msrb3	-0.77	0.000	protein_coding	ENSMUSG00000051236.13	320183
Gprc5b	-0.76	0.000	protein_coding	ENSMUSG00000008734.9	64297
Gm15943	-0.76	0.046	processed_transcript	ENSMUSG00000086801.1	NA
Syt8	-0.76	0.046	protein_coding	ENSMUSG00000031098.18	55925
Gm43807	-0.76	0.049	sense_intronic	ENSMUSG00000107048.1	NA
Col12a1	-0.76	0.007	protein_coding	ENSMUSG00000032332.17	12816

Gm5113	0.69	0.004	protein_coding	ENSMUSG00000066647.6	330503	*Fermt2*	-0.75	0.000	protein_coding	ENSMUSG00000037712.15	218952
B9d2	0.68	0.027	protein_coding	ENSMUSG00000063439.7	232987	*Slc25a30*	-0.75	0.027	protein_coding	ENSMUSG00000022003.6	67554
Nlrc5	0.68	0.040	protein_coding	ENSMUSG00000074151.13	434341	*Hook1*	-0.75	0.004	protein_coding	ENSMUSG00000028572.13	77963
Iqcg	0.68	0.024	protein_coding	ENSMUSG00000035578.15	69707	*Gas1*	-0.75	0.002	protein_coding	ENSMUSG00000052957.7	14451
Gm7967	0.68	0.036	lincRNA	ENSMUSG00000100009.6	NA	*Bmp2*	-0.75	0.018	protein_coding	ENSMUSG00000027358.6	12156
Cdc14a	0.67	0.041	protein_coding	ENSMUSG00000033502.14	229776	*Dennd2c*	-0.75	0.013	protein_coding	ENSMUSG00000007379.15	329727
Parp10	0.67	0.009	protein_coding	ENSMUSG00000063268.12	671535	*Mab21l1*	-0.75	0.039	protein_coding	ENSMUSG00000056947.5	17116
Tm6sf1	0.67	0.033	protein_coding	ENSMUSG00000038623.9	107769	*Tspan8*	-0.75	0.012	protein_coding	ENSMUSG00000034127.14	216350
Fam13a	0.67	0.012	protein_coding	ENSMUSG00000037709.13	58909	*Mrln*	-0.74	0.012	processed_transcript	ENSMUSG00000019933.7	69563
Evc2	0.67	0.001	protein_coding	ENSMUSG00000050248.11	68525	*Plekho1*	-0.74	0.002	protein_coding	ENSMUSG00000015745.9	67220
Rfx5	0.66	0.005	protein_coding	ENSMUSG00000005774.12	53970	*Gm22362*	-0.74	0.037	snoRNA	ENSMUSG00000065036.1	115486329
Ldhd	0.66	0.006	protein_coding	ENSMUSG00000031958.16	52815	*Prkab2*	-0.73	0.004	protein_coding	ENSMUSG00000038205.12	108097
App	0.66	0.008	protein_coding	ENSMUSG00000022892.10	11820	*Homer1*	-0.73	0.000	protein_coding	ENSMUSG00000007617.17	26556
Ltbp1	0.65	0.004	protein_coding	ENSMUSG00000001870.15	268977	*Rhobtb1*	-0.73	0.012	protein_coding	ENSMUSG00000019944.14	69288
Fam110a	0.65	0.031	protein_coding	ENSMUSG00000027459.16	73847	*Eya1*	-0.73	0.000	protein_coding	ENSMUSG00000025932.14	14048
Plet1os	0.65	0.024	antisense	ENSMUSG00000101304.1	69631	*Six2*	-0.73	0.016	protein_coding	ENSMUSG00000024134.11	20472
2900052L18Rik	0.65	0.009	processed_transcript	ENSMUSG00000043993.6	NA	*Anxa1*	-0.73	0.046	protein_coding	ENSMUSG00000024659.14	16952
Flnc	0.65	0.014	protein_coding	ENSMUSG00000068699.12	68794	*Osbpl6*	-0.73	0.001	protein_coding	ENSMUSG00000042359.18	99031
Il6ST	0.65	0.013	protein_coding	ENSMUSG00000010358.13	70110	*Shtn1*	-0.73	0.045	protein_coding	ENSMUSG00000041362.16	71653
H2-T24	0.65	0.012	protein_coding	ENSMUSG00000053835.17	15042	*Capg*	-0.73	0.015	protein_coding	ENSMUSG00000056737.14	12332
Klhl33	0.64	0.013	protein_coding	ENSMUSG00000090799.1	546611	*Gm10762*	-0.73	0.034	protein_coding	ENSMUSG00000074807.2	NA
Tpm2	0.64	0.003	protein_coding	ENSMUSG00000028464.16	22004	*Nudt3*	-0.72	0.000	protein_coding	ENSMUSG00000024213.13	56409
AW011738	0.64	0.021	protein_coding	ENSMUSG00000078349.2	100382	*Gfer*	-0.72	0.009	protein_coding	ENSMUSG00000040888.9	11692
Sesn3	0.64	0.004	protein_coding	ENSMUSG00000032009.8	75747	*Prkcd*	-0.72	0.008	protein_coding	ENSMUSG00000021948.15	18753
Pex6	0.64	0.017	protein_coding	ENSMUSG00000002763.16	224824	*Cd24a*	-0.72	0.010	protein_coding	ENSMUSG00000047139.8	12484
Cyp4f13	0.64	0.035	protein_coding	ENSMUSG00000024055.14	170716	*Tgif1*	-0.72	0.017	protein_coding	ENSMUSG00000047407.17	21815
Chmp1	0.64	0.006	protein_coding	ENSMUSG00000041189.9	11443	*Dagla*	-0.71	0.005	protein_coding	ENSMUSG00000056735.10	269060
Hspb1	0.64	0.010	protein_coding	ENSMUSG00000044951.10	15507	*Gpi2*	-0.71	0.002	protein_coding	ENSMUSG00000031706.11	109682
Mpc1-ps	0.64	0.009	processed_pseudogene	ENSMUSG00000091498.4	NA	*E130308A19Rik*	-0.71	0.038	protein_coding	ENSMUSG00000045071.13	230259
Cox6a2	0.64	0.002	protein_coding	ENSMUSG00000030785.8	12862	*Efemp1*	-0.71	0.016	protein_coding	ENSMUSG00000020467.15	216616
Fam73b	0.64	0.050	protein_coding	ENSMUSG00000026858.18	108958	*Musk*	-0.71	0.015	protein_coding	ENSMUSG00000057280.15	18198
4930513N20Rik	0.63	0.007	TEC	ENSMUSG00000109225.1	NA	*Slc10a7*	-0.71	0.002	protein_coding	ENSMUSG00000031684.11	76775
Gm15337	0.63	0.045	antisense	ENSMUSG00000085289.1	NA	*Tdrp*	-0.70	0.048	protein_coding	ENSMUSG00000050052.12	72148
Gm11613	0.63	0.006	processed_transcript	ENSMUSG00000085586.1	NA	*Samd1*	-0.70	0.033	protein_coding	ENSMUSG00000079003.2	666704
Pnpla2	0.63	0.012	protein_coding	ENSMUSG00000025509.15	66853	*Tab2*	-0.70	0.000	protein_coding	ENSMUSG00000015755.16	68652
4632428C04Rik	0.63	0.047	lincRNA	ENSMUSG00000097184.1	100043102	*Elfd1*	-0.70	0.042	protein_coding	ENSMUSG00000026255.15	98363
Ins1	0.63	0.011	protein_coding	ENSMUSG00000055980.2	16367	*Vps72*	-0.69	0.001	protein_coding	ENSMUSG00000008958.14	21427
Gm17197	0.63	0.013	antisense	ENSMUSG00000090990.1	NA	*Ppp1r14b*	-0.69	0.002	protein_coding	ENSMUSG00000056612.6	18938
Plekhn1	0.63	0.038	protein_coding	ENSMUSG00000078485.2	231002	*Ociad2*	-0.69	0.039	protein_coding	ENSMUSG00000029153.11	433904
Zfp827	0.63	0.029	protein_coding	ENSMUSG00000071064.13	622675	*Ldlrad4*	-0.69	0.010	protein_coding	ENSMUSG00000024544.8	52662
Arhgap4	0.62	0.036	protein_coding	ENSMUSG00000031389.17	171207	*Cmya5*	-0.68	0.000	protein_coding	ENSMUSG00000047419.5	76469
D330041H03Rik	0.62	0.017	processed_transcript	ENSMUSG00000073437.10	654822	*Klf4*	-0.68	0.030	protein_coding	ENSMUSG00000003032.8	16600
Uck1	0.62	0.039	protein_coding	ENSMUSG00000002550.16	22245	*Rxrg*	-0.68	0.005	protein_coding	ENSMUSG00000015843.10	20183
Runx1	0.62	0.023	protein_coding	ENSMUSG00000022952.16	12394	*RP24-343P7.1*	-0.68	0.018	processed_pseudogene	ENSMUSG00000110644.1	NA
Fahd1	0.62	0.004	protein_coding	ENSMUSG00000045316.4	68636	*Ddit4l*	-0.68	0.003	protein_coding	ENSMUSG00000046818.7	73284
Gm43162	0.62	0.027	TEC	ENSMUSG00000104724.1	NA	*9530086O07Rik*	-0.68	0.003	TEC	ENSMUSG00000108076.1	NA
Gm38344	0.62	0.024	TEC	ENSMUSG00000102452.1	NA	*Plhf7*	-0.68	0.004	protein_coding	ENSMUSG00000021902.6	71838
Gm37953	0.62	0.005	TEC	ENSMUSG00000104061.1	NA	*Ppp1r3c*	-0.68	0.038	protein_coding	ENSMUSG00000067279.2	53412
Tpra1	0.62	0.032	protein_coding	ENSMUSG00000002871.14	24100	*Zfp788*	-0.67	0.019	protein_coding	ENSMUSG00000074165.10	67607
Fer1l6	0.62	0.010	protein_coding	ENSMUSG00000037106.8	631797	*Snrpn*	-0.67	0.003	protein_coding	ENSMUSG00000102252.5	20646
Fdxr	0.62	0.011	protein_coding	ENSMUSG00000018861.8	14149	*Bhlhe40*	-0.67	0.031	protein_coding	ENSMUSG00000030103.11	20893
Dmpk	0.62	0.002	protein_coding	ENSMUSG00000030409.15	13400	*Tmod2*	-0.67	0.004	protein_coding	ENSMUSG00000032186.14	50876
Lmod3	0.62	0.010	protein_coding	ENSMUSG00000044086.8	320502	*Mllt11*	-0.66	0.002	protein_coding	ENSMUSG00000053192.9	56772
Mettl21a	0.61	0.004	protein_coding	ENSMUSG00000025956.10	67099	*Usp6nl*	-0.66	0.010	protein_coding	ENSMUSG00000039046.15	98910
Trim7	0.61	0.002	protein_coding	ENSMUSG00000040350.15	94088	*Hmga1*	-0.65	0.023	protein_coding	ENSMUSG00000046711.15	15361
Cdc42ep2	0.61	0.003	protein_coding	ENSMUSG00000045664.4	104252	*Fgf2*	-0.65	0.033	protein_coding	ENSMUSG00000037225.13	14173
Stat1	0.61	0.012	protein_coding	ENSMUSG00000026104.14	20846	*Reep1*	-0.65	0.000	protein_coding	ENSMUSG00000052852.8	52250
Abr	0.61	0.002	protein_coding	ENSMUSG00000017631.18	109934	*Gm42651*	-0.65	0.047	TEC	ENSMUSG00000104877.1	NA
Vars2	0.60	0.002	protein_coding	ENSMUSG00000038838.15	68915	*Gm43953*	-0.65	0.011	TEC	ENSMUSG00000108067.1	NA
Klf5	0.60	0.025	protein_coding	ENSMUSG00000005148.7	12224	*Ankrd44*	-0.65	0.007	protein_coding	ENSMUSG00000052331.14	329154
Ppil	0.60	0.009	protein_coding	ENSMUSG00000021868.6	105675	*Epn15*	-0.65	0.000	protein_coding	ENSMUSG00000028552.13	13858
Cntrob	0.60	0.039	protein_coding	ENSMUSG00000032782.19	216846	*Rsph3b*	-0.65	0.029	protein_coding	ENSMUSG00000023806.9	100037282
Fut2	0.60	0.049	protein_coding	ENSMUSG00000055978.5	14344	*Tnfrsf21*	-0.65	0.021	protein_coding	ENSMUSG00000023915.4	94185
B3galt1	0.60	0.024	protein_coding	ENSMUSG00000034780.6	26877	*Fhl3*	-0.65	0.010	protein_coding	ENSMUSG00000032643.12	14201
Fv1	0.60	0.042	protein_coding	ENSMUSG00000070583.1	14349	*Mcm3*	-0.65	0.042	protein_coding	ENSMUSG00000041859.10	17215
Ndc1	0.60	0.002	protein_coding	ENSMUSG00000028614.14	72787	*5330439B14Rik*	-0.65	0.050	antisense	ENSMUSG00000104234.1	321015
Calr3	0.60	0.037	protein_coding	ENSMUSG00000019732.14	73316	*Gm26911*	-0.64	0.037	antisense	ENSMUSG00000097834.2	NA
Neat1	0.59	0.001	lincRNA	ENSMUSG00000092274.2	66961	*Pcdhga11*	-0.64	0.030	protein_coding	ENSMUSG00000102742.1	93723
Acsl1	0.59	0.030	protein_coding	ENSMUSG00000018796.13	14081	*Ubald2*	-0.64	0.008	protein_coding	ENSMUSG00000050628.6	319370
Tlc7	0.59	0.004	protein_coding	ENSMUSG00000036918.15	225049	*Srebf1*	-0.64	0.040	protein_coding	ENSMUSG00000020538.15	20787
Adam1a	0.59	0.046	protein_coding	ENSMUSG00000072647.5	280668	*Otub2*	-0.64	0.007	protein_coding	ENSMUSG00000021203.15	68149
Acot9	0.59	0.009	protein_coding	ENSMUSG00000025287.15	56360	*Csde1*	-0.64	0.000	protein_coding	ENSMUSG00000068823.10	229663
Tnfsf10	0.58	0.024	protein_coding	ENSMUSG00000039304.11	22035	*Abca1*	-0.64	0.009	protein_coding	ENSMUSG00000015243.4	11303
Nme1	0.58	0.004	protein_coding	ENSMUSG00000037601.11	18102	*Hrasls*	-0.64	0.006	protein_coding	ENSMUSG00000022525.13	27281
Cst6	0.58	0.025	protein_coding	ENSMUSG00000024846.5	73720	*Npc1*	-0.64	0.001	protein_coding	ENSMUSG00000024413.13	18145
Rab20	0.58	0.044	protein_coding	ENSMUSG00000031504.6	19332	*Ldha-ps2*	-0.64	0.013	processed_pseudogene	ENSMUSG00000083836.1	NA
Gm42507	0.58	0.035	TEC	ENSMUSG00000107168.1	NA	*Rora*	-0.64	0.001	protein_coding	ENSMUSG00000032238.17	19883
Rnf122	0.58	0.011	protein_coding	ENSMUSG00000039328.10	68867	*Dynk2*	-0.64	0.017	protein_coding	ENSMUSG00000028630.8	69181
Gtpbp6	0.58	0.035	protein_coding	ENSMUSG00000033434.15	107999	*Fam122a*	-0.63	0.008	protein_coding	ENSMUSG00000074922.1	68034
Art5	0.58	0.010	protein_coding	ENSMUSG00000070424.12	11875	*Ammecr1*	-0.63	0.011	protein_coding	ENSMUSG00000042225.3	56068
Tldc1	0.58	0.020	protein_coding	ENSMUSG00000034105.9	74347	*Vldlr*	-0.63	0.040	protein_coding	ENSMUSG00000024924.14	22359
Gm11361	0.58	0.024	processed_pseudogene	ENSMUSG00000061330.7	NA	*Maoa*	-0.63	0.044	protein_coding	ENSMUSG00000025037.6	17161
L3mbtl3	0.57	0.003	protein_coding	ENSMUSG00000039098.14	237339	*Pkd4*	-0.62	0.025	protein_coding	ENSMUSG00000061273.15	18802
Cars	0.57	0.001	protein_coding	ENSMUSG00000010755.17	27267	*Gm7332*	-0.62	0.043	processed_pseudogene	ENSMUSG00000080875.4	NA
Atrnl1	0.57	0.003	protein_coding	ENSMUSG00000054843.8	226255	*Rab12*	-0.62	0.001	protein_coding	ENSMUSG00000023460.12	19328
Hspb6	0.57	0.029	protein_coding	ENSMUSG00000036854.14	243912	*Smad7*	-0.62	0.007	protein_coding	ENSMUSG00000025880.11	17131
Slc25a22	0.57	0.047	protein_coding	ENSMUSG00000019082.18	68267	*Cbfb*	-0.62	0.004	protein_coding	ENSMUSG00000031885.14	12400
H2-T23	0.56	0.021	protein_coding	ENSMUSG00000067212.8	15040	*Jak2*	-0.62	0.018	protein_coding	ENSMUSG00000024789.12	16452
Cenpq	0.56	0.027	protein_coding	ENSMUSG00000023919.7	83815	*Gm43947*	-0.62	0.002	TEC	ENSMUSG00000107448.1	NA
Trappc12	0.56	0.008	protein_coding	ENSMUSG00000020628.15	217449	*Rai14*	-0.61	0.030	protein_coding	ENSMUSG00000022246.13	75646
Etv5	0.56	0.014	protein_coding	ENSMUSG00000013089.15	104156	*Optn*	-0.61	0.002	protein_coding	ENSMUSG00000026672.11	71648
Prepl	0.56	0.046	protein_coding	ENSMUSG00000024127.14	13760	*Tmcc1*	-0.61	0.001	protein_coding	ENSMUSG00000030126.17	330401
Sh3bgrl3	0.56	0.032	protein_coding	ENSMUSG00000028843.8	73723	*Mylip*	-0.61	0.007	protein_coding	ENSMUSG00000038175.9	218203
Cdc123	0.56	0.006	protein_coding	ENSMUSG00000039128.13	98828	*Dbn1*	-0.61	0.030	protein_coding	ENSMUSG00000034675.17	56320
Dtx3l	0.56	0.003	protein_coding	ENSMUSG00000049502.16	209200	*Lrrn4cl*	-0.61	0.006	protein_coding	ENSMUSG00000071656.6	68852
Ivd	0.55	0.009	protein_coding	ENSMUSG00000027332.11	56357	*Phospho1*	-0.61	0.020	protein_coding	ENSMUSG00000050860.6	237928
Pitx2	0.55	0.022	protein_coding	ENSMUSG00000028023.16	18741	*C2cd2l*	-0.61	0.004	protein_coding	ENSMUSG00000032120.10	71764
Got2	0.55	0.007	protein_coding	ENSMUSG00000031672.8	14719	*Gpd2*	-0.60	0.009	protein_coding	ENSMUSG00000026827.12	14571
Tm7sf2	0.55	0.049	protein_coding	ENSMUSG00000024799.14	73166	*Fmnl2*	-0.60	0.018	protein_coding	ENSMUSG00000036053.16	71409
Fads6	0.55	0.036	protein_coding	ENSMUSG00000044788.10	328035	*Lbx1*	-0.60	0.014	protein_coding	ENSMUSG00000025216.9	16814
Exog	0.55	0.047	protein_coding	ENSMUSG00000042787.13	208194	*Tenm3*	-0.60	0.031	protein_coding	ENSMUSG00000031561.16	23965
Gca	0.55	0.046	protein_coding	ENSMUSG00000026893.4	227960	*Lysmd2*	-0.60	0.033	protein_coding	ENSMUSG00000032184.4	70082
Slc4a3	0.54	0.050	protein_coding	ENSMUSG00000006576.16	20536	*Sub1*	-0.60	0.002	protein_coding	ENSMUSG00000022205.15	20024
Pdzd7	0.54	0.040	protein_coding	ENSMUSG00000074818.12	100503041	*Spin1*	-0.60	0.003	protein_coding	ENSMUSG00000021395.10	20729
Ddit3	0.54	0.013	protein_coding	ENSMUSG00000025408.15	13198	*Vezf1*	-0.60	0.001	protein_coding	ENSMUSG00000018377.10	22344
Ldlrap1	0.54	0.003	protein_coding	ENSMUSG00000037295.7	100017	*Gm28229*	-0.60	0.026	sense_intronic	ENSMUSG00000101335.1	NA
Crem	0.54	0.006	protein_coding	ENSMUSG00000063889.16	12916	*Pole4*	-0.60	0.031	protein_coding	ENSMUSG00000030042.15	66979
Rnf213	0.54	0.010	protein_coding	ENSMUSG00000070327.14	672511	*Tfdp1*	-0.60	0.002	protein_coding	ENSMUSG00000038482.11	21781
Lcmt2	0.53	0.027	protein_coding	ENSMUSG00000074890.4	329504	*Eef1akmt1*	-0.59	0.021	protein_coding	ENSMUSG00000021951.5	68043
Ppp1r11	0.53	0.018	protein_coding	ENSMUSG00000036398.13	76497	*Rab2a*	-0.59	0.004	protein_coding	ENSMUSG00000047187.9	59021
Myom2	0.53	0.003	protein_coding	ENSMUSG00000031461.4	17930	*Pctp*	-0.59	0.032	protein_coding	ENSMUSG00000020553.8	18559
Abcg2	0.53	0.009	protein_coding	ENSMUSG00000029802.13	26357	*Mical2*	-0.59	0.028	protein_coding	ENSMUSG00000038244.13	320878
Gm37314	0.53	0.007	TEC	ENSMUSG00000104094.1	NA	*Gatsl2*	-0.59	0.027	protein_coding	ENSMUSG00000015944.9	80909
Trim35	0.53	0.011	protein_coding	ENSMUSG00000022043.18	66854	*Skil*	-0.59	0.001	protein_coding	ENSMUSG00000027660.16	20482
Rnaseh2c	0.53	0.020	protein_coding	ENSMUSG00000024925.10	68209	*Tbkbp1*	-0.58	0.027	protein_coding	ENSMUSG00000038517.15	73174
RP23-425N12.2	0.52	0.046	lincRNA	ENSMUSG00000106981.1	NA	*Fmr1*	-0.58	0.049	protein_coding	ENSMUSG00000030838.17	14265
F11r	0.52	0.011	protein_coding	ENSMUSG00000038235.4	16456	*Fez2*	-0.58	0.006	protein_coding	ENSMUSG00000056121.15	225020
Eci1	0.52	0.019	protein_coding	ENSMUSG00000024132.5	13177	*Angptl7*	-0.58	0.013	protein_coding	ENSMUSG00000028989.3	654812
Arl6ip5	0.52	0.002	protein_coding	ENSMUSG00000035199.6	65106	*Tmem63a*	-0.58	0.001	protein_coding	ENSMUSG00000026519.16	208795
Ppara	0.52	0.033	protein_coding	ENSMUSG00000022383.13	19013	*Cpeb4*	-0.58	0.002	protein_coding	ENSMUSG00000020300.14	67579
Nudt8	0.52	0.024	protein_coding	ENSMUSG00000024869.9	NA	*Tada2a*	-0.58	0.031	protein_coding	ENSMUSG00000018651.14	217031
Abi2	0.52	0.005	protein_coding	ENSMUSG00000026782.15	329165	*Rxra*	-0.58	0.001	protein_coding	ENSMUSG00000015846.14	20181
Shmt2	0.52	0.009	protein_coding	ENSMUSG00000025403.4	108037	*Spire1*	-0.57	0.019	protein_coding	ENSMUSG00000024533.15	68166
Wbp1	0.52	0.005	protein_coding	ENSMUSG00000030035.14	22377	*2610203C20Rik*	-0.57	0.004	processed_transcript	ENSMUSG00000074415.11	73144
Usp54	0.52	0.045	protein_coding	ENSMUSG00000034235.16	78787	*Phc1*	-0.57	0.030	protein_coding	ENSMUSG00000040669.14	13619
Mrpl47	0.52	0.024	protein_coding	ENSMUSG00000037531.8	74600	*Slc26a6*	-0.57	0.021	protein_coding	ENSMUSG00000023259.16	171429
Kyat3	0.52	0.027	protein_coding	ENSMUSG00000040213.13	229905	*Zfp946*	-0.57	0.029	protein_coding	ENSMUSG00000071266.13	74149
Acss1	0.51	0.039	protein_coding	ENSMUSG00000027452.11	68738	*Ankrd6*	-0.57	0.026	protein_coding	ENSMUSG00000040183.13	140577
Dis3	0.51	0.004	protein_coding	ENSMUSG00000033166.10	72662	*Setbp1*	-0.57	0.001	protein_coding	ENSMUSG00000024548.11	240427
AA474408	0.51	0.029	TEC	ENSMUSG00000073867.2	NA	*Acvr1*	-0.57	0.014	protein_coding	ENSMUSG00000026836.15	11477
Camk2d	0.51	0.017	protein_coding	ENSMUSG00000053819.16	108058	*Eepd1*	-0.57	0.002	protein_coding	ENSMUSG00000036611.5	67484
Lmo7	0.51	0.004	protein_coding	ENSMUSG00000033060.15	380928	*Gm43672*	-0.57	0.010	lincRNA	ENSMUSG00000106019.1	NA
Oxnad1	0.51	0.009	protein_coding	ENSMUSG00000021906.13	218885	*Tnnt3*	-0.57	0.010	protein_coding	ENSMUSG00000061723.18	21957
Sars	0.51	0.002	protein_coding	ENSMUSG00000068739.13	20226	*Tlc7b*	-0.57	0.015	protein_coding	ENSMUSG00000033530.7	104718
Sec61a2	0.51	0.006	protein_coding	ENSMUSG00000025816.15	57743	*Htra1*	-0.57	0.004	protein_coding	ENSMUSG00000006205.13	56213
Parp12	0.51	0.011	protein_coding	ENSMUSG00000038507.6	243771	*Fbxl4*	-0.57	0.016	protein_coding	ENSMUSG00000040410.14	269514
Pacsin2	0.51	0.008	protein_coding	ENSMUSG00000016664.14	23970	*Tmem123*	-0.57	0.005	protein_coding	ENSMUSG00000050912.15	71929
Krt1	0.51	0.041	protein_coding	ENSMUSG00000035047.9	215194	*Hlx2*	-0.57	0.002	protein_coding	ENSMUSG00000038403.10	69585
Ptprd	0.51	0.037	protein_coding	ENSMUSG00000028399.18	19266	*Abi3bp*	-0.57	0.003	protein_coding	ENSMUSG00000035258.14	320712
Mdh1	0.50	0.007	protein_coding	ENSMUSG00000020321.15	17449	*Ostpl10*	-0.57	0.046	protein_coding	ENSMUSG00000040875.12	74486
Gm20712	0.50	0.016	sense_overlapping	ENSMUSG00000093677.1	NA	*Gnptab*	-0.56	0.001	protein_coding	ENSMUSG00000035311.16	432486
Cyb5r1	0.50	0.002	protein_coding	ENSMUSG00000026456.18	72017	*Gm15446*	-0.56	0.032	protein_coding	ENSMUSG00000090015.8	100642166
Ifitm3	0.50	0.037	protein_coding	ENSMUSG00000025492.6	66141	*Arl4a*	-0.56	0.003	protein_coding	ENSMUSG00000047446.18	11861
Pfkfb2	0.50	0.004	protein_coding	ENSMUSG00000026409.14	18640	*Bpgm*	-0.56	0.001	protein_coding	ENSMUSG00000038871.5	12183
						Slc16a9	-0.56	0.021	protein_coding	ENSMUSG00000037762.6	66859
						Inafm2	-0.56	0.019	antisense	ENSMUSG00000074918.4	100043272

Rassf1	-0.56	0.025	protein_coding	ENSMUSG00000010067.13	56289
Serinc3	-0.56	0.015	protein_coding	ENSMUSG00000017707.9	26943
Smad3	-0.56	0.008	protein_coding	ENSMUSG00000032402.12	17127
Lsp1	-0.55	0.014	protein_coding	ENSMUSG00000018819.10	16985
Lgals1	-0.55	0.025	protein_coding	ENSMUSG00000068220.5	16852
Abca6	-0.55	0.024	protein_coding	ENSMUSG00000044749.13	76184
Eif4ebp2	-0.55	0.003	protein_coding	ENSMUSG00000020091.14	13688
Cited4	-0.55	0.027	protein_coding	ENSMUSG00000070803.6	56222
Pip5k1a	-0.55	0.003	protein_coding	ENSMUSG00000028126.16	18720
Lpar1	-0.55	0.027	protein_coding	ENSMUSG00000038668.14	14745
Slc16a2	-0.55	0.028	protein_coding	ENSMUSG00000033965.10	20502
Zmiz2	-0.55	0.003	protein_coding	ENSMUSG00000041164.15	52915
Slc7a8	-0.55	0.034	protein_coding	ENSMUSG00000022180.6	50934
Amigo1	-0.55	0.002	protein_coding	ENSMUSG00000050947.9	229715
Mtum	-0.54	0.048	protein_coding	ENSMUSG00000038065.13	68235
Cd9	-0.54	0.024	protein_coding	ENSMUSG00000030342.8	12527
Klf13	-0.54	0.020	protein_coding	ENSMUSG00000052040.10	50794
Thbs2	-0.54	0.009	protein_coding	ENSMUSG00000023885.8	21826
Klf3c	-0.54	0.003	protein_coding	ENSMUSG00000020668.9	16570
Relt	-0.54	0.025	protein_coding	ENSMUSG00000008318.10	320100
Zfp9	-0.54	0.013	protein_coding	ENSMUSG00000072623.6	22750
RP23-478B10.1	-0.53	0.033	processed_pseudogene	ENSMUSG00000109600.1	NA
9030617O03Rik	-0.53	0.006	protein_coding	ENSMUSG00000021185.15	217830
Tnrc18	-0.53	0.040	protein_coding	ENSMUSG00000039477.16	231861
Stxbp6	-0.53	0.038	protein_coding	ENSMUSG00000046314.15	217517
Slc44a2	-0.53	0.002	protein_coding	ENSMUSG00000057193.7	68682
Ap1ar	-0.53	0.001	protein_coding	ENSMUSG00000074238.6	211556
Fxd7	-0.53	0.018	protein_coding	ENSMUSG00000041075.8	14369
Slc35f5	-0.53	0.020	protein_coding	ENSMUSG00000026342.10	74150
Qser1	-0.53	0.002	protein_coding	ENSMUSG00000074994.4	99003
Mfap5	-0.53	0.045	protein_coding	ENSMUSG00000030116.14	50530
Dlg1	-0.53	0.002	protein_coding	ENSMUSG00000022770.16	13383
Smyd2	-0.53	0.029	protein_coding	ENSMUSG00000026603.13	226830
Gm7236	-0.53	0.043	processed_pseudogene	ENSMUSG00000090389.1	NA
Dcn	-0.53	0.016	protein_coding	ENSMUSG00000019929.15	13179
Casq1	-0.53	0.028	protein_coding	ENSMUSG00000007122.11	12372
Ccl11	-0.52	0.006	protein_coding	ENSMUSG00000020676.2	20292
Gm15910	-0.52	0.016	processed_transcript	ENSMUSG00000087480.1	100504616
Peli2	-0.52	0.046	protein_coding	ENSMUSG00000021846.8	93834
Itpr1	-0.52	0.004	protein_coding	ENSMUSG00000030102.11	16438
St8sia5	-0.52	0.005	protein_coding	ENSMUSG00000025425.17	225742
4930453N24Rik	-0.52	0.001	protein_coding	ENSMUSG00000059920.9	67609
Aven	-0.52	0.038	protein_coding	ENSMUSG00000003604.14	74268
Hoxc10	-0.52	0.001	protein_coding	ENSMUSG00000022484.7	209448
Ccdc134	-0.52	0.015	protein_coding	ENSMUSG00000068114.6	76457
Klhl31	-0.51	0.002	protein_coding	ENSMUSG00000044938.8	244923
Vkorc1l1	-0.51	0.010	protein_coding	ENSMUSG00000066735.8	69568
Prkar2a	-0.51	0.001	protein_coding	ENSMUSG00000032601.13	19087
Sort1	-0.51	0.033	protein_coding	ENSMUSG00000068747.14	20661
Spast	-0.51	0.001	protein_coding	ENSMUSG00000024068.6	50850
Cdkn2aipnl	-0.51	0.019	protein_coding	ENSMUSG00000020392.8	52626
Ppp2cb	-0.51	0.005	protein_coding	ENSMUSG00000009630.10	19053
Lingo3	-0.51	0.029	protein_coding	ENSMUSG00000051067.7	237403
Tmod4	-0.51	0.007	protein_coding	ENSMUSG00000005628.12	50874
Ifitg1	-0.51	0.009	protein_coding	ENSMUSG00000031703.8	71927
Polm	-0.51	0.044	protein_coding	ENSMUSG00000020474.11	54125
Dnase1	-0.51	0.047	protein_coding	ENSMUSG00000005980.15	13419
Fgd4	-0.51	0.013	protein_coding	ENSMUSG00000022788.16	224014
Rab10	-0.51	0.001	protein_coding	ENSMUSG00000020671.8	19325
Lpin1	-0.51	0.003	protein_coding	ENSMUSG00000020593.14	14245
Mb21d2	-0.51	0.025	protein_coding	ENSMUSG00000051065.8	239796
Jak1	-0.51	0.002	protein_coding	ENSMUSG00000028530.14	16451
Ergic1	-0.50	0.005	protein_coding	ENSMUSG00000001576.14	67458
Jph1	-0.50	0.009	protein_coding	ENSMUSG00000042686.5	57339
Bmpr1b	-0.50	0.044	protein_coding	ENSMUSG00000052430.15	12167
Ube2r2	-0.50	0.006	protein_coding	ENSMUSG00000036241.3	67615
Ghr	-0.50	0.002	protein_coding	ENSMUSG00000055737.12	14600

Table S11. Indirect calorimetry analysis in thermoneutral conditions (31°C) after two-week acclimatization period of male (55 weeks of age) Euploid and MAC21 mice fed a high-fat diet (18 weeks on diet).

	Eu	**MAC21**	***P***	**Eu**	**MAC21**	***P***	**Eu**	**MAC21**	***P***
High-fat diet (Male)	***Ad-libitum* (dark cycle)**			***Ad-libitum* (light cycle)**			***Ad-libitum* (24 hr)**		
N	5	4		5	4		5	4	
Body weight (g)							**58.1 ± 6.18**	**36.0 ± 7.39**	**0.0020**
Food intake (kcal)							7.67 ± 3.42	8.27 ± 3.87	0.814
VO2 (mL/kg lean mass/h)	**3185 ± 120**	**4182 ± 103**	**<0.001**	**2480 ± 103**	**3134 ± 144**	**0.007**	**2833 ± 103**	**3658 ± 112**	**<0.001**
VCO2 (mL/kg lean mass/h)	**2230 ± 91**	**3017 ± 150**	**0.002**	**1766 ± 70**	**2360 ± 221**	**0.025**	**1998 ± 76**	**2688 ± 183**	**0.007**
RER (VCO2/VO2)	0.70 ± 0.006	0.72 ± 0.024	0.342	0.71 ± 0.007	0.75 ± 0.033	0.245	0.70 ± 0.006	0.73 ± 0.028	0.282
EE (kcal/kg lean mass/h)	**14.9 ± 0.57**	**19.7 ± 0.55**	**<0.001**	**11.6 ± 0.48**	**14.9 ± 0.82**	**0.009**	**13.3 ± 0.48**	**17.3 ± 0.64**	**0.001**

Eu: Euploid; VO2: rate of oxygen consumption; VCO2: rate of carbon dioxide production; RER: respiratory exchange ratio; EE: energy expenditure

Table S12. With the exeption of *Myl4*, none of the genes are significantly upregulated above log2(FC) of 0.5

Atrophy-related genes

Gene Symbol	Log2(FC)	Adj.p-Value	Gene Type	GencodeID	EntrezID
Becn1	-0.243	0.0567	protein_coding	ENSMUSG00000035086.13	56208
Capn2	-0.018	0.9199	protein_coding	ENSMUSG00000026509.15	12334
Fbxo32	-0.465	0.0045	protein_coding	ENSMUSG00000022358.6	67731
Mustn1	0.461	0.1410	protein_coding	ENSMUSG00000042485.6	66175
Nedd4	-0.052	0.6234	protein_coding	ENSMUSG00000032216.14	17999
Psma6	0.100	0.5439	protein_coding	ENSMUSG00000021024.14	26443
Psmb2	0.196	0.2092	protein_coding	ENSMUSG00000028837.8	26445
Trim55	-0.265	0.0606	protein_coding	ENSMUSG00000060913.6	381485
Trim63	-0.315	0.0572	protein_coding	ENSMUSG00000028834.13	433766

Contractile and Structural genes

Gene Symbol	Log2(FC)	Adj.p-Value	Gene Type	GencodeID	EntrezID
Des	0.027	0.8863	protein_coding	ENSMUSG00000026208.9	13346
Dysf	-0.003	0.9892	protein_coding	ENSMUSG00000033788.15	26903
Mybpc1	0.344	0.2387	protein_coding	ENSMUSG00000020061.17	109272
Mybpc2	-0.152	0.3554	protein_coding	ENSMUSG00000038670.11	233199
Myh1	0.801	0.0879	protein_coding	ENSMUSG00000056328.14	17879
Myh2	-0.045	0.9449	protein_coding	ENSMUSG00000033196.17	17882
Myh3	-0.020	0.9831	protein_coding	ENSMUSG00000020908.14	17883
Myh7	0.420	0.7271	protein_coding	ENSMUSG00000053093.15	140781
Myh7b	0.340	0.7350	protein_coding	ENSMUSG00000074652.3	668940
Myh8	-0.155	0.7391	protein_coding	ENSMUSG00000055775.16	17885
Myl1	0.097	0.6449	protein_coding	ENSMUSG00000061816.15	17901
Myl3	-0.016	0.9928	protein_coding	ENSMUSG00000059741.13	17897
Myl4	**-1.214**	**0.0329**	**protein_coding**	**ENSMUSG00000061086.12**	**17896**
Mypn	0.079	0.4802	protein_coding	ENSMUSG00000020067.7	68802
Tnni2	-0.332	0.1263	protein_coding	ENSMUSG00000031097.15	21953

Fibrosis and Injury Repair related genes

Gene Symbol	Log2(FC)	Adj.p-Value	Gene Type	GencodeID	EntrezID
Col1a1	-0.410	0.1196	protein_coding	ENSMUSG00000001506.10	12842
Col1a2	-0.297	0.0738	protein_coding	ENSMUSG00000029661.16	12843
Col3a1	-0.075	0.8063	protein_coding	ENSMUSG00000026043.18	12825
Col4a1	0.217	0.6216	protein_coding	ENSMUSG00000031502.11	12826
Col4a2	0.114	0.7705	protein_coding	ENSMUSG00000031503.13	12827
Col4a3	0.080	0.7762	protein_coding	ENSMUSG00000079465.8	12828
Col4a3bp	-0.134	0.2699	protein_coding	ENSMUSG00000021669.14	68018
Col4a4	0.024	0.9291	protein_coding	ENSMUSG00000067158.9	12829
Col4a5	0.072	0.7762	protein_coding	ENSMUSG00000031274.16	12830
Col4a6	0.445	0.4745	protein_coding	ENSMUSG00000031273.16	94216
Col6a1	-0.201	0.3954	protein_coding	ENSMUSG00000001119.7	12833
Col6a2	-0.301	0.2191	protein_coding	ENSMUSG00000020241.13	12834
Col6a3	-0.036	0.8902	protein_coding	ENSMUSG00000048126.16	12835
Col6a6	0.099	0.6784	protein_coding	ENSMUSG00000043719.14	245026
Eln	-0.111	0.6890	protein_coding	ENSMUSG00000029675.12	13717
Mmp2	-0.230	0.2256	protein_coding	ENSMUSG00000031740.8	17390
Mmp14	-0.231	0.5334	protein_coding	ENSMUSG00000000957.9	17387
Scx	-0.239	0.5406	protein_coding	ENSMUSG00000034161.7	20289
Timp1	-0.528	0.5704	protein_coding	ENSMUSG00000001131.11	21857
Timp2	-0.467	0.0395	protein_coding	ENSMUSG00000017466.9	21858

Muscle Wasting related genes

Gene Symbol	Log2(FC)	Adj.p-Value	Gene Type	GencodeID	EntrezID
Aldh2	0.418	0.0280	protein_coding	ENSMUSG00000029455.14	11669
Apc	-0.152	0.2303	protein_coding	ENSMUSG00000005871.14	11789
Bnip3	0.176	0.3012	protein_coding	ENSMUSG00000078566.8	12176
Ccl2	0.284	0.8355	protein_coding	ENSMUSG00000035385.5	20296
Foxo1	0.101	0.4669	protein_coding	ENSMUSG00000044167.6	56458
Il6ra	-0.386	0.1657	protein_coding	ENSMUSG00000027947.11	16194
Il6st	0.018	0.9020	protein_coding	ENSMUSG00000021756.12	16195
Ly6c1	-0.160	0.6728	protein_coding	ENSMUSG00000079018.10	17067
Map1lc3a	-0.008	0.9780	protein_coding	ENSMUSG00000027602.9	66734
Ptprc	-0.091	0.8671	protein_coding	ENSMUSG00000026395.16	19264
Rela	-0.016	0.9408	protein_coding	ENSMUSG00000024927.7	19697
Xrcc5	0.135	0.5156	protein_coding	ENSMUSG00000026187.8	22596
Zmpste24	-0.036	0.8016	protein_coding	ENSMUSG00000043207.10	230709

Table S13. Tissue weights of male MAC21 and Euploid littermates (55 weeks of age) housed at thermoneutrality (31°C) and fed an HFD (18 weeks on diet).

	Eu	MAC21	*P*
N	5	4	
Body weight (g)	**60.3 ± 2.85**	**36.9 ± 3.71**	**0.001**
Gondal fat (gWAT, g)	1.62 ± 0.22	1.07 ± 0.05	0.065
Inguinal fat (iWAT, g)	**1.60 ± 0.11**	**0.58 ± 0.11**	**<0.001**
Liver (g)	**3.03 ± 0.33**	**1.66 ± 0.19**	**0.013**
BAT (g)	**0.25 ± 0.02**	**0.10 ± 0.02**	**<0.001**
Pancreas (g)	**0.44 ± 0.02**	**0.34 ± 0.03**	**0.015**

Eu: Euploid; gWAT: gondal white adipose tissue; iWAT: inguinal white adipose tissue; BAT: brown adipose tissue

Table S14 Skeletal muscle (HFD, 31℃)

Human genes expressed

Gene Symbol	Log(Fold Change)	Adj.p-Value	Gene Type	GencodeID	EntrezID
SH3BGR	12.10	1.374E-05	protein_coding	ENSG00000185437.13	6450
ATP5J	11.77	1.074E-05	protein_coding	ENSG00000154723.12	522
AGPAT3	11.06	1.809E-05	protein_coding	ENSG00000160216.18	56894
MAP3K7CL	10.85	1.826E-03	protein_coding	ENSG00000156265.15	56911
NDUFV3	10.82	1.506E-05	protein_coding	ENSG00000160194.17	4731
USP16	10.60	1.809E-05	protein_coding	ENSG00000156256.14	10600
ATP5O	10.56	1.374E-05	protein_coding	ENSG00000241837.6	539
SON	10.22	4.835E-05	protein_coding	ENSG00000159140.18	6651
DYRK1A	9.79	5.371E-05	protein_coding	ENSG00000157540.19	1859
SOD1	9.73	5.317E-05	protein_coding	ENSG00000142168.14	6647
HLCS	9.69	2.292E-05	protein_coding	ENSG00000159267.14	3141
DIP2A	9.60	2.003E-05	protein_coding	ENSG00000160305.17	23181
SUMO3	9.59	7.614E-05	protein_coding	ENSG00000184900.15	6612
DSCR3	9.48	2.143E-05	protein_coding	ENSG00000157538.13	10311
PIGP	9.48	2.003E-05	protein_coding	ENSG00000185808.13	51227
GABPA	9.38	2.487E-05	protein_coding	ENSG00000154727.10	2551
POFUT2	9.30	2.292E-05	protein_coding	ENSG00000186866.16	23275
ETS2	9.28	2.292E-05	protein_coding	ENSG00000157557.11	2114
IFNAR1	9.23	4.923E-05	protein_coding	ENSG00000142166.12	3454
UBE2G2	9.22	3.893E-04	protein_coding	ENSG00000184787.18	7327
PTTG1IP	9.13	2.331E-04	protein_coding	ENSG00000183255.11	754
CCT8	9.13	7.614E-05	protein_coding	ENSG00000156261.12	10694
BRWD1	9.03	1.774E-04	protein_coding	ENSG00000185658.13	54014
N6AMT1	9.03	2.421E-05	protein_coding	ENSG00000156239.11	29104
TRAPPC10	8.98	2.767E-05	protein_coding	ENSG00000160218.12	7109
IFNGR2	8.94	2.292E-05	protein_coding	ENSG00000159128.14	3460
MCM3AP	8.89	1.277E-04	protein_coding	ENSG00000160294.10	8888
SLC37A1	8.73	3.382E-05	protein_coding	ENSG00000160190.13	54020
CLIC6	8.71	4.700E-05	protein_coding	ENSG00000159212.12	54102
RRP1B	8.68	5.371E-05	protein_coding	ENSG00000160208.12	23076
BACH1	8.54	3.647E-05	protein_coding	ENSG00000156273.15	571
GART	8.46	3.576E-04	protein_coding	ENSG00000159131.16	2618
URB1	8.43	2.435E-04	protein_coding	ENSG00000142207.6	9875
RWDD2B	8.42	4.700E-05	protein_coding	ENSG00000156253.6	10069
MX2	8.37	4.835E-05	protein_coding	ENSG00000183486.12	4600
WRB	8.30	1.779E-04	protein_coding	ENSG00000182093.14	7485
PKNOX1	8.30	7.295E-05	protein_coding	ENSG00000160199.14	5316
ITSN1	8.29	4.700E-05	protein_coding	ENSG00000205726.14	6453
CYYR1	8.28	4.700E-05	protein_coding	ENSG00000166265.11	116159
C21orf33	8.28	9.855E-05	protein_coding	ENSG00000160221.16	8209
MX1	8.25	1.003E-04	protein_coding	ENSG00000157601.13	4599
CSTB	8.23	4.416E-04	protein_coding	ENSG00000160213.5	1476
SLC5A3	8.22	4.700E-05	protein_coding	ENSG00000198743.6	6526
CH507-9B2.3	8.14	1.161E-04	protein_coding	ENSG00000280071.3	102724023
SYNJ1	8.03	4.835E-05	protein_coding	ENSG00000159082.17	8867
PDXK	8.01	8.893E-04	protein_coding	ENSG00000160209.18	8566
APP	7.98	1.770E-03	protein_coding	ENSG00000142192.20	351
HMGN1	7.91	8.444E-04	protein_coding	ENSG00000205581.10	3150
PCNT	7.84	3.454E-04	protein_coding	ENSG00000160299.16	5116
ADAMTS1	7.82	6.390E-05	protein_coding	ENSG00000154734.14	9510
MRPL39	7.81	1.278E-04	protein_coding	ENSG00000154719.13	54148
PSMG1	7.81	1.938E-04	protein_coding	ENSG00000183527.11	8624
SETD4	7.80	1.003E-04	protein_coding	ENSG00000185917.13	54093
CBR1	7.79	1.693E-04	protein_coding	ENSG00000159228.12	873
URB1-AS1	7.77	7.722E-05	lincRNA	ENSG00000256073.3	84996
TMEM50B	7.75	1.265E-03	protein_coding	ENSG00000142188.16	757
CRYZL1	7.68	3.101E-04	protein_coding	ENSG00000205758.11	9946
TTC3	7.67	2.025E-03	protein_coding	ENSG00000182670.13	7267
RRP1	7.58	1.277E-04	protein_coding	ENSG00000160214.12	8568
PRMT2	7.53	5.059E-04	protein_coding	ENSG00000160310.16	3275
RUNX1	7.49	1.934E-04	protein_coding	ENSG00000159216.18	861
TSPEAR-AS1	7.49	2.963E-04	antisense	ENSG00000235890.2	NA
LINC00649	7.47	7.202E-04	antisense	ENSG00000237945.7	100506334
FAM207A	7.46	1.672E-04	protein_coding	ENSG00000160256.12	85395
PAXBP1	7.44	1.431E-03	protein_coding	ENSG00000159086.14	94104
MRPS6	7.39	1.938E-04	protein_coding	ENSG00000243927.5	64968
BACE2	7.36	1.161E-04	protein_coding	ENSG00000182240.15	25825
IFNAR2	7.36	1.505E-04	protein_coding	ENSG00000159110.19	3455
PRDM15	7.34	1.277E-04	protein_coding	ENSG00000141956.13	63977
JAM2	7.29	3.163E-04	protein_coding	ENSG00000154721.14	58494
CH507-9B2.5	7.28	1.743E-04	protein_coding	ENSG00000275464.4	102724159
C21orf59	7.25	1.476E-04	protein_coding	ENSG00000159079.18	56683
ADARB1	7.20	1.804E-04	protein_coding	ENSG00000197381.15	104
S100B	7.20	1.968E-04	protein_coding	ENSG00000160307.9	6285
BTG3	7.16	1.824E-02	protein_coding	ENSG00000154640.14	10950
SCAF4	7.15	2.025E-03	protein_coding	ENSG00000156304.14	57466
TSPEAR-AS2	7.12	1.733E-04	antisense	ENSG00000182912.6	NA
LTN1	7.09	1.733E-04	protein_coding	ENSG00000198862.13	26046
DNAJC28	6.87	3.618E-04	protein_coding	ENSG00000177692.11	54943
HSPA13	6.78	6.158E-04	protein_coding	ENSG00000155304.5	6782
C2CD2	6.71	1.520E-03	protein_coding	ENSG00000157617.16	25966
CHAF1B	6.61	5.064E-04	protein_coding	ENSG00000159259.7	8208
DONSON	6.56	7.755E-04	protein_coding	ENSG00000159147.17	29980
ITGB2	6.42	1.265E-03	protein_coding	ENSG00000160255.17	3689
ZBTB21	6.27	8.513E-03	protein_coding	ENSG00000173276.13	49854
SIM2	6.24	7.158E-04	protein_coding	ENSG00000159263.15	6493
WDR4	6.21	2.038E-03	protein_coding	ENSG00000160193.11	10785
LINC00310	6.13	1.236E-03	lincRNA	ENSG00000227456.7	114036
UMODL1	6.10	2.512E-03	protein_coding	ENSG00000177398.18	89766
PFKL	6.09	9.476E-03	protein_coding	ENSG00000141959.16	5211
TIAM1	6.09	1.250E-03	protein_coding	ENSG00000156299.13	7074
IL10RB	6.04	1.250E-03	protein_coding	ENSG00000243646.9	3588
C21orf58	5.95	1.250E-03	protein_coding	ENSG00000160298.17	54058
RCAN1	5.93	2.088E-03	protein_coding	ENSG00000159200.17	1827
DOPEY2	5.91	4.912E-03	protein_coding	ENSG00000142197.12	9980
EVA1C	5.77	2.323E-03	protein_coding	ENSG00000166979.12	59271
CBSL	5.66	1.484E-02	protein_coding	ENSG00000274276.4	102724560
U2AF1	5.60	3.793E-03	protein_coding	ENSG00000160201.11	7307
LCA5L	5.36	6.233E-03	protein_coding	ENSG00000157578.13	150082
LINC00205	5.14	1.198E-02	lincRNA	ENSG00000223768.1	NA
BX322557.10	5.14	1.428E-02	processed_transcript	ENSG00000215447.7	NA
KCNE2	5.12	1.180E-02	protein_coding	ENSG00000159197.3	9992
TSPEAR	5.06	3.148E-02	protein_coding	ENSG00000175894.14	54084
CBS	5.03	2.947E-02	protein_coding	ENSG00000160200.17	875
MORC3	5.02	4.033E-02	protein_coding	ENSG00000159256.12	23515
DSCR4	4.96	1.823E-02	protein_coding	ENSG00000184029.9	10281
PAXBP1-AS1	4.92	1.428E-02	antisense	ENSG00000238197.5	100506215
LINC01436	4.77	3.027E-02	lincRNA	ENSG00000231106.2	NA
RSPH1	4.77	3.187E-02	protein_coding	ENSG00000160188.9	89765
YBEY	4.46	4.033E-02	protein_coding	ENSG00000182362.13	54059

Mouse up-regulated genes

Gene Symbol	Log(Fold Change)	Adj.p-Value	Gene Type	GencodeID	EntrezID
Eif3s6-ps2	5.04	0.010	processed_pseudogene	ENSMUSG00000091697.1	NA
Gm13534	4.81	0.029	processed_pseudogene	ENSMUSG00000053472.3	NA
RP23-162M13.9	4.76	0.021	processed_pseudogene	ENSMUSG00000110569.1	NA
Dmp1	4.74	0.019	protein_coding	ENSMUSG00000029307.7	13406
Myo1a	4.71	0.040	protein_coding	ENSMUSG00000025401.8	432516
Fut1	4.39	0.040	protein_coding	ENSMUSG00000008461.6	14343
Ccdc92	3.77	0.047	protein_coding	ENSMUSG00000037979.13	215707
Mtfr1d2	3.70	0.003	protein_coding	ENSMUSG00000005667.8	17768
Slc7a5	3.58	0.002	protein_coding	ENSMUSG00000040010.10	20539
Asns	3.30	0.007	protein_coding	ENSMUSG00000029752.12	27053
Aldh18a1	2.60	0.002	protein_coding	ENSMUSG00000025007.13	56454
E2f2	2.35	0.004	protein_coding	ENSMUSG00000018983.9	242705
A930003A15Rik	2.30	0.029	protein_coding	ENSMUSG00000075330.3	NA
Cpne2	2.19	0.001	protein_coding	ENSMUSG00000034361.10	234577
Ankrd1	2.01	0.001	protein_coding	ENSMUSG00000024803.8	107765
Aldh1l2	1.83	0.045	protein_coding	ENSMUSG00000020256.14	216188
Atf5	1.82	0.001	protein_coding	ENSMUSG00000038539.15	107503
Tceal7	1.81	0.002	protein_coding	ENSMUSG00000079428.8	100040972
Spag5	1.71	0.018	protein_coding	ENSMUSG00000002055.9	54141
Itga9	1.66	0.003	protein_coding	ENSMUSG00000039115.13	104099
Tnfaip2	1.55	0.001	protein_coding	ENSMUSG00000021281.15	21928
Cdkn1a	1.52	0.001	protein_coding	ENSMUSG00000023067.13	12575
Slc7a1	1.49	0.019	protein_coding	ENSMUSG00000041313.14	11987
Sesn2	1.49	0.041	protein_coding	ENSMUSG00000028893.8	NA
Lrp2bp	1.45	0.001	protein_coding	ENSMUSG00000031637.13	67620
Abra	1.35	0.029	protein_coding	ENSMUSG00000042895.5	NA
Otud1	1.33	0.046	protein_coding	ENSMUSG00000043415.5	71198
A930018M24Rik	1.32	0.021	protein_coding	ENSMUSG00000091089.1	NA
Ctnna3	1.32	0.018	protein_coding	ENSMUSG00000060843.11	216033
A830010M20Rik	1.31	0.011	protein_coding	ENSMUSG00000044060.18	NA
Ift122	1.30	0.001	protein_coding	ENSMUSG00000030323.13	81896
6430548M08Rik	1.27	0.024	protein_coding	ENSMUSG00000031824.15	234797
Gadd45a	1.26	0.025	protein_coding	ENSMUSG00000036390.8	13197
Slc47a1	1.24	0.027	protein_coding	ENSMUSG00000010122.14	67473
Zfp870	1.23	0.018	protein_coding	ENSMUSG00000095325.1	240066
Clu	1.16	0.000	protein_coding	ENSMUSG00000022037.14	12759
Nnt	1.16	0.001	protein_coding	ENSMUSG00000025453.16	18115
Angpt1	1.09	0.007	protein_coding	ENSMUSG00000022309.8	11600
Tmem47	1.09	0.049	protein_coding	ENSMUSG00000025666.16	192216
Camta1	1.06	0.039	protein_coding	ENSMUSG00000014592.19	100072
Rcan1	1.05	0.013	protein_coding	ENSMUSG00000022951.15	54720
Iars	1.03	0.029	protein_coding	ENSMUSG00000037851.13	105148
Klf10	0.97	0.025	protein_coding	ENSMUSG00000037465.9	21847
Cars	0.93	0.017	protein_coding	ENSMUSG00000010755.17	27267
Rb1	0.93	0.029	protein_coding	ENSMUSG00000022105.6	19645
Pacsin2	0.92	0.024	protein_coding	ENSMUSG00000016664.14	23970
Extl1	0.87	0.021	protein_coding	ENSMUSG00000028838.11	56219
Clic4	0.85	0.020	protein_coding	ENSMUSG00000037242.8	29876
Cebpg	0.84	0.025	protein_coding	ENSMUSG00000056216.9	12611
Fads6	0.80	0.031	protein_coding	ENSMUSG00000044788.10	NA
Prss23	0.79	0.026	protein_coding	ENSMUSG00000039405.7	76453
Gars	0.76	0.040	protein_coding	ENSMUSG00000029777.10	353172
Lmod3	0.74	0.008	protein_coding	ENSMUSG00000044086.8	320502
Sars	0.73	0.031	protein_coding	ENSMUSG00000068739.13	20226
Palld	0.66	0.017	protein_coding	ENSMUSG00000058056.16	72333
Yars	0.65	0.037	protein_coding	ENSMUSG00000028811.11	NA
Tob1	0.62	0.040	protein_coding	ENSMUSG00000037573.5	22057
Nars	0.60	0.035	protein_coding	ENSMUSG00000024587.9	70223
Dmpk	0.57	0.023	protein_coding	ENSMUSG00000030409.15	13400

Mouse down-regulated genes

Gene Symbol	Log(Fold Change)	Adj.p-Value	Gene Type	GencodeID	EntrezID
Cdh4	-3.28	0.008	protein_coding	ENSMUSG00000000305.12	12561
Shc2	-2.79	0.034	protein_coding	ENSMUSG00000020312.11	216148
Nhs	-2.73	0.021	protein_coding	ENSMUSG00000059493.13	195727
Cntnap2	-2.42	0.020	protein_coding	ENSMUSG00000039419.17	66797
Gdf11	-2.34	0.000	protein_coding	ENSMUSG00000025352.6	NA
Pla2g7	-2.20	0.003	protein_coding	ENSMUSG00000023913.17	27226
Aurka	-2.11	0.029	protein_coding	ENSMUSG00000027496.15	20878
Ctxn3	-1.90	0.001	protein_coding	ENSMUSG00000069372.3	629147
Mss51	-1.80	0.001	protein_coding	ENSMUSG00000021815.3	74843
Col24a1	-1.77	0.023	protein_coding	ENSMUSG00000028197.4	71355
Mib1	-1.69	0.002	protein_coding	ENSMUSG00000024294.13	225164
Ces1d	-1.67	0.047	protein_coding	ENSMUSG00000056973.6	104158
Aebp1	-1.60	0.000	protein_coding	ENSMUSG00000020473.13	11568
Gm45123	-1.56	0.027	lincRNA	ENSMUSG00000108322.1	71368
Nos1	-1.48	0.046	protein_coding	ENSMUSG00000029361.18	18125
Wbscr17	-1.48	0.018	protein_coding	ENSMUSG00000034040.16	212996
Col22a1	-1.46	0.003	protein_coding	ENSMUSG00000079022.9	69700
Sorbs2	-1.43	0.002	protein_coding	ENSMUSG00000031626.17	234214
2310065F04Rik	-1.39	0.029	lincRNA	ENSMUSG00000087410.7	74184
Enox2	-1.35	0.013	protein_coding	ENSMUSG00000031109.16	209224
Tpbgl	-1.35	0.022	protein_coding	ENSMUSG00000096606.2	100503386
mt-Te	-1.29	0.035	Mt_tRNA	ENSMUSG00000064369.1	NA
Mettl11b	-1.26	0.027	protein_coding	ENSMUSG00000040113.14	240879
Mstn	-1.25	0.001	protein_coding	ENSMUSG00000026100.6	17700
Rasd2	-1.24	0.001	protein_coding	ENSMUSG00000034472.13	75141
Cpeb1	-1.20	0.005	protein_coding	ENSMUSG00000025586.17	12877
Clec3b	-1.19	0.014	protein_coding	ENSMUSG00000025784.4	21922
Gpx3	-1.19	0.035	protein_coding	ENSMUSG00000018339.11	14778
Pmepa1	-1.12	0.029	protein_coding	ENSMUSG00000038400.15	65112
Smox	-1.11	0.026	protein_coding	ENSMUSG00000027333.18	228608
Ttll7	-1.10	0.004	protein_coding	ENSMUSG00000036745.15	70892
Calm3	-1.09	0.001	protein_coding	ENSMUSG00000019370.10	12315
Myoc	-1.09	0.016	protein_coding	ENSMUSG00000026697.10	17926
Plekho1	-1.09	0.021	protein_coding	ENSMUSG00000015745.9	67220
Slc16a3	-1.09	0.010	protein_coding	ENSMUSG00000025161.16	80879
Me1	-1.05	0.001	protein_coding	ENSMUSG00000032418.15	17436
Ppp1r14b	-1.01	0.009	protein_coding	ENSMUSG00000056612.6	18938
Vasp	-0.98	0.029	protein_coding	ENSMUSG00000030403.9	22323
Plekhb1	-0.96	0.023	protein_coding	ENSMUSG00000030701.17	27276
Zfp467	-0.92	0.018	protein_coding	ENSMUSG00000068551.12	68910
Net1	-0.90	0.009	protein_coding	ENSMUSG00000021215.14	56349
Sms	-0.88	0.002	protein_coding	ENSMUSG00000071708.11	20603
Ccnk	-0.88	0.013	protein_coding	ENSMUSG00000021258.9	12454
Lgals1	-0.82	0.021	protein_coding	ENSMUSG00000068220.5	16852
Mylk2	-0.81	0.002	protein_coding	ENSMUSG00000027470.9	228785
Calm1	-0.81	0.018	protein_coding	ENSMUSG00000001175.13	12313
Rxrg	-0.78	0.032	protein_coding	ENSMUSG00000015843.10	20183
Drap1	-0.75	0.022	protein_coding	ENSMUSG00000024914.16	66556
Ankrd9	-0.74	0.010	protein_coding	ENSMUSG00000037904.14	74251
Kmt5a	-0.63	0.031	protein_coding	ENSMUSG00000049327.17	67956
Ccdc50	-0.61	0.040	protein_coding	ENSMUSG00000038127.14	67501
Ttc7b	-0.57	0.050	protein_coding	ENSMUSG00000033530.7	104718
Cdc34	-0.55	0.047	protein_coding	ENSMUSG00000020307.14	216150
Csde1	-0.53	0.034	protein_coding	ENSMUSG00000068823.10	229663

Table S15. List of primers used for qPCR analysis of gene expression.

Gene Symbol	Gene Name	Forward Sequence	Reverse Sequence
Acadm, Mcad	Acyl-Coenzyme A dehydrogenase, medium chain	AGGGTTTAGTTTTGAGTTGACGG	CCCCGCTTTTGTCATATTCCG
Acc	Acetyl-CoA carboxylase	TGACAGACTGATCGCAGAGAAAG	TGGAGAGCCCCACACACA
Acox1	Acyl-Coenzyme A oxidase 1, palmitoyl	AGATTGGTAGAAATTGCTGCAAA	ACGCCACTTCCTTGCTCTTC
Adgre1, F4/80	Adhesion G protein-coupled receptor E1	CCCCAGTGTCCTTACAGAGTG	GTGCCCAGAGTGGATGTCT
Arg1	Arginase 1	CTCCAAGCCAAAGTCCTTAGAG	AGGAGCTGTCATTAGGGACATC
Atp2a1	ATPase, Ca2+ transporting, fast twitch 1, Serca1	TGTTTGTCCTATTTCGGGGTG	AATCCGCACAAGCAGGTCTTC
Atp2a2	ATPase C2+ transporting slow twitch 2, Serca2a	GAGAACGCTCACACAAAGACC	CAATTCGTTGGAGCCCCAT
Atp5a1	ATP synthase, H+ transporting, mitochondrial F1 complex, alpha subunit 1	TCTCCATGCCTCTAACACTCG	CCAGGTCAACAGACGTGTCAG
Calm2	Calmodulin 2	ACGGGGATGGGACAATAACAA	CACACGGAATGCTTCTCTAATCT
Ccl3	Chemokine (C-C motif) ligand 3	TTCTCTGTACCATGACACTCTGC	CGTGGAATCTTCCGGCTGTAG
Ccl4	Chemokine (C-C motif) ligand 4	TTCCTGCTGTTTCTCTTACACCT	CTGTCTGCCTCTTTTGGTCAG
Ccr7	Chemokine (C-C motif) receptor 7	TGTACGAGTCGGTGTGCTTC	GGTAGGTATCCGTCATGGTCTTG
CD206	Mannose receptor, C type 1	CTCTGTTCAGCTATTGGACGC	CGGAATTTCTGGGATTCAGCTTC
CD36	CD36 molecule	ATGGGCTGTGATCGGAACTG	AGCCAGGACTGCACCAATAAC
CD68	CD68 antigen	TTCTGCTGTGGAAATGCAAG	CAATGATGAGAGGCAGCAAG
Cebpa	CCAAT/enhancer binding protein alpha	CAAGAACAGCAACGAGTACCG	GTCACTGGTCAACTCCAGCAC
Cidea	Cell death-inducing DNA fragmentation factor, alpha subunit-like effector A	TGACATTCATGGGATTGCAGAC	GGCCAGTTGTGATGACTAAGAC
Cidec	Cell death-inducing DFFA-like effector c	ATGGACTACGCCATGAAGTCT	CGGTGCTAACACGACAGGG
Ckb	Brain/BAT isoform fo CK	AGTTCCCTGATCTGAGCAGC	GAATGGCGTCGTCCAAAGTAA
Ckm	Creatine kinase, muscle	CTGACCCCTGACCTCTACAAT	CATGGCGGTCCTGGATGAT
Col1a1	Collagen, type I, alpha 1	GCTCCTCTTAGGGGCCACT	CCACGTCTCACCATTGGGG
Col3a1	Collagen, type III, alpha 1	GGGTTTCCCTGGTCCTAAAG	CCTGGTTTCCCATTTTCTCC
Col6a1	Collagen, type VI, alpha 1	GATGAGGGTGAAGTGGGAGA	CAGCACGAAGAGGATGTCAA
Cox8b	Cytochrome c oxidase subunit 8B	TGTGGGGATCTCAGCCATAGT	AGTGGGCTAAGACCCATCCTG
Cpt1a	Carnitine palmitoyltransferase 1a, liver	CACCAACGGGCTCATCTTCTA	CAAAATGACCTAGCCTTCTATCGAA
Cpt1b	Carnitine palmitoyltransferase 1b, muscle	GGTCCCATAAGAAACAAGACCTCC	CAGAAAGTACCTCAGCCAGGAAAG
Dgat1	Diacylglycerol O-acyltransferase 1	GCCTTACTGGTTGAGTCTATCAC	GCACCACAGGTTGACATCC
Dgat2	Diacylglycerol O-acyltransferase 2	GCGCTACTTCCGAGACTACTT	GGGCCTTATGCCAGGAAACT
Dio2	Deiodinase, iodothyronine, type II	AATTATGCCTCGGAGAAGACCG	GGCAGTTGCCTAGTGAAAGGT
Dio3	Deiodinase, iodothyronine type III	CACGGCCTTCATGCTCTGG	CGGTTGTCGTCTGATACGCA
F4/80	Adhesion G protein-coupled receptor E1	CCCCAGTGTCCTTACAGAGTG	GTGCCCAGAGTGGATGTCT
Fasn	Fatty acid synthase	GGAGGTGGTGATAGCCGGTAT	TGGGTAATCCATAGAGCCCAG
Gatm	Glycine amidinotransferase (L-arginine:Gglycine amidotransferase), mitochondrial protein nuclear encoded	GCTTCCTCCCGAAATTCCTGT	CCTCTAAAGGGTCCCATTCGT
Gpat1, Gpam	Glycerol-3-phosphate acyltransferase, mitochondrial	CATCCTCTTTTGCCACAACAT	ACAGAATGTCTTTGCGTCCA
Gpat2	Glycerol-3-phosphate acyltransferase 2, mitochondrial	CACTGCTCCAGGTTTTGATG	AGGTTGGCAGCAATTCCATAC
Gpat4	Glycerol-3-phosphate acyltransferase 4	AGCTTGATTGTCAACCTCCTG	CCGTTGGTGTAGGGCTTGT
Hnf4a	Hepatic nuclear factor 4, alpha	CACGCGGAGGTCAAGCTAC	CCCAGAGATGGGAGAGGTGAT
Il-10	Interleukin 10	TAGTCCTTCCTACCCCAATTTCC	TTGGTCCTTAGCCACTCCTTC
Il-1β	Interleukin 1 beta	GCTCTTACTGACTGGCATGAG	CGCAGCTCTAGGAGCATGTG
IL6	Interleukin 6	GCCACCTTTTGACAGTGATGAG	GACAGCCCAGGTCAAAGGTT
Lcad, Acadl	Acyl-Coenzyme A dehydrogenase, long-chain	TCTTTTCCTCGGAGCATGACA	GACCTCTCTACTCACTTCTCCAG
Lipe	Lipase, hormone sensitive	CCAGCCTGAGGGCTTACTG	CTCCATTGACTGTGACATCTCG
Mb	Myoglobin	CTGTTTAAGACTCACCCTGAGAC	GGTGCAACCATGCTTCTTCA
Mcad	Acyl-Coenzyme A dehydrogenase, medium chain	AGGGTTTAGTTTTGAGTTGACGG	CCCCGCTTTTGTCATATTCCG
Mcp1	chemokine (C-C motif) ligand 2	TTAAAAACCTGGATCGGAACCAA	GCATTAGCTTCAGATTTACGGGT
Mct10	Slc16a10, olute carrier family 16, member 10; Tat1	GAGGTGGAGCTGACGAGGT	CATGGACACGAAGAGCACCC
Mct8	Slc16a2, monocarboxylic acid transporter, member 2, Xpct	CGGCTGGATAGTGGTGTTTG	CAGAGTTATGGATGCCGAAGATG
Mgl2	Macrophage galactose N-acetyl-galactosamine specific lectin 2	GCATGAAGGCAGCTGCTATTGGTT	TAGGCCCATCCAGCTAAGCACATT
Mlxipl, ChREBP	MLX interacting protein-like	AGATGGAGAACCGACGTATCA	ACTGAGCGTGCTGACAAGTC
mt-Co2	Mitochondrial cytochrome c oxidase II	GCCGACTAAATCAAGCAACA	CAATGGGCATAAAGCTATGG
mt-Cytb	Mitochondrially encoded cytochrome b	CATTTATTATCGCGGCCCTA	TGTTGGGTTGTTTGATCCTG
myh1	Myosin heavy chain 2x, myosin 1	GCGAATCGAGGCTCAGAACAA	GTAGTTCCGCCTTCGGTCTTG
myh2	Myosin heavy chain 2a, myosin 2	AAGTGACTGTGAAAACAGAAGCA	GCAGCCATTTGTAAGGGTTGAC
Myh4, MyhII2b	Myosin, heavy polypeptide 4, skeletal muscle	CTTTGCTTACGTCAGTCAAGGT	AGCGCCTGTGAGCTTGTAAA
Myh7	Myosin hevy chain polypeptide 7	ACTGTCAACACTAAGAGGGTCA	TTGGATGATTTGATCTTCCAGGG
Myl2	Myosin light poplypeptide 2	ATCGACAAGAATGACCTAAGGGA	ATTTTTCACGTTCACTCGTCCT
Myod1	Myogenic differentiation 1	CCACTCCGGGACATAGACTTG	AAAAGCGCAGGTCTGGTGAG
Myog	Myogenin	GAGACATCCCCCTATTTCTACCA	GCTCAGTCCGCTCATAGCC
Ndufa1	NADH:ubiquinone oxidoreductase subunit A1	ATGTGGTTCGAGATTCTCCCT	TGGTACTGAACACGAGCAACT
Nos2	Nitric oxide synthase 2, inducible	GTTCTCAGCCCAACAATACAAGA	GTGGACGGGTCGATGTCAC
Nr1h4, Fxr	Nuclear receptor subfamily 1, group H, member 4	GCTTGATGTGCTACAAAAGCTG	CGTGGTGATGGTTGAATGTCC
P2rx5	Purinergic receptor P2X, ligand-gated ion channel, 5	TGGAAGGGGTTCGTGTTGTC	AGGGAAGTGTCAATGTCCTGA
Pln	Phospholamban	CTCGCTCGGCTATCAGGAGAG	AGCATCACAATGATGCAGATCAG
Pnpla2, Atgl	Patatin-like phospholipase domain containing 2	TGTGGCCTCATTCCTCCTAC	TCGTGGATGTTGGTGGAGCT
Ppara	Peroxisome proliferator activated receptor alpha	CTATAATTTGCTGTGGAGATCGGC	GGATGGTTGCTCTGCAGGT
Ppard	Peroxisome proliferator activated receptor delta	TCCATCGTCAACAAAGACGGG	ACTTGGGCTCAATGATGTCAC
Ppargc1a, Pgc1a	Peroxisome proliferative activated receptor, gamma, coactivator 1 alpha	TATGGAGTGACATAGAGTGTGCT	CCACTTCAATCCACCCAGAAAG
Ppargc1b, Pgc1b	Peroxisome proliferative activated receptor, gamma, coactivator 1 beta	TCCTGTAAAAGCCCGGAGTAT	GCTCTGGTAGGGGCAGTGA
Pparγ	Peroxisome proliferator activated receptor gamma	TCGCTGATGCACTGCCTATG	GAGAGGTCCACAGAGCTGATT
Prdm16	PR domain containing 16	CAGCACGGTGAAGCCATTC	GCGTGCATCCGCTTGTG
Ptgs2, Cox2 (COXII)	Prostaglandin-endoperoxide synthase 2	GCCGACTAAATCAAGCAACA	CAATGGGCATAAAGCTATGG
Retnla	Resistin like alpha	CCAATCCAGCTAACTATCCCTCC	ACCCAGTAGCAGTCATCCCA
Rplp0, 36B4	Ribosomal protein, large, P0	AGATTCGGGATATGCTGTTGGC	TCGGGTCCTAGACCAGTGTTC
Scd1	Stearoyl-Coenzyme A desaturase 1	TTCTTGCGATACACTCTGGTGC	CGGGATTGAATGTTCTTGTCGT
Sirt1	Sirtuin 1	GCTGACGACTTCGACGACG	TCGGTCAACAGGAGGTTGTCT
Slc6a8	Solute carrier family 6 (neurotransmitter transporter, creatine), member 8	GCAGGGTGTGCATATCTCCAA	TACCCCCACTCACATCAGTCA
Sln	Sarcolipin	TGTGCCCCTGCTCCTCTTC	TGATTGCACACCAAGGCTTG
Srebf1, Srebp1c	Sterol regulatory element binding transcription factor 1	GGAGCCATGGATTGCACATT	GGCCCGGGAAGTCACTGT
Srebf2	Sterol regulatory element binding factor 2	GCGTTCTGGAGACCATGGA	ACAAAGTTGCTCTGAAAACAAATCA
Tbp	TATA-box binding protein	TGGTGTGCACAGGAGCCAAG	TTCACATCACAGCTCCCCAC
Thra1	Thyroid hormone receptor alpha, nr1a1	CTGACCTCCGCATGATCGG	GGTGGGGCACTCGACTTTC
Thrb	Thyroid hormone receptor beta	CCAGAGGTACACGAAGTGTGC	AGGTTTCCAGGGTAACTACAGG
Tnfa	tumor necrosis factor alpha	ATGCTGGGACAGTGACCTGG	CCTTGATGGTGGTGCATGAG
Tnnc1	Troponin C	GCGGTAGAACAGTTGACAGAG	CCAGCTCCTTGGTGCTGAT
Tnni1	Troponin I, skeletal, slow 1	ATGCCGGAAGTTGAGAGGAAA	TCCGAGAGGTAACGCACCTT
Tnnt1	Troponin T1	CCTGTGGTGCCTCCTTTGATT	TGCGGTCTTTTAGTGCAATGAG
Tnnt2	Troponin T2	GAGCTACAGACTCTGATCGAGG	CCGCTCATTGCGAATACGC
Tpm3	Tropomyosin 3, gamma	ACCACCATCGAGGCGGTAA	CCCTTTCCTCCGCATCATCA
Ucp1	Uncoupling protein 1 (mitochondrial, proton carrier)	AGGCTTCCAGTACCATTAGGT	CTGAGTGAGGCAAAGCTGATTT
Ucp3	Uncoupling protein 3 (mitochondrial, proton carrier)	CCGATTTCAAGCCATGATACGC	GGCATCCATAGTCCCTCTGTATT